

4th ANNUAL EARTH RESOURCES PROGRAM REVIEW

VOLUME III
U.S. GEOLOGICAL
SURVEY PROGRAMS



68952
(NASA-TM-X-~~60398~~) FOURTH ANNUAL EARTH
RESOURCES PROGRAM REVIEW. VOLUME 3: US
GEOLOGICAL SURVEY PROGRAMS (NASA) 21 Jan.
1972 309 p CSCI 08G
G3/13 37075
N72-29355
thru
N72-29377
Unclas



Presented at the
Manned Spacecraft Center
Houston, Texas

January 17 to 21, 1972

Reproduced by
**NATIONAL TECHNICAL
INFORMATION SERVICE**
U.S. Department of Commerce
Springfield VA 22151

309

FOREWORD

A review of various aspects of the Earth Resources Program was held at the Manned Spacecraft Center, Houston, Texas, January 17 to 21, 1972. Particular emphasis was placed on the results of analysis of data obtained with the Manned Spacecraft Center and other aircraft which have contributed data to the program.

The review was divided into the disciplinary areas of Geology, Geography, Hydrology, Agriculture, Forestry, and Oceanography. Program investigators presented the results of their work in each of these areas. The material presented is published in five volumes:

VOLUME I - NATIONAL AERONAUTICS AND SPACE ADMINISTRATION PROGRAMS - *N72-29302*
VOLUME II - UNIVERSITY PROGRAMS *N72-29327*
VOLUME III - U.S. GEOLOGICAL SURVEY PROGRAMS *N72-29355*
VOLUME IV - NATIONAL OCEANIC AND ATMOSPHERIC ADMINISTRATION PROGRAMS AND
U.S. NAVAL RESEARCH LABORATORY PROGRAMS *N72-29378*
VOLUME V - AGRICULTURE AND FORESTRY PROGRAMS *N72-29407*

The review provided a current assessment of the program for both management and technical personnel. Note that the material presented represents the current status of ongoing programs and complete technical analyses will be available at a later date.

Where papers were not submitted for publication or were not received in time for printing, abstracts are used.

FRONT COVER

The map on the front cover depicts the NASA Earth Resources
aircraft coverage of the United States through June 1971.

ORIGINAL CONTAINS
COLOR ILLUSTRATIONS

THE ORIGINAL REPORT USED FOR
PRINTING THIS COPY CONTAINS
COLOR PLATES AND ARE REPRO-
DUCED HERE IN BLACK AND WHITE.
OTHER HALFTONES ARE OF POOR
QUALITY AND MAY BE BETTER
STUDIED ON MICROFICHE.

PRECEDING PAGE BLANK NOT FILMED

CONTENTS OF VOLUME I

Section	Page
FOREWORD	iii
<u>AMES RESEARCH CENTER</u>	
1 AMES RESEARCH CENTER SR&T PROGRAM AND EARTH OBSERVATIONS	1-1
by Ilia G. Poppoff	
<u>WALLOPS STATION</u>	
2 DEVELOPMENT OF CHESAPEAKE BAY TEST SITE FOR REMOTE SENSING APPLICATIONS	2-1
by James Bettie	
<u>GODDARD SPACE FLIGHT CENTER</u>	
3 DEVELOPMENT OF EARTH RESOURCES SURVEY TECHNIQUES AT GSFC - OVERVIEW	3-1
by William Nordberg	
4 RADIOMETRIC IMAGES OF IR RESTSTRAHLEN EMISSION FROM ROCK SURFACES	4-1
by Warren A. Hovis	
5 NIMBUS HYDROLOGICAL OBSERVATIONS OVER THE WATERSHEDS OF THE NIGER AND INDUS RIVERS	5-1
by Vincent V. Salomonson and Norman H. MacLeod	
6 SPECTRAL REFLECTANCE MEASUREMENTS OF PLANT-SOIL COMBINATIONS	6-1
by Norman MacLeod	
7 ANALYSIS OF MULTISPECTRAL IMAGES SIMULATING ERTS OBSERVATIONS	7-1
by Nicholas M. Short and Norman H. MacLeod	

<p>Preceding page blank</p>

Section		Page
8	MICROWAVE EMISSION MEASUREMENTS OF SEA SURFACE ROUGHNESS, SOIL MOISTURE, AND SEA ICE STRUCTURE . . .	8-1
	by P. Gloersen, T. Wilheit, and T. Schmugge	
9	RADIOMETRIC OCEAN COLOR SURVEYS THROUGH A SCATTERING ATMOSPHERE	9-1
	by Robert J. Curran and Warren A. Hovis	
10	A MULTISPECTRAL METHOD OF MEASURING SEA SURFACE TEM- PERATURES FROM SATELLITES	10-1
	by William E. Shenk and Vincent V. Salomonson	
	<u>MISSISSIPPI TEST FACILITY</u>	
11	A SUMMARY OF ACTIVITIES OF THE EARTH RESOURCES LABORA- TORY AT THE MISSISSIPPI TEST FACILITY DURING 1971	11-1
	by Robert O. Filand	
12	SUMMARY OF 1971 WATER REMOTE SENSING INVESTIGATIONS	12-1
	by Edward L. Tilton, III	
13	MISSISSIPPI SOUND REMOTE SENSING STUDY	13-1
	by B. H. Atwell and G. C. Thomann	
14	SUMMARY OF 1971 LAND REMOTE SENSING INVESTIGATIONS . . .	14-1
	by Darden W. Mooneyhan	
15	SUMMARY OF 1971 PATTERN RECOGNITION PROGRAM DEVELOPMENT	15-1
	by Sidney L. Whitley	
	<u>LEWIS RESEARCH CENTER</u>	
16	LEWIS RESEARCH CENTER EARTH RESOURCES PROGRAM	16-1

Section		Page
	<u>MARSHALL SPACE FLIGHT CENTER</u>	
17	ENVIRONMENTAL APPLICATIONS ACTIVITY AT MARSHALL SPACE FLIGHT CENTER	17-1
	by Charles T. N. Paludan	
	<u>LANGLEY RESEARCH CENTER</u>	
18	EARTH RESOURCES PROGRAMS AT THE LANGLEY RESEARCH CENTER. PART I. ADVANCED APPLICATIONS FLIGHT EXPERIMENTS (AAFE) AND MICROWAVE REMOTE SENSING PROGRAM	18-1
	by Robert N. Parker	
19	EARTH RESOURCES PROGRAMS AT THE LANGLEY RESEARCH CENTER. PART II. COASTAL ZONE OCEANOGRAPHY PROGRAM . . . :	19-1
	by Walter E. Bressette	
	<u>MANNED SPACECRAFT CENTER</u>	
20	MSC SUPPORTING RESEARCH AND TECHNOLOGY	20-1
	by Dallas Evans	
21	HOUSTON AREA TEST SITE	21-1
	by Bryan Erb	
22	PUBLIC HEALTH APPLICATIONS OF REMOTE SENSING	22-1
	by Charles E. Fuller	
23	A BREADBOARD HYBRID MULTISPECTEAL PROCESSING SYSTEM	23-1
	by Donald Hayden	
24	CONSTRUCTING AND MANIPULATING COLOR IMAGERY FROM DIGITAL DATA	24-1
	by J. E. Davis, C. A. Helmke, T. R. Kell, M. J. Arldt, and E. L. Wilson	

Section		Page
25	SALINITY SURVEYS USING AN AIRBORNE MICROWAVE RADIOMETER	25-1
	by J. F. Paris, J. D. Droppleman, and D. E. Evans	
26	MICROWAVE BRIGHTNESS TEMPERATURE OF A WINDBLOWN SEA	26-1
	by Forrest G. Hall	
27	DETECTION OF OIL SPILLS USING 13.3-GHz RADAR SCATTEROMETER	27-1
	by Kumar Krishen	

CONTENTS OF VOLUME II

Section		Page
	FOREWORD	iii
	<u>UNIVERSITY OF MICHIGAN</u>	
28	A SUMMARY OF MICHIGAN PROGRAM FOR EARTH RESOURCES INFORMATION SYSTEMS	28-1
	by Jon D. Erickson	
29	INFORMATION EXTRACTION TECHNIQUES FOR MULTI- SPECTRAL SCANNER DATA	29-1
	by William A. Malila, Robert B. Crane, Wyman Richardson, and Robert E. Turner	
30	USER ORIENTED MULTISPECTRAL DATA PROCESSING AT THE UNIVERSITY OF MICHIGAN	30-1
	by Frederick J. Thomson	
31	PREDICTION OF DIRECTIONAL REFLECTANCE OF A CORN FIELD UNDER STRESS	31-1
	by Gwynn H. Suits, Gene Safir, and A. Ellingboe	
32	CLASSIFICATION OF SPATIALLY UNRESOLVED OBJECTS	32-1
	by Richard F. Nalepka, Harold M. Horwitz, Peter D. Hyde, and James P. Morgenstern	
33	EXPERIMENTAL METHODS FOR GEOLOGICAL REMOTE SENSING	33-1
	by Robert K. Vincent	
34	MICHIGAN EXPERIMENTAL MULTISPECTRAL SCANNER SYSTEM	34-1
	by Philip G. Hasell, Jr.	
35	MULTISPECTRAL IMAGING RADAR	35-1
	by L. J. Porcello and R. A. Rendleman	

Section		Page
	<u>UNIVERSITY OF KANSAS</u>	
36	SURFACE CONFIGURATION AS AN EXPLANATION FOR LITHOLOGY-RELATED CROSS-POLARIZED RADAR IMAGE ANOMALIES	36-1
	by James R. McCauley	
37	THE STATUS OF PARAMETRIC STUDIES IN RADAR AGRICULTURE	37-1
	by Stanley A. Morain	
38	DATA PROCESSING AT THE UNIVERSITY OF KANSAS	38-1
	by Robert M. Haralick	
39	RADAR SIGNATURE AND SYSTEMS STUDIES AT KANSAS UNIVERSITY	39-1
	by Richard K. Moore	
	<u>UNIVERSITY OF CALIFORNIA</u>	
40	AN INTEGRATED STUDY OF EARTH RESOURCES IN THE STATE OF CALIFORNIA USING REMOTE SENSING TECHNIQUES . . .	40-1
	by Robert N. Colwell	
	<u>SOUTH DAKOTA STATE UNIVERSITY</u>	
41	REMOTE SENSING OF SOILS, LAND FORMS, AND LAND USE IN THE NORTHERN GREAT PLAINS IN PREPARATION FOR ERTS APPLICATIONS	41-1
	by C. J. Frazee, F. C. Westin, J. Gropper, and V. I. Myers	
42	PATTERN RECOGNITION SYSTEM AND PROCEDURES	42-1
	by Gerald D. Nelson and David V. Serreyn	
	<u>COLORADO SCHOOL OF MINES</u>	
43	BONANZA PROJECT — 1971	43-1
	by Keenan Lee	

Section		Page
	<u>TEXAS A & M UNIVERSITY</u>	
44	A COACTIVE INTERDISCIPLINARY RESEARCH PROGRAM WITH NASA	44-1
	by John W. Rouse, Jr.	
45	SPECTRAL REFLECTANCE MEASUREMENTS OF A VIRUS HOST MODEL	45-1
	by Robert W. Toler and N. K. Shankar	
	<u>UNIVERSITY OF WISCONSIN</u>	
46	APPLICATION OF REMOTE SENSING TO WATER RESOURCES PROBLEMS	46-1
	by James L. Clapp	
	<u>PURDUE UNIVERSITY</u>	
47	DIFFERENTIATING ELEMENTS OF THE SOIL-VEGETATION COMPLEX	47-1
	by M. F. Baumgardner and Staff	
48	LAND UTILIZATION AND WATER RESOURCE INVENTORIES OVER EXTENDED TEST SITES	48-1
	by Roger M. Hoffer and Staff	
49	MEASUREMENTS PROGRAM IN REMOTE SENSING AT PURDUE UNIVERSITY	49-1
	by LeRoy F. Silva and Staff	
50	DATA PROCESSING I: ADVANCEMENTS IN MACHINE ANALYSIS OF MULTISPECTRAL DATA	50-1
	by Philip H. Swain and Staff	
51	DATA PROCESSING II: ADVANCEMENTS IN LARGE-SCALE DATA PROCESSING SYSTEMS FOR REMOTE SENSING	51-1
	by David Landgrebe and Staff	

Section		Page
	<u>JET PROPULSION LABORATORY</u>	
52	OVERVIEW OF THE EARTH RESOURCES PROGRAM OF THE JET PROPULSION LABORATORY	52-1
	by Donald P. Burcham	
53	MICROWAVE PROPERTIES OF GEOLOGICAL MATERIALS: STUDIES OF PENETRATION DEPTH AND MOISTURE EFFECTS	53-1
	by John C. Blinn, III and Jack G. Quade	
54	POLARIZATION EFFECTS WITH A COMBINED RADAR-RADIOMETER	54-1
	by David Martin	

CONTENTS OF VOLUME III

Section		Page
	FOREWORD	iii
	<u>GEOLOGY, MINERAL, AND LAND RESOURCES</u>	
55	AN OVERVIEW OF RESEARCH BY USDI GEOLOGY, MINERAL, AND LAND RESOURCES WORKING GROUP by Douglas Carter	55-1 ¹⁷⁰ 170
56	SATELLITE RELAY TELEMETRY IN THE SURVEILLANCE OF ACTIVE VOLCANOES AND MAJOR FAULT ZONES by Jerry P. Eaton and Peter L. Ward	56-1 ✓ ⁵⁶
57	ANALYSIS OF THERMAL PATTERNS OF GEOCHEMICALLY STRESSED TREES AT CATHEART MOUNTAIN, MAINE by F. C. Canney, T. D. Hessin, and W. G. Burge	57-1 ¹⁷⁰ 170
58	APPLICATIONS OF INFRARED REMOTE SENSING METHODS TO GEOLOGICAL AND ENGINEERING PROBLEMS OF THE ARCTIC by Gordon W. Greene	58-1 ¹⁷⁰ 170
59	GEOLOGIC MATERIAL DISCRIMINATION FROM NIMBUS SATELLITE DATA by H. A. Pohn, T. W. Offield, and Kenneth Watson	59-1 ⁵⁷
60	NEAR-INFRARED IRON ABSORPTION BANDS: APPLICATIONS TO GEOLOGIC MAPPING AND MINERAL EXPLORATION by Lawrence C. Rowan	60-1 ⁵⁸
61	MAPPING OF TERRAIN BY COMPUTER CLUSTERING TECHNIQUES USING MULTISPECTRAL SCANNER DATA AND USING COLOR AERIAL FILM by Harry W. Smedes, Harold J. Linnerud, Lawrence B. Woolaver, Ming-Yang Su, and Robert R. Jayroe	61-1 ⁵⁹

Section		Page	
62	FUNCTIONS AND ACTIVITIES OF THE ARIZONA REGIONAL ECOLOGICAL TEST SITE	62-1	✓ 66
	by L. K. Lepley		
63	APPLICATIONS OF REMOTE SENSOR DATA BY STATE AND FEDERAL USER AGENCIES IN ARIZONA	63-1	✓ 61
	by Herbert H. Schumann		
64	REMOTE SENSING ON INDIAN AND PUBLIC LANDS	64-1	✓ 62
	by Grover B. Torbert and Arthur M. Woll		
65	THE REMOTE SENSING OF AIR POLLUTION FROM COAL UTILIZATION	65-1	✓ 63
	by Brian M. Harney, Donald H. McCrea, and Albert J. Forney		
66	REMOTE SENSING OF WET LANDS IN IRRIGATED AREAS	66-1	✓ 64
	by Herbert H. Ham		
67	SHORT PULSE RADAR MEASUREMENTS OF LAYERED ICE AND SNOW	67-1	✓ 65
	by R. S. Vickers and G. C. Rose		
68	EARTH RESOURCES CARTOGRAPHY PROGRAM	68-1	✓ 66
	by Alden P. Colvocoresses		
69	AUTOMATIC THEMATIC MAPPING IN THE EROS PROGRAM	69-1	✓ 67
	by Dean T. Edson		
	<u>GEOGRAPHY, HUMAN, AND CULTURAL RESOURCES</u>		
70	THE GEOGRAPHY AND HUMAN - CULTURAL RESOURCES WORKING GROUP OF THE EROS PROGRAM	70-1	✓ 68
	by Arch C. Gerlach		
71	AN AUTOMATED MAP AND MODEL OF LAND USE IN THE PHOENIX QUADRANGLE	71-1	✓ 69
	by John L. Place		

Section		Page
72	CENTRAL ATLANTIC REGIONAL ECOLOGICAL TEST SITE	72-1 <i>79</i>
	by Robert H. Alexander	
73	THE CENSUS CITIES PROJECT: A STATUS REPORT FOR 1971	73-1 <i>78</i>
	by James R. Wray	
74	BUREAU AND AGENCY REPORTS	74-1 <i>72</i>
	by George L. Loelkes	
	<u>HYDROLOGY AND WATER RESOURCES</u>	
75	HYDROLOGIC APPLICATIONS PROGRAM SUMMARY	75-1 <i>NO 74</i>
	by Morris Deutsch	
76	SIMULATION STUDIES OF ERTS-A&B DATA FOR HYDROLOGIC STUDIES IN THE LAKE ONTARIO BASIN	76-1 <i>NO 74</i>
	by Joseph MacDowall, Allan Falconer, and Keith P. B. Thomson	
77	COURT PRECEDENT FOR ACCEPTANCE IN EVIDENCE OF REMOTELY- SENSED DATA AND THEIR INTERPRETATION, CROSS-FLORIDA BARGE CANAL	77-1 <i>NO 74</i>
	by Aaron L. Higer, Milton C. Kolipinski, and Eldon Lucas	
78	WETLANDS DELINEATION BY SPECTRAL SIGNATURE ANALYSIS AND LEGAL IMPLICATIONS	78-1 <i>73</i>
	by Richard R. Anderson and Virginia Carter	
79	DISCRIMINATION OF FLUORIDE AND PHOSPHATE CONTAMINA- TION IN CENTRAL FLORIDA FOR ANALYSES OF ENVIRONMENTAL EFFECTS	79-1 <i>74</i>
	by A. E. Coker, R. Marshall, and F. Thomson	
80	RELAY OF QUANTITATIVE RESOURCES DATA BY ERTS-A	80-1 <i>NO 74</i>
	by James F. Daniel	

Section		Page
81	APPLICATIONS OF SPECTROSCOPY TO REMOTE DETERMINATION OF WATER QUALITY.	81-1 ✓ 25
	by Marvin C. Goldberg and Eugene R. Weiner	
82	SPECTRAL REFLECTANCE OF SELECTED AQUEOUS SOLUTIONS FOR WATER QUALITY APPLICATIONS	82-1 ✓ 76
	by M. R. Querry, R. C. Waring, W. E. Holland, W. Nijm, and G. M. Hale	
83	QUANTITATIVE RELATIONSHIP BETWEEN REFLECTANCE AND TRANSPIRATION OF PHREATOPHYTES — GILA RIVER TEST SITE	83-1 ✓ 27
	by R. C. Culler, J. E. Jones, and R. M. Turner	

CONTENTS OF VOLUME IV

Section	Page
FOREWORD	iii
<u>NATIONAL OCEANIC AND ATMOSPHERIC ADMINISTRATION</u>	
84 MICROWAVE CHARACTERISTICS OF THE OCEAN SURFACE IN THE 1-10 GHz BAND	84-1
by Alan E. Strong and Ronald A. Porter	
85 OBSERVATIONS OF OCEANIC WHITE CAPS FOR MODERATE TO HIGH WIND SPEEDS	85-1
by Duncan B. Ross and Vincent Cardone	
86 THE CONSTRAINT OF SUN GLINT ON VISIBLE DATA GATHERED BY EARTH SATELLITES	86-1
by Alan E. Strong	
87 SPECIAL DISPLAYS OF SATELLITE INFRARED DATA FOR SEA ICE MONITORING	87-1
by E. Paul McClain	
88 APPLICATION OF SATELLITE INFRARED MEASUREMENTS TO MAPPING SEA ICE	88-1
by James C. Barnes	
89 MICROWAVE EMISSION CHARACTERISTICS OF SEA ICE	89-1
by A. T. Edgerton and G. Poe	
90 REGIONAL STUDIES USING SEA SURFACE TEMPERATURE FIELDS DERIVED FROM SATELLITE INFRARED MEASUREMENTS	90-1
by Alan E. Strong	
91 FISHERIES RESOURCE IDENTIFICATION AND ASSESSMENT STUDIES	91-1
by William H. Stevenson	

Section		Page
92	COMPARISON OF REMOTE SENSORS FOR SOIL MOISTURE AND OTHER HYDROLOGIC STUDIES	92-1
	by Donald R. Wiesnet	
93	SOIL MOISTURE MAPPING BY GROUND AND AIRBORNE MICROWAVE RADIOMETRY	93-1
	by G. Poe and A. T. Edgerton	
94	DETERMINATION OF THAWING SNOW AND ICE SURFACES USING EARTH SATELLITE DATA	94-1
	by Donald R. Wiesnet and David F. McGinnis	
95	SNOW STUDIES USING THERMAL INFRARED OBSERVATIONS FROM EARTH SATELLITES	95-1
	by James C. Barnes	
	<u>U. S. NAVAL RESEARCH LABORATORY</u>	
96	LABORATORY INVESTIGATIONS RELATED TO MICROWAVES . . .	96-1
	by Omar H. Shemdin	
97	THE EXTRAPOLATION OF LABORATORY AND AIRCRAFT RADAR SEA RETURN DATA TO SPACECRAFT ALTITUDES	97-1
	by Willard J. Pierson and Richard K. Moore	
98	MISSION 119 PASSIVE MICROWAVE RESULTS	98-1
	by J. P. Hollinger and R. A. Mennella	
99	GROUND TRUTH INVESTIGATIONS FOR AIDJEX 71	99-1
	by William Campbell	
100	APPLICATION OF THERMAL RADIATION DATA TO FISHERY OCEANOGRAPHY	100-1
	by Merritt Stevenson and Forrest Miller	

Section		Page
101	THE CASE FOR OCEAN COLOR	101-1
	by Henry J. Yotko	
102	DETECTION OF OCEAN CHLOROPHYLL FROM EARTH ORBIT . . .	102-1
	by Seibert Q. Duntley	
103	A TECHNIQUE FOR THE REDUCTION AND ANALYSIS OF OCEAN SPECTRAL DATA	103-1
	by Peter G. White	
104	AIRBORNE DIFFERENTIAL RADIOMETER MEASUREMENTS OF CHLOROPHYLL IN WATER	104-1
	by John C. Arvesen	
105	REMOTE MEASUREMENT OF CHLOROPHYLL CONCENTRATION AND SECCHI-DEPTH USING THE PRINCIPAL COMPONENTS OF THE OCEAN'S COLOR SPECTRUM	105-1
	by James L. Mueller	
106	SURFACE TRUTH MEASUREMENTS OF OPTICAL PROPERTIES OF THE WATERS IN THE NORTHERN GULF OF CALIFORNIA	106-1
	by Roswell W. Austin	
107	PRACTICAL UTILITY OF THE BLUE SPECTRAL REGION	107-1
	by Donald S. Ross	
108	EVALUATION OF FACTORS AFFECTING RESOLUTION OF SHALLOW-WATER BOTTOM FEATURES	108-1
	by Curtis C. Mason, Dean R. Norris, and I. Dale Browne	
109	MULTISPECTRAL OBSERVATIONS OF MARINE ENVIRONMENTS	109-1
	by Fabian C. Polcyn	
110	COASTAL AND ESTUARINE APPLICATIONS OF MULTISPECTRAL PHOTOGRAPHY	110-1
	by Edward Yost and Sondra Wenderoth	

Section		Page
111	EFFLUENT MIXING IN THE MISSISSIPPI REGION DELTA, LOUISIANA	111-1
	by James Coleman, Lyn Wright, and Ronald Becker	
112	A STUDY OF TEMPORAL ESTUARINE FLOW DYNAMICS	112-1
	by Robert L. Mairs and Dennis K. Clark	
113	THE TONGUE OF THE OCEAN AS A REMOTE SENSING OCEAN COLOR CALIBRATION RANGE	113-1
	by Leo V. Strees	
114	A PROGRAM TO ASSESS A THERMAL DISCHARGE ON TRINITY BAY, TEXAS	114-1
	by James B. Zaitzeff and Victor S. Whitehead	

CONTENTS OF VOLUME V

Section		Page
	FOREWORD	iii
	<u>AGRICULTURE AND FORESTRY</u>	
115	DEVELOPMENT OF ANALYSIS TECHNIQUES FOR REMOTE SENSING OF VEGETATION RESOURCES	115-1
	by William C. Draeger	
116	RESOURCE ANALYSIS AND LAND USE PLANNING WITH SPACE AND HIGH ALTITUDE PHOTOGRAPHY	116-1
	by Barry J. Schrumph	
117	THE USE OF KODAK AEROCROME INFRARED COLOR FILM, TYPE 2443 AS A REMOTE SENSING TOOL	117-1
	by G. R. Cooper, R. L. Bowen, and H. W. Gausman	
118	MEASUREMENTS FROM AIRCRAFT TO CHARACTERIZE WATERSHEDS	118-1
	by Bruce J. Blanchard	
119	DISCRIMINANT ANALYSES OF BENDIX SCANNER DATA	119-1
	by A. J. Richardson, C. L. Wiegand, R. W. Leamer, A. H. Gerbermann, and R. J. Torline	
120	DEVELOPMENT AND FIELD TEST OF AN ERTS - MATCHED FOUR - CHANNEL SPECTROMETER	120-1
	by Frederick P. Weber	
121	MICROSCALE PHOTO INTERPRETATION OF FOREST AND NONFOREST LAND CLASSES	121-1
	by Robert C. Aldrich and Wallace J. Greentree	
122	POTENTIALITY FOR OBTAINING PORIA DISEASE SIGNATURES IN THE OREGON CASCADES FROM ORBITAL ALTITUDES	122-1
	by John F. Wear	

Section	Page
123	PATTERN RECOGNITION OF NATIVE PLANT COMMUNITIES — MANITOU COLORADO TEST SITE 123-1
	by Richard S. Driscoll
	<u>CORN BLIGHT</u>
124	CORN BLIGHT WATCH EXPERIMENT RESULTS 124-1
	by C. J. Johannsen, M. E. Bauer, and Staff
125	THE CORN BLIGHT PROBLEM — 1970 AND 1971 125-1
	by Marvin E. Bauer
126	CORN BLIGHT REVIEW — SAMPLING MODEL AND GROUND DATA MEASUREMENTS PROGRAM 126-1
	by Richard Allen
127	AIRCRAFT DATA ACQUISITION 127-1
	by Ronald K. Blilie
128	1971 CORN BLIGHT WATCH EXPERIMENT DATA PROCESSING, ANALYSIS, AND INTERPRETATION 128-1
	by Terry L. Phillips and Staff
129	EXPERIMENT RESULTS GROUND MEASUREMENTS, PHOTO AND MULTISPECTRAL MACHINE ANALYSIS 129-1
	by Phillip Swain
130	DETAILED INTERPRETATION AND ANALYSIS OF SELECTED CORN BLIGHT WATCH DATA SETS 130-1
	by R. F. Nalepka, J. P. Morgenstern, and W. L. Brown
131	1971 CORN BLIGHT WATCH EXPERIMENT 131-1
	by J. W. Clifton

SECTION 55

AN OVERVIEW OF RESEARCH BY USDI
GEOLOGY, MINERAL, AND LAND RESOURCES

WORKING GROUP

by Douglas Carter
U.S. Geological Survey

ABSTRACT

(Not available)

SECTION 56

N72-29356

SATELLITE RELAY TELEMETRY IN THE SURVEILLANCE OF
ACTIVE VOLCANOES AND MAJOR FAULT ZONES

by

Jerry P. Eaton and Peter L. Ward
U.S. Geological Survey
National Center for Earthquake Research
345 Middlefield Road
Menlo Park, California 94025

INTRODUCTION

This project was initiated in 1968, soon after the U.S. Geological Survey's National Center for Earthquake Research began to develop a dense, telemetered microearthquake network in central California to study the mechanics of earthquake generation along the San Andreas fault. It has been closely tied to the overall effort to develop and evaluate the improved instruments and data transmission, recording, and analysis systems required in the earthquake research program. It has also received important stimulus from interaction with the microearthquake and strain studies at Kilauea Volcano, in Hawaii, which are carried out jointly by NCER and the Survey's Hawaiian Volcano Observatory.

In this report we would like first to review very briefly the work on this project that has been accomplished to date. Next, we shall outline the principal elements and objectives of our ERTS-A proposal, "Prototype Volcano Surveillance Network," which is an outgrowth of the earlier work. Finally, we shall describe some aspects of the central California microearthquake network and the results obtained from it as well as some promising experiments in computerized record processing that promise to reduce the data flow from such a network by 5 orders of magnitude. Such a reduction would bring its data transmission requirements into the range of a system like ERTS.

PRE ERTS-A

The project began as a feasibility study of the use of satellite relay telemetry in earthquake prediction research. It was concluded that satellite relay telemetry of data would have important advantages over conventional techniques because 1) it could provide access to remote areas that lack dense communications networks and 2) because it would not be

destroyed by large earthquakes at a time when it is most needed.

Reliable, low power, radio data links were needed to collect seismic signals from a cluster of stations into a central point for multiplexing onto a phone line or satellite relay channel; so the development of such links was stimulated by a development contract. These radio links have been very successful and are now in routine operation in 6 western states, including Hawaii and Alaska (Figure 1).

The low data-handling capacity of the ERTS system limits its usefulness in microearthquake networks like those now in operation. As noted below, research on automatic processing of data from clusters of seismographs may lead to a sufficient reduction in the data flow from such a cluster that a system like ERTS-A could be used.

On the other hand, the data capacity of the ERTS system should be adequate for monitoring seismic events and tilt changes at volcanoes, and its potential worldwide coverage would permit it to serve as the core of a worldwide volcano surveillance system.

Requirements for the ground-based instruments that would be needed to evaluate the use of ERTS-A in a volcano surveillance system were specified, and work on the development and testing of this equipment was then begun:

a) The prototype Multilevel Event Counter is shown in Figure 2. Six units of the first version of this 4-level event counter are on hand and are being tested. Modifications in design that improve the response and reliability of these instruments have been incorporated into specifications for the next version.

b) Development of a 2-component borehole tiltmeter has been completed. Several instruments are being fabricated to permit further testing of methods of implanting the tiltmeter in shallow boreholes to minimize the effects of the ground surface. A tiltmeter will be available for installation in the Hawaii test area before the end of March.

c) A portable visible recording seismograph has been designed, built, and tested (Figure 3). Ten of these seismographs are available for the ERTS-A program. Six of them incorporate a low-power radio link (Figure 1) to permit the seismometer to be placed high on the volcano and the recorder to be placed in a convenient location at its foot. Two of these instruments are now in use in the Hawaii test area and a third was operated temporarily on most of the volcanoes proposed for study under ERTS-A in Central America.

d) The telemetered seismic network in the Hawaii test area has been expanded and modernized by addition of radio-telemetered remote seismic stations (like those used in the San Andreas Network) (Figure 4) and by

installation of 16 mm strip film seismic recorders (Develocorders).

ERTS-A

A primary goal of our ERTS-A project is to develop and test a relatively inexpensive prototype system for monitoring large numbers of volcanoes and determining when a given volcano is in a sufficiently rest-less state to warrant more detailed studies and concern over possible eruptions. One of the principal problems in volcanology is that, with present approaches, only a very small number of volcanoes can be monitored routinely. In the past, local observatories have been set up only to decay because the volcanoes of interest either were not sufficiently active to warrant the continuing expense, or became inactive. Thus, there is a great need for a widespread system to identify potentially hazardous volcanoes and to notify scientists when more detailed studies are needed.

We have chosen to monitor earthquakes and ground tilt because these have repeatedly proven in the past to be the most reliable indicators of increased volcanic activity in Hawaii, Japan, the West Indies, and other such regions where volcanoes are being studied intensively.

The ERTS Data Collection System, while requiring a large amount of data compression, still provides an unprecedented opportunity to collect data relatively easily from a number of volcanoes. Techniques for data compression have already been developed earlier in this project. The need now is to learn how to emplace these instruments so that the compressed data will relate directly to more conventional data. The principal short-range objectives of our study will be:

1. To fabricate and test multilevel event counters and tiltmeters based on prototypes already developed.
2. To identify and solve problems encountered in placing these instruments on different types of volcanoes in different environments.
3. To compare the condensed data collected by these instruments with the more standard types of data and to evaluate the adequacy of these condensed data for characterizing the internal state of a volcano.
4. To develop and refine relationships between earthquake counts, ground surface deformational activity, and volcanic outbursts at various types of volcanoes.
5. Finally, our main goal is to determine the feasibility of extending the prototype network to form a global volcano surveillance

system aimed at identifying which "dormant" volcanoes are becoming active at a particular time.

To meet these objectives it will be necessary to study volcanoes in a variety of geographical locations. We have spent considerable effort in recent months trying to clearly identify which volcanoes should be studied to meet these objectives and in which areas logistical problems are least likely to prevent success. From these considerations we feel that a minimum program should include observations on the following volcanoes:

	<u>Event Counters</u>	<u>Seismographs</u>	<u>Tiltmeters</u>
<u>Central America</u>			
1. San Cristobal, Telica, Cerro Negro; Nicaragua	5	3	
2. Pacaya, Agua, Fuego; Guatemala	5	3	2
3. Santiaguito; Guatemala	2	1	
4. Izalco; El Salvador	2	1	
<u>Cascades</u>			
Lassen, Baker, St. Helens, Rainier	4	4	1
<u>Alaska</u>			
St. Augustine, Spurr	4	3	

Hawaii will be used as a testing area for two additional event counters and one tiltmeter (without Data Collection Platforms) because Kilauea volcano is the best instrumented volcano in the world, and it is by far the best place to compare these compressed observations with standard observations. Because of the extensive USGS facilities at Kilauea, these tests can be carried out at very little cost. The purpose of the studies in Hawaii is not to examine another volcano but to prove that the data compression techniques are accurate and the results are interpretable.

Familiarization trips to most of these volcanoes have been made by project personnel and local contacts are being actively developed (Figure 5).

POST ERTS

Volcanoes pose a serious threat to life in many countries. Current interest in developing improved methods for monitoring volcanoes and forecasting eruptions is widespread. International cooperation in this area is growing. In recent years a team of volcano geophysicists has worked in the USA (at Kilauea, in cooperation with HVO), in Costa Rica, in the Philippines, and in Indonesia. At the IUGG meetings in Moscow last August, an international Working Group for the Mitigation of Volcanic Disasters was established within IAVCEI. This group will advise UNESCO on the mission and composition of an international team of experts to be dispatched by UNESCO to volcanoes that threaten disaster to the populace around them.

If the Volcano Surveillance System to be tested with ERTS-A is successful, it should be possible to establish a worldwide system operated cooperatively by volcano scientists from many countries. In such a network, it would be desirable to employ a satellite-to-ground communications system with relatively inexpensive ground-based data receiving stations so that the maximum geographical coverage could be attained at minimum cost.

Automatic processing of microearthquake network data.- A large dense microearthquake network is an indispensable requirement of an earthquake prediction system. With present instrumentation, 8 seismic stations can be multiplexed on a single voice-grade communication circuit; so about 12 such channels are required for a 100 station network. We estimate that an earthquake prediction system for California and western Nevada may contain up to 600 seismometers that would require up to 75 voice-grade communication channels, all in continuous use.

Most of the transmitted record is of little or no interest; but with conventional data reduction and analysis techniques employing human "readers" it must all be recorded. A computer-based automatic system for analyzing seismic network data has been under development at NCER for several years. Very promising versions of both on-line and off-line systems have been tested, but both still need some coaching from their human trainers.

A small process-control computer can monitor records from at least 30 stations, detecting and timing earthquake P-wave onsets and measuring their amplitudes. Reduction of one day's record to such data for 10 earthquakes would constitute a 10^5 reduction in the data to be transmitted. Twenty 30-station clusters, each with its own processor, could replace a 600-station network and reduce its data flow to a level that could be accommodated by intermittent service from a synchronous satellite or by a tape-equipped polar satellite.

The central California microearthquake network consists of about 80 stations (Figure 6) with their signals transmitted to Menlo Park for recording. The field stations are those shown in Figure 1. Signals from

8 stations are multiplexed over a single phone line to Menlo Park (Figure 7). Undiscriminated "phone line" signals are recorded on analog magnetic tape for optional subsequent playback, and discriminated signals are displayed, 16 stations at a time, on 16 mm film strip recorders (Develocorders). The recording system permits discriminated signals from 32 stations to be fed into the computer on a real time basis. Alternatively, the master tape can be played back, 2 "tracks" at a time, and 16 stations can be fed at one time into the computer for analysis.

Currently, earthquakes are timed from the Develocorder films and the foci are calculated by computer using a layered half-space velocity model. Microearthquakes outline currently active (sliding) sections of the major faults in the San Francisco Bay Area (Figure 8). Quiet zones along known active faults reveal regions of elastic strain accumulation. Projections of foci onto vertical planes perpendicular and parallel the Sargent Fault (Figure 9), which runs diagonally between the San Andreas and Calaveras faults northwest of Hollister. These cross-sections show how earthquakes are distributed at depth. The fault is nearly vertical, and no earthquakes occur deeper than 15 km.

The automatic processor has been designed to consider the same parameters that a human does in analyzing a seismogram (Figure 10). Sharp onsets of signal level changes are noted and timed. If the signal persists for a sufficient length of time, it is considered to be a "probable earthquake." Such onsets at several neighboring stations are required before an event is labeled "Earthquake" and its hypocenter is computed.

SUMMARY

There is an ongoing program at the Geological Survey's National Center for Earthquake Research aimed at utilizing satellites to collect seismic data efficiently for the purpose of earthquake prediction and volcano surveillance. Satellites provide an unprecedented opportunity for collecting data from widespread areas particularly in regions without dense ground communication networks. Furthermore, satellite relays should not be interrupted by major earthquakes or volcanic eruptions. Our evaluation has shown that substantial compression of seismic data will be necessary unless many continuous voice-grade communication channels will be available. We have successfully developed a relatively simple data compressing instrument for use on volcanoes and look forward to deploying a number of these instruments on volcanoes this year as part of ERTS. Such relatively inexpensive earthquake counters may provide the most effective method yet available for identifying potentially active volcanoes throughout a large region. Far more sophisticated data compression techniques are required for prediction of eruptions and prediction of earthquakes. We have operated for several years large networks connected on-line and off-line to a small computer. Results to date demonstrate the feasibility and value of this approach. Such networks connected by satellite to a central data center could provide a bold new approach to forecasting volcanic eruptions and predicting destructive earthquakes.

REFERENCES CITED

- Eaton, J. P., W. H. K. Lee, and L. C. Pakiser, 1970, Use of microearthquakes in the study of the mechanics of earthquake generation along the San Andreas Fault in Central California: Tectonophysics, v. 9, p. 259-282.
- Lee, W. H. K., J. C. Roller, and J. P. Eaton, 1970, Microearthquake mapping of the San Andreas fault system in Central California [abs.]: Geol. Soc. America Abs. with Programs 1970, v. 2, no. 2, p. 111-112.
- Stewart, S. W., W. H. K. Lee, and J. P. Eaton, 1971, Location and real-time detection of microearthquakes along the San Andreas Fault System in Central California: Bull. Roy. Soc. New Zealand, v. 9, p. 205-209.

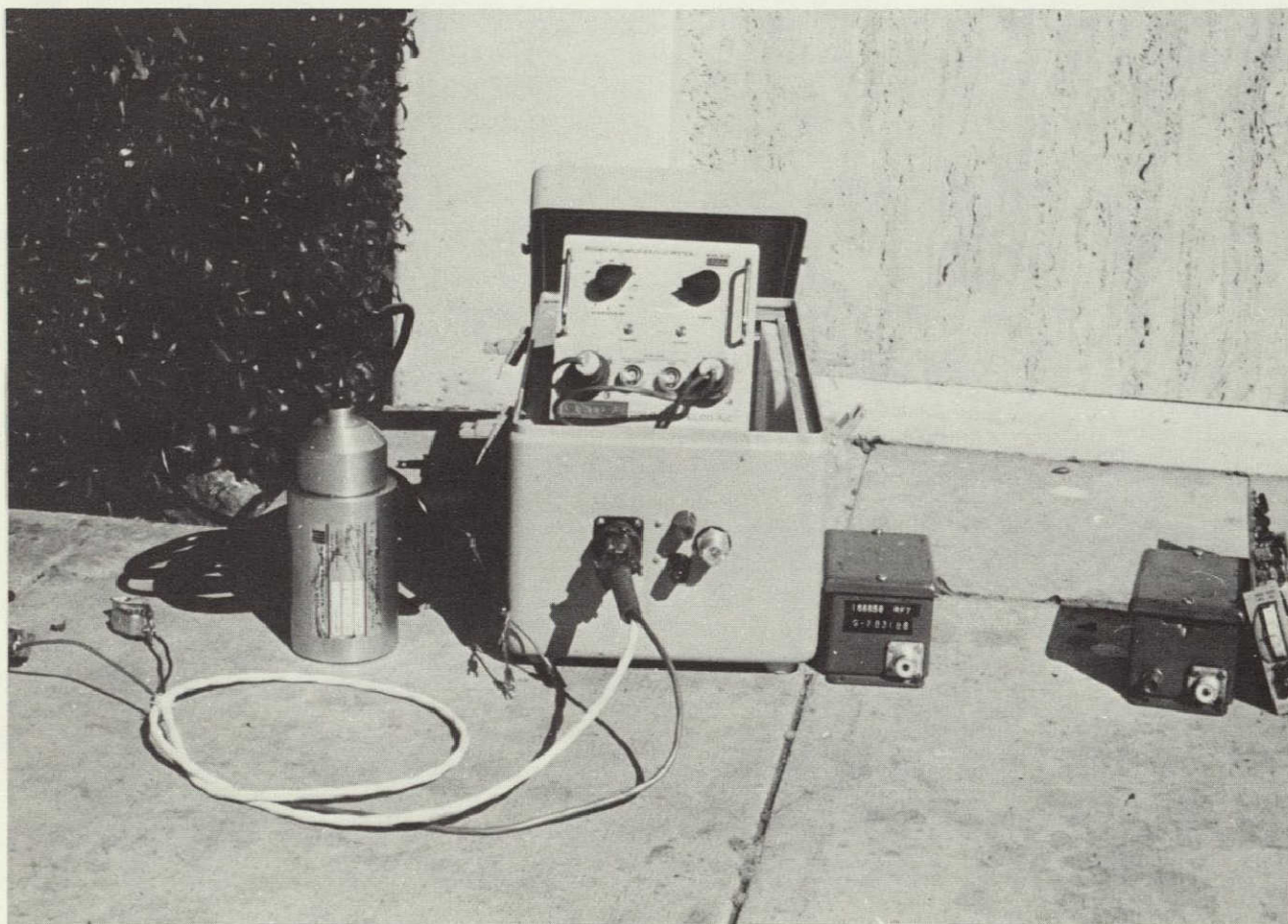


Figure 1.- Geophone, amplifier and FM modulator, transmitter, receiver, and discriminator used for recording and telemetering seismic data to a central location. The transmitter and receiver boxes are about 7 cm wide, 7 cm high and 10 cm long.

This page is reproduced again at the back of this report by a different reproduction method so as to furnish the best possible detail to the user.



Figure 2.- Prototype multilevel seismic event counter and sensor.
The counter is about 28 cm long and 18 cm wide.

This page is reproduced again at the back of this report by a different reproduction method so as to furnish the best possible detail to the user.

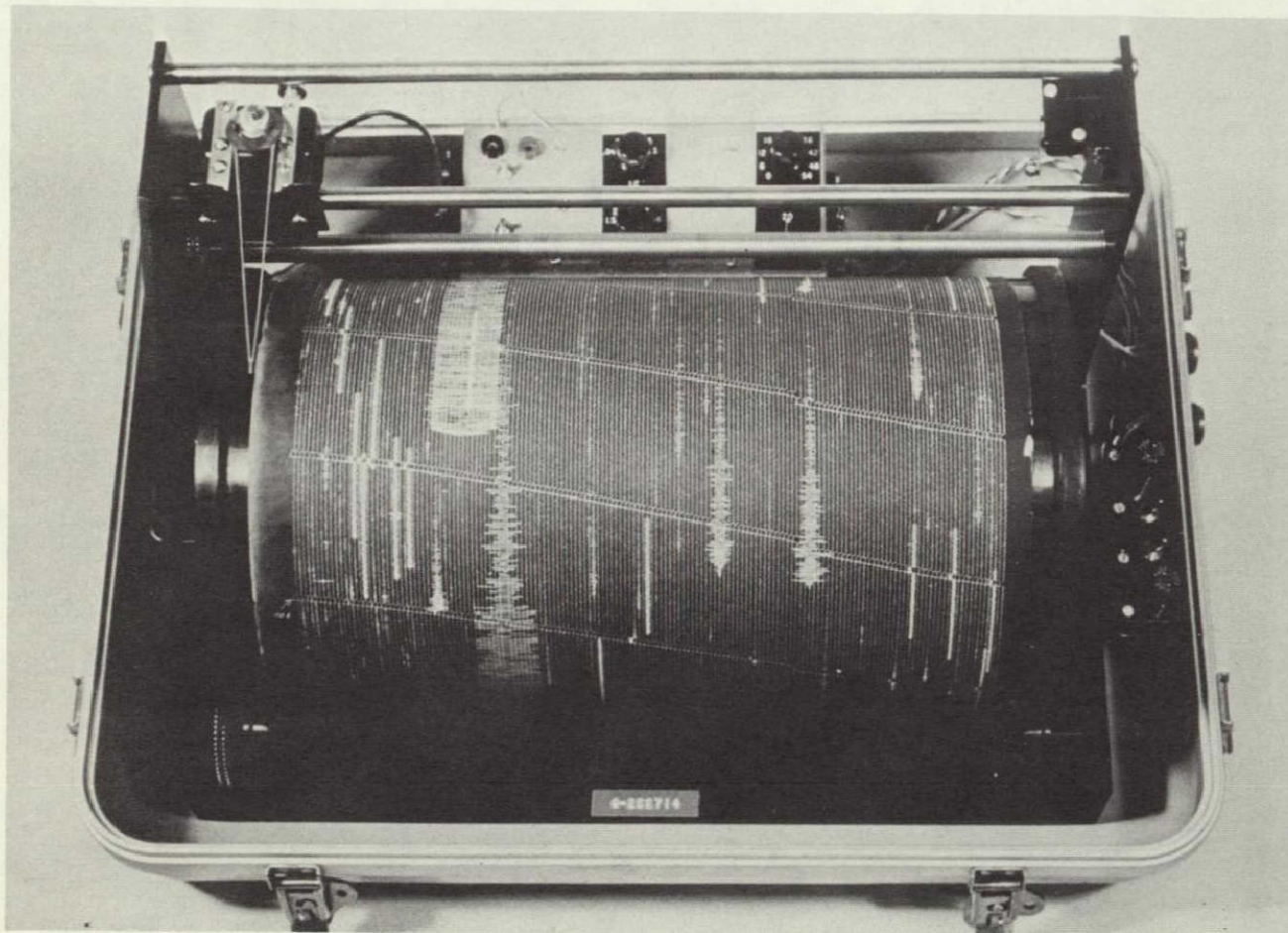


Figure 3.- Portable visible recording seismograph. The recording drum is about 19 cm in diameter and 35 cm wide.

This page is reproduced again at the back of this report by a different reproduction method so as to furnish the best possible detail to the user.

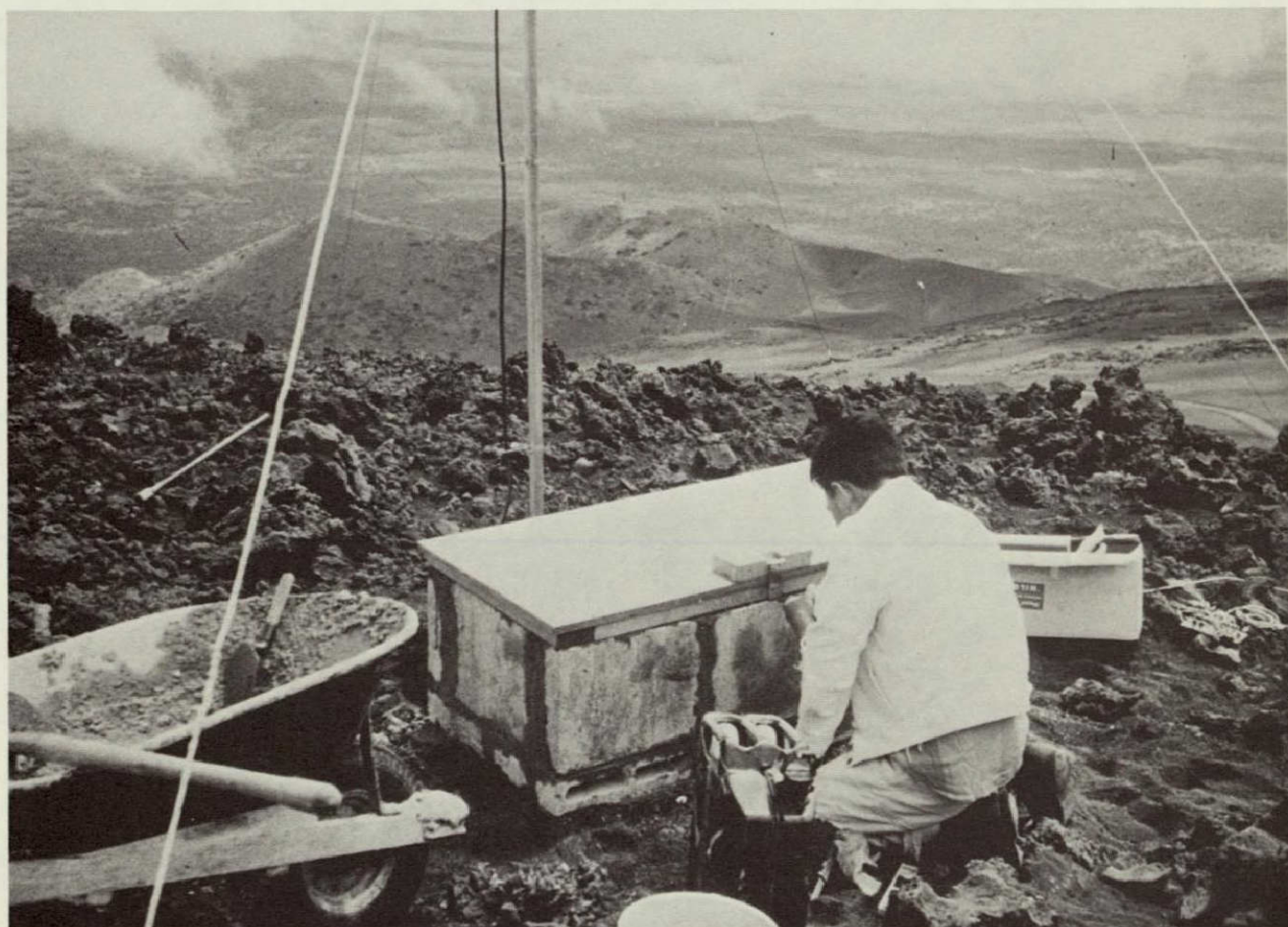


Figure 4.- Remote seismic station being completed on
Mauna Kea volcano, Hawaii.

This page is reproduced again at the back of
this report by a different reproduction method
so as to furnish the best possible detail to the
user.



Figure 5.- Summit of San Cristobal Volcano, near Leon, Nicaragua, Central America, on December 3, 1971. This volcano was dormant between 1685 and early May, 1971.

This page is reproduced again at the back of this report by a different reproduction method so as to furnish the best possible detail to the user.

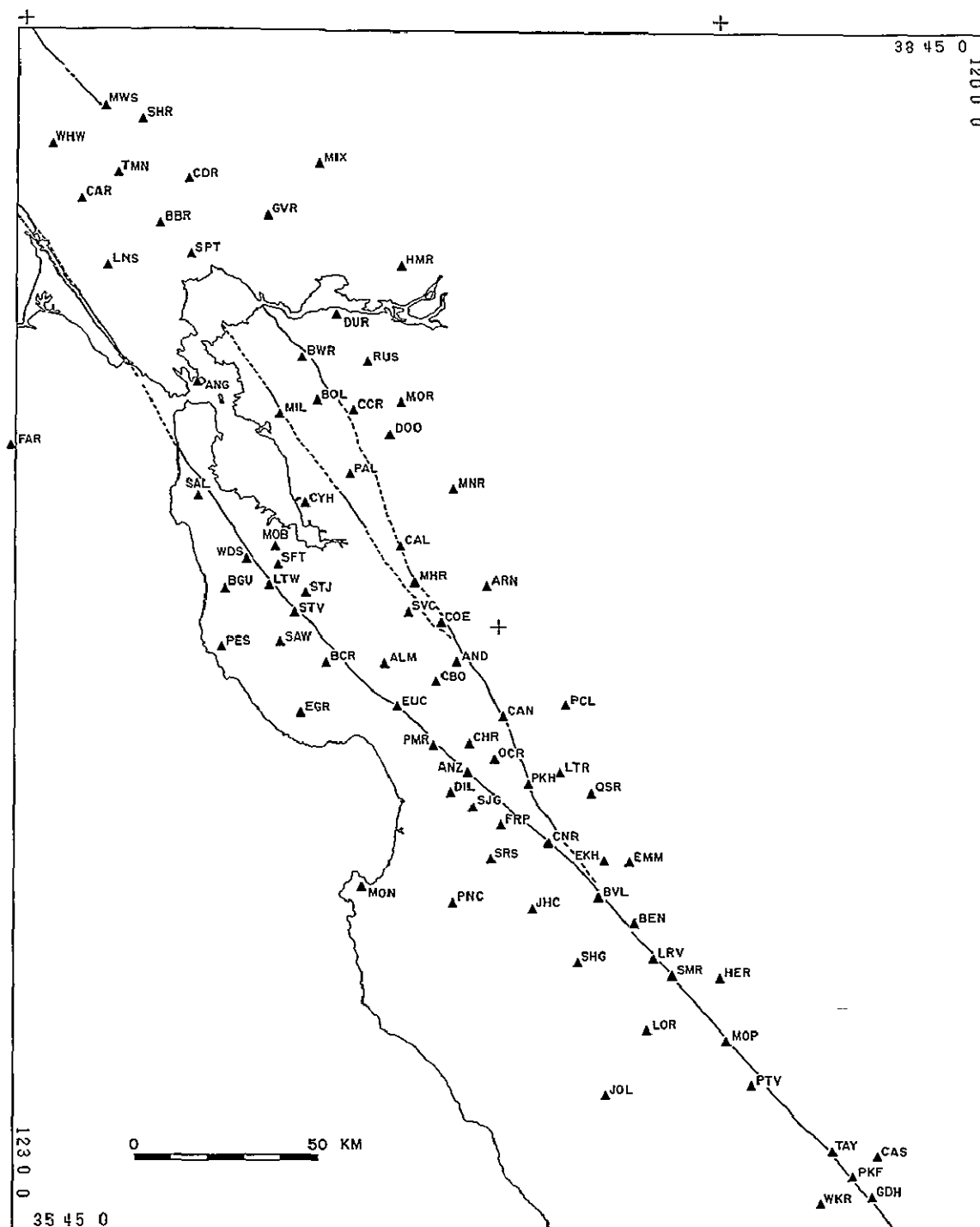


Figure 6.-- Locations of seismic stations operated by the National Center for Earthquake Research in the San Francisco area, California. Data for these stations are recorded in Menlo Park (near station MOB) (Lee et al., 1970).

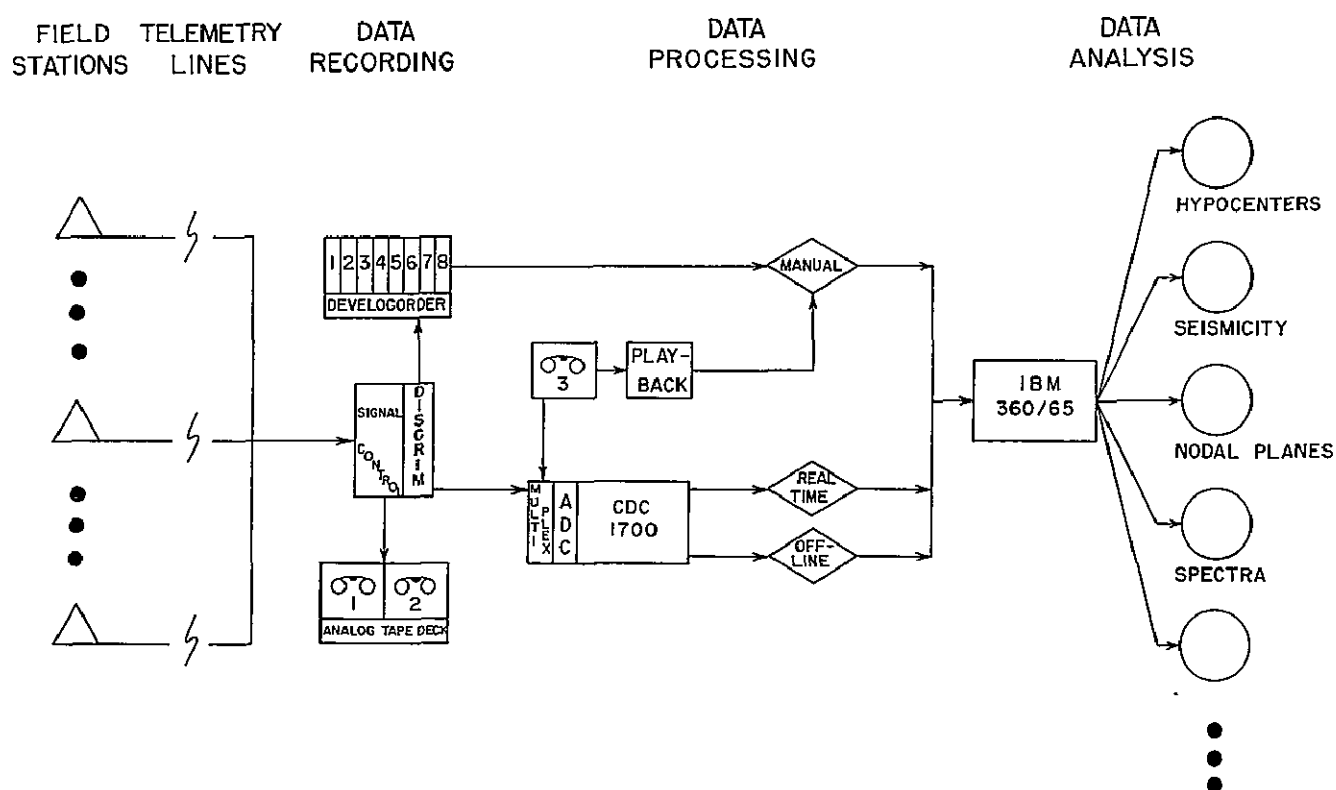


Figure 7.- Block diagram of the data recording, processing, and analysis system in Menlo Park, California.

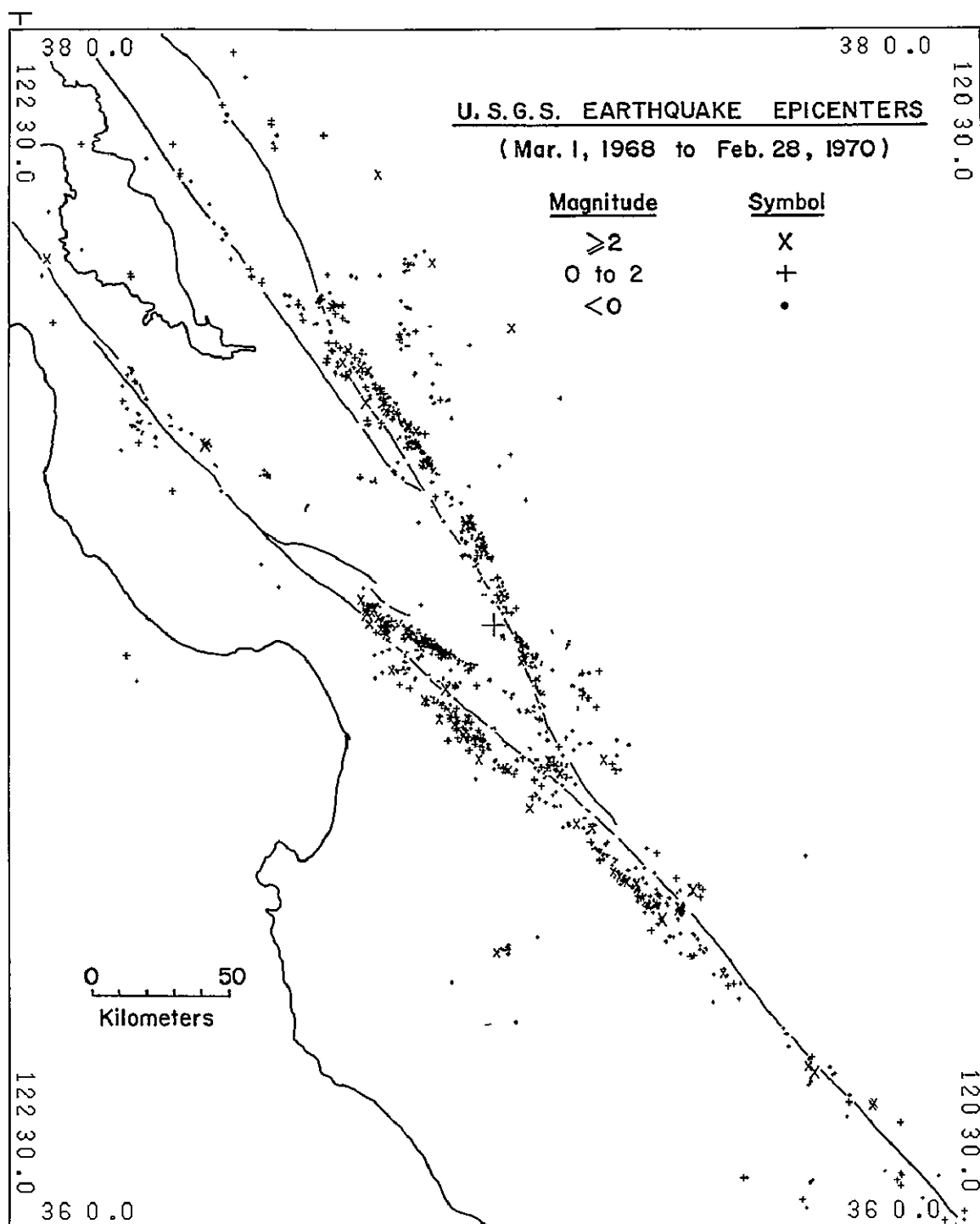


Figure 8.- Epicenters of earthquakes located with data from the USGS net (Figure 6) between March 1, 1968 and February 28, 1970 (Lee et al., 1970).

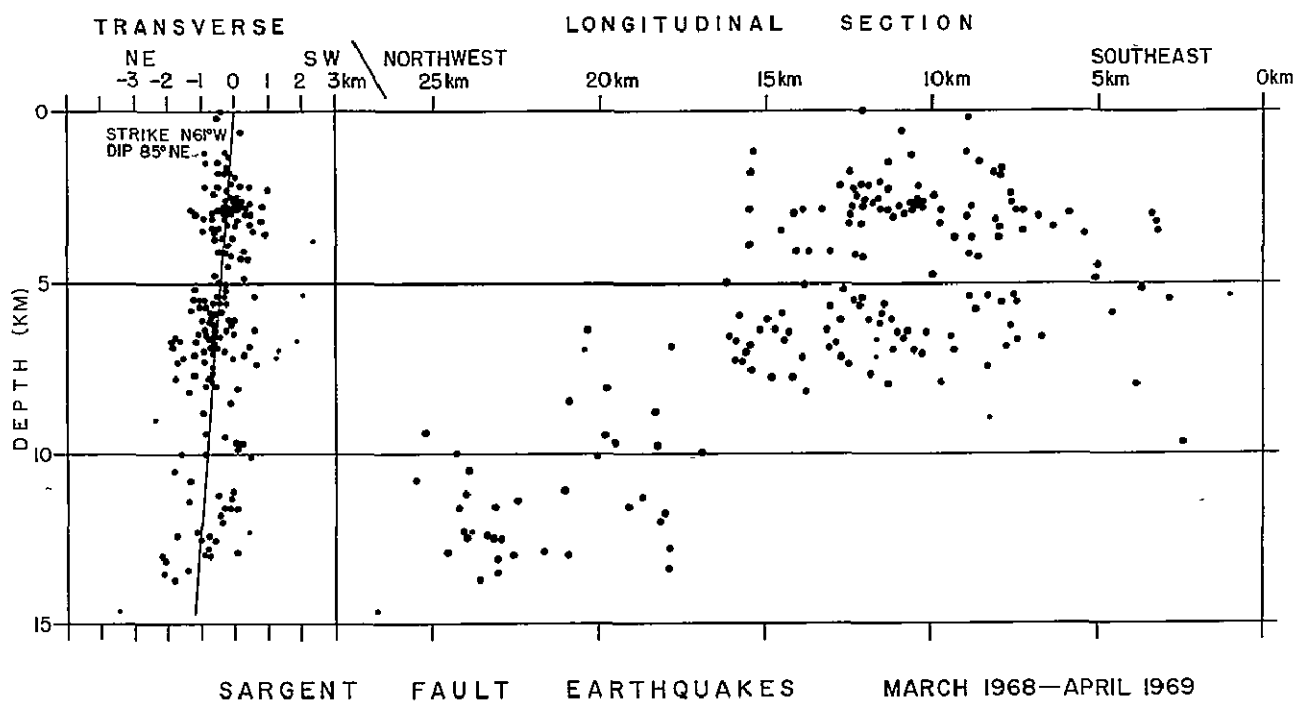


Figure 9.— Earthquakes in the Sargent fault hypocentral zone projected onto vertical planes perpendicular (left) and parallel (right) to the surface trace of the plane fitted by least squares to the hypocenter. (Eaton et al., 1970).

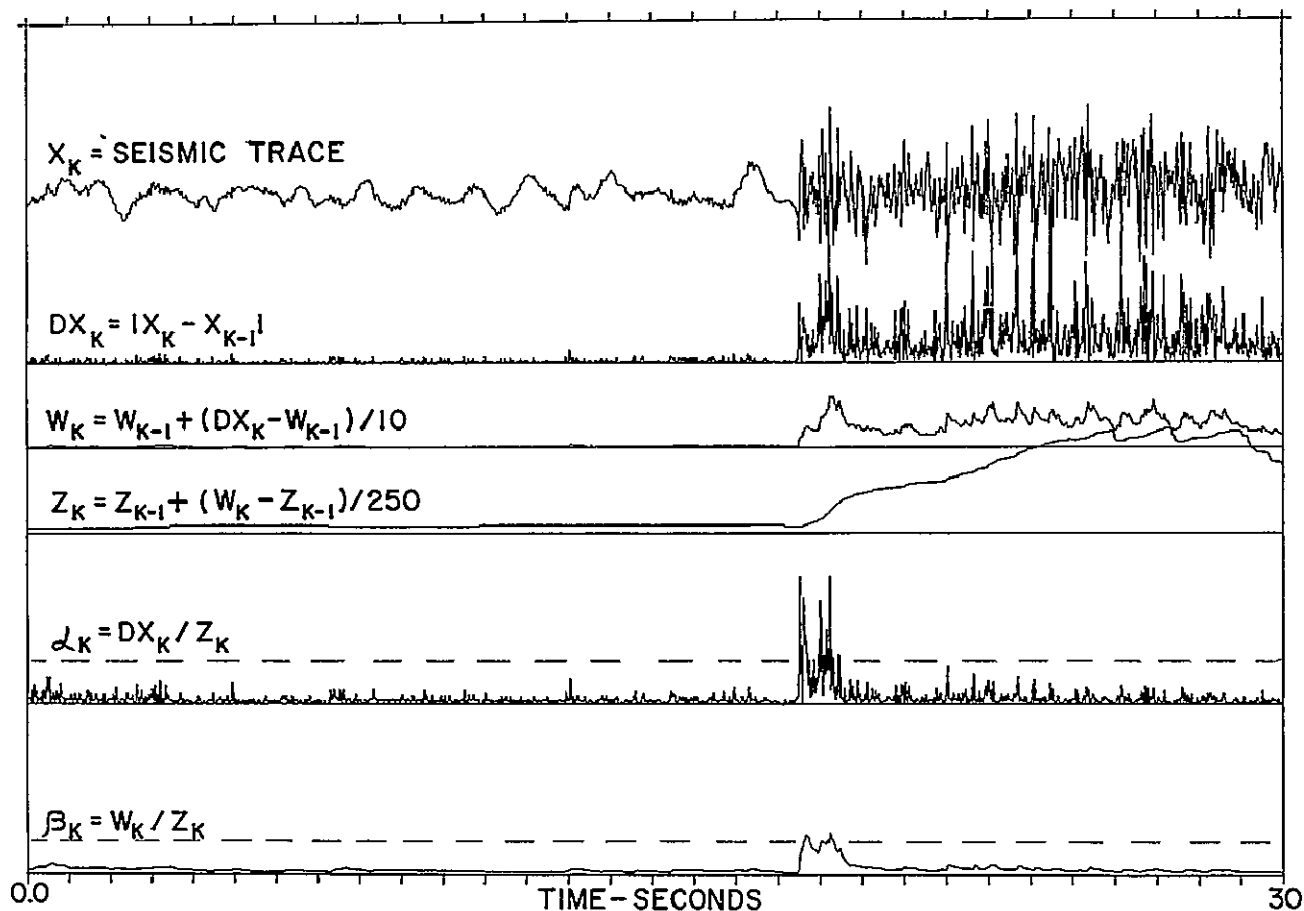


Figure 10.- An example of some of the functions applied to an earthquake signal by the automatic earthquake processor. (Stewart et al., 1971).

SECTION 57

ANALYSIS OF THERMAL PATTERNS OF GEOCHEMICALLY STRESSED

TREES AT CATHEART MOUNTAIN, MAINE

by

F. C. Canney and T. D. Hessin
U.S. Geological Survey
Denver, Colorado

and

W. G. Burge
Willow Run Laboratories
University of Michigan
Ann Arbor, Michigan

ABSTRACT

Thermal-emission data were collected on August 27, 1970, at Catheart Mountain, Maine (NASA Site 240), during mission 21M by the University of Michigan aircraft and support personnel. At this site large areas of soil contain anomalously high contents of copper and molybdenum genetically related to a copper-molybdenum mineral deposit concealed beneath the soil on the heavily forested mountainside. This site has been used since 1968 to study the feasibility of the remote detection of geochemical soil anomalies. Previous ground studies have shown that spruce and fir trees rooted in metal-rich soils differ significantly in their spectral signatures from normal trees, thus apparently indicating a geochemical stress.

Missions were flown under marginal weather conditions at midday and in the early evening over a 4-mile flight line that crossed the geochemical anomaly. The thermal imagery of the 8.2-13.5- μ m band was sliced into 10 density increments, and composite color-coded prints were prepared. The image of the noon flight at 2,000 feet above mean terrain showed nothing of interest. However, on both the postsunset runs (2,600 and 1,500 feet) pronounced and well-defined warmer areas were noted that correlated crudely with the areas of metal-rich soils. Analyses of the thermal patterns were also made in terms of differences in altitude, slope angle and exposure, and variation in tree species. These comparisons were made difficult by the distortion in the imagery caused by the large variation in topographic relief along the flight path (>1,000 feet) and other factors, but the best correlation, though imperfect, was with the geochemistry. Thus, measurable differences may exist in thermal infrared emission between geochemically stressed trees and normal trees; further study is clearly justified.

SECTION 58

APPLICATIONS OF INFRARED REMOTE SENSING METHODS TO
GEOLOGICAL AND ENGINEERING PROBLEMS OF THE ARCTIC

by

Gordon W. Greene
U S. Geological Survey
Menlo Park, California 94025

ABSTRACT

Thermal infrared imagery provides significant information concerning surface water drainage needed for site selection and trafficability studies in regions underlain by permafrost. Sources of sand and gravel for construction can be identified in well-drained areas. Deep lakes capable of providing fresh water throughout the winter can often be distinguished from shallow lakes by observing the rate of surface temperature changes during a diurnal cycle. Spring discharges likely to cause icings of the ground surface can be located, and where temperature contrasts exist, the discharge of ground water into streams can be detected. Modification of the surface thermal regime by man's activities can be monitored.

Reliable estimates of active layer thicknesses may be made from aerial photographs of tree cover. Color infrared film is especially useful in this application, because differences in tree species and relative vigor in a given species may be discerned.

Collection of infrared remote sensing data must be scheduled carefully with respect to season, time of day, and weather conditions (both present and in the recent past) to ensure that desired thermal or vegetative anomalies are present.

N72-29357

59-1

SECTION 59

GEOLOGIC MATERIAL DISCRIMINATION FROM NIMBUS SATELLITE DATA*

by

H. A. Pohn, T. W. Offield, and Kenneth Watson
U.S. Geological Survey
Denver, Colorado 80225

ORIGINAL CONTAINS

COLOR ILLUSTRATIONS

INTRODUCTION

Digital data on day and night surface temperatures and daytime reflectance are available from Nimbus satellites which cover the globe daily. Nominal resolution of the Nimbus radiometers is about 8 km. Quantitative analysis of these data has been done for a test area in the Arabian Peninsula in order to assess the value of the information in determining physical properties of surface materials and to develop analytical techniques applicable to handling data of much better resolution from future earth resources or meteorological satellites.

Examination of film-strip photofacsimiles of Nimbus radiometer data generally has proved of little use in geologic studies. Computer-generated maps of reflectance and day or night temperatures have been used individually for study of very large features [1], but have not appeared to provide much information useful in geologic mapping, and this has generally been attributed to the coarse resolution. The different approach described here shows that resolution is not a serious limit on extracting useful information, but rather that different data treatment is required to make maximum use of Nimbus observations. This approach is based on a computer modeling technique developed by Watson [2], in which day-night temperature range and reflectance are used to calculate the thermal inertias of surface materials. The ground temperature is dependent not only on the thermal inertia and albedo of the ground (at a given latitude and sun's declination) but also on such factors as emissivity, sky radiation, elevation, and topographic slope. However by computing the day-night temperature difference we minimize these effects and maximize the effects of thermal inertia. Using results of the computer thermal model for a range of thermal inertias and albedos, an empirical relationship can be constructed of thermal inertia as a function of albedo and day-night temperature difference, and this relationship can be used to derive thermal inertias from the satellite observations. Figure 1 shows theoretically derived curves for diurnal temperature variations of materials having different thermal inertia. The determination of this physical property presents a means of discriminating some materials and

*Publication authorized by the Director, U.S. Geological Survey.

in some instances provides information by which remote identification may be achieved. Data from which thermal inertias can be calculated are provided at noon and midnight daily by Nimbus IV THIR (10.5-12.5 μ m) and at noon by Nimbus III HRIR (0.7-1.3 μ m). Noon and midnight observations do not define the maximum diurnal temperature range, as can be seen from figure 1, but are suitable for the present analysis.

DISCUSSION

An area in the Oman Mountains region of the Arabian Peninsula was selected for study because large geologic units spanning a wide range of thermal inertias occur with little or no vegetative cover. The available 1:2,000,000-scale reconnaissance geologic map (fig. 2) seemed adequate for comparison with data at 8-km resolution. Figure 3 is a Nimbus III HRIR photofacsimile of the Arabian Peninsula; the Oman Mountains range is a discrete dark area, but very little geologic detail is discernible. Figure 4 and 5 show this region in photofacsimiles of Nimbus IV THIR data taken at noon and midnight, respectively. No ground detail within the Oman Mountains region is apparent in the daytime data, and even the coastlines are indistinguishable in the nighttime data.

The specific test area, around Jebel Akhdar in the Oman Mountains range, is shown in figure 6, an enlargement of the outlined area shown in the U.S. Geological Survey geologic map (fig. 2). This part of the map displays reconnaissance information compiled by the Arabian-American Oil Company. Figure 7 shows this map with superposed contours representing day-night temperature differences measured by Nimbus IV. Although a general correlation exists between the geologic map units and the thermal data, numerous well-defined temperature anomalies do not relate to the geology.

Some of these discrepancies relate to the fact that the satellite radiometer observed only the surface materials, whereas the geologic map is constructed to show bedrock configuration and omits the details of thin surficial cover. A better portrayal of the actual surface units is obtained from a map of the Oman desert sedimentary environments [3] (fig. 8), and from a Gemini IV photograph (fig. 9). This information was used to modify the geologic base map to show more accurately the distribution of surface units (fig. 10). Comparison of the new map with the day-night temperature-difference contours (fig. 11) shows most of the previously unexplained high-difference anomalies to correspond to wadi sediments overlying the bedrock units shown in the original geologic map (fig. 7).

The thermal data shown offer reasonable capability of discriminating different surface areas, even at 8-km resolution. By combining these data

with reflectance information, a step may be taken toward possible identification of the surface materials in the discriminated areas. Figure 12 is a plot of means of day-night temperature difference vs reflectivity for various geologic units shown in figure 10; four groupings of materials are distinctive: 1) units Pzu and Kse (Paleozoic limestone and dolomite, and an ophiolite suite); 2) units Kh (chert, limestone and shale) and Klm and Tml (marly limestone); 3) wadi deposits and unit Qtga (alluvium and gravels); 4) Qe (eolian sand located outside area shown in map figures). With data of better resolution, both the discrimination and identificational groupings may be improved. Where the groups contain diverse lithologies, addition of other types of information such as that obtained photogeologically might suffice to reduce the ambiguities and achieve truly remote identification of geologic units from satellite.

By using temperature-difference and reflectance data in the computer modeling technique, a thermal-inertia map was produced (fig. 13). This map showed better correlation with the geologic map in most areas, but also showed some important noncorrelated anomalies of markedly high thermal inertia in the area of the Jebel Akhdar massif (at the southern end of the Oman Mountains) and along the ophiolite belt. Because of the good general correlation of thermal inertia and mapped rock units, it was suspected that the anomalous areas were ones where the 8-km satellite data might be more correct than the broad reconnaissance mapping information. This prompted further search for maps of the Oman Mountains area, and a recent detailed map of the Jebel Akhdar Massif by H. H. Wilson [4, fig. 16, p. 650-651] was found. The new presentation of geology was significantly different, and showed a belt of dolomite and quartzite to match the zone of high thermal inertia across the massif (fig. 14). No new information is available northward along the ophiolite belt, but the sharply defined high thermal-inertia anomalies are believed to indicate huge unmapped blocks within the ultramafic mass. The thermal inertia values are so high that such blocks probably must be dolomite, quartzite, or unserpentinized dunite.

FUTURE APPLICATIONS

A significant advance can be achieved when Nimbus V data at 700-m resolution become available. This information should permit sufficient discrimination of surface materials to improve existing reconnaissance geologic maps for remote or poorly accessible parts of the world. The system should also be suitable for mapping near-surface moisture distribution in soils and along fracture zones because of the influence of water on the thermal inertias of soils. Although ERTS-B will provide thermal data at 300-m resolution, a midmorning orbit time will limit the extraction of thermal-inertia data and hence restrict the capability of

discriminating geologic units. It should be noted that the technique described here is immediately applicable to the geologic mapping of extraterrestrial bodies.

REFERENCES

- [1] Poquet, Jean, 1969; Geopedological features derived from satellite measurements in the 3.4-4.2 μ m and 0.7-1.3 μ m spectral regions: NASA-Goddard Spaceflight Center preprint X-622-69-437, 27 p.
- [2] Watson, Kenneth, 1970, A, Introduction and Summary, B, Data analysis techniques, in remote sensor application studies progress report July 1, 1968, to June 30, 1969: National Technical Information Service, PB-197-098; Watson, Kenneth, 1971, A thermal model for analysis of infrared images: NASA 3rd Ann. Earth Resources Aircraft Status Review, Houston, Texas, v. 1, sec: 13, p. 1-16; Watson, Kenneth, Rowan, L. C., and Offield, T. W., 1971; Application of thermal modeling in the geologic interpretation of IR images: in Proceedings of the 7th International Symposium on Remote Sensing of Environment, v. III, p. 2017-2041; Watson, Kenneth, 1971, A computer program of thermal modeling for interpretation of infrared images: National Technical Information Service, PB-203-578.
- [3] Glennie, K. W., 1970, Desert sedimentary environments: Elsevier Publ. Co., 222 p.
- [4] Wilson, H. H., 1969, Late Cretaceous eugeosynclinal sedimentation, gravity tectonics, and ophiolite emplacement in Oman Mountains, southeast Arabia: Am. Assoc. Petroleum Geologists Bull., v. 53, no. 3; p. 626-671, 30 figs.

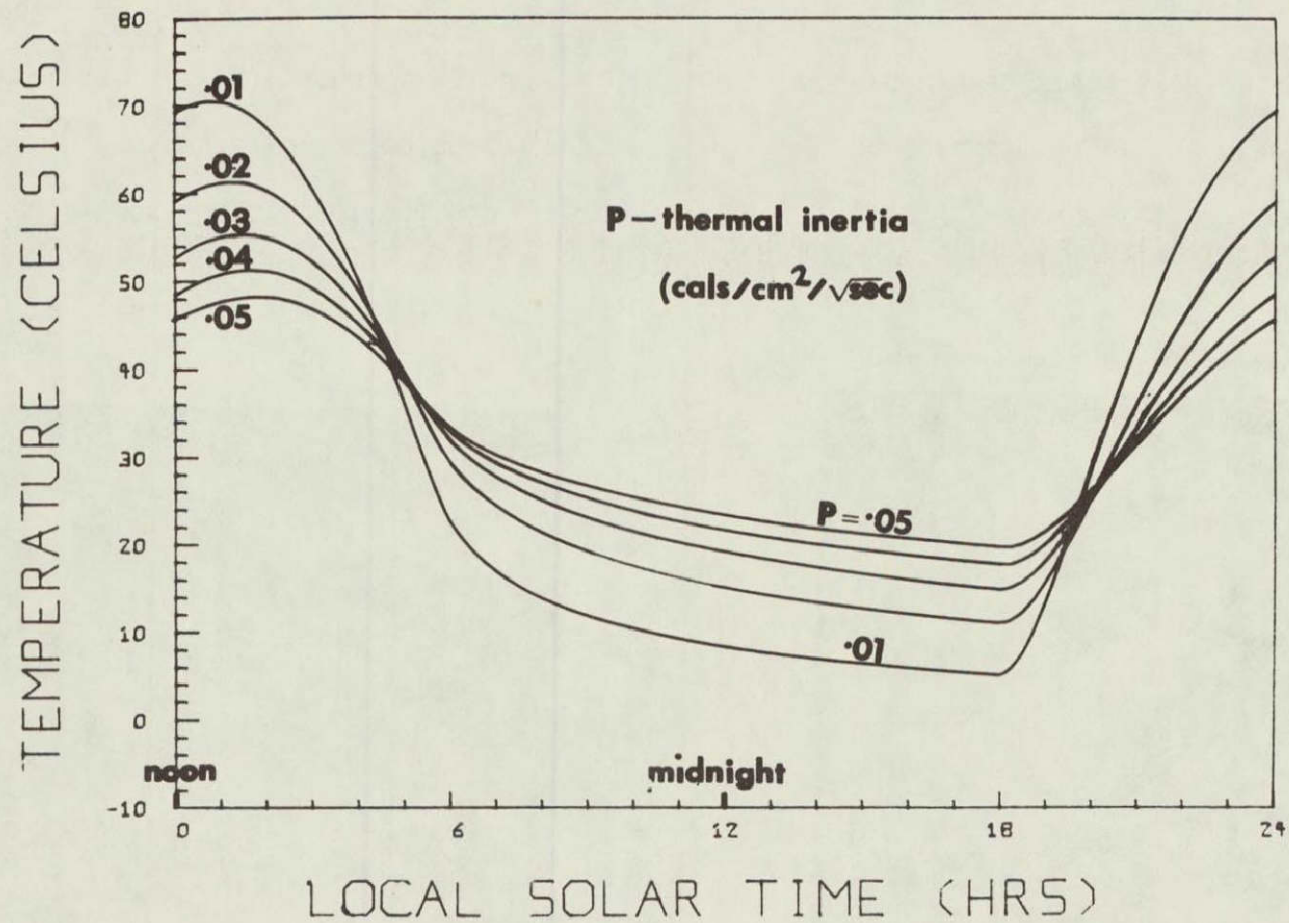


Figure 1 - Diurnal temperature variations of materials with different thermal inertias.

This page is reproduced again at the back of this report by a different reproduction method so as to furnish the best possible detail to the user.



Figure 2 - Portion of geologic map of Arabian Peninsula (U.S. Geological Survey map I-270a); study area outline.



NIMBUS III HRIR DAYTIME ORBIT 711 6 JUNE 1969

Figure 3 - Nimbus III daytime HRIR photofacsimile of the Arabian Peninsula (study area outlined).

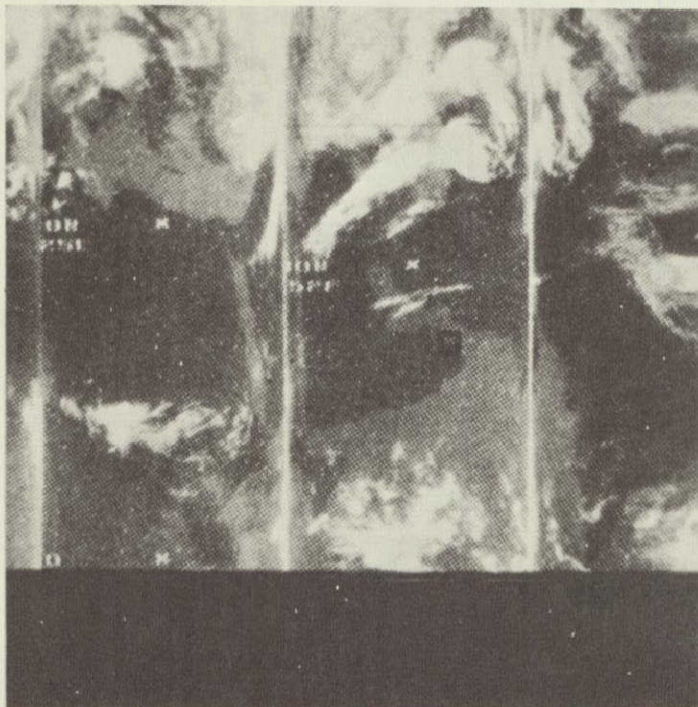


Figure 4 - Nimbus IV daytime THIR photo-facsimile of the Arabian Peninsula;
(study area outlined).

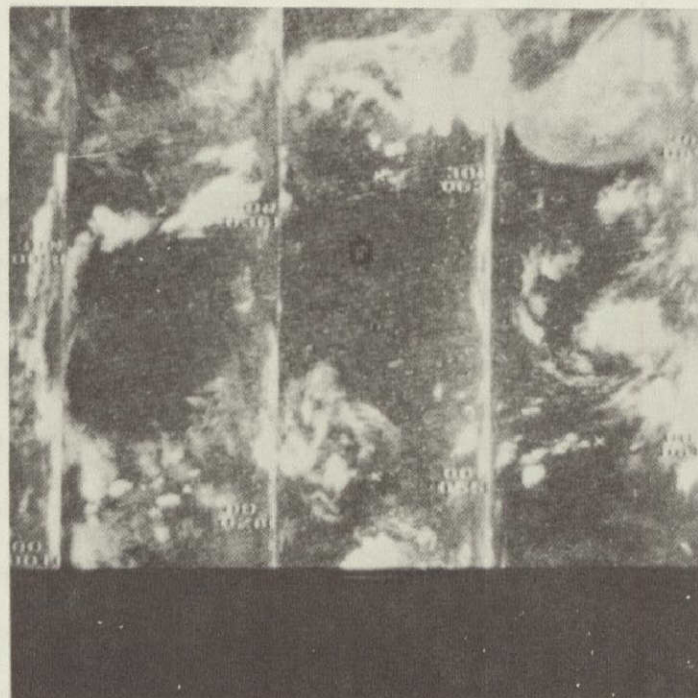


Figure 5 - Nimbus IV nighttime THIR photo-facsimile of the Arabian Peninsula;
(study area outlined).

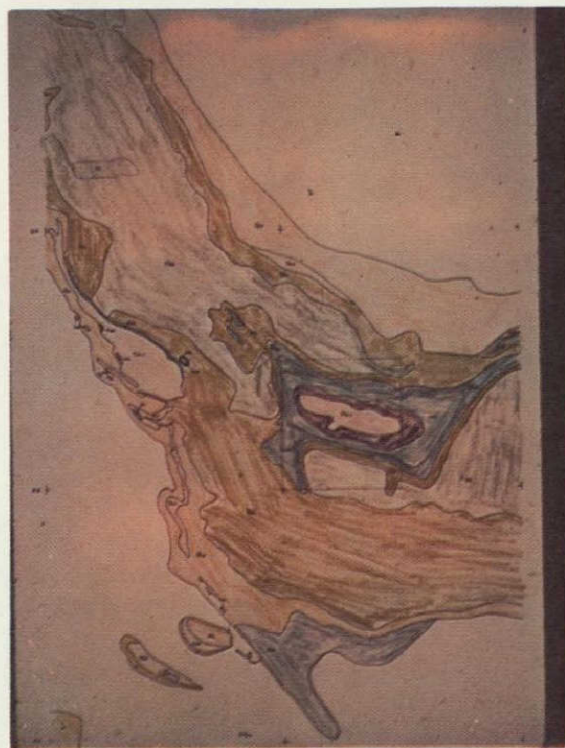


Figure 6 - Geologic map of Jebel Akhdar
area, Oman range; data from USGS map
I-270a.

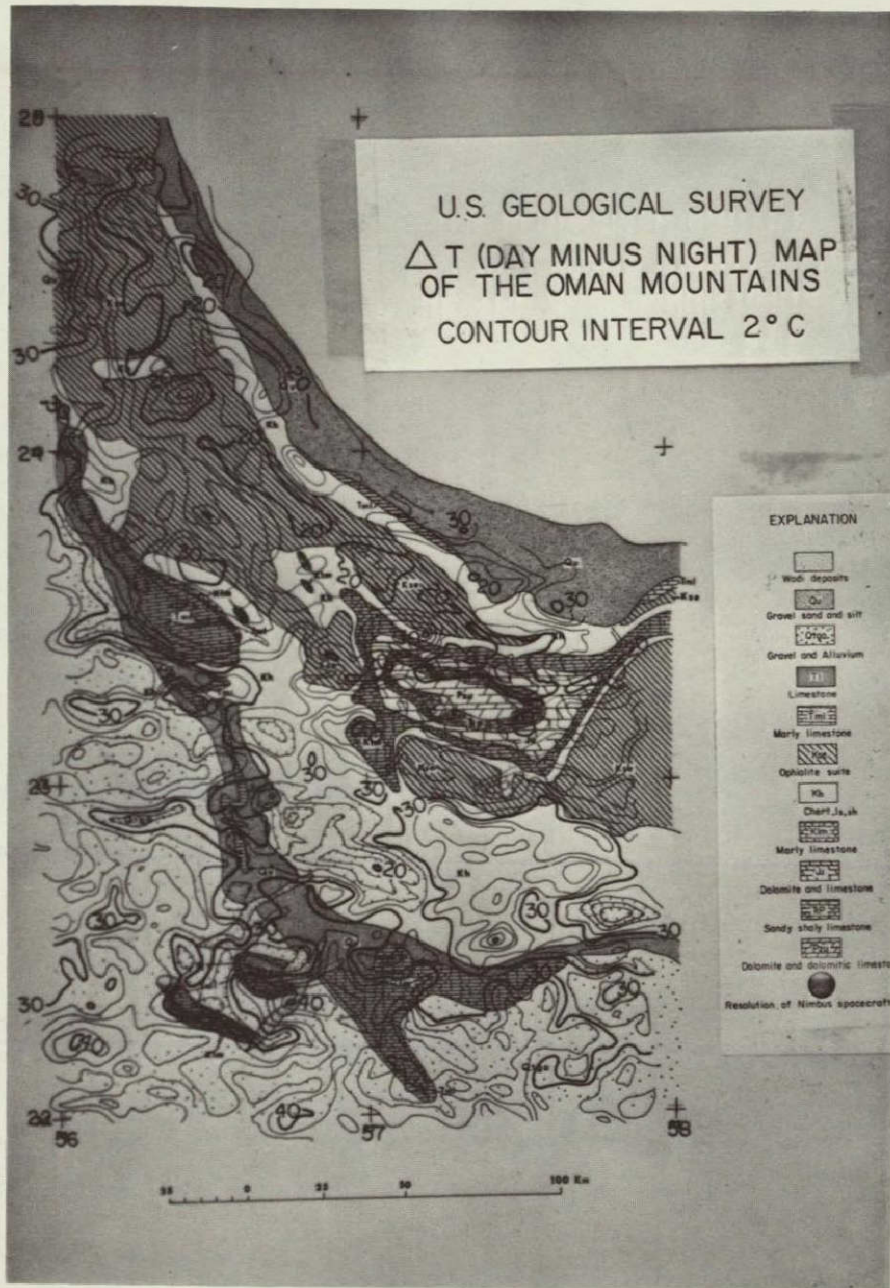


Figure 7 - Day-night temperature difference contoured on geologic map (fig. 6).



Figure 8 - Desert environment map of Glennie [3, enclosure 3] (western part of area in figs. 6 and 10).

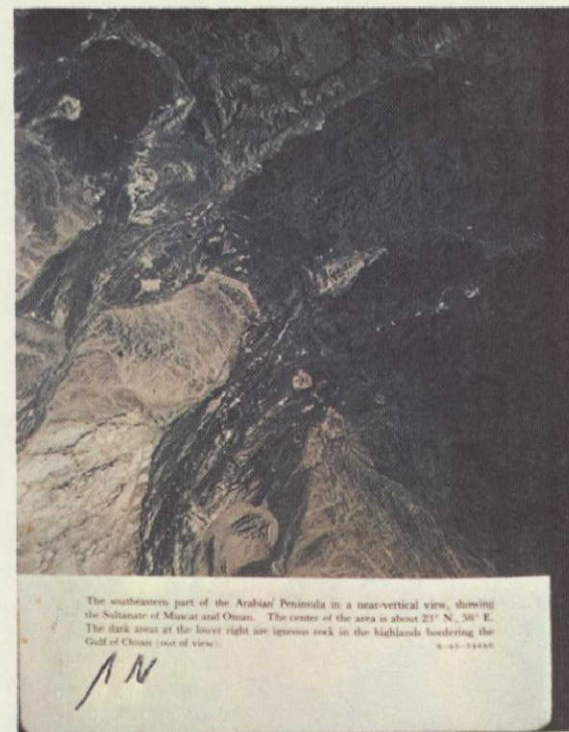


Figure 9 - Gemini IV photograph showing part of Jebel Akhdar area. See fig. 10 for location of photographic coverage.

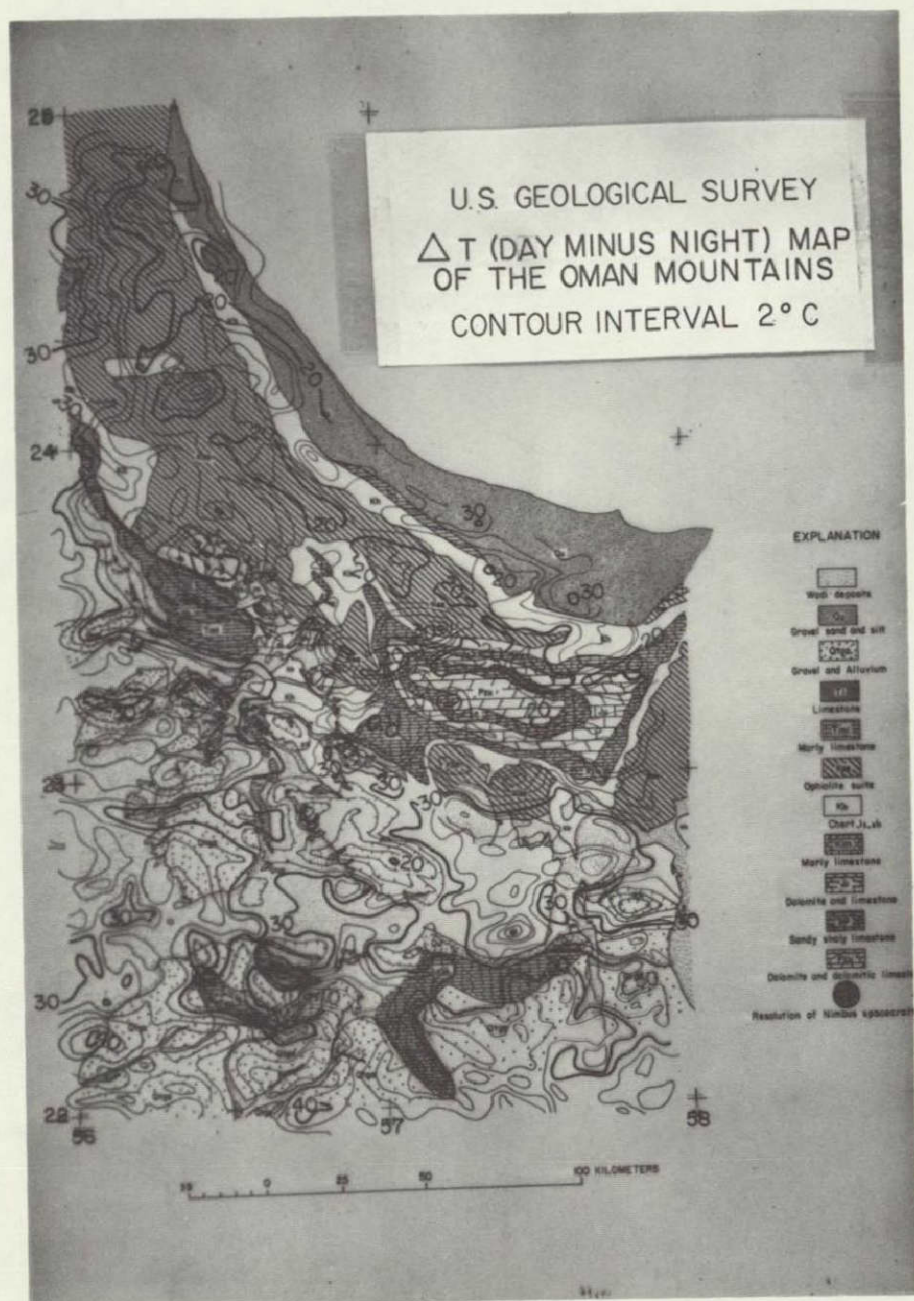


Figure 11 - Day-night temperature difference contoured
 on modified geologic map (fig. 10).

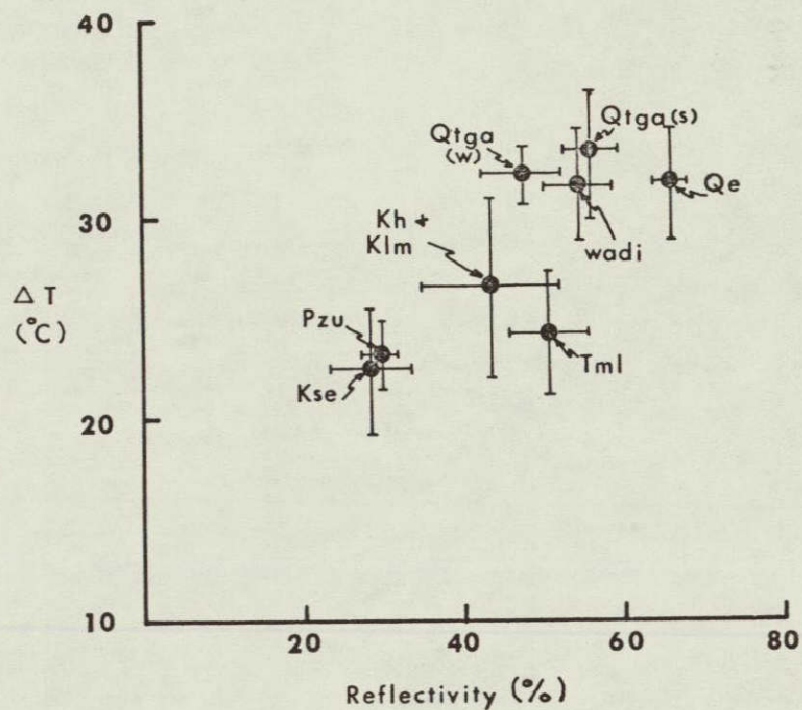


Figure 12 - Day-night temperature difference (ΔT) vs reflectivity for geologic units shown in fig. 10 (means and standard deviations shown by crosses). Unit Qtga discriminated as to west (w) and south (s) areas. Other units explained in text.

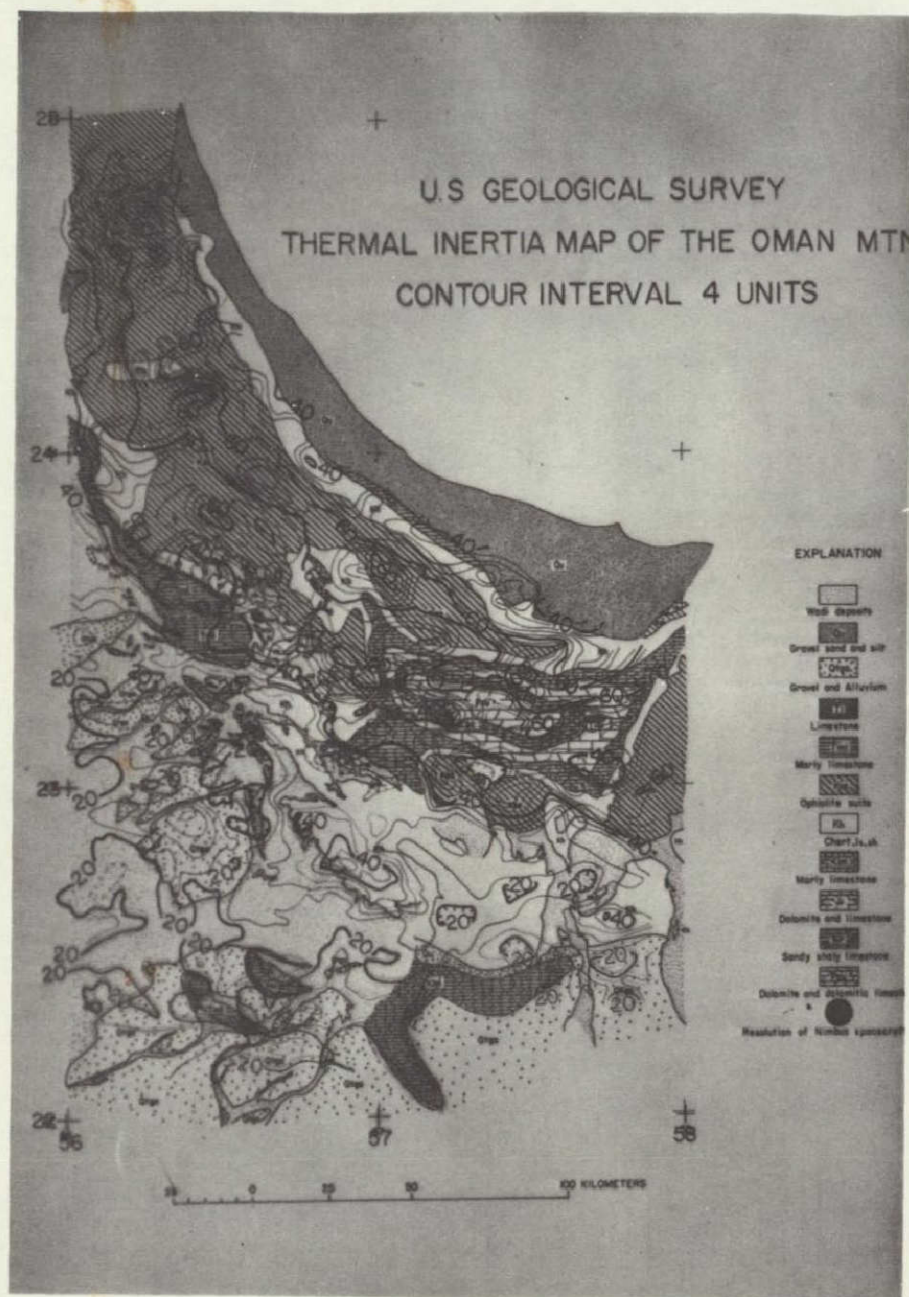


Figure 13 - Thermal inertia contours on modified geologic map (fig. 10).

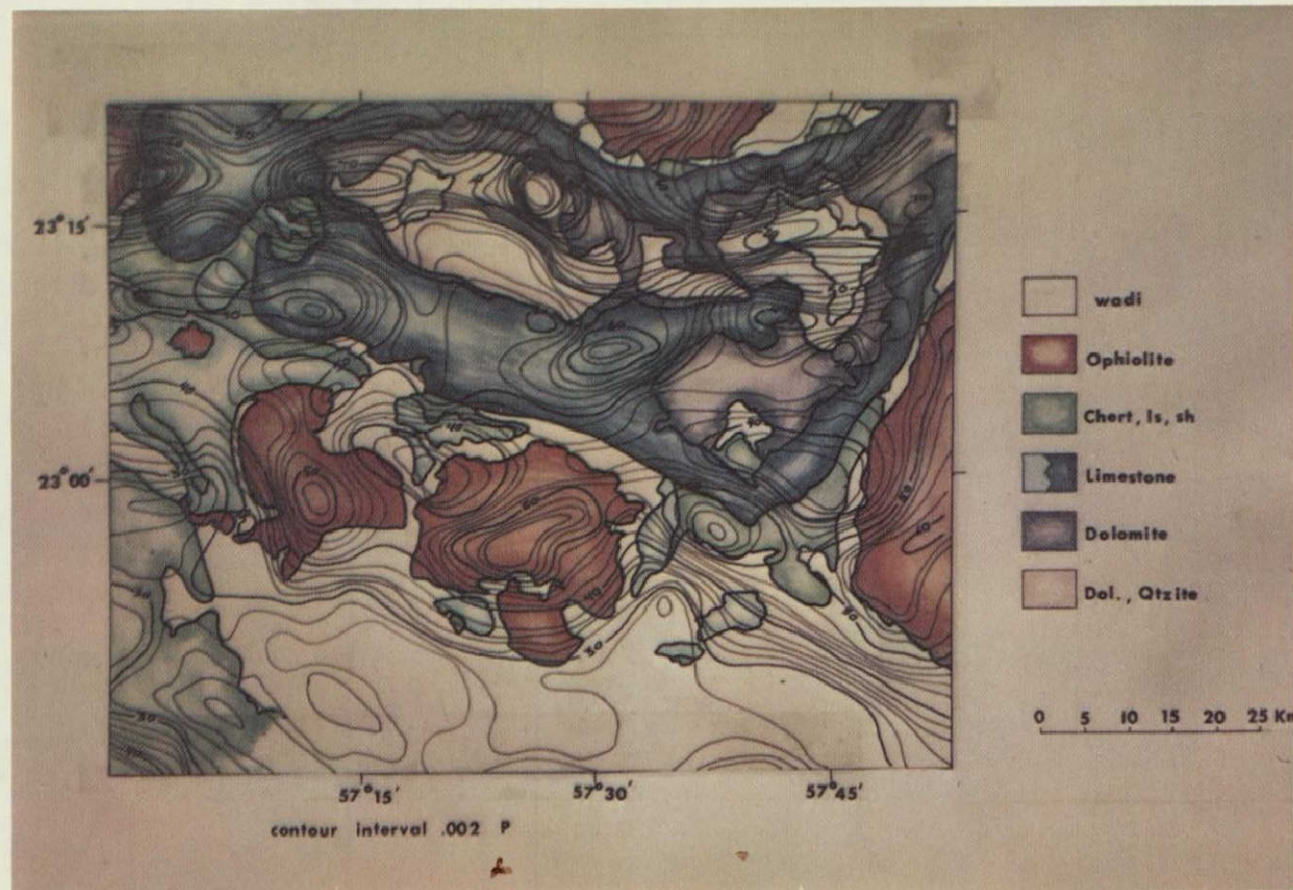


Figure 14 - Thermal inertia contours on geologic map of Jebel Akhdar by H. H. Wilson. [4] Red is ophiolite (Kse), green is chert (Kh), blue is limestone, lavender is dolomite-limestone-quartzite mixed unit, clear is wadi deposits.

NEAR-INFRARED IRON ABSORPTION BANDS: APPLICATIONS
TO GEOLOGIC MAPPING AND MINERAL EXPLORATION*

by

Lawrence C. Rowan
U.S. Geological Survey
Denver, Colorado 80225

ORIGINAL CONTAINS
COLOR ILLUSTRATIONS

INTRODUCTION

During the last 5-6 years, laboratory studies [1, 2, 3, 4] have shown that broad reflectance minima occur in the near-infrared spectra as well as in the visible spectra of iron-bearing minerals. These minima are due to optical absorption caused by electronic transitions in the ferric and ferrous ions. Minor amounts of iron sometimes cause decreased reflectance in the near-infrared, but, as the data presented here show, these minima are generally less intense than those measured in "iron-rich" minerals. Thus, spectral differences between "iron-rich" and "iron-poor" minerals, rocks, and soils are significant. These differences in spectral radiance commonly are 20-30 percent and constitute much greater image contrast between important rock and soil types than do those of normal photographs and afford application of band-ratioing techniques to provide information on the relative proportions of total iron and perhaps on the oxidation state of the iron. Data of this type are directly applicable to metallic-mineral exploration and geologic mapping of large areas from near-infrared and visible satellite images. In this preliminary report, I present briefly the pertinent laboratory spectroscopic data, the application of these spectral differences to the discrimination of two important metamorphic rock types and to mineral exploration by aircraft in the Beartooth Mountains, Montana, and a consideration of the application of this technique from the ERTS and Skylab satellite systems.

SPECTROSCOPIC MEASUREMENTS

Although most of the dependable and pertinent spectroscopic data have been obtained from crushed samples in the laboratory, with planetary exploration problems in mind, these data are entirely adequate to demonstrate the relative intensity of the absorption bands in iron-rich and iron-poor minerals and rocks.

*Publication authorized by the Director, U.S. Geological Survey.

Mineral Spectra

The visible and near-infrared reflectance spectra for several important rock-forming minerals shown in figure 1 show marked contrast between iron-rich and iron-poor minerals. Iron-poor mineral spectra, such as those for quartz, orthoclase, and albite, simply increase in reflectance from short to long wavelengths; in contrast, iron-rich minerals, such as augite, fayalite, and hornblende, decrease markedly in reflectance between 0.60 and 1.20 μm owing to the presence of ferric and ferrous absorption bands. One of the most important iron-rich minerals in ore-deposit exploration is limonite; it is associated with many metallic ore deposits as a surficial secondary mineral. Limonite shows diagnostic absorption bands at about 0.92 μm and 0.65 μm and a reflectance maximum at about 0.80 μm (fig. 2). The positions of the iron-absorption bands depend on the oxidation state and coordination of the iron ions [4]; the most intense ferric bands are centered at about 0.70 and 0.87 μm , whereas the most intense ferrous band is at about 1.00 μm .

Rock Spectra

The most significant spectral differences between felsic and mafic rocks are due to optical absorption in the mafic minerals. The visible and near-infrared laboratory spectra for selected felsic and mafic rocks [5] are shown in figure 3. Visible and near-infrared albedo differences are obvious, and the general slopes of the two sets of curves are significantly different, particularly beyond about 0.60 μm , where the mafic rock reflectances either decrease or remain constant and the felsic rock reflectances increase. The largest reflectance contrast is in the near-infrared. The spectral differences can be exploited through several techniques, but the most economical and widely available means is multi-band photography.

MULTIBAND PHOTOGRAPHS

Multiband photographic techniques are particularly applicable to discrimination and identification of iron-rich mineral deposits, rocks, and soils, because the wavebands of interest are spectrally broad and the reflectance differences are of a magnitude sufficient to be recorded on film.

In August 1971, a mission was flown by the U.S. Geological Survey over the Beartooth Mountains of Montana; this mission made use of an International Imaging Systems (I²S) camera and Kodak 2424 infrared-sensitive film. This camera places four images on 9-in. film simultaneously at specific wavebands. The band passes for the four filters

used are shown in figure 4; band 4 actually is effective to about $0.92\mu\text{m}$ where the film response is about 5-10 percent. One of the main objectives of this mission was the determination of the effectiveness of the iron-absorption band technique for metallic-mineral exploration. Two geologically different mineralized zones were examined in this experiment: (a) chromite-bearing ultramafic rocks in the eastern Beartooth Mountains, and (b) a zoned breccia pipe that contained disseminated gold and copper in the southern part of the Beartooth Mountains.

Chromite-bearing ultramafic rocks occur in the eastern Beartooth Mountains as pod-shaped bodies [6]. During World War II, many of these bodies were mined for chromite; they are now inactive, but the Stillwater ultramafic complex in the northwestern part of the range is being explored actively. I²S multiband photographs of one of the bodies in the eastern Beartooth Mountains are shown in figure 5. The ultramafic rocks, consisting of serpentinite with minor hornblende and pyroxene layers as well as magnetite [6], are dark in all four bands, but the contrast between these rocks and the host rocks, mainly granitic gneiss, on the south side of the mine (fig. 5) is significantly higher in band 4. The general scene contrast in this band is due somewhat to the high spectral contrast between outcrop and vegetation in this part of the spectrum; but within the vegetation-free mine area, the high contrast between the chromitic ultramafic rocks and the gneiss is enough to permit mapping the dark body with this remote-sensing technique and to identify it as a target of prospecting interest.

Visible and near-infrared spectra for the ultramafic rocks (fig. 6) and the gneisses (fig. 8) show that the contrast between these rocks seen in band 4 is due to near-infrared reflectance differences. The gneiss spectra have minor absorption bands, due mainly to biotite, and generally increasing reflectances in the near-infrared band, whereas the ultramafic rock spectra have generally decreasing reflectance. It is noteworthy that although the gneisses have about 1 percent iron, the effect of absorption is much greater in the ultramafic spectrum. Thus, in mapping and prospecting for ultramafic rocks of this type, infrared photographs may be much more useful than visible-wavelength photographs, because the scene contrast is enhanced when the host rocks are iron-poor. Ektachrome-infrared photographs, though broad-band, are particularly useful also for iron-poor rocks because the distribution of verdent vegetation can be determined and distinguished from rock outcrops.

Perhaps the most interesting results of this photographic experiment thus far deals with preliminary-stage mapping in the Homestake Mine area located in the New World mining district, Montana, just north of Yellowstone National Park. The general structure is a zoned Tertiary breccia pipe which has copper and gold mineralization (James Elliott, USGS, unpub. data). The central zone of the pipe, where the mine is located, is dacite breccia which has about 25 percent biotite and hornblende

phenocrysts and a minable percentage of disseminated copper and gold. The peripheral zone consists of approximately 70 percent Paleozoic limestone including some shale and 30 percent dacite breccia; mineralization is pyrite and hematite with limonite alteration and some disseminated copper and gold. The host rocks beyond the peripheral zone are limestone and minor amounts of shale.

In the visible-wavelength I²S bands [1, 2, and 3] little contrast is shown between the central and peripheral zones (fig. 7). The infrared band (No. 4), however, shows very high contrast between the two zones; density tracings across the two zones as they are exposed in the cliff show that the contrast between these zones is 35-40 percent greater in band 4 than in the visible bands. No significant density contrast was found among the visible bands. Because the contrast exists in the vegetation-free cliff as well as on the sparsely but uniformly vegetated plateau, reflectance contrast clearly is not due to differences in vegetation distribution.

The most adequate explanation for the spectral contrast between the two breccia-pipe zones is the distribution of the ferrous and perhaps the ferric iron: the central zone is rich in ferrous iron relative to the peripheral zone, because biotite and hornblende phenocrysts are about three times more abundant in the central zone. As previously mentioned, electronic transitions in the ferrous ion cause broad absorption bands centered at about 1.0 μ m. Hornblende and biotite contain ferric iron also, which, in some photographs, result in an absorption band at 0.87 μ m. These absorption bands decrease the reflectance in band 4 and would account for the high film density of the central zone. An additional factor may be the presence of limonite on the surface of the peripheral zone. Limonite has, as shown in figure 2, a broad reflectance maximum centered at about 0.80 μ m which would result in relatively high reflectance in band 4 in the peripheral zone. Thus, the enhancement in band 4 may be a twofold effect related to the distribution of ferric and ferrous iron.

Although data concerning the detailed distribution of copper and gold are not available at present, field observations and the location of the mine adit in the central zone suggest that the mineralization is directly associated with the dacite breccia intrusion. Definition of this zone in the breccia pipe is achieved best on the near-infrared photograph, apparently because of the distribution of ferric and ferrous iron.

EKTACHROME-INFRARED PHOTOGRAPHS

Ektachrome-infrared photographs have been used in the Beartooth Mountains, Montana, since 1969, to facilitate discrimination of

amphibolite, basaltic dikes, and chromite-bearing ultramafic rocks from granitic rocks [7, 8]. In the southeastern part of the range, thick amphibolite bands are interlayered with granitic gneiss; their distributions define the trend of the major regional folds and are therefore of regional structural significance. Comparison among conventional black-and-white photographs and Ektachrome and Ektachrome-infrared photographs obtained for this area from 52,000 feet shows significantly higher contrast between the amphibolite and gneiss in the Ektachrome-infrared photographs. Part of the study area is shown in a conventional black-and-white-photographic mosaic in figure 8. West of Becker Lake, a band of amphibolite contrasts poorly with the gneiss and blends in tone with the alpine vegetation in this photograph. In an Ektachrome photograph (fig. 9a) taken with a 6-in. lens from 52,000 feet above terrain during NASA/ERS mission 102, this amphibolite band is seen to contrast somewhat with the gneiss but to blend with the vegetation. An Ektachrome-infrared photograph (fig. 9b) taken simultaneously with the Ektachrome photograph, but with a 12-in. lens, shows significantly improved contrast between these two rock types; the amphibolite, in fact, can be mapped with reasonable accuracy on this photograph.

To evaluate the contrast differences seen in these photographs visible and near-infrared spectra were obtained for the gneiss and amphibolite in the field in August 1970 with an ISCO model SR spectroradiometer. The gneiss reflectance increases almost linearly with increasing wavelength (fig. 10), whereas the amphibolite, which contains 10-12 percent iron, has markedly decreased reflectance in the near-infrared owing to intense absorption bands at about 0.7 and 1.0 μ m. The spectra for the two gneiss samples, which contain 1-2 percent iron, also show the effects of optical absorption, but the absorption bands are relatively weak. The difference in reflectance for these rocks is 25-40 percent higher between about 0.65 and 0.80 μ m than in the visible. The Ektachrome-IR film is far more responsive in this spectral region than are Ektachrome and conventional black-and-white films and shows improved contrast.

CONCLUSIONS

The results of these studies show that the image contrast between iron-rich and iron-poor rocks can be significantly enhanced by recording energy reflected in specific visible and near-infrared wave-length bands. In addition, multiband images and photographs can provide information concerning the relative proportions of total iron and the state of the iron. In the Homestake Mine area, for example, similar film-density levels for the central and peripheral zones in the visible bands but high contrast between them in the near-infrared indicate a high ferrous-ferric iron ratio in the central zone and a low ratio in the peripheral zone. Data of this type should be especially useful in mineralized areas

where the ore distribution is either indirectly or directly related to the distribution of iron. Ektachrome-infrared photographs are useful also for discriminating iron-rich and iron-poor rocks and soils.

The experiments described here were conducted from aircraft at both low and high altitudes. This technique should be even more useful from the RBV (returned beam vidicon) and MSS (multispectral scanner) systems, because atmospheric transmission over the spectral region of prime interest is good ($0.4\text{--}1.2\mu\text{m}$), the iron absorption bands are spectrally broad, and especially because large mineralized areas can be explored efficiently and economically. Although the ERTS MSS and RBV bands are not optimum for this kind of study, they should prove to be adequate, as table 1 shows, especially when they are used in conjunction with the EREP S190 (photographic) and S192 (multispectral scanner) data. The most critical band, $0.90\text{--}1.10\mu\text{m}$, will be imaged by the MSS system, but the band is broader ($0.80\text{--}1.1\mu\text{m}$) than is desirable because it includes the $0.87\mu\text{m}$ ferric band. More desirable band passes would be $0.85\text{--}0.95$ and $0.95\text{--}1.10\mu\text{m}$; these would provide a possible means of distinguishing the main ferrous band and the ferric band which is common to limonite, hematite, and goethite. None of the four systems optimally covers the second most important absorption band, $0.70\mu\text{m}$, mainly because these band passes are centered at either about 0.65 or about $0.75\mu\text{m}$. The $0.58\text{--}0.68\mu\text{m}$ waveband is important, because limonite, a common surface-alteration product in metallic-mineral deposits, has a secondary minimum in this area; it is optimally covered by the RBV system. The other band of importance shown in table 1, $1.70\text{--}1.82\mu\text{m}$, is directed toward a very specific problem: detection of layered ultramafic bodies which, though not numerous, are commonly fairly large and contain important ore minerals. This band is not imaged by either system and should be considered in future satellite experiments.

The data obtained by the ERTS imaging systems should be adequate to evaluate the potential of the iron-absorption band technique for discriminating felsic and mafic rocks and detecting areas of prospecting interest for metallic-ore deposits from satellite altitudes; this capability will be improved greatly by using both the ERTS and EREP bands. Demonstration of the technique should justify more appropriate band passes for use in future satellite systems. Visible and near-infrared spectral measurements have been confined mainly to the laboratory, but a field-measurement program has been initiated by the Remote Sensing Geophysics group to provide a statistically sound basis for optimum use of these band passes.

ACKNOWLEDGMENTS:

Robert Watson assisted in making the spectral reflectance measurements and in compiling the spectral curves. James Elliott correlated the geology and the reflectance data of the Homestake Mine.

REFERENCES

- [1] Bancroft, G. M. and Burns, R. G., 1967, Interpretation of the electronic spectra of iron in pyroxenes: Amer. Mineralogist, v. 52, nos. 9-10, p. 1278-1287.
- [2] White, W. B. and Keester, K. L., 1966, Optical absorption spectra of iron in the rock-forming silicates: Amer. Mineralogist, v. 51, p. 774-791.
- [3] Adams, John B., 1968, Lunar and Martian surfaces: petrologic significance of absorption bands in the near-infrared: Science, v. 159, p. 1453-1455.
- [4] Hunt, G. R. and Salisbury, J. W., 1970, Visible and near-infrared spectra of minerals and rocks: I, Silicate minerals: Modern Geol., v. 1, p. 283-300.
- [5] Ross, H. P., Adler, J.E.M., and Hunt, G. R., 1969, A statistical analysis of the reflectance of igneous rocks from 0.2 to 2.65 microns: Icarus, v. 11, p. 46-54.
- [6] James, H. L., 1944, Chromite deposits near Red Lodge, Carbon County, Montana: U.S. Geol. Survey Bull. 945-F, p. 151-189 [1947].
- [7] Offield, T. W., Rowan, L. C., and Watson, R. D., 1971, Linear geologic structure and mafic rock discrimination as determined from infrared data: Third annual earth resources program review, v. 1, sec. 11, p. 1-12.
- [8] Rowan, L. C. and Vincent, R. K., 1971, Discrimination of iron-rich zones using visible and near-infrared spectral analysis in Abstracts with programs: Geol. Soc. Amer., Annual Meeting, Washington, D. C., v. 3, no. 7, p. 691.

Table 1 - Optimum band passes for application of the iron-absorption band technique from satellite and the manner in which these bands are covered by ERTS/Skylab systems *, optimally; x, partially; -, none.

ERTS and EREP Systems	OPTIMUM BAND PASSES (in micrometers)					
	0.58-0.68	0.65-0.75	0.75-0.85	0.85-0.95	0.95-1.10	1.70-1.82
MSS	*	x	x	x	x	-
RBV	*	x	x	-	-	-
S190	*	x	x	x	-	-
S192	*	x	x	x	*	-

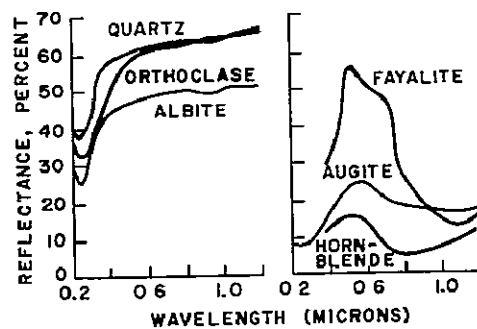


Figure 1 - Visible and near-infrared reflectance spectra for selected iron-rich and iron-poor rock-forming minerals showing the reflectance minima in the near-infrared in the iron-rich mineral spectra. Spectra obtained from crushed grains: 750-1200 μ m for hornblende and fayalite [from ref. 4]; 400-500 μ m for quartz, orthoclase, augite, and albite [from ref. 5].



Figure 2 - Visible and near-infrared reflectance spectrum for limonite.

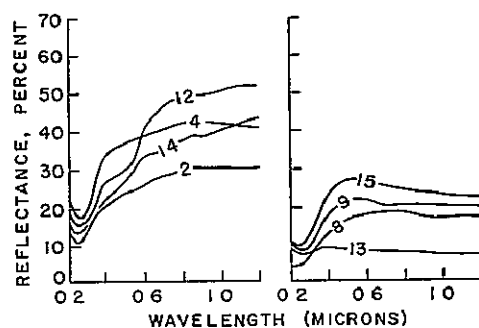


Figure 3 - Visible and near-infrared reflectance spectra for selected felsic rocks, granite (14), rhyolite (12), granodiorite (2), and rhyolite (4) and for selected mafic rocks, basalt (13), gabbro (9), serpentinite (15), and peridotite (8), showing decreased reflectance in the near-infrared for the mafic rocks. Spectra of samples with grain sizes in the 400-500 μ m range [from ref. 5].

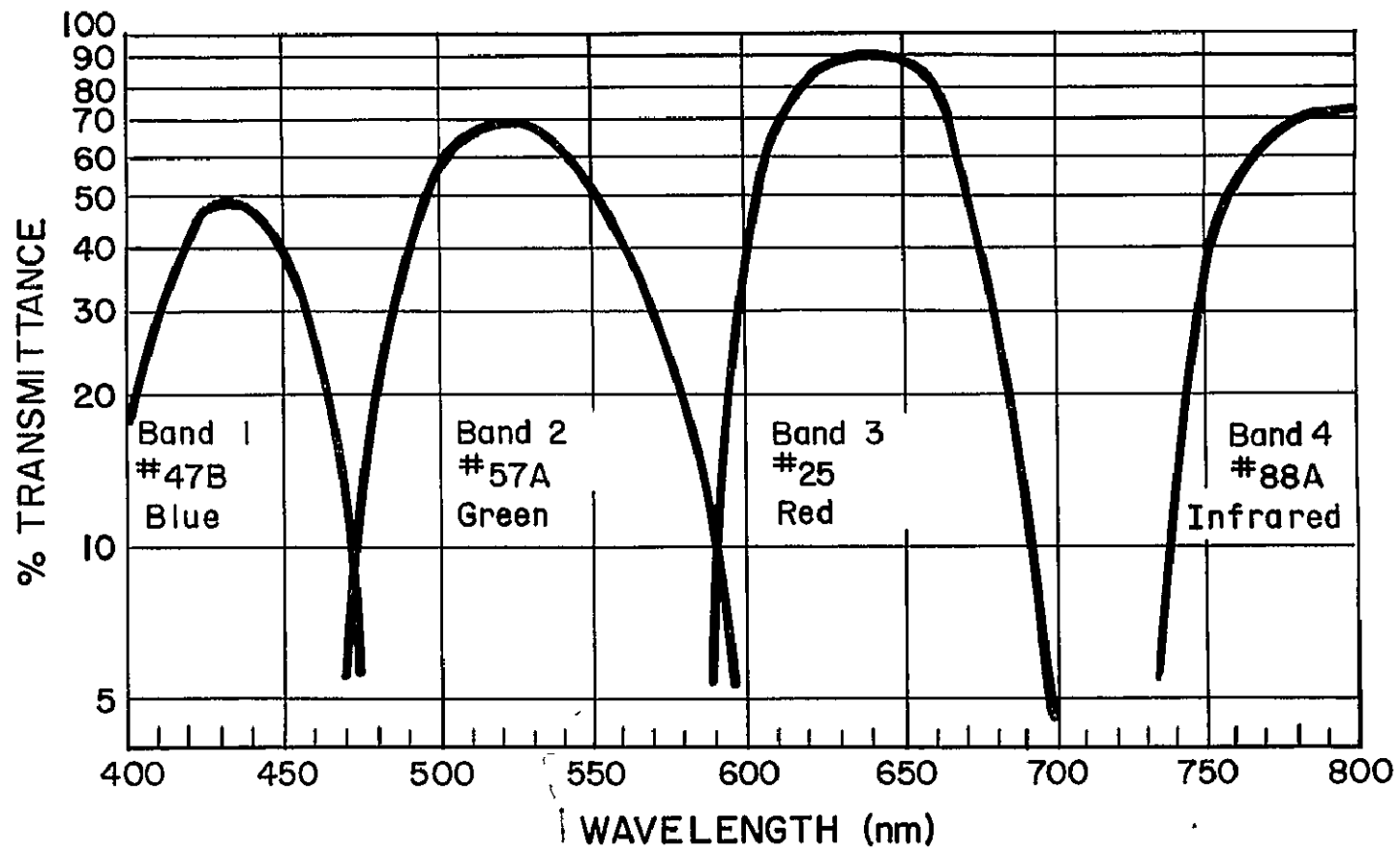


Figure 4 - Spectral response of blue, green, red, and near-infrared band-pass filters used in I²S camera used to photograph selected areas in the Beartooth Mountains in August 1971.

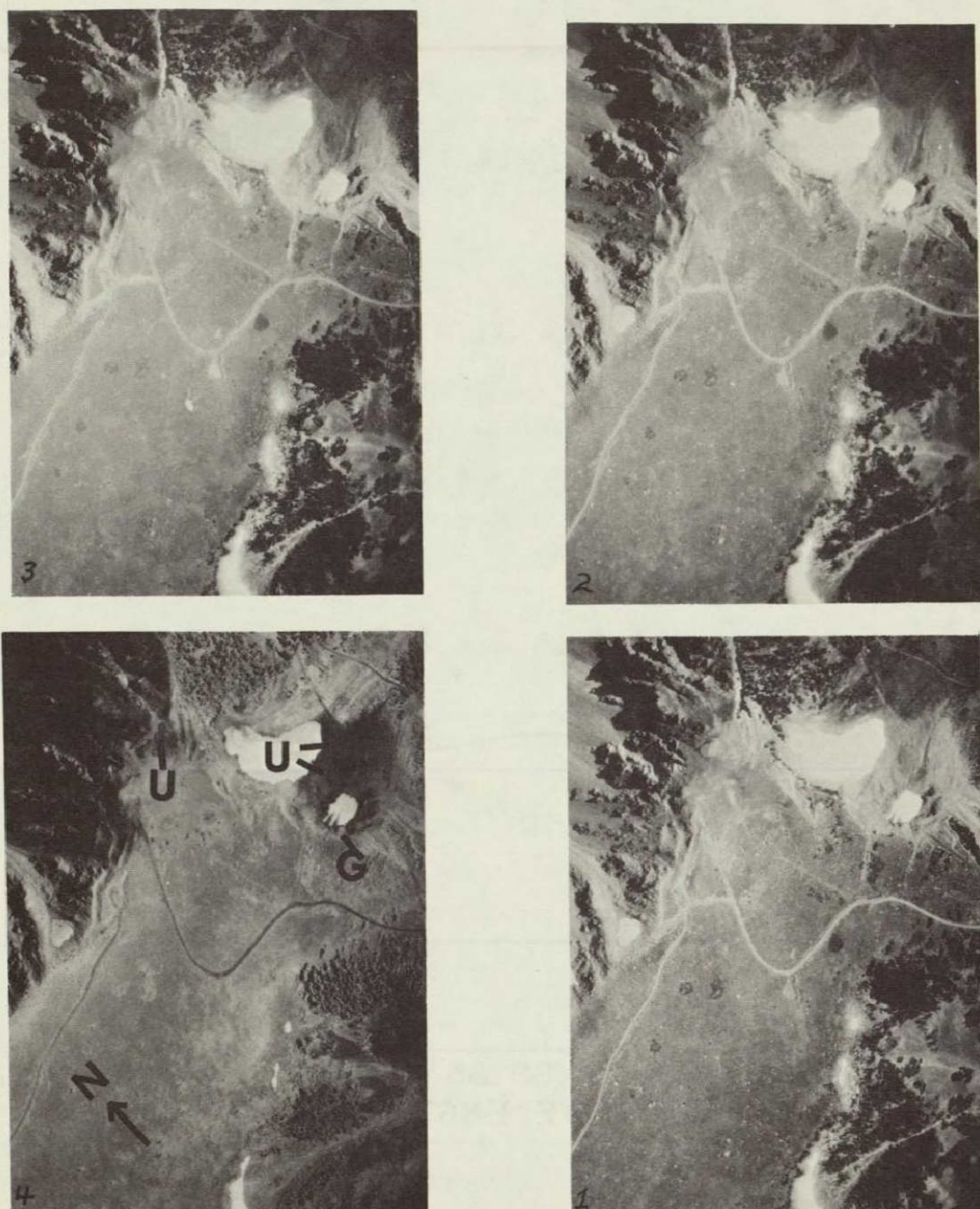


Figure 5 - I²S Multiband photographs of a chromite-bearing ultramafic deposit in the eastern Beartooth Mountains, Montana, showing increased photographic contrast between the ultramafic (U) and host rocks (G) in the near-infrared band. Scale is 550 m across frames.

This page is reproduced again at the back of this report by a different reproduction method so as to furnish the best possible detail to the user.

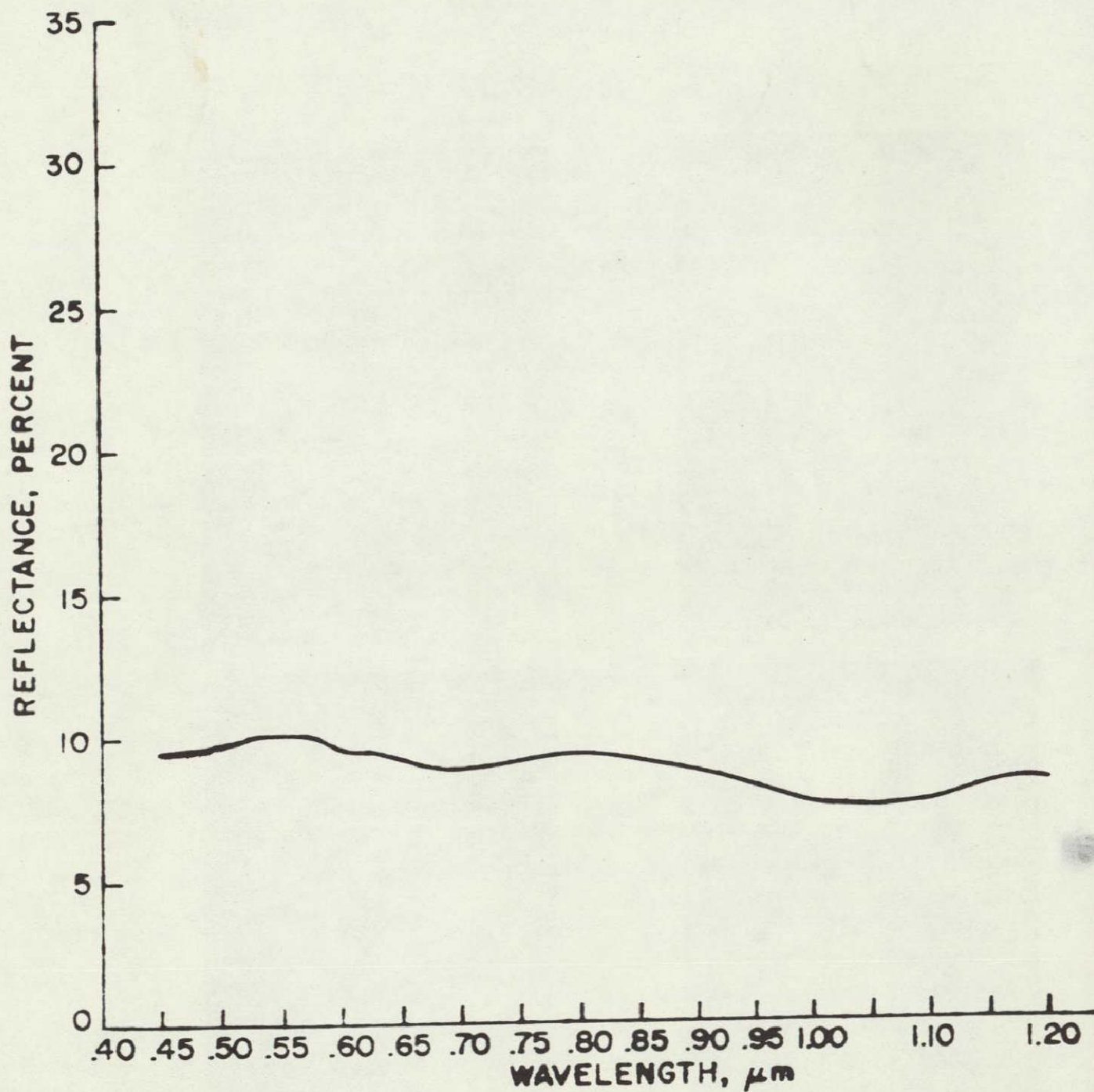


Figure 6 - Visible and near-infrared reflectance spectra for chromitic ultramafic rock shown in figure 5.

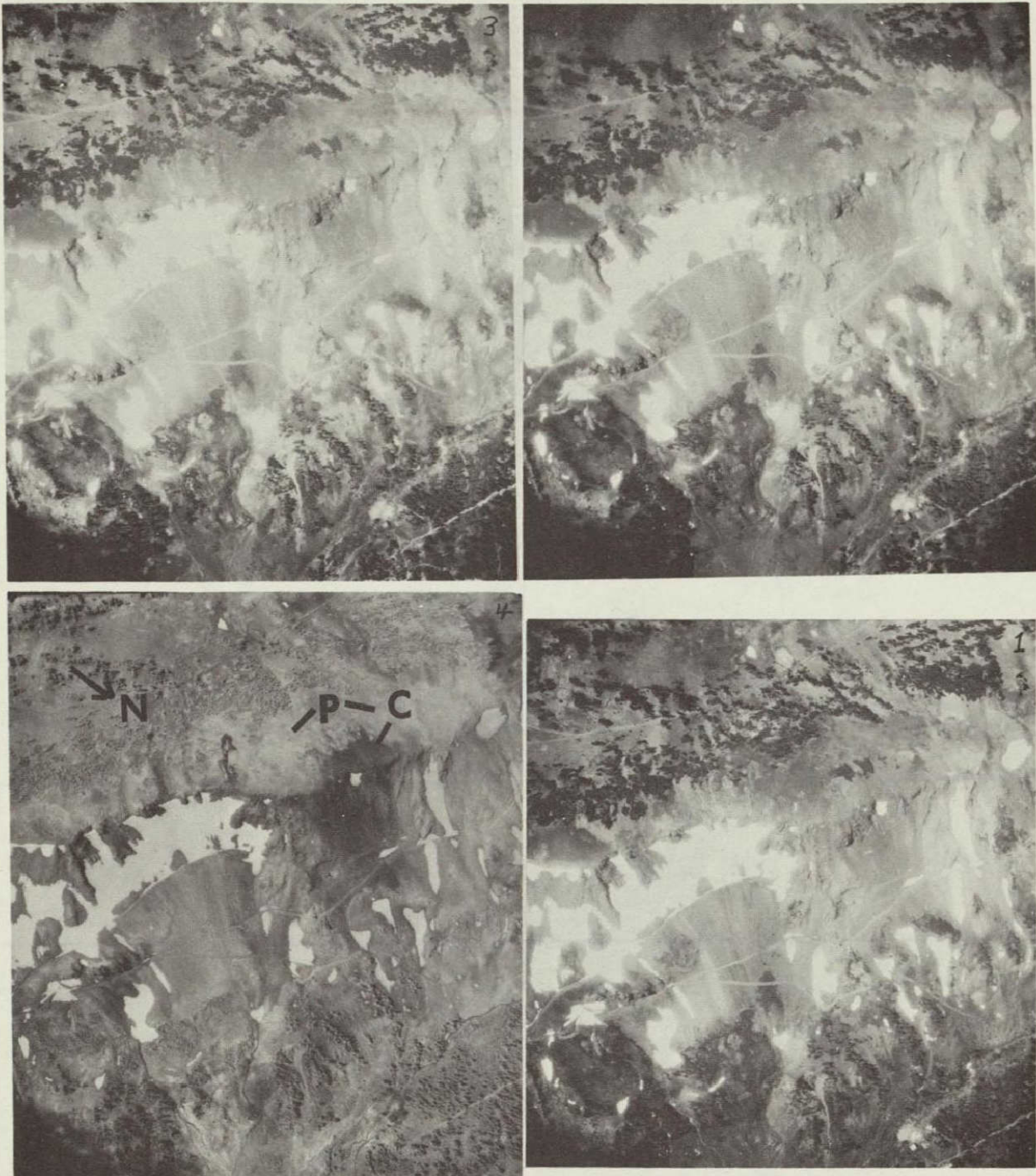


Figure 7 - I²S Multiband photographs of the Homestake Mine area, Montana, showing the increased photographic contrast between the central (C) and peripheral (P) zones of a breccia pipe in the near-infrared band. Scale is 870 m across frame.

This page is reproduced again at the back of this report by a different reproduction method so as to furnish the best possible detail to the user.

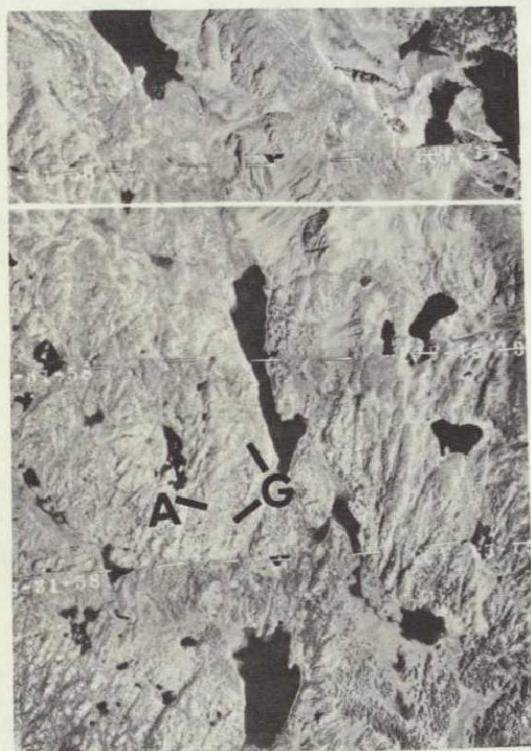


Figure 8 - Conventional black-and-white aerial photo-mosaic of the Becker Lake (center of mosaic) area in the southeastern Beartooth Mountains, Montana, showing the photographic density between granitic gneiss (G) and amphibolite (A). North at top. Becker Lake is about 1.5 km long.

This page is reproduced again at the back of this report by a different reproduction method so as to furnish the best possible detail to the user.

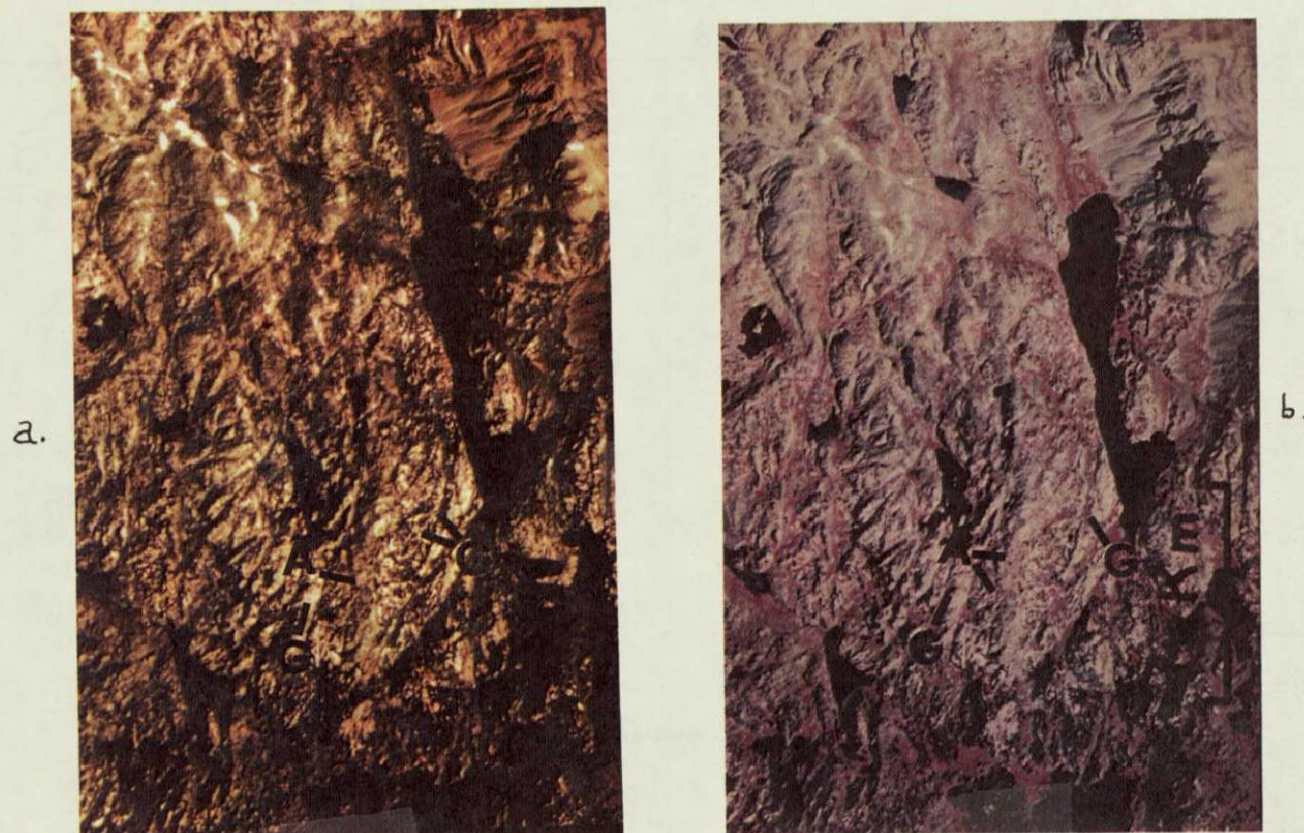


Figure 9 - (a) Ektachrome (2448 film with HF-3 and Av filters) and (b) Ektachrome-infrared (S0-117 film with 0.50 μ m filter) photographs of the Becker Lake area in the southeastern Beartooth Mountains, Montana, showing the photographic contrast between granitic gneiss (G) and amphibolite (A). North at top.

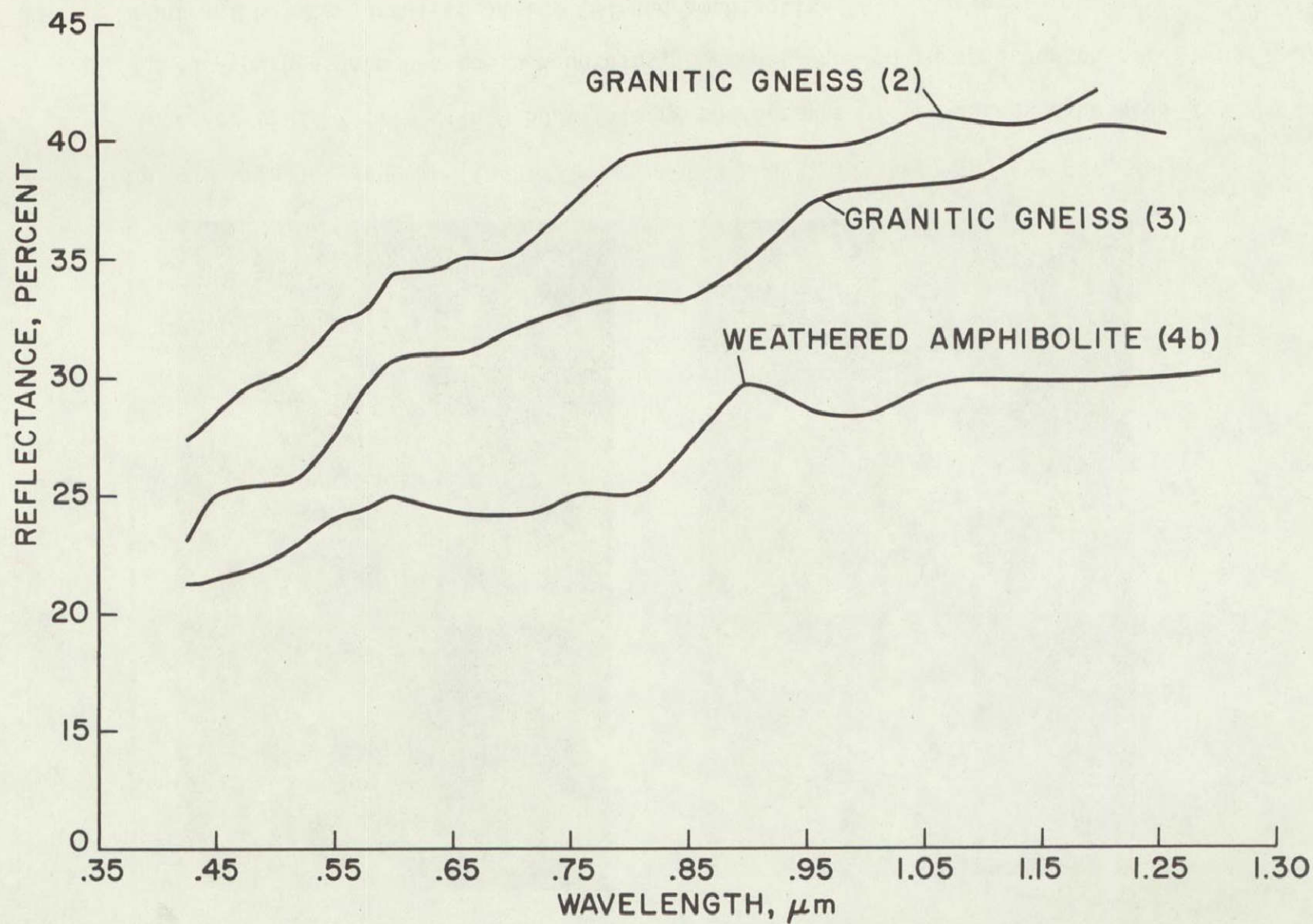


Figure 10 - Visible and near-infrared reflectance spectra for Becker Lake amphibolite (4b) and two samples of granitic gneiss (2 and 3) showing the reflectance minima at about 0.70 and 1.00 μm in the amphibolite. Spectra obtained from about 1-foot-diameter outcrops.

SECTION 61

MAPPING OF TERRAIN BY COMPUTER CLUSTERING TECHNIQUES USING
MULTISPECTRAL SCANNER DATA AND USING COLOR AERIAL FILM

by

Harry W. Smedes
U.S. Department of the Interior
Geological Survey
Denver, Colorado

Harold J. Linnerud and Lawrence B. Woolaver
E G & G, Inc.
Bedford, Massachusetts

Ming-Yang Su
Northrop Services, Inc.
Huntsville, Alabama
and
Robert R. Jayroe
National Aeronautics and Space Administration
George C. Marshall Space Flight Center
Huntsville, Alabama

ABSTRACT

ORIGINAL CONTAINS
COLOR ILLUSTRATIONS

Two clustering techniques were used for terrain mapping by computer of test sites in Yellowstone National Park. One test was made with multispectral scanner data using a composite technique which consists of (1) a strictly sequential statistical clustering which is a sequential variance analysis, and (2) a generalized K-means clustering. In this composite technique, the output of (1) is a first approximation of the cluster centers. This is the input to (2) which consists of steps to improve the determination of cluster centers by iterative procedures.

Another test was made using the three emulsion layers of color-infrared aerial film as a three-band spectrometer. The aerial film was scanned by a trichromatic microdensitometer which simultaneously samples all three emulsion layers. Relative film densities were analyzed using a simple clustering technique in three-color space.

The multispectral composite clustering technique utilized a 6x6-m ground-resolution cell. In that test, 12 units representing six terrain classes were mapped with an accuracy of about 80 percent. Pre-processing techniques to reduce illumination differences due to scan angle and shadows were not employed.

The color-film technique utilized a ground-resolution cell 9 meters in diameter. In that test, 12 units representing nine terrain classes were mapped with an accuracy of about 85 percent. The computer produced terrain maps which can be directly overlaid on enlargements of the photographs.

Improvements are being made in both computer techniques. Important advantages of clustering techniques over conventional supervised computer programs are (1) human intervention, preparation time, and manipulation of data are reduced, and (2) the resulting map gives an unbiased indication of where best to select the reference ground control data. Additional advantages of the color-film technique are that the film is relatively inexpensive and easy to acquire, and the geometric distortions can easily be rectified by simple standard photogrammetric techniques.

INTRODUCTION

This report summarizes the results of preliminary studies of digital computer processing of data using clustering techniques with multispectral scanner data and with color aerial film. These studies are part of a comprehensive program for testing of automatic mapping of terrain by computer techniques. A summary of results of that program has been published (ref. 1).

PREVIOUS STUDIES

Multispectral data have been used in the past for pattern recognition of terrain classes. Traditionally, these data have been from multispectral airborne scanning spectrometers (ref. 2, 3, 4) or from multi-lens aerial cameras using black and white film (ref. 5, 6, 7).

Scanner Systems

Scanning spectrometers record each wavelength band as a separate synchronized signal on magnetic tape so that analog and digital computers can be used to determine spectral signatures of terrain classes. Using these signatures, each datum point is categorized according to its terrain class.

Conventional computer mapping programs are based on supervised techniques, wherein the reference spectral signatures are obtained directly from training sites which form parts of the test area. The general procedure is:

- a) Training areas are selected for some arbitrary number of classes.
- b) Data from these training areas are used to establish reference spectral signatures.
- c) Using these spectral signatures, the computer maps the entire area, assigning each datum point to one of the predetermined classes or to a null class.
- d) The computer map is compared with the control data to determine whether it is "good enough".
- e) Steps a through d are repeated until the resulting map is "good enough" or until further iteration no longer results in improved accuracy. Much human intervention and manipulation of the data are involved, and detailed ground control is required in order to know when the computer has been sufficiently trained and the map is "good enough".

Camera Systems

Multiband camera systems conventionally use (ref. 5, 6, 7) one to four separate rolls of black and white film which are exposed synchronously by as many as nine lenses, each lens filtered to pass only a limited wavelength band and each lens exposing a separate image. The resulting multiple-image sets generally have been studied optically by superimposing projected images on a screen, each projector using a different colored filter, or by printing the images as different colored transparencies and superimposing several of them. The object is to select a combination of filters that will enhance certain terrain features.

PRESENT STUDY

To avoid or minimize human intervention, extensive preparation time, and the other disadvantages of supervised techniques, unsupervised digital computer techniques were applied. These techniques utilize the fact that the radiance of different materials tends to cluster in different places in n-dimensional space. The programs, in effect, allow the computer to determine these clusters and to plot each class based on clustering, whatever that class may be (ref. 8, 9).

One such natural class might be printed in map form by the letter S, for example; and, although you would not know what that class really was, you would know everywhere it occurred. Limited field checking or photo interpretation would then give an identity to each of the classes mapped by this clustering technique.

In this sense, the application of clustering techniques to the multispectral data analysis is in reverse order to that of the supervised classification techniques. An advantage of processing the data in the order of the clustering techniques is that we will know better where to select the reference ground control data.

No prior knowledge is required for the computer to make a map. In addition there is the further advantage that because data points within a cluster are highly similar, clustering procedures constitute an irreversible data-flow compression that could save much data transmission from satellites without loss of information, since cluster codes could be transmitted rather than multidimensional data points (ref. 9). The resulting data would not overload existing computer facilities (Dr. F. R. Krause, oral communication, 1971).

Data Set

The data studied were acquired by contract with the University of Michigan, and consist of one set of data from their 12-channel reflective scanner (see table) and color aerial photographs taken at the same time the scanner data were acquired. The flight was at approximately 1400 hours, Sept. 19, 1967. The test site (Fig. 1) is about 31 km² in the north-central part of Yellowstone National Park (ref. 2, 9, 10). The area has a wide range of terrain types, and about 600 meters of relief (Fig. 2).

WAVELENGTH BANDS OF UNIVERSITY OF MICHIGAN MULTISPECTRAL SYSTEM

Channel number	Wavelength band in micrometers (μ m)	Channel number	Wavelength band in micrometers (μ m)
Scanner No. 1			
1	0.40-0.44	7	0.55-0.58
2	0.44-0.46	8	0.58-0.62
3	0.46-0.48	9	0.62-0.66
4	0.48-0.50	10	0.66-0.72
5	0.50-0.52	11	0.72-0.80
6	0.52-0.55	12	0.80-1.00

MULTISPECTRAL SCANNER DATA

A technique was developed (ref. 11, 12) which is a composite of two clustering techniques:

- 1) A Sequential Statistical Clustering along line-scan segments (ref. 13).

2) A Generalized K-Means Clustering (ref. 14).

The multispectral data are processed first by the Sequential Statistical Clustering program which classifies the given sequences of multispectral data along a scan line into an arbitrary number of classes, such that the variation within classes is insignificant compared to the differences between classes. This is accomplished in a truly sequential manner, with only one pass of the entire data sequence.

The outputs from this program consist of the mean spectral vectors and variance of the clusters. They serve as the initial cluster centers (as inputs) for the Generalized K-Means Clustering program, which consists of steps to improve the location of cluster centers by iterative procedures.

The accuracy of classification by each of these techniques alone is less than that obtained using supervised classification techniques (ref. 1, 11, 12); however, the composite technique produces classification of the data nearly as accurate as the supervised techniques, without using any training sets.

TERRAIN CLASSES

A terrain map was obtained by this unsupervised composite clustering technique from the raw multispectral data using channels 2, 9, 10, and 12. Coloring (by hand) enables each of the 12 classes to be distinguished clearly (Fig. 3). Comparison with the ground control data indicated that several classes were subunits of a single terrain class and should be merged and given the same color code (Fig. 4). The resulting map (Fig. 4) depicts the following terrain classes, plus shadow:

- 1) Bedrock
- 2) Vegetated bedrock rubble
- 3) Meadows and grassland underlain by glacial deposits
- 4) Forest
- 5) Talus and water, undivided

Descriptions and illustrations of these classes are given in references 1 and 10.

COLOR AERIAL FILM

In the present study, density data from the three emulsion layers of 70-mm color-infrared aerial film were entered into a digital computer programmed to produce terrain maps by using clustering techniques.

FILM RESPONSE

Ektachrome color and color-infrared film are sensitive to radiance in the range 0.35- .70 μ m (Fig. 5) and 0.50- .90 μ m (Fig. 6), respectively, each in three broad bands. This three-band sensitivity and the ability to calibrate films (ref. 15, 16) to account for sensitivity overlap make it possible to use color film for computer classification and mapping of terrain.

MICRODENSITOMETRY

Original 70-mm film transparencies were scanned by a Mann Trichromatic Microdensitometer at a resolution of 450 μ , corresponding to a spot 9 meters in diameter on the ground. All three color-film layers were sampled simultaneously by means of beam splitters and filters (Fig. 7). Because they have a common base and were sampled simultaneously, the data from all three layers are in perfect register, thus eliminating the registration problems inherent in conventional multiband photographic studies (ref. 8) and also reducing the scanning time by a factor of three. The triads of density values for each area element on the film transparency were digitized and recorded on magnetic tape.

DIGITAL COMPUTER PROCESSING

The data were processed on an IBM 360/40 computer using existing FORTRAN software. For selecting the spectral signatures, a clustering technique was applied. Each datum point was assigned a position in three-color space on the basis of its density values for the red, blue, and green film layers. The coordinates of this three-color space are percent green, percent blue, and total density (Fig. 8). Because the total density is dependent on all three color film layers, the coordinate of total density is in effect a function of the density of the red layer (the only remaining independent variable) and was plotted in this way simply to make use of existing computer programs that had been developed for other purposes.

The data were arbitrarily divided into 22 increments of percent blue, 22 of percent green, and 22 for total density (the sum of blue, green, and red). From this three-color space, density clusters were determined by inspection of computer printouts. Figure 9 illustrates how four clusters appear in the seventh layer of green/blue space. This layer is seventh up from lowest total density and is therefore of relatively bright objects (layer 22 would be for the darkest objects).

Computer printouts of the 22 layers of green/blue space were examined and coordinates of clusters determined by inspection. These coordinates were entered into the computer along with letter symbols, which were arbitrarily assigned to each cluster. The computer then mapped each datum point as belonging to one of these clusters, based on its spectral signature. Separate computer printouts were made for each terrain class determined by this cluster technique. The steps in this three-color technique are summarized in the schematic diagram of Figure 10. The computer printouts directly fit photographic enlargement of the original film transparencies.

Preliminary analysis showed that the color IR film had greater separation of clusters and wider range of spectral signatures than did the true color film, so the processing was done on two different color IR transparencies. The first one processed was used as a training ground for the second one (Fig. 11). After cluster classes had been determined in the first image, the computer was asked to identify areas in the second image having spectral signatures matching those in the first image.

The computer print for evergreen trees in the second image is shown in Figure 12. Simple drafting techniques and inexpensive color diazo transparencies can be used to convert all the separate overlays into a colored map (Fig. 13).

TERRAIN CLASSES

By overlaying the computer-generated terrain maps on enlargements of the photos and comparing the maps with the ground control data, each class was identified as to true terrain type. The following nine classes were assembled from the twelve* clusters mapped by the computer:

1. meadow and grasslands underlain by glacial till
2. meadow and grasslands underlain by glacial kame
3. felsic bedrock, largely granitic gneiss, and rhyolite tuff (in a quarry)
4. mafic bedrock, largely basalt lava and amphibolite
5. talus
6. evergreen trees
7. deciduous trees, bushes, and bogs
8. rock and talus in shade
9. shade of trees and cliffs

* Several of the clusters simply represented a single terrain unit under different illumination conditions. Presumably, too fine a distinction was made, and wider limits should have been set for most of the clusters.

Preprocessing techniques (ref. 17) might result in reduction of these last two shadow categories. Descriptions and illustration of these classes are given in references 1 and 10.

COMPARISON WITH ERTS WAVELENGTH BANDS

The widths and positions of the spectral bands used in this study are similar to those of the Earth Resources Technology Satellite RBV Camera System:

<u>Color IR Film</u>	<u>ERTS RBV Cameras</u>
0.50- .59 μ m	0.48- .58 μ m
.59- .68	.62- .72
.68- .90	.72- .80

The accuracy of classification (better than 85 percent) indicates how well the ERTS sensor might be expected to perform in classifying similar terrain and agrees closely with the results of ERTS simulations made using scanner data (ref. 1, 10).

ACCURACY

The ranking and overall approximate accuracies of maps made by different computer techniques are shown in Table I, and are based on ground control data (Fig. 16).

It is not possible to compare each map directly with the others because different classes are shown. For example, water and talus are shown as an undivided unit on the cluster map (Fig. 4), and one is tempted to conclude that the accuracy for talus or for water is, therefore, poor. However, for the combined class of water plus talus, the accuracy is very good. Reconnaissance photo interpretation would allow one to separate the two readily.

Cloud shadows were most accurately classified on the supervised map without preprocessing (Fig. 14), and one would assume that that was the best map. However, shadows are not terrain features, and one would like to know what lies under the shadow. In that regard the supervised map made from preprocessed data is best because it minimized the area of shadow and correctly classified the terrain unit that lay under the shadow.

Some insight can be gained into the distinctness of classes by means of a special boundary map printed by the computer by means of a program developed by one of us (RRJ). On such a boundary map (Fig. 17),

three symbols are used to indicate whether the change across the boundary is greater than 70, 80, or 90 percent, respectively, of the rest of the data. These represent degrees of change in Euclidean distance (squared) from neighboring elements in north-south or east-west direction. Blank areas are homogeneous.

All four of the maps are highly satisfactory terrain maps which portray physiographic units or unique rock-soil-vegetation association units. In all cases, where terrain classes were areally extensive they were correctly identified by the computer. Most inaccuracies occurred where the units were small and where some were below the ground-resolution cell size; accordingly, the radiance for a given resolution cell was a complex combination of several categories (see Fig. 16).

ADVANTAGES AND DISADVANTAGES

SCANNER VS AERIAL PHOTOGRAPHS

Advantages of scanning spectrometers are that they have high spectral resolution (12-24 channels of narrow band width), that the data are directly amenable to computer programs capable of sophisticated statistical decision rules, and the data are in perfect register. Disadvantages are the low spatial resolution (2.5-3 mrad angle subtended by the scanner), the fact that scanner data are sparse and expensive to acquire (ref. 10) and the serious handicap of various kinds of inherent geometric distortion.

Advantages of multiband aerial photographs are that they are becoming increasingly easy and inexpensive to acquire, that they have high spatial resolution, and that the inherent geometric distortion can be rectified by using standard photogrammetric techniques. Disadvantages are the lower spectral resolution--as many as nine overlapping spectral band widths, but more commonly four images, each recorded over rather broad bands--the fact that most* processing techniques result in an image (not a map) on which only one or two terrain classes are enhanced, and problems of register (ref. 8).

Advantages of the color-film clustering technique over scanner data are threefold:

* There are exceptions, such as the University of Kansas IDECS system (ref. 17), which is computer-programmable, and other optical-electronic systems (ref. 5, 18), all of which are more sophisticated systems but of severely limited availability.

1. Color film is inexpensive to acquire, and much is already available. Scanner data are very expensive to obtain, and very little are already available (in terms of different areas covered).
2. The geometric distortion in aerial color film can be rectified using stereoscopic pairs of photos and simple standard photogrammetric techniques; in fact, that is the way our present day accurate base maps are made. The geometric distortions inherent in scanner data can be reduced only in areas where there are numerous distinct shapes of class boundaries, or road intersections, etc., and then only at great computer cost.
3. The color image is of considerable interpretive value alone and can be used as a valuable reference to study specific anomalies brought to light by the computer mapping program.

Disadvantages of the color film technique over scanner data are twofold:

1. There is poorer spectral resolution due to the broader spectral response band width of the three film layers (average $0.13 \mu\text{m}$) compared to the narrow band width of the scanner channels (average $0.04 \mu\text{m}$).
2. The wavelength range of the film is more limited than that of the scanner. The film used (color IR) has a response range of about $0.40 \mu\text{m}$; whereas the Michigan 12-channel scanner has a range of about $0.60 \mu\text{m}$, and the new Bendix scanner has a range of about 20 times that of the Michigan scanner.

At present, both of these disadvantages are only theoretical inasmuch as the accuracy of the color film method is approximately the same as the scanner method. This may be due to a chance selection of photographs that were better suited to the method than others would have been, although attempts were made to select representative photographs.

COLOR VS MULTIBAND PHOTOGRAPHY

Advantages of the three-color technique over conventional multi-band photography are that all three film layers are in register and were scanned simultaneously, thus reducing the scanning time by a factor of three.

CONCLUSIONS

Considering the various advantages and disadvantages, the color film technique seems suitable for studies involving a broad range of terrain classes, rather than highly specific targets, where the spectral signatures can adequately be characterized within the wavelength range of color or color-infrared film response. Where these constraints are not met, the scanner technique will probably be required.

SUPERVISED VS UNSUPERVISED TECHNIQUES

Three disadvantages of conventional supervised computer technique are:

1. Prior knowledge of the site is required in order to select training areas.
2. Areas chosen for training may not be fully representative of that terrain class throughout the test site.
3. Variability of the reference spectral signatures with differing atmospheric conditions, time of day, season, recency of rain, sensor scan angle, and other factors (some known and some unknown in the process of data-gathering) make it impractical if not impossible to use a given set of signatures for a different set of data over the same site or even for the same set of data but at great distance from the training areas. As a result, training areas must be selected and used for each different set of data.

Advantages of the unsupervised techniques are:

1. No prior knowledge of the site is required.
2. Human intervention, manipulation of the data, and bias are eliminated or minimized.
3. Because spectral signatures are not used, the problem of data preparation described in 3, above, is not encountered, and much time is saved.
4. The resulting map gives an unbiased indication of where to select the reference ground control data so that they will be more representative of that terrain class throughout the test site.
5. Resulting classification (maps) are nearly as accurate as those made by the supervised techniques, but at a great savings in time and cost.

Both of these tests of clustering techniques were feasibility studies which demonstrated the effectiveness and usefulness of the methods. Consequently, joint studies are continuing, in an effort to determine optimum technique, computer programs, and applications, and to test and define the limits of applicability. As part of those studies, the density data from color film will be used as input to the composite sequential K-means clustering technique.

ACKNOWLEDGEMENTS

As shown by the authorship, this study is a cooperative effort. We thank our many colleagues who have contributed to these studies through discussion, and wish especially to thank Dr. Fritz R. Krause of NASA's Marshall Space Flight Center and Dr. Kenneth L. Pierce, Dr. Harold J. Prostka, and Miss Jeanne T. Hemphill of the U.S. Geological Survey.

REFERENCES

1. Smedes, H. W., 1971, Automatic Computer Mapping of Terrain, in Proceedings of the International Workshop on Earth Resources Survey Systems, v. 2, 334-406, illustrated; U.S. Government Printing Office.
2. Landgrebe, D. A., 1968, LARSYSAA, A Processing System for Airborne Earth Resources Data: LARS Information Note 091968, Purdue Univ.
3. Marshall, R. E., and Kriegler, F. J., 1970, Multispectral recognition techniques: present status and a planned hybrid recognition system: Proc. of the 1970 I.E.E.E. Symposium on Adapter Processes Decision and Central; The University of Texas at Austin, December 1970, p. 1-2.
4. Nalepka, R. F., 1970, Investigation of Multispectral Discrimination Techniques: Report 2264-12-F, Infrared and Optics Laboratory, The University of Michigan, 186 p.
5. Brooke, R. K., Jr., 1971, Display technology for multiband photography: Convention of the American Society of Photogrammetric and the American Congress on Surveying and Mapping, 20 p.
6. Colwell, R. N., 1964, Aerial photograph--a valuable sensor for the scientist: American Scientist, March 1964, p. 16-49.
7. Cronin, J. F., and Molineaux, C. E., 1967, Multispectral photographic sensing of terrestrial features: Proc. Symposium Electromagnetic Sensing of the Earth from Satellite, Polytechnic Press, Polytechnic last of Brooklyn.
8. Hoffer, R. M., Anuta, P. E., and Phillips, T. L., 1971, Application of ADP techniques to multiband and multiemulsion digitized photography: Paper 71-345, Convention of the American Society of Photogrammetry and the American Congress on Surveying and Mapping, 19 p.
9. Haralick, R. M., and Dinstein, I., 1971, An iterative clustering procedure: in Institute of Electrical and Electronic Engineers Trans. Systems Science and Cybernetics, 11 p.
10. Smedes, H. W., Pierce, K. L., Tanguay, M. G., and Hoffer, R. M., 1970, Digital Computer Terrain Mapping from Multispectral Data, Journal of Spacecraft and Rockets, v. 1, no. 9, p. 1025-1031.
11. Su, Ming-Yang, 1972, An unsupervised statistical clustering technique, with application to remote earth observation: Fourth Annual Earth Resources Program Review, NASA, MSC, Houston.

12. Su, M. Y., Hand, C. G., and Pooley, J. C., 1971, Applications of a composite sequential K-Means clustering technique to remotely sensed agricultural data: TR-220-1009, prepared for NASA, Marshall Space Flight Center Aero-Astrodynamics Laboratory by Northrop Services, Inc., 59 p.
13. Su, M. Y., 1970, Algorithms for sequential classification of multispectral observation into homogeneous populations: Northrop-Huntsville Memorandum M-794-808.
14. Su, M. Y., 1971, A generalized K-Means algorithm for clustering multispectral observations: Northrop-Huntsville Memorandum M-794-964.
15. Smedes, H. W., Linnerud, H. J., Woolaver, L. B., and Howks, S. V., 1971, Digital Computer Mapping of Terrain by Clustering Technique Using Color Film as a Three-Band Sensor: Proc. Seventh International Symposium on Remote Sensing of Environment, Univ. of Michigan, v. 3, p. 2057-2071.
16. Buckner, J., and Maciel, R., 1969, "Three-Band Source Spectra From Color Film," EG&G Report no. B-3968 (EGG 1183-484) 21 March 1969, 29 p., illustrated.
17. Smedes, H. W., Spencer, M. M., and Thomson, F. J., 1971, "Preprocessing of Multispectral Data and Simulations of ERTS Data Channels to Make Computer Terrain Maps of Yellowstone National Park Test Site," in Proceedings of the Seventh International Symposium on Remote Sensing of Environment, University of Michigan.
18. Dalke, G. W., 1968, "Multi-image Correlation Systems for MGI Phase II," prepared for the U.S. Army Engineering Topographic Laboratories by the Center For Research, Inc., University of Kansas, 139 p., illustrated.
19. Smedes, H. W., 1970, "Geologic Studies of Yellowstone National Park Imagery Using an Electronic Image Enhancement System: U.S. Geological Survey Open File Report, 24 p., illustrated.

TABLE I.- RANKING AND OVERALL ACCURACY OF CLASSIFICATION OF
DIFFERENT COMPUTER TECHNIQUES

[1 = best; 4 = worst; -- = not present in area covered by map, or
not mapped separately]

Techniques using multispectral scanner data				Technique using color film
Feature (Fig. 15)	Supervised without preprocessing (Fig. 14)	Supervised with preprocessing (Fig. 15)	Nonsupervised without preprocessing (Fig. 14)	Nonsupervised without preprocessing (Fig. 13)
A	2	1	--	3
B	1	2	--	--
A, B undivided	2	4	1	3
C	2	--	1	--
D	1	--	3	2
C, D undivided	2	1	2	--
E	3	1	2	--
F	3	4	2	1
G	1	2	2	--
H	1	1	1	--
I	3	2	4	1
J	2	3	1	--
K	3	1	2	--
All talus	1	2	3	1
All water	2	3	1	--
Forest	1	2	3	2
Bog	1	2	--	--
Elimination of shadow	3	1	2	3
Approximate over- all accuracy (percent)	86	88	80	85

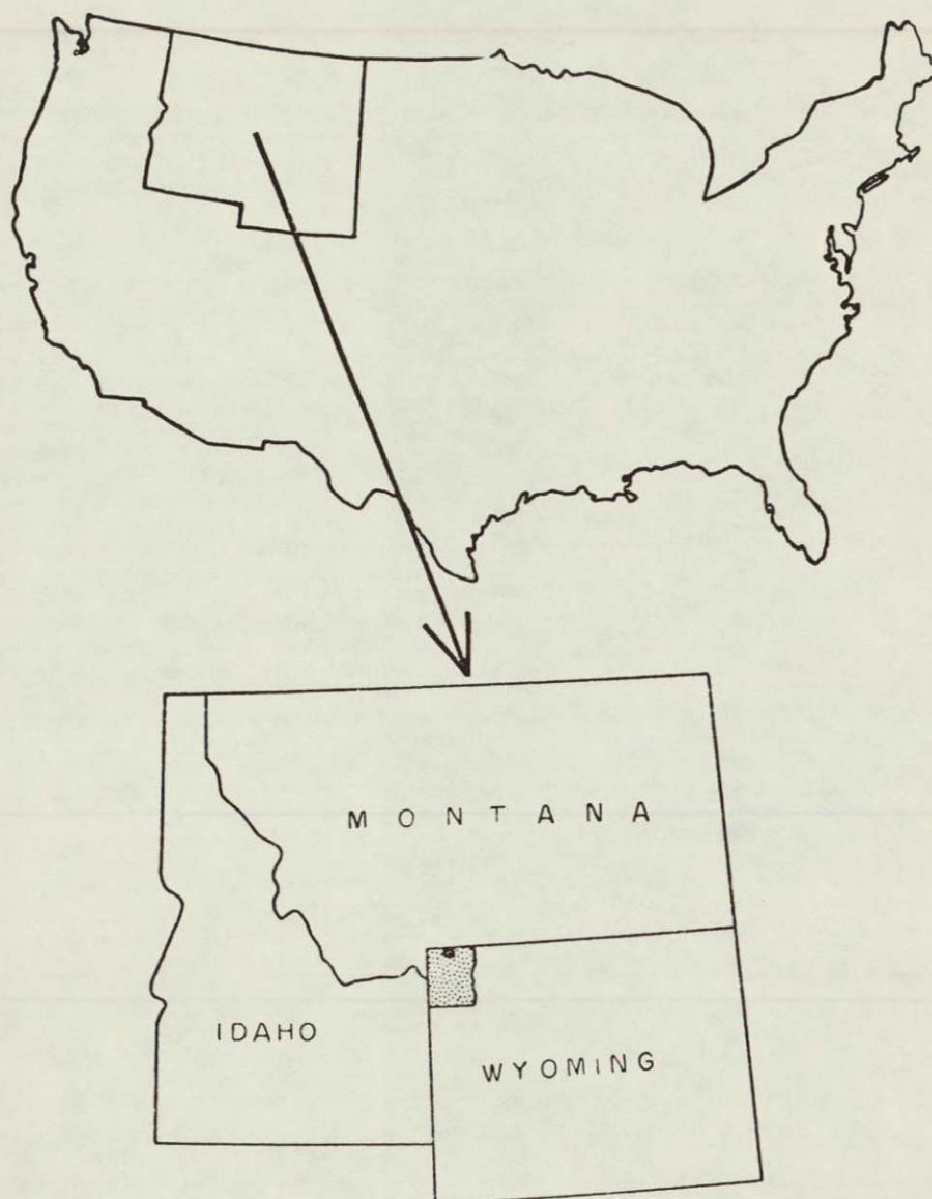


Figure 1. Index map of United States showing location of Yellowstone National Park (shaded) and the test site (black).



Figure 2.- Panorama of the test site, looking west from near the east edge.

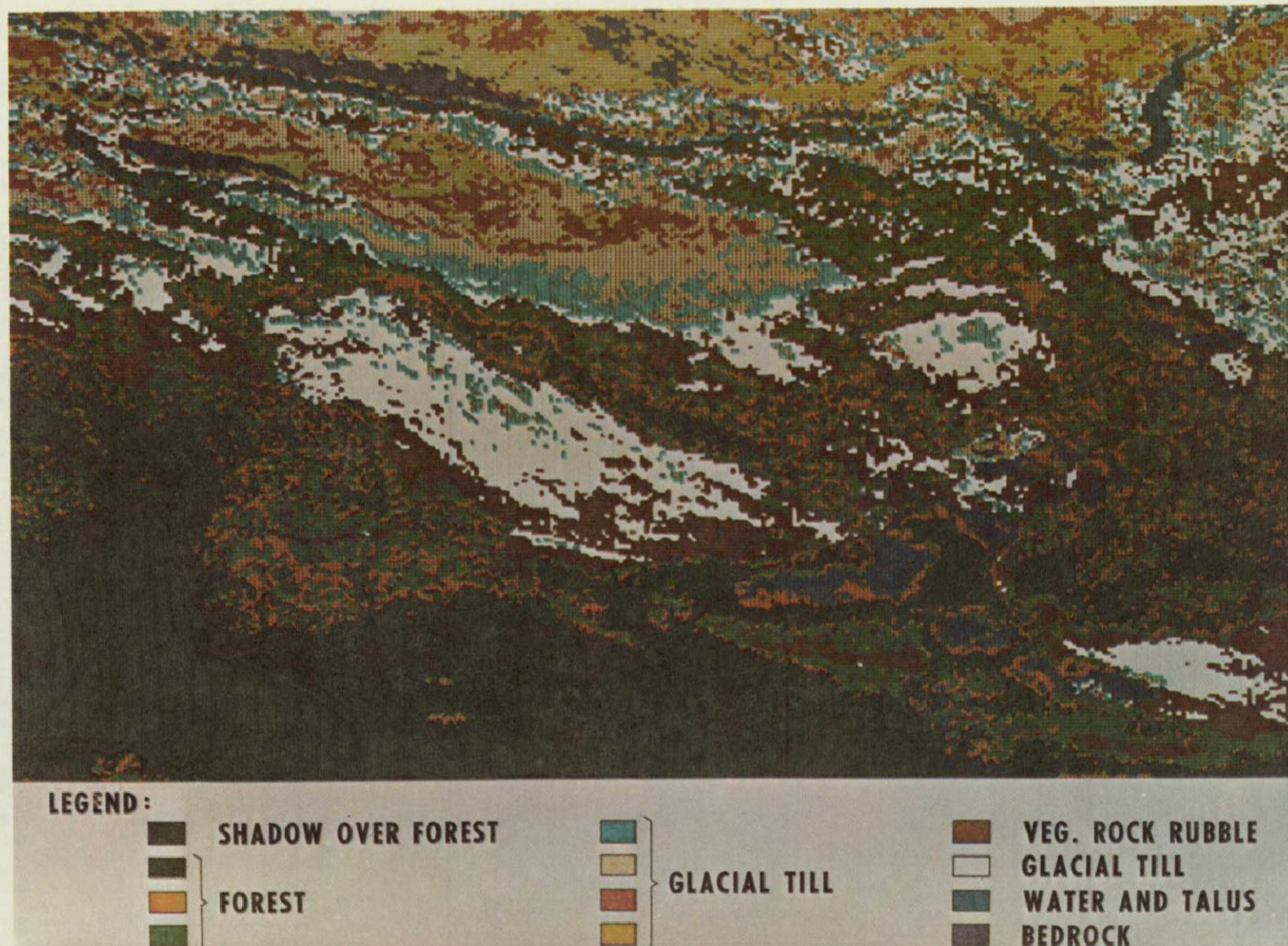


Figure 3. Terrain map of test site made by digital computer using unsupervised composite sequential K-means clustering technique. Hand colored coding distinguishes the 12 classes detected by this procedure. Computer processing by NASA/MSFC using channels 2, 9, 10, and 12.

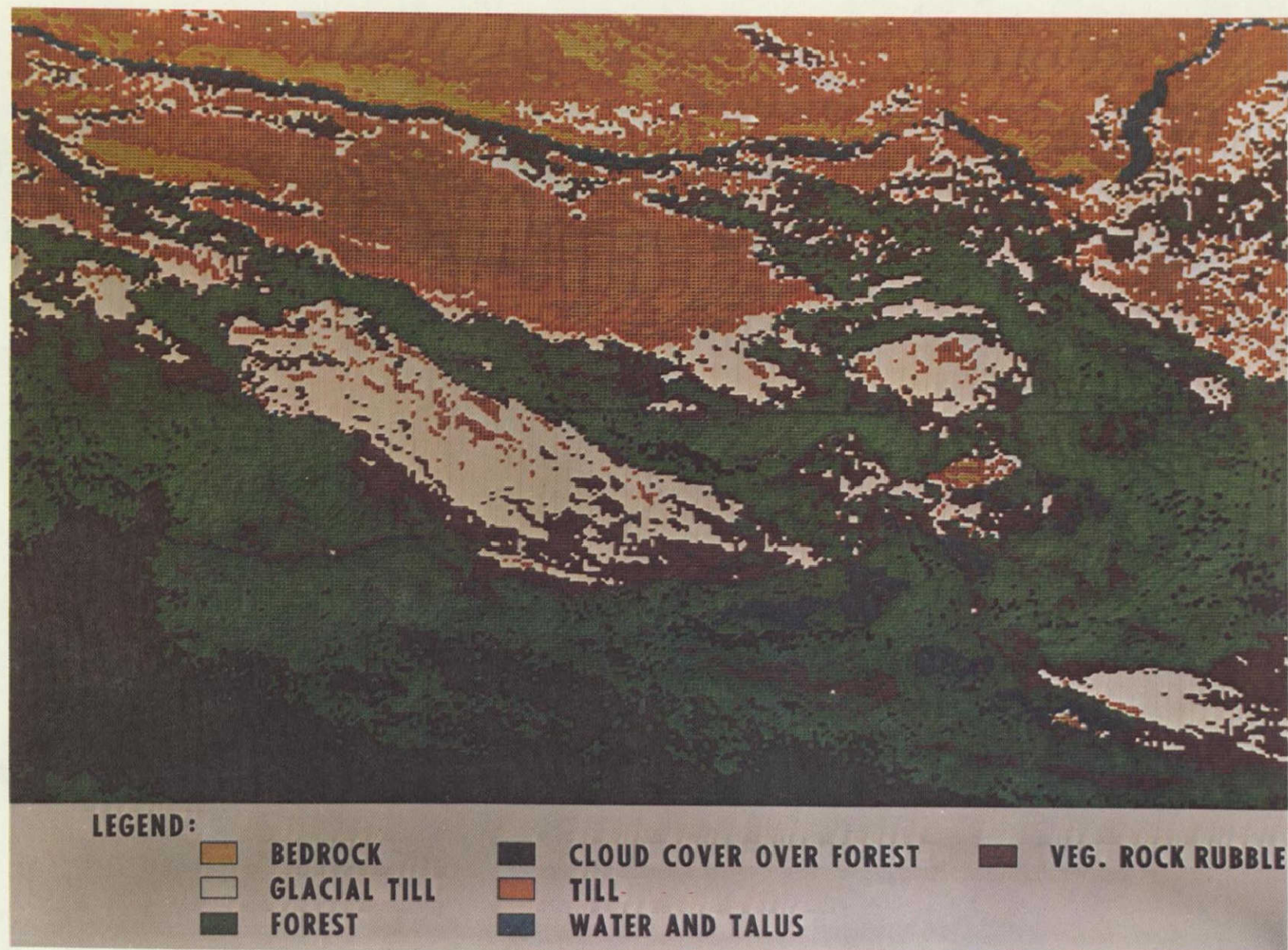


Figure 4. Terrain map of test site made by digital computer, generalized from the data of Figure 3 by merging several of the classes on the basis of ground control data.

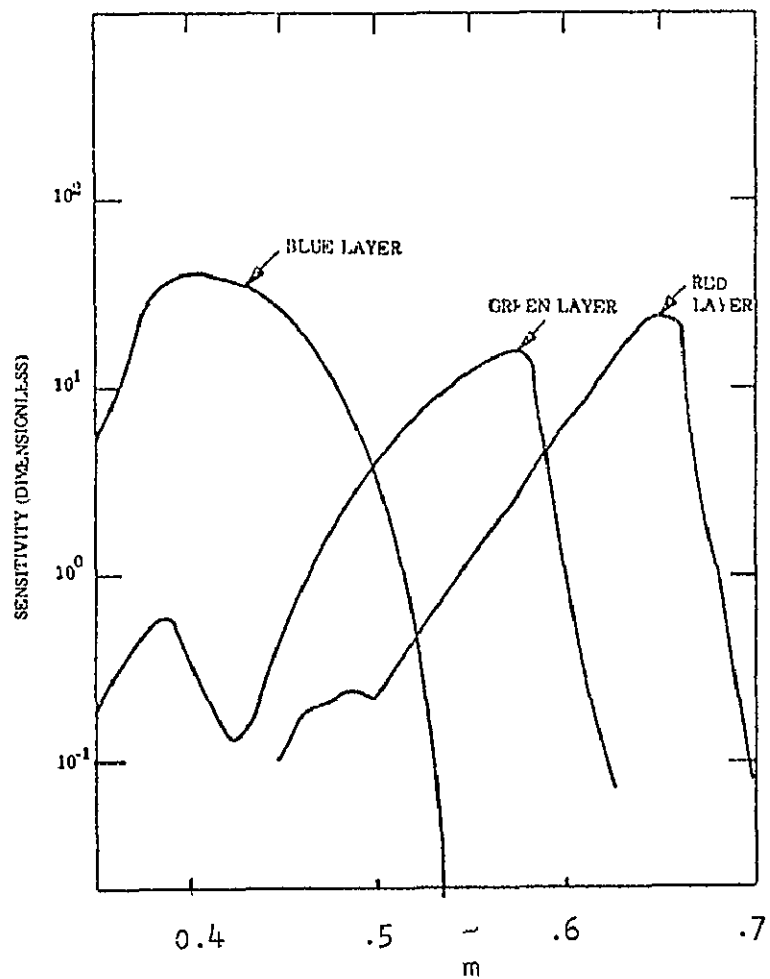


Figure 5.- Spectral sensitivity of Ektachrome color film.

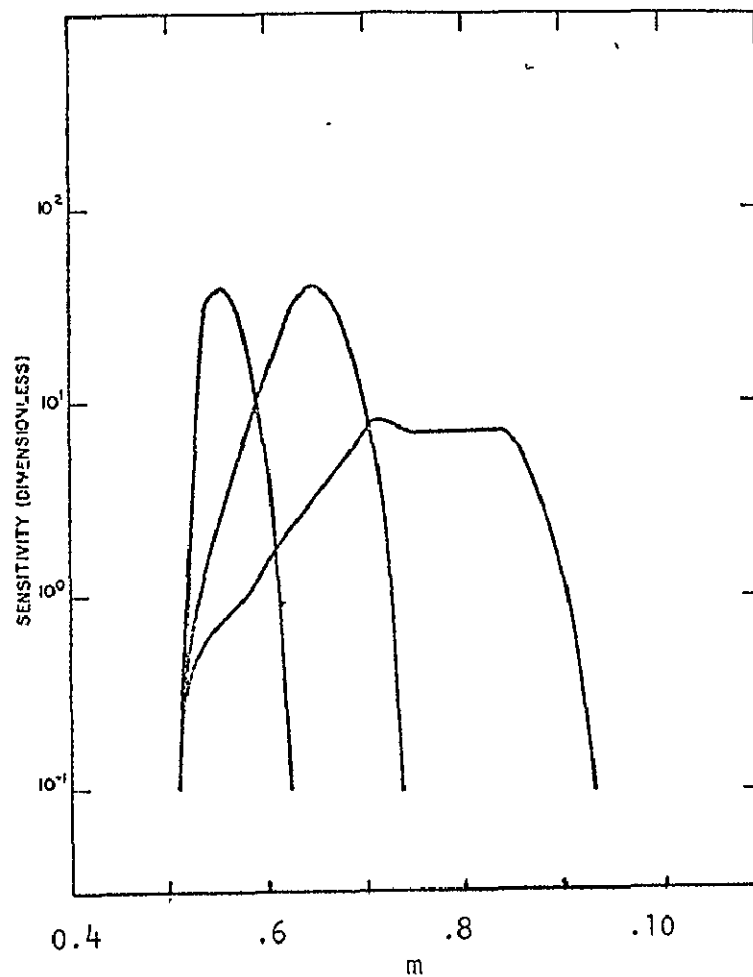


Figure 6.- Spectral sensitivity of Ektachrome color infrared film, plus G15 filter.

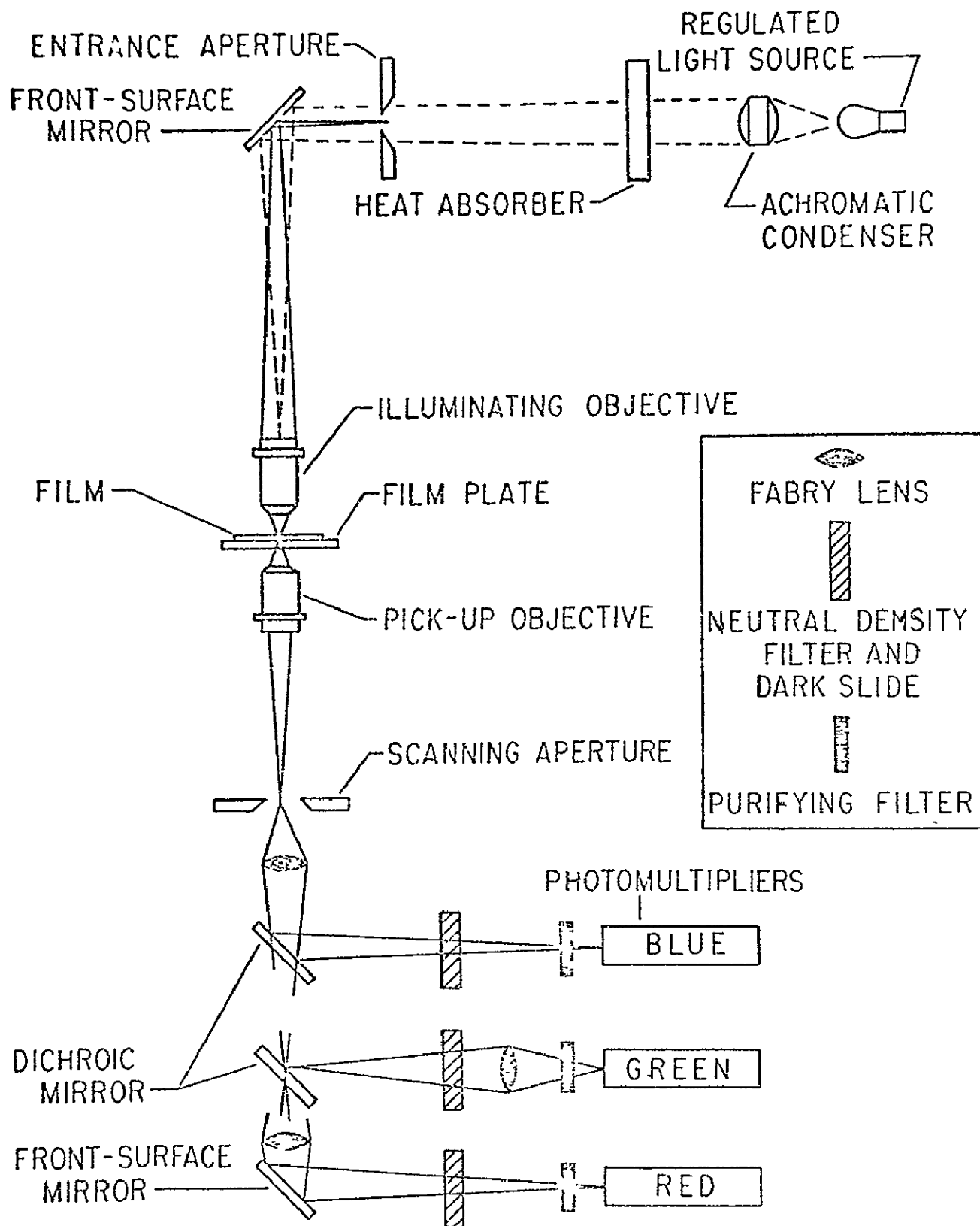


Figure 7.- Schematic diagram of trichromatic microdensitometer.

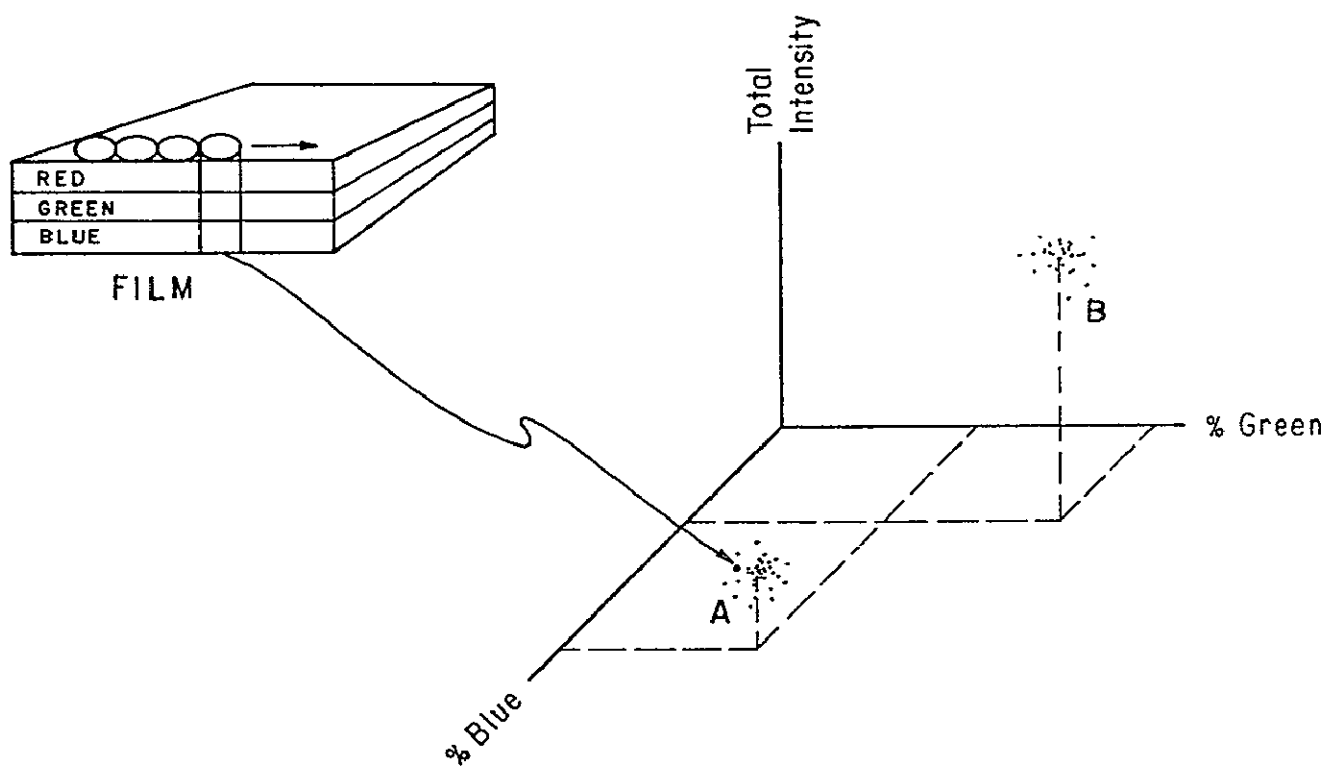


Figure 8. Schematic diagram of three-color space. Clusters of density data for two different classes (A and B) are indicated by dots.

SLICE 7

	1	2	3	4	5	6	7	8	9	10	11	12	13	14	15	16	17	18	19	20	21	22	23	24
1	0	0	0	0	0	0	0	0	0	0	0	0	0	0	0	0	0	0	0	0	0	0	0	0
2	0	0	0	0	0	0	0	0	0	0	0	0	0	0	0	0	0	0	0	0	0	0	0	0
3	0	0	0	0	0	0	0	0	0	0	0	0	0	0	0	0	0	0	0	0	0	0	0	0
4	0	0	0	0	0	0	0	0	0	0	0	0	0	0	0	0	0	0	0	0	0	0	0	0
5	0	0	0	0	0	0	0	0	0	0	0	0	0	0	0	0	0	0	0	0	0	0	0	0
6	0	0	0	0	0	0	0	0	0	0	0	0	0	0	0	0	0	0	0	0	0	0	0	0
7	0	0	0	0	0	1	0	0	0	0	0	0	0	0	0	0	0	0	0	0	0	0	0	0
8	0	0	0	0	2	12	2	0	4	2	0	0	0	0	0	0	0	0	0	0	0	0	0	0
9	0	0	0	1	1	6	11	13	9	32	31	15	3	0	0	0	0	0	0	0	0	0	0	0
10	0	0	0	0	0	1	8	11	12	11	12	10	1	0	0	0	0	0	0	0	0	0	0	0
11	0	0	0	0	0	1	4	10	15	6	2	4	0	0	0	0	0	0	0	0	0	0	0	0
12	0	0	0	0	0	0	0	5	12	18	9	3	1	0	0	0	0	0	0	0	0	0	0	0
13	0	0	0	0	0	0	0	5	19	21	8	3	0	0	1	1	1	0	0	0	0	0	0	0
14	0	0	0	0	0	0	0	2	22	30	28	5	0	0	2	1	0	0	0	0	0	0	0	0
15	0	0	0	0	0	0	0	0	5	31	47	24	1	1	0	0	0	0	0	0	0	0	0	0
16	0	0	0	0	0	0	0	0	0	4	14	25	4	0	0	0	0	0	0	0	0	0	0	0
17	0	0	0	0	0	0	0	0	0	0	2	5	1	0	0	0	0	0	0	0	0	0	0	0
18	0	0	0	0	0	0	0	0	0	0	0	0	0	0	0	0	0	0	0	0	0	0	0	0
19	0	0	0	0	0	0	0	0	0	0	0	0	0	0	0	0	0	0	0	0	0	0	0	0
20	0	0	0	0	0	0	0	0	0	0	0	0	0	0	0	0	0	0	0	0	0	0	0	0
21	0	0	0	0	0	0	0	0	0	0	0	0	0	0	0	0	0	0	0	0	0	0	0	0
22	0	0	0	0	0	0	0	0	0	0	0	0	0	0	0	0	0	0	0	0	0	0	0	0

61-22

Figure 9.- Seventh layer of green-blue space showing frequency distribution of data that depict four terrain classes. This layer is 7/22 of the way between least and greatest densities, and is therefore of relatively bright objects. Computer processing by E G&G, Inc.

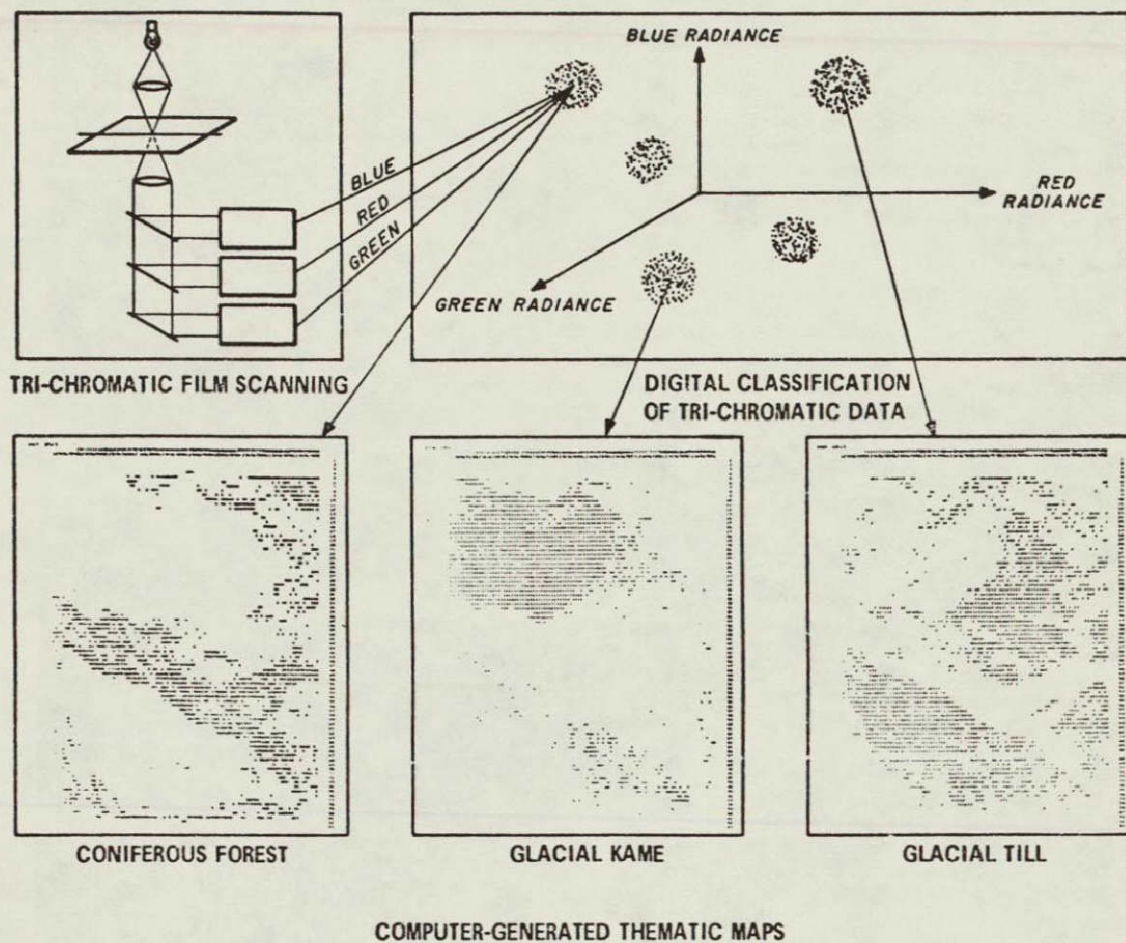


Figure 10.- Schematic diagram showing three-color method of producing terrain maps using computer clustering technique.

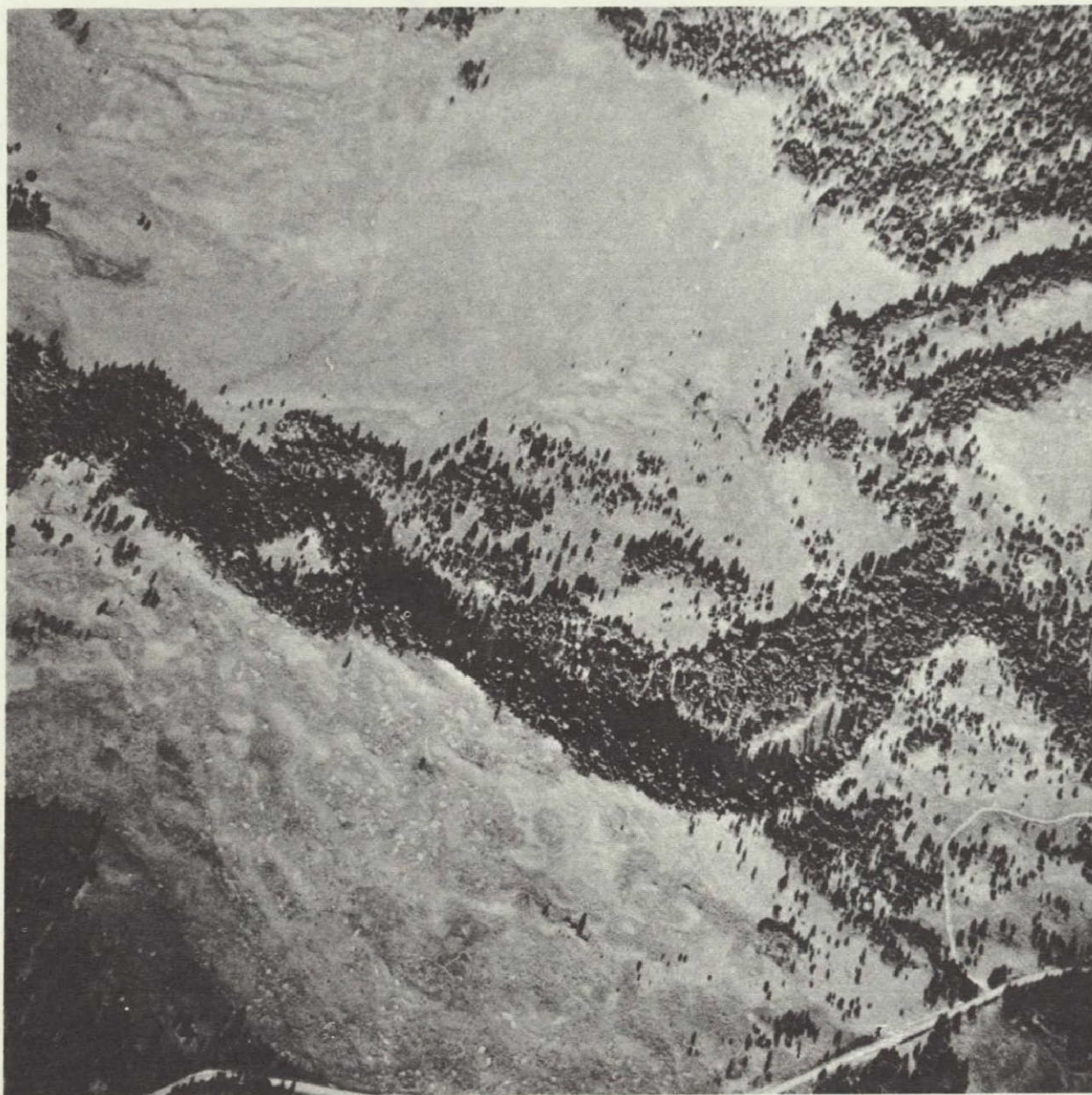
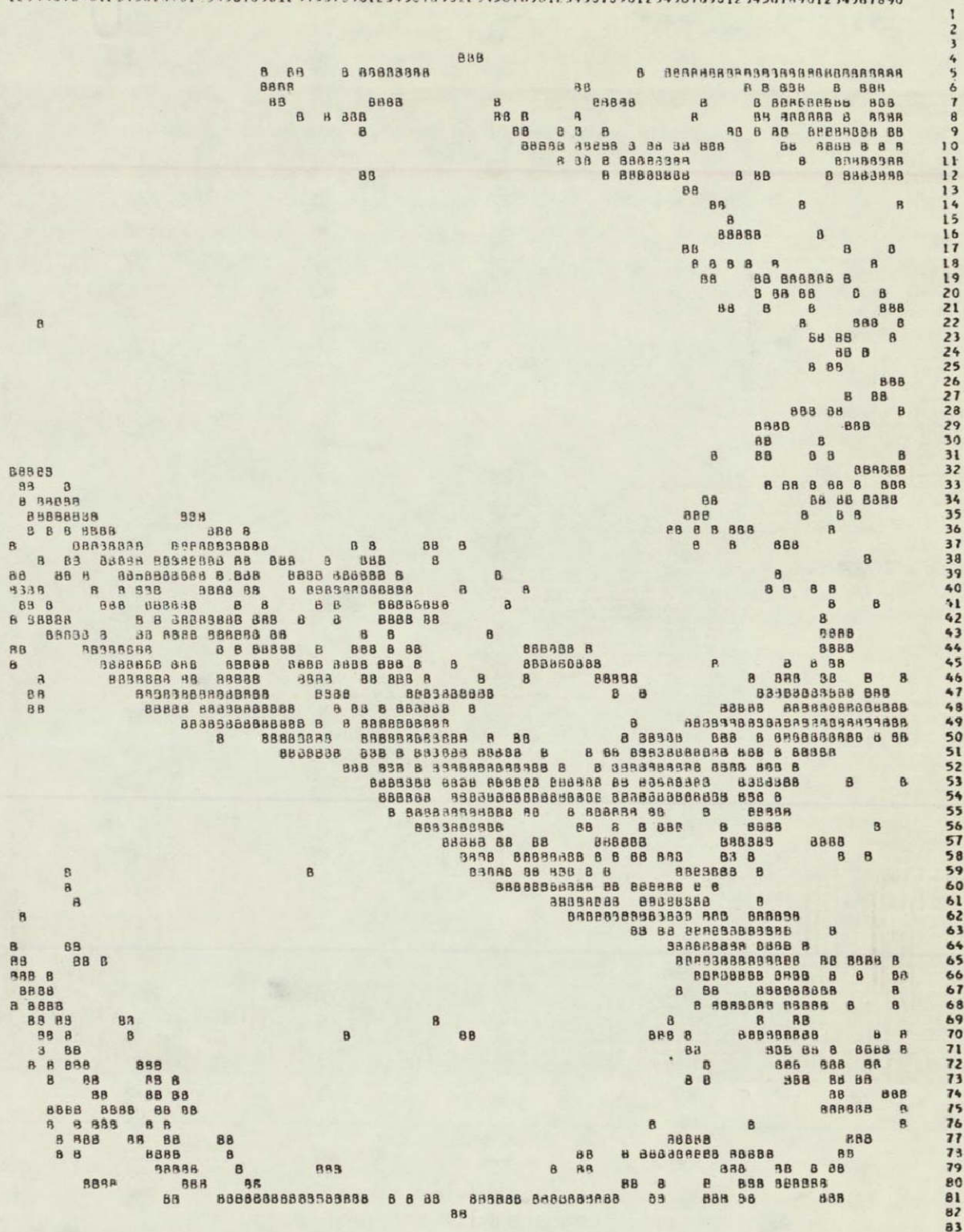


Figure 11.- Photographic copy of the second color infrared image studied. Compare with map of Figure 13.

This page is reproduced again at the back of this report by a different reproduction method so as to furnish the best possible detail to the user.

11111111122222222223333333333344444444445555555555566666666666777777777788888888889999999999
 12345678901234567890123456789012345678901234567890123456789012345678901234567890



(Illustration not received for publication)

Figure 13.- Map showing distribution of five terrain units plus shadows. Made by drafting and color-coding the separate computer maps of classes.

Color code

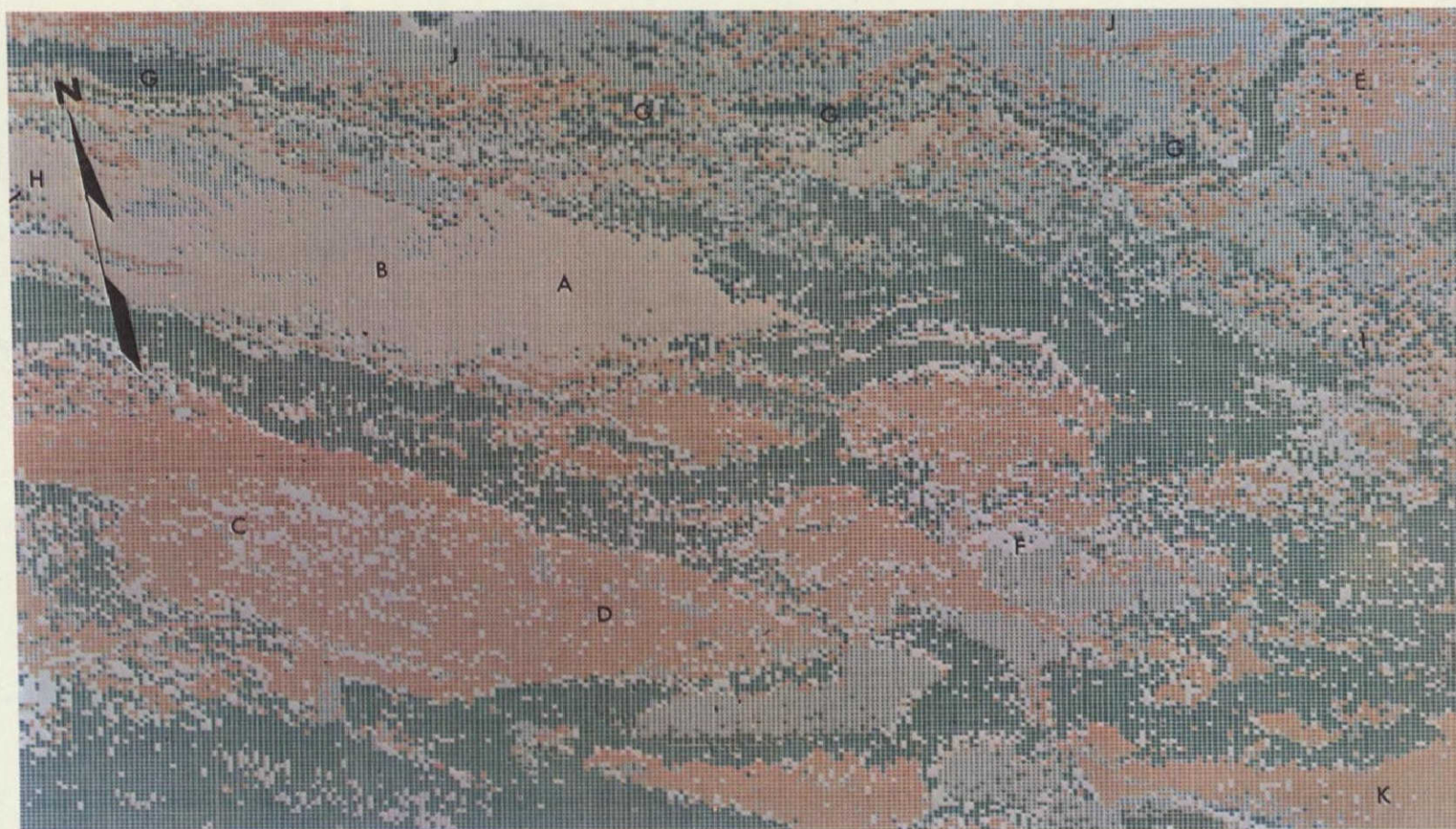
Orange	Meadow underlain by glacial kame	Green	Deciduous trees and bushes
Yellow	Meadow underlain by glacial till	Gray	Talus
		Black	Shadows
Blue	Evergreen trees	White	Other



Figure 14. Terrain map of test site made by digital computer using supervised techniques. This hand-colored computer printout depicts eight terrain classes plus shadows. Computer processing LARS, Purdue University, using channels 2, 9, 10, and 12.

Color code

Red	Bedrock	Dark green	Conifers
Dark brown	Vegetated bedrock rubble	Light green	Marsh and bog
Purple	Talus	Blue	Water
Light brown	Glacial till	Black	Shadows
Yellow	Glacial kame	White	Other (reject)



0 | 1 km

Figure 15.- Terrain map of test site made with digital computer using supervised technique and preprocessing to normalize the data as a function of scan angle (ref. 17). This computer-colored printout depicts eight terrain classes plus shadows. Computer processing by WRL, University of Michigan, using channels 2, 5, and 12. Letters indicate areas referred to in Table 1.

Color code

Dark blue	Bedrock	Dark green	Forest
Light blue	Vegetated bedrock rubble	Light green	Bog
Dark red	Glacial till	Black	Water
Light red	Glacial kame	Light gray	Shadow
Medium gray	Talus	White	Other (reject)

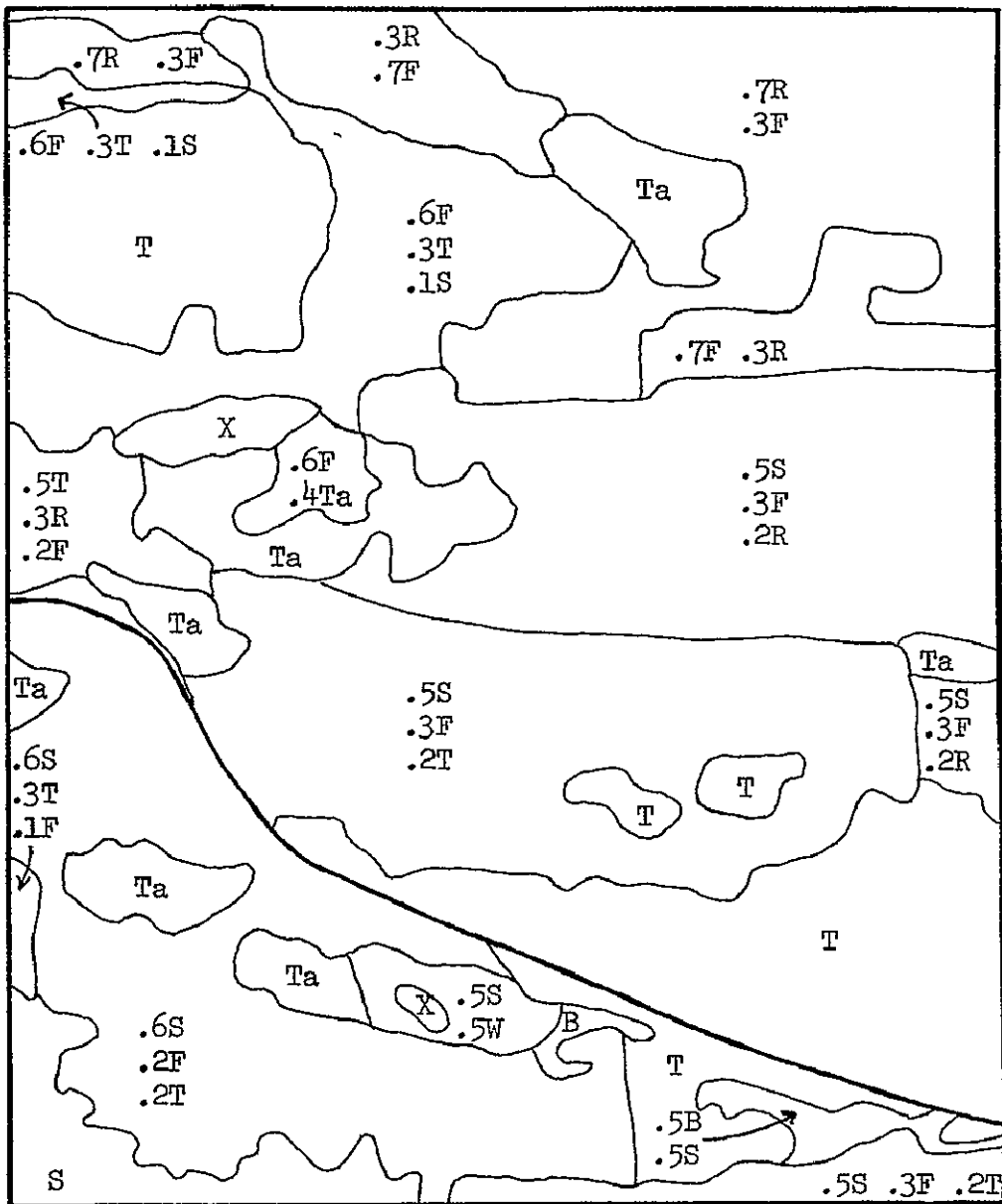
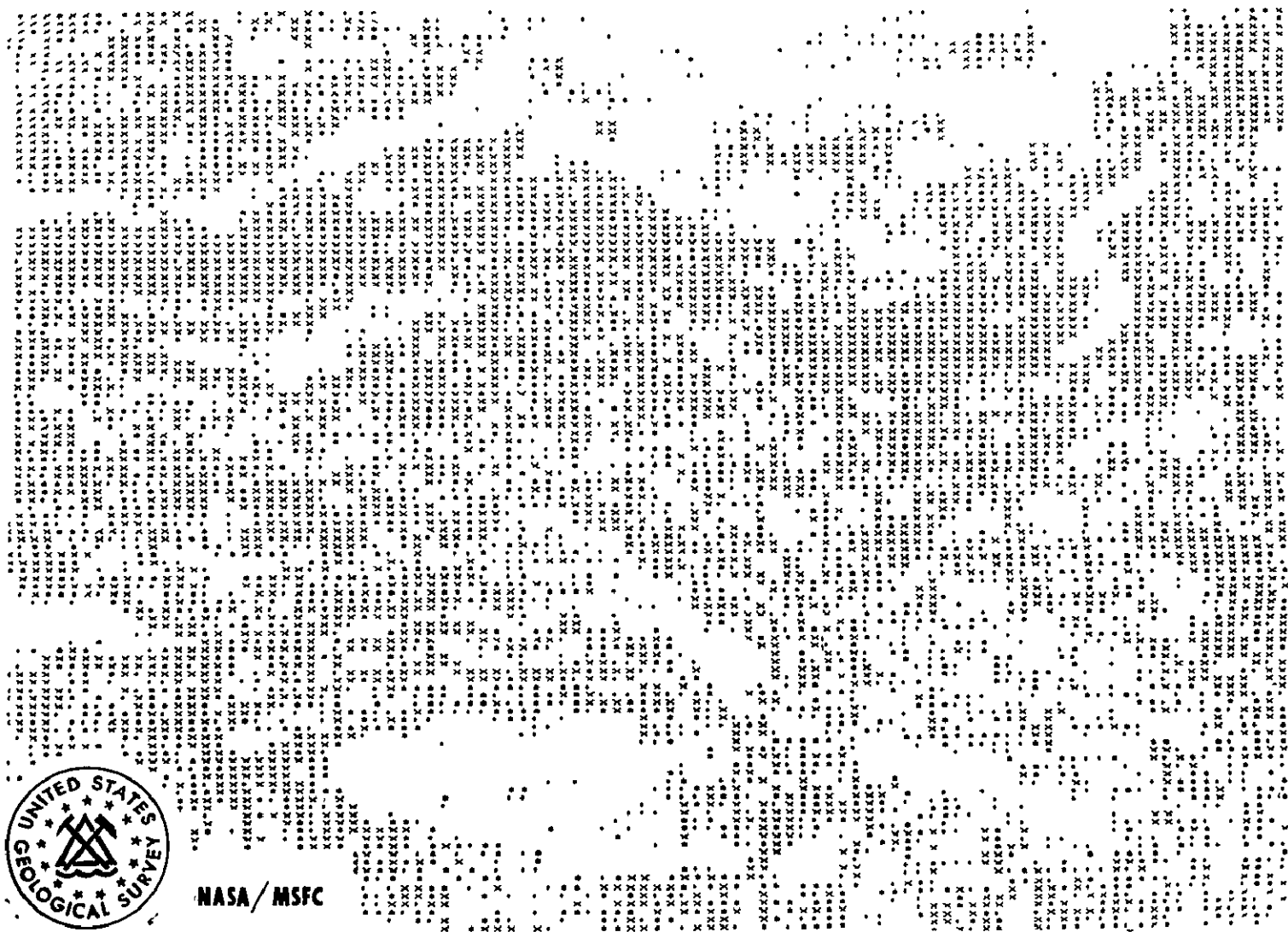


Figure 16.- Generalized ground control map of part of test site. Numbers indicate decimal proportion of classes present in each outlined area. Classes are indicated by letters:
 T Meadow and grassland underlain by glacial till,
 K Same as T but underlain by glacial kame;
 Ta Talus; X bedrock; R vegetated bedrock rubble,
 F forest; B bog, W water; S shadow;
 The dark line is a road.



NASA / MSFC

Figure 17.- Computer-generated boundary map of part of the test site. Distinctness of classes is indicated by whether the change in n-dimensional reflectance across the boundary is greater than 70, 80, or 90 percent of the rest of the data, shown by ., **, and x, respectively. Blank areas are homogeneous. Segment corresponds with NE part of area shown in Figures 3, 4, 14, and 15. Curved blank area is part of Yellowstone River. Computer processing by NASA/MSFC.

SECTION 62

FUNCTIONS AND ACTIVITIES OF THE
ARIZONA REGIONAL ECOLOGICAL TEST SITE

by

L. K. Lepley
Office of Arid Lands Studies
University of Arizona
Tucson, Arizona

INTRODUCTION

After one year of operation, the Arizona Regional Ecological Test Site has established in Tucson and Phoenix, staff and facilities for the coordination and transfer to the public the technology of application of remote sensing to earth resources and environmental problems in Arizona.

ARETS is administered through the Office of Arid Lands Studies, College of Earth Sciences, in the University of Arizona. The ARETS Project Manager is myself and the ARETS branch office in Phoenix is under the management of Herbert Schumann.

OBJECTIVES

The objectives of the ARETS Project are:

1. to establish a multidiscipline resources and environment team in Arizona capable of applying satellite and supporting aircraft data to expedite remote sensing technology transfer to user-agencies;
2. to conduct coordinated multidiscipline experiments in the use of ERTS data;
3. to determine future resources and environment information needs for Arizona;

4. to provide and recommend facilities, instruments and training necessary to support the practical uses of remote sensing data.

PROCEDURES AND RESULTS

1. ARETS coordinates the ERTS and EREPS investigations in the Arizona area. The figure shows, under the label of ARETS '71, the outlines of the Mission 155 flown by NASA's RB-57 in January, 1971. This area bounded most of the Arizona disciplinary sites active one year ago. Mission 155 was to provide base data for all of the investigators in the area but was only partially successful in that incomplete coverage was obtained with somewhat overexposed and low-contrast color and multispectral photography and only a small percentage of the area was covered with metric infrared color.

Almost one year ago, one of the first efforts of the ARETS headquarters was to recruit and assist in the preparation of ERTS-A proposals by potential Arizona investigators. The figure shows the approximate geographic areas of the ARETS/ERTS-A investigations, indicating the geographic expansion of ARETS north to the Nevada border and south to include the northern Gulf of California, and east to 109 degrees longitude.

We have established agreement among several of the approved ERTS investigators to coordinate field work and attempt to establish compatible legend systems, especially for the vegetation studies.

2. We have established film libraries and data processing centers in Tucson and Phoenix which include films from Mission 155, 101, the U-2 ERTS-simulating flights and others including some non-NASA photography.

We have at both locations large light tables and polyfax film copiers and in Tucson, we have an I²S multispectral viewer. We have recently received copies of the U-2 ERTS-simulating multispectral photography for which the I²S is particularly useful. Our film libraries have had intensive use by exploration geologists from the copper mining industry in the Tucson area, by students conducting thesis research in geology, soils, forestry studies, etc. at the University and by state and federal agencies in the Phoenix area.

3. To expedite technology transfer, we have devoted considerable effort to training, and public information in the general application of remote sensing in the use of high-altitude aerial photography and satellite data. The ARETS Project Manager and the Phoenix Coordinator have provided several public lectures describing ARETS and the ERTS programs. Our staff has devoted considerable time in advice and consultation in the use of ERTS and other remote sensing data.

The Office of Arid Lands Studies has initiated a remote sensing service project entitled, "Research for Applications of Remote Sensing to State and Local Governments". The objective of this project is to establish a service-oriented remote sensing agency to assist state and local agencies in the use of high-altitude photography in planning, zoning and environmental monitoring and assessment. Its Advisory Committee includes the Planning Directors of the State of Arizona, Cochise and Pima counties and members of the University of Arizona including the ARETS Project Manager.

The first ARETS symposium was the Workshop conducted in October 1970. In November 1971 the second ARETS symposium entitled, "Applied Remote Sensing in Arizona", attracted 172 speakers and participants, most of whom are potential users of NASA's present and future remote sensing data acquired in Arizona.

The Project Manager has taught a one semester university course in remote sensing with emphasis on the use of small scale imagery and on the optical physics of the earth's surface.

There is considerable need and demand here in Arizona for a remote sensing short course available to local government agencies, institutions and industries. This short course is now under development at ARETS.

ARETS publishes at irregular intervals an information bulletin pertaining to the ERTS program in this area.

4. We have established a center for ground truth technology.

Mr. Christopher Thompson, of the Optical Science Center, University of Arizona, is now designing and assembling a miniaturized optical ground truth instrument package for ARETS which includes a low-cost camera-size field spectrometer, a low-cost camera-size thermal radiometer, and 35 mm. camera clusters. This package is for general use by ERTS investigators.

5. We are conducting in-house demonstration pilot projects in remote sensing. Two of these projects by ARETS headquarters are in the fields of (1) geothermal prospecting, and (2) air pollution mapping. The U. S. Army has agreed to provide aerial thermal imagery over certain potential geothermal areas. Considerable interest in the use of remote sensing techniques as an aid in geothermal exploration in Arizona has been generated. In Tucson, we have been conducting multispectral, multipolarization photographic experimentation in the detection and mapping of air pollution from the copper smelters in this region. We have obtained multispectral and multipolarization photography from mountain top fire stations, low and medium altitude light planes, and are presently analyzing the U-2 ERTS-simulation photography for this application.

These in-house remote sensing projects have two purposes: (1) to generate public interest in the application of remote sensing to visible problems; and (2) to recruit ERTS-B proposals from within Arizona institutions, agencies and corporations.

6. We have encouraged international cooperation in the experimental use and application of remote sensing through contacts with Mexican federal agencies and the University of Sonora. One of the new University of Arizona ARETS/ERTS-A investigations involves the study of the marine environment of the northern Gulf of California. This investigation will be carried out in cooperation with the University of Sonora and Mexican federal agencies, thus bringing international aspects to ARETS.

The U. S. Office of Economic Opportunity has agreed to support a project whose end purpose is to domesticate a wild desert shrub found in Southern Arizona and particularly on the Indian Reservations. This shrub, *Simmondsia*, known locally as jojoba, produces a nut rich in a liquid wax having characteristics making it a possible raw material for the manufacture of the following:

1. cosmetics
2. hard crystalline wax
3. high temperature lubricant
4. most importantly, a possible replacement for sperm whale oil now used as automatic transmission fluid.

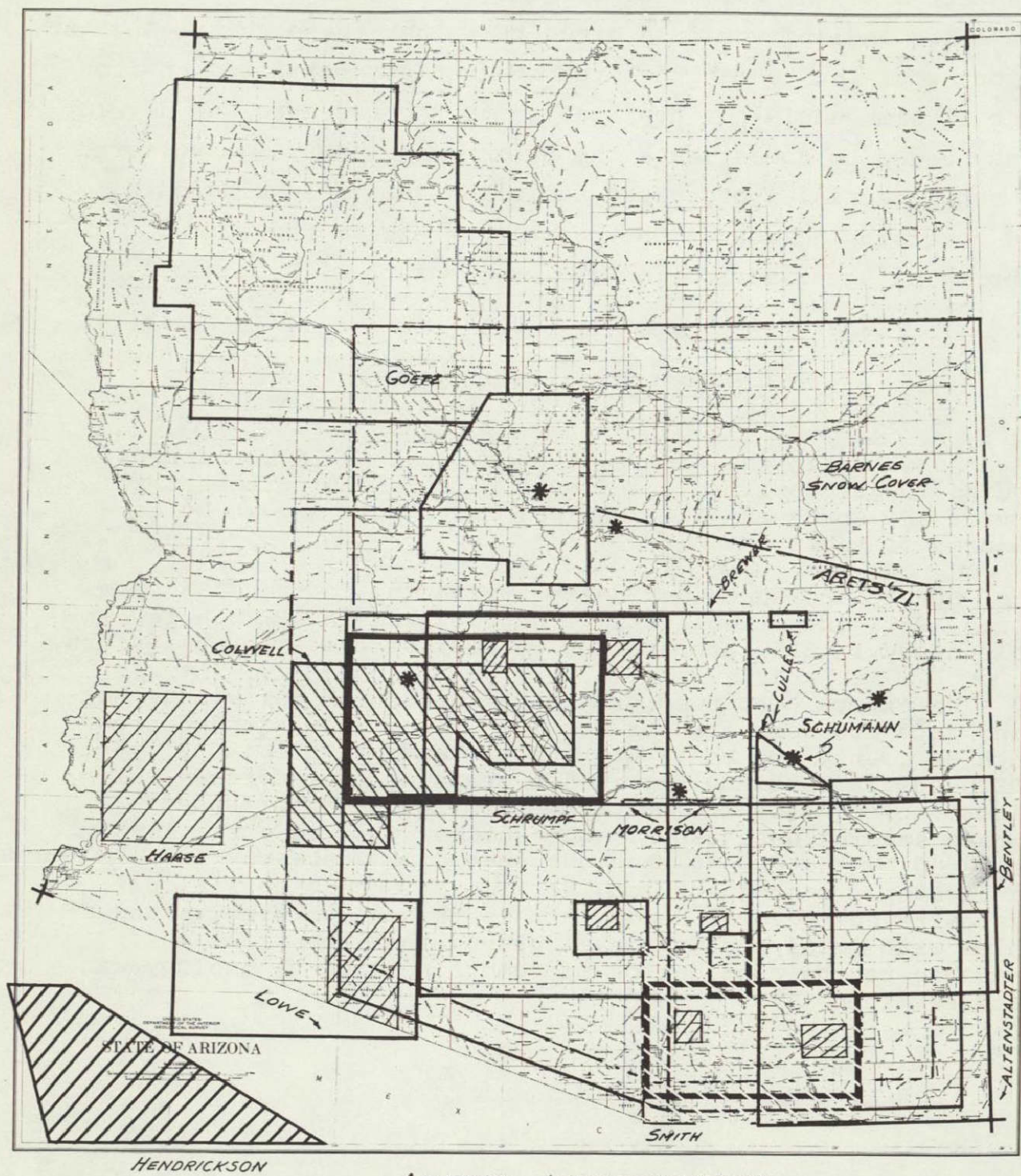
The first step would be to gather sufficiently large quantities of the wild nuts for large scale industrial test of the oil. Indians would be hired to gather these nuts. Another effort would be to map the distribution and preferred environment of Simmondsia for application to the research and development needed to domesticate the Simmondsia. ARETS has offered to supply aerial photography and other remote sensing data and to train Indians as photo interpreters in the aerial mapping of the distribution and environment of Simmondsia.

DISCUSSION AND CONCLUSIONS

As shown in the figure, the original ARETS boundaries are no longer applicable and must be expanded northwest to Nevada and southwest into Mexico, and should herein be considered flexible.

Due to the announced delay in funding to the NASA sponsored ARETS investigations, we expect here in ARETS a regrettable delay in ERTS preparation by most of these investigators.

We expect continued growth in the use of our remote sensing data and need for our services to non-NASA funded groups such as county and state governments and private industry. ARETS should continue to provide training and advisory services, information and encouragement to the "non-funded" remote sensing data users. Our success will be partially measured by the extent that our subsidized research is able to develop a cost-justified, service-oriented, operational system keyed to local needs. It is through working relationships with local working-level groups that the problems amenable to the application of remote sensing technology can be determined.



ARETS INVESTIGATION
SITES

SECTION 63

N72-29361

APPLICATIONS OF REMOTE SENSOR DATA BY STATE AND
FEDERAL USER AGENCIES IN ARIZONA

by

Herbert H. Schumann
U.S. Geological Survey
Water Resources Division
Phoenix, ArizonaABSTRACT

The Arizona Regional Ecological Test Site (ARETS) project was established in the fall of 1970 by the U.S. Geological Survey at the request of NASA to consolidate research efforts and to develop a multidisciplinary team in Arizona capable of applying remote sensor data to the State's environmental and resources problems in a timely and effective fashion. During the past year local, State, and Federal agencies in Arizona for the first time have had direct access to remote sensor data collected over the State through the ARETS project.

The U.S. Bureaus of Indian Affairs and Land Management are using NASA high altitude aerial photography (Mission 155) of southeastern Arizona to develop a natural resources information system for Federal lands. The Geological Survey has used high altitude aerial photography to develop an orthophotomosaic of Maricopa County, and has produced orthophotoquads covering the Phoenix metropolitan area. These products together with high altitude aerial photography are being used by local, State, and Federal agencies in connection with geologic mapping projects, water resources investigations, and land use studies to determine the alignment of a proposed major aqueduct.

Arizona governmental agencies are using NASA high altitude aerial photography in connection with land use planning, to detect changes in land use, to confirm land ownership boundaries, and for legislative reapportionment mapping. Other applications include mapping vegetative cover, evaluation of changes in wildlife habitat, location of deer kills, and as a base for recording telemetry data from radio-collared big game animals.

The Arizona Regional Ecological Test Site (ARETS) project was initiated in October of 1970 by U. S. Geological Survey (USGS) Earth Resources Observation System (EROS) program at the request of NASA to consolidate research efforts designated to test and evaluate air and spaceborne remote sensor methods and applications to environmental and resource problems in southern Arizona. The ARETS project has as a major objective to develop a multidiscipline resources and environmental team in Arizona capable of utilizing data to be acquired by satellites and supporting aircraft in a timely and effective fashion. The project also has as a major objective to determine the future information needs of the Arizona resources and environmental community and prepare recommendations on the types of facilities, instrumentation, and training that should be developed to support the community.

Early in the project it became apparent that, because of the large size of the test site (approximately 33,000 square miles) and the State's population distribution (approximately 50 percent of the population resides in central Arizona in Maricopa County), it would be necessary to establish two ARETS data centers to provide the remote sensor data necessary to meet the project objectives. One data center was established at the University of Arizona in Tucson, Arizona under the direction of Dr. L. K. Lepley. The second data center was established at the Federal Building in Phoenix, Arizona, under the direction of the author. Because all State and Federal governmental agencies responsible for management of Arizona's resources are headquartered in Phoenix, the State Capital, the author was assigned special responsibility for coordination of ARETS activities with State and Federal agencies in Arizona.

The assistance, guidance, and support of Mr. William A. Fischer and Mr. W. D. Carter of the EROS office is gratefully acknowledged. The encouragement and support of the Honorable Jack Williams, Governor of Arizona, and his staff is also gratefully acknowledged. Mr. Herbert E. Skibitzke of the USGS research facility in Prescott, Arizona, and Mr. James Webster, Chief of the Photogrammetry & Mapping Division of the Arizona Highway Department have both furnished aircraft and photographic support during

the past year. Mr. O. E. Zeitler and his staff at NASA-MSC have furnished NASA imagery in a timely manner.

During the past year local, State, and Federal agencies in Arizona for the first time have had direct access to NASA air and spaceborne remote sensor data through the ARETS data centers.

The lack of reproducible copies of the color and color infrared photography has been a major limitation to making evaluations and applications of this imagery by user agencies. However, the development of the photographic laboratory within the EROS Data Center near Sioux Falls, South Dakota should solve this problem during the coming year.

This report will summarize preliminary evaluations and applications of the high altitude aerial photography and other remote sensor data by State and Federal user agencies in Arizona during the past year.

ARIZONA LAND OWNERSHIP

To understand the needs of the State and Federal user agencies, responsible for management of Arizona's resources, it is instructive to examine the distribution of land ownership. Nearly 72 percent of Arizona is controlled, owned, or managed by the Federal government. Included in this amount are nineteen Indian reservations, seven National forests, and eighteen National monuments. Roughly 13 percent of Arizona is owned by the State and about 15 percent of the land is privately owned. Although only 28 percent of Arizona is state and private land, these lands are scattered throughout the more than 113, 000 square miles of the State.

The widely scattered distribution of land ownership, together with a very rapid population growth and resultant land use changes, necessitates the acquisition of timely and accurate land use information for use by State and Federal land and resources management agencies. During the past year, the Arizona Land Use Committee, composed of representatives of both State and Federal agencies, recommended to Governor Jack Williams that a comprehensive land use inventory be developed in Arizona.

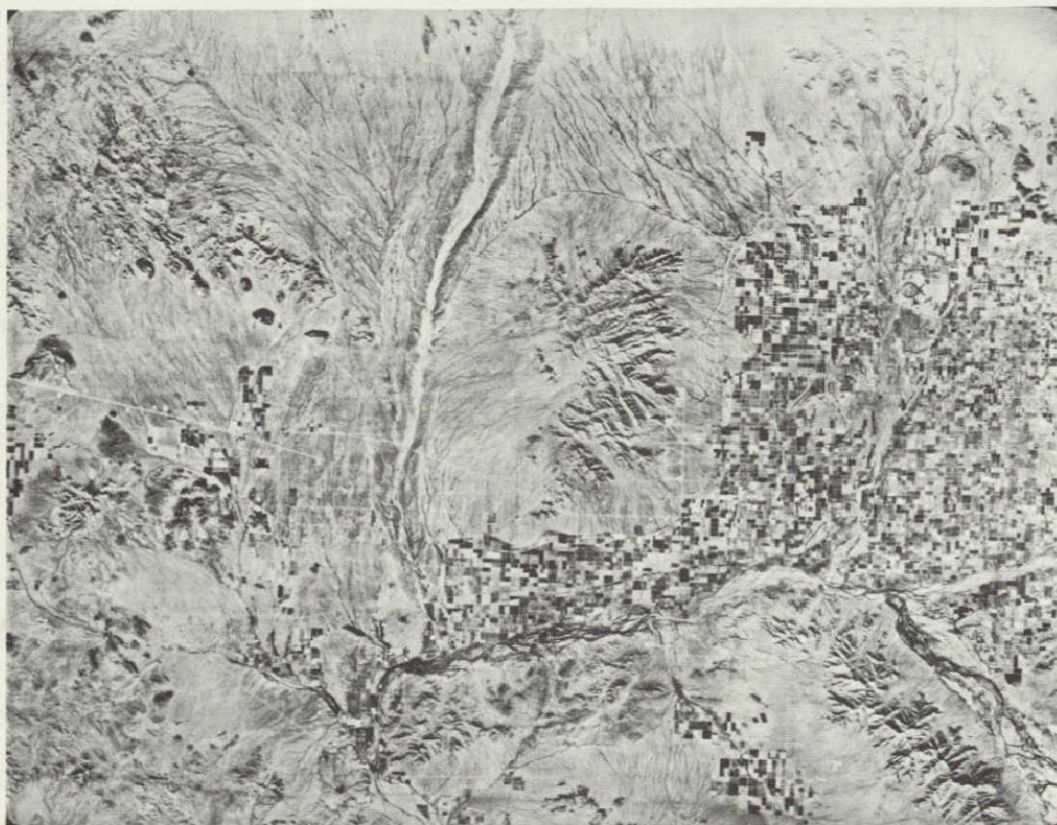


Figure 1. - Orthophotomosaic of western Maricopa County,
Arizona. Original compiled at 1:125,000 scale

In August of 1971, Governor Jack Williams initiated the Arizona Resources Information System project (ARIS) to develop a comprehensive land use inventory of Arizona. This project, under the direction of Mr. Carl C. Winikka of the Governor's Office, will make extensive use of remote sensor data.

APPLICATIONS BY FEDERAL AGENCIES

U. S. BUREAU OF INDIAN AFFAIRS AND BUREAU OF LAND MANAGEMENT

The U. S. Bureau of Indian Affairs (BIA) and the Bureau of Land Management (BLM) have the combined responsibility of managing nearly half the land in Arizona. During the past year, BIA and BLM have contracted Boeing Computer Services, Inc. to develop a natural resources information system for Federal lands. This system is being developed using NASA high altitude aerial photography (Mission 155) of southeastern Arizona.

The Bureau of Land Management plans to use ERTS-A imagery during the coming year to attempt to predict ephemeral and perennial range quantity and quality in southern Arizona. This project will involve active participation of BLM field personnel to develop applications of repetitive space imagery to aid in the solution of range management problems.

U. S. GEOLOGICAL SURVEY

The U. S. Geological Survey has developed a 1:125,000 scale orthophotomosaic covering approximately 8,000 square miles of Maricopa County (figure 1) and six orthophotoquads covering the Phoenix metropolitan area at a 1:24,000 scale using high altitude aerial photography (DOD photography and NASA Mission 155) as part of the USGS Arizona Urban Area Pilot Study. The orthophotomosaic consists of two sheets and was developed primarily for use in connection with land use planning. This mosaic is also being used by local, State, and Federal agencies in connection with geologic

mapping projects, water resources investigations, flood control studies, and to determine the alignment of a proposed major aqueduct.

The Geological Survey has also developed 1:24,000 and 1:50,000 scale orthophotoquads in the Mesa area that meet National map accuracy standards (figure 2). State and Federal agencies are presently evaluating the orthophotoquad as a map base for land use studies in Arizona.

The Geological Survey has used NASA high altitude aircraft and Apollo photography in various water resources investigations to map cultivated acreage, to make drainage area studies, to assist in site selection for hydrologic instrumentation, and as a base for the delineation of flooded areas.

During the coming year the Geological Survey, in cooperation with local water user agencies, plan to use the ERTS-A Data Collection System to transmit information from stream gages and precipitation gages located in remote areas of central Arizona to provide near real-time data to assist in making water management decisions. ERTS-A imagery will be used to study evapotranspiration in the Gila River Basin and to map the distribution of phreatophytic vegetation along major rivers and streams in southern Arizona.

APPLICATIONS BY ARIZONA STATE AGENCIES

During the past year, several State agencies have evaluated high altitude photography of Arizona received from the NASA Manned Spacecraft Center in Houston and through the ARETS Data Center in Phoenix. Uses and applications of this imagery by State agencies have been documented by Mr. Carl C. Winikka and the following is a summary of Mr. Winikka's report.

ARIZONA STATE PARKS BOARD

Arizona State Parks Board has used enlargements of NASA Mission 101 photography of Picacho Peak and vicinity to develop an

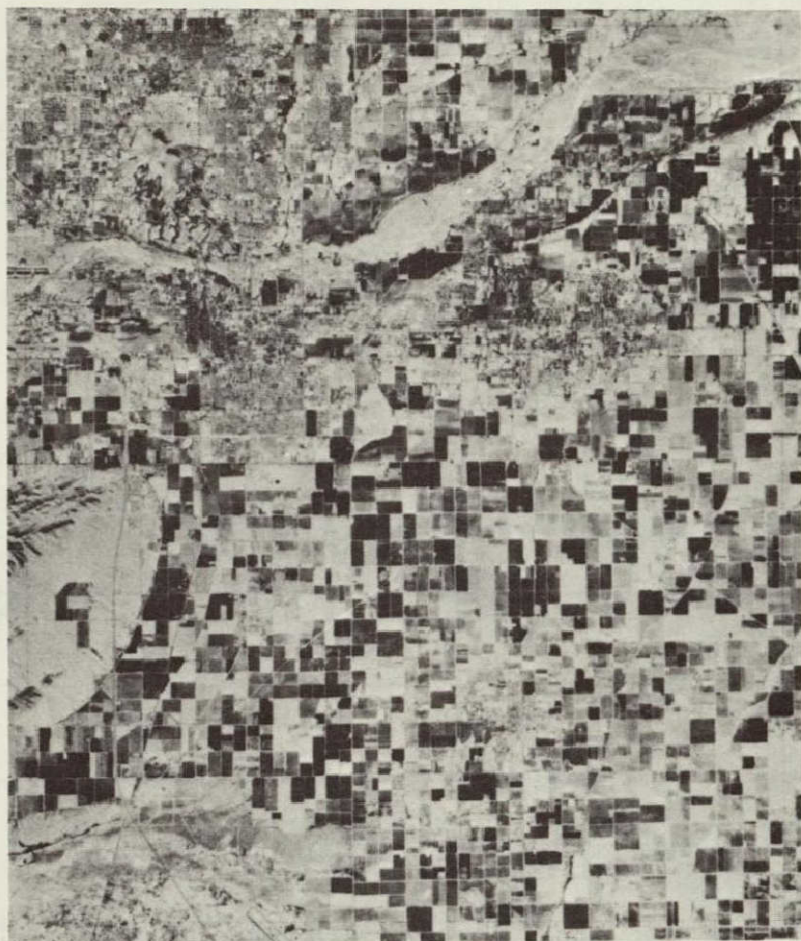


Figure 2. - Orthophotomosaic of the Mesa 15 Minute Quadrangle, Arizona. Original compiled at 1:50,000 scale.

environmental study of the Picacho Peak State Park. The Park is adjacent to Interstate Highway 10 approximately 40 miles northwest of Tucson, Arizona.

ARIZONA DEPARTMENT OF PROPERTY VALUATION

Arizona Department of Property Valuation has used 1:24,000 scale enlargements of NASA Mission 101 photography over the 100,000-acre San Carlos Irrigation Project in central Arizona to confirm land ownership boundaries and to verify legal descriptions of property. During the past 40 years, many land exchanges have occurred between private, State, and Federal lands within the project area and records of these transactions contain serious inconsistencies that are difficult to resolve.

ARIZONA GAME AND FISH DEPARTMENT

Arizona Game and Fish Department has used NASA Mission 158 photography of the Three Bar Wildlife Areas, near Roosevelt Lake in central Arizona, for vegetative cover mapping, hunter orientation, and field location of deer kills. This study indicates deer hunters had little difficulty in determining precise locations of deer kills with only minimum orientation and instruction in use of the photography by the Arizona Game and Fish Department personnel. The resulting map of deer kills is probably the most accurate map of this type prepared to date in Arizona.

Other applications by the Arizona Game & Fish Department include the use of enlarged Mission 101 photography as base for recording radio-telemetry data for tracking Javelina herds in the Totalita Mountains of southeastern Arizona. Future plans include the use of enlargements of Mission 155 photography of southern Yavapai County in central Arizona as a base for recording activities of radio-collared mountain lions.

ARIZONA HIGHWAY DEPARTMENT

The Arizona Highway Department has used high altitude aerial photography from NASA Missions 101, 146, 155, and 158 in connection with its county mapping program to analyze and map urban change, for updating road locations and cultural detail, and for planning low level aerial photography missions. Other applications include use of Mission 158 photography for drainage studies southwest of Tucson, Arizona and Mission 101 photography to prepare a photomosaic of the Tucson metropolitan area for use by the Arizona Highway Engineer in making public presentations of proposed locations for new freeways. This mosaic will also be used in the design of the Tucson freeway system.

LEGISLATIVE REAPPORTIONMENT MAPPING

NASA Mission 123 photography flown on March 16, 1970 was used as a reference for reapportionment mapping of the greater Phoenix area. The court requirement was for data as of April 1, 1970 for the reapportionment mapping. Although the Mission 123 photography was not the most recent photography available, it was very timely for this application.

SUMMARY AND CONCLUSIONS

During the past year several State and Federal user agencies in Arizona for the first time have had access to remote sensor data through the ARETS Data Centers. Although the lack of reproducible copies of the color and color infrared imagery did present a major limitation to the evaluations and applications of the imagery, it is believed this limitation will soon be removed by the development of the photographic laboratory facility at the EROS Data Center near Sioux Falls, South Dakota.

Preliminary evaluations of application of remote sensor data by user agencies in Arizona indicate a wide variety of potential and actual applications of high altitude aerial and satellite photography to aid in solution of Arizona's resources and environmental problems. The

consensus of the user agencies participating in these evaluations is that they have only begun to explore the potential applications of high altitude photography and they anticipate the spaceborne imagery from the ERTS and Sky-Lab experiments will have even wider applications.

Evaluations by user agencies indicate the high value of existing imagery as a permanent historical record of land use patterns, conditions of wildlife habitat, and distributions of vegetative cover. This record will prove invaluable as a base for future change detection studies.

C. 3 .

REMOTE SENSING ON INDIAN AND
PUBLIC LANDS

by

Grover B. Torbert
Bureau of Land Management
Washington, D. C.

and Arthur M. Woll
Bureau of Indian Affairs
Washington, D. C.

INTRODUCTION

Although black and white aerial photography has been used by the BLM and BIA since the late 1930's, the present day Bureaus' managers, through the efforts of the Interior's Program EROS, are beginning to look beyond B-W aerial photography. He is asking for the more sophisticated types of sensor data, color, false color and ultra high altitude aerial photography, and infrared and radar imagery. He is asking for more complete and up-to-date inventories of the natural resources. He is more conscious of the part "remote sensing" can play when making management decisions, planning resource programs, writing environmental impact statements, and monitoring his entire program.

Because of his awareness of the possible uses of remote sensing from all platforms the Bureaus' managers have stepped into the aerospace program.

BUREAU OF INDIAN AFFAIRS PROJECTS

The following projects on American Indian lands utilized both aircraft and spacecraft data furnished by NASA.

ARIZONA REGIONAL ECOLOGICAL TEST SITE

The Arizona Regional Ecological Test Site (ARETS) encompasses or is adjacent to a number of Indian Reservations. The topography varies from near sea level to approximately 10,000 feet elevation. The vegetative cover ranges from the Sonora Desert to heavy stands of pine and spruce. There is also a diversity of pressure upon the reservations from urban sprawl within the test site.

PAPAGO RESERVATION

The objective of this project was to complement conventional black-and-white and color aerial photography as well as aeromagnetic data by using satellite and ultra-high altitude multiband aerial photography for mineral exploration.

The study emphasized the need for data from all levels of observation and how each level complemented the succeeding level.

The EROS program office is preparing a report of the study that will be presented to the Papago Tribe. The report will include a recommendation for the continuation of this type of study on the reservation, and expand it to include the work of Stephen Gawarecki of the USGS.

FORT APACHE RESERVATION

This study was designed to furnish an early warning of beetle infestation in the Engleman spruce trees by thermal means. Insect eradication required detection before stress is detectable by false color infrared photography or discoloration of the needles on the trees.

The project did not receive NASA aircraft support and alternate aircraft thermal scanner failures delayed collection of data until November, 1970. Snow and seasonal lateness prevented spatial temperature variations between sick and healthy trees of sufficient differences to analysis.

Continuous monitoring of the beetle infestation by BIA has shown a marked decrease in the beetle population. This may have been caused by cutting practices and natural causes. No additional efforts were made to obtain new thermal data. While trying to develop temperature differences from the high altitude photography, it became apparent that tree size and crown could be counted by computer methods. This was a decided side benefit from the project.

SAN CARLOS RESERVATION

The discovery of the circular feature on Apollo 9 photography and Morenci copper deposits lead to further geological work in the area. The report states..."the area is decidedly anomalous relative to its surroundings..."

The report will be forwarded to the tribe and the tribe's desires will be followed in future activities.

SOUTH DAKOTA

The objective of this study is to use remote sensing data to assist in making land use decisions for Indian lands in southwestern South Dakota. This project is contracted to Dr. Victor Myers of the Remote Sensing Institute of South Dakota University. The contract is unique to the BIA's program because it assigns BIA personnel to RSI , to assist in analysis of the data.

BUREAU OF LAND MANAGEMENT PROJECTS

CADASTRAL SURVEYS USING INFRARED IMAGERY

The objective of this project was to determine the feasibility of using infrared scanned imagery over a forested area to execute a cadastral (property boundary) survey.

The imagery was obtained by the University of South Dakota Remote Sensing Institute as funded by the EROS program. Several flights were made at varying altitudes both during the day and night. Panels of aluminum foil were placed at all corners and control points. The foil, a cool target, was used because of the prohibition of hot targets in a forested area.

The targets placed in openings in the trees were visible on the imagery when enhanced through the computer. However, the ambient temperature of trees corresponded too closely to the targets and positive identification was impractical in the timbered areas or when targets were placed under large trees.

Through its own resources the BLM has financed the following studies which involve remote sensing as the prime input for the data base.

THE CALIFORNIA DESERT STUDY

The goal of the Bureau in this study is to meet the major predicted needs of the 1980's for the California Desert, 11 million acres, and its resources. This includes a full understanding of and a regard for protection of the desert's environmental values. To meet this goal would require: (1) data collection and comprehensive planning; and (2) immediate critical management action.

A small pilot project in data collection using ultra-high aircraft photography was performed by Dr. Dillard Gates and BLM personnel on 100,000 acres. The classification of the plant community was performed using the classification system developed by Dr. Charles Poulton.

The plan as developed includes remote sensing for the inventory and planning phases.

APPLICATION OF ECOLOGY AND REMOTE SENSING IN THE ANALYSIS OF RANGE WATERSHEDS

The purpose of this study was to develop an inventory of the kinds, amounts, distribution, and conditions of each specific ecosystem (vegetation-soil system) found in a management unit area. The study was conducted under Dr. C. E. Poulton of Oregon State University.

Ecosystems were mapped using high quality aerial photography from which a descriptive legend and key for ecological resources were prepared.

NATURAL RESOURCES INFORMATION SYSTEM

INTRODUCTION

The most significant study in terms of impact and potential good to the land managers, to come from the research in remote sensing involving the BLM and BIA, is the "Natural Resources Information System."

The BIA has 50 million acres of land to manage and the BLM has 470 million acres of land plus the outer continental shelf to manage. The size of these areas and the diversity of management problems would indicate a great need for all types of data. Present planning and programming systems provide for maps and numerous overlays as an essential tool for resource managers.

OBJECTIVE

The objective of the study is to develop, demonstrate and deliver a Natural Resources Information System. The system must have the capability of storing, retrieving, processing, and displaying earth resources data derived from ground and remote sensing data.

User Survey. - Starting with top management 120 BLM/BIA employees were interviewed. In addition, 50 non BLM/BIA personnel concerned with resources management or computer application to resources management were interviewed. Reporting forms, procedural manuals, maps, photographs and reports were obtained during these interviews.

The importance of the user survey was that it started at "top management," and developed the goals and objectives of the Bureaus. This permitted the contractor to decide what types and classes of data were relevant to meet the goals and objectives.

Data Collection. - The fact that the demonstration area is in the ARETS project simplified data collection. The data was obtained from the Phoenix Coordinator of the ARETS project.

Other data, maps, and tabulations were obtained from the San Carlos and Apache Indian Reservations and the BLM Safford District Office.

Data Analysis.- Several techniques for automating data handling will be demonstrated.

Density Slicing: To display a selected photographic density and prepare a high contrast overlay to assist in interpretation of data, a monochromatic transparency is electronically scanned and digitized. The data is input into a computer; specified levels of intensity are selected for reproduction; and the processed data is photographically reconstructed either as a continuous tone photograph or overlay.

Datachrome Process: Enhances images by color display.

Color Discrimination: To locate and identify areas of similar spectral characteristics; discriminate object classes; or provide a color index for automated files, the operator will select the region for classification on a color transparency. The density of the three colors are measured and other areas of the image may be quantitatively compared. The areas selected are compiled into automated locations. The output is an index number system and a monochrome transparency.

The results of the techniques plus a review of the literature will be used to recommend subsequent utilization of remote sensing data for information systems.

System Design.- Several information systems were studied to determine the system to best fit the objectives of BLM/BIA. The systems studied were the Canada Land Inventory Earth Resources Information System (University of California), Clari, BLM Systems, Forest Service, State of Minnesota, and Illinois "NARIS."

The system is designed to input from photography, existing maps or other data, and field survey results. The data will be classified as required and digitized, either manual or mechanical. Code, classification, and descriptive data is entered at this time.

During a meeting sponsored by the Geographic Working Group of the EROS program on land classification, it was our understanding that Dr. Anderson's land classification system would be used as a base upon which to build a national land classification system. With this understanding, we adopted it as the base to classify land in the information system.

After the necessary computer routines of reduction, classification, assigning coordinates, etc., data is stored. The data may be processed in combinations and formats as required by the land manager. This may take the form of maps or tabulations.

Demonstration Project.- The contractor, Boeing Computer Services has been right on schedule throughout the contract. We feel he will be prepared to demonstrate the final information system during the month of March as provided in the contract.

The demonstration will display boundaries of resources as polygons. By computer the manager will be able to analyze and synthesize resource data; file reports with in-place data; settle land use and capability conflicts. All the resource data is tied to an overall land use classification.

SUMMARY

In summary there has been a wide diversity of experiments executed by the BIA and BLM. Funding has been from NASA, EROS and in house, and we believe we are gaining the confidence of the land manager as we enter the aero-space era.

SECTION 65

THE REMOTE SENSING OF AIR POLLUTION FROM COAL UTILIZATION

by

Brian M. Harney, Donald H. McCrea, and Albert J. Forney
U. S. Department of the Interior
Bureau of Mines
Pittsburgh, Pennsylvania 15213

INTRODUCTION

ORIGINAL CONTAINS

COLOR ILLUSTRATIONS

The purpose of this project is to investigate the utility of applying data obtained through the Earth Resources Observation System (EROS) of the Department of Interior to the detection and monitoring of air pollution, particularly air pollution caused by coal utilization. Since the EROS program sensors, which use the visible, near, and thermal infrared bands, cannot be used to identify gaseous pollutants per se, it was decided to focus on the detection of the effects of such pollutants. One of the possible effects is air pollution damage to vegetation which can occur at low ambient concentrations^{1/}. Since the near infrared band is often useful in showing changes in vegetative vigor^{2/}, it was thought that this band could be applied to detecting and monitoring vegetative stress caused by air pollution.

A test site was chosen which includes three very large coal-fired power plants and a complex of beehive-type coke ovens. The test site is in a rural area which contains a large number of coniferous trees. These trees are known to be sensitive to low concentrations of pollutants emitted by power plants, especially sulfur dioxide (SO₂). The power plants, relatively new units, burn medium sulfur coal (2 to 3 percent) resulting in stack emissions of up to 2,000 ppm SO₂. The plants are equipped with high-efficiency electrostatic precipitators and have very tall stacks (700 to 1,000 ft). The coke ovens, on the other hand, are quite old and have almost no air pollution controls. These ovens, pyrolyzing coal to coke, emit large quantities of hydrogen sulfide, particulates, and various benzene based organics^{3/}.

For a sensor, a dual 35-mm camera bank was utilized so that color and color infrared film could be exposed simultaneously. This system was chosen for a number of reasons. First, the photogrammetric precision of conventional aerial photography was thought not to be necessary for the scope of this project. In addition, the test site chosen was subject to relatively unpredictable and frequent ground haze conditions. It was thought that a simple camera system would result in needed flexibility in planning the overflights. A third feature was the favorable economy of such a system.

Underlined numbers refer to items in the list of references at the end of this report.

ORIGINAL CONTAINS

COLOR ILLUSTRATIONS

As part of the overall project, a variety of Gemini and Apollo orbital imagery was examined for evidence of air pollution. Several photographs were found in which individual sources of air pollution could be detected, and the dispersal patterns of the resultant plumes observed.

The author would like to acknowledge the aid of Mr. Thomas Starkey, forester with the Ecological Research Division of the Environmental Protection Agency, for providing invaluable assistance in obtaining ground truth for this project. Acknowledgment is also made to Mr. Edward Zeitler, chairman, NASA Earth Resources Data Facility Index, for cooperation in providing samples of Gemini and Apollo imagery.

AERIAL PHOTOGRAPHY

APPARATUS AND PROCEDURE

The sensor utilized consisted of two 35-mm Nikon* Photomic FTN cameras equipped with 50 mm Nikon lenses. Kodak Ektachrome infrared film (35-mm cassettes) was used in one camera, and Kodachrome II color film was used in the other. A Wratten No. 12 filter was used with the infrared film and a No. 1A skylight filter with the color film. The cameras were mounted on an aluminum bar about 40 cm long, equipped with two handles. ASA settings of 25 for the color and 100 for the color infrared and a shutter speed of 1/500 sec for both films produced good results. Cable releases were used to expose the same scene on both films. Exposure settings for the photographs varied with light conditions and were set via "thru-the-lens" individual light meters attached to each camera. The settings worked well for the color film. The exposure, however, was not always correct for the infrared film, and it was found useful to bracket the f stop indicated by the meter by one-half an f stop. Three exposures were, therefore, made, and the photograph with the correct exposure was selected from these.

The aircraft used was a Cessna 150 two-seat, single-engine aircraft. This is a high wing plane offering the advantages of low stalling speed and very good maneuverability. The window of the plane was completely open while the photographs were taken.

The aerial photographic missions were started in May 1971 and continued through September 1971. An additional flight was made in January 1972. The flights were on a weekly basis initially, but they were changed to a bi-weekly basis about midway through the summer. Photographs were made at altitudes from 400 to 3,000 ft above the ground. During the first part of the summer, flights were arranged so that a series of photographs were taken along a line northeast and southwest of each plant. In the second half of the summer, an

* Mention of equipment is for identification only and does not imply endorsement by the Bureau of Mines.

area of Eastern white pine near one of the power plants and the area surrounding the coke ovens were photographed. Immediately after each flight, the exposed film was mailed to the nearest Kodak processing laboratory and was returned processed in a few days. Ground truth was obtained by visiting a number of the areas photographed and examining individual trees in these areas.

DISCUSSION OF THE RESULTS

Figure 1 shows the relative locations of the power plants and the coke ovens along with the prevailing wind path. Eastern white pine, Scotch pine, Austrian pine, and Norway spruce are present in the area. The original assumption was that any detectable damage would be found in the direction of the prevailing wind path. Photographic overflights were initiated along a line northeast (the prevailing wind path) of each plant. Photographs were also taken along a southwest line for comparison. About midway through the summer, it was decided to abandon this procedure owing to the lack of air pollution damage detectable from the aerial photography. A large stand of conifers about 5 miles west of one of the power plants was then examined. It contained areas affected by both air pollution and a fungus-type injury (lophodermium). These areas were photographed with color and color infrared film at varying altitudes.

The utility of infrared film in discriminating types of vegetation was quite useful. There were, however, some problems with infrared renditioning. The first few rolls of film used had been stored commercially for a number of months at room temperature. In this film the deciduous trees are distinguished by a bright magenta color, while the conifers appear a very deep red and purple. When film obtained directly from the factory was used, deciduous trees appear a very bright magenta, while conifers are shades of dark red. It is known that as the film ages, the contribution of cyan in the photograph increases. Refrigerating or freezing the film when it is received will prevent this and keep the film fresh. Interestingly enough, the increased cyan contribution is helpful in bringing out more contrast for the stressed vegetation against the background. However, contrast will be reduced by excessive cyan. The use of a color-compensating filter that shifts the color balance to cyan could help by adding a controlled amount of cyan in the fresh film.

Figures 2 and 3 are color and color infrared photographs of Eastern white pine in the test area, which exhibited symptoms typical of air pollution damage, specifically ozone. Ozone concentrations have been measured in ranges of 12-25 pphm (parts per hundred million) in this region. Although the symptoms were typical of ozone damage, it is known that low levels of sulfur dioxide can also be a contributing factor. Ozone and sulfur dioxide exhibit a synergistic effect whereby nonlethal concentrations of ozone and nonlethal concentrations of SO_2 can combine to form a lethal mixture for many species of conifers¹. Eastern white pine is one of the most sensitive species. The physical appearance of the stressed Eastern white pine is that of an early loss and severe yellowing of needles. The

yellowing of the needles can be seen in figure 2, and the decrease in infrared reflectance for the stressed trees can be observed in figure 3. These photographs were taken from an altitude of approximately 400 ft.

Figures 4 and 5 are aerial color and color infrared views of the coke-oven complex. They show the large amount of effluent from the coke ovens, and its effect on the adjacent hill is obvious. Figure 5 also demonstrates the haze penetrability of the infrared. Although the vegetation on the hill is green, the sparcity of it is readily apparent and contrasts greatly with areas further away from the ovens.

CONCLUSIONS

The use of a simple hand-held camera operated manually from a small aircraft has proved to be successful and has a number of advantages over conventional aerial photography. The chief benefits are economy, ease of operation, and flexibility. Rental of a small plane with a pilot costs about \$25/hr, whereas conventional aerial photography would cost approximately \$400/hr. If one does not require the large coverage or photogrammetric precision of the conventional aerial cameras, this type of operation should be considered. Color infrared film is helpful in discriminating tree species and in cutting haze. Its ability to identify stressed trees is better than color film in some cases, marginal in others. This property apparently varies with cyan contribution in the image.

The air pollution damage to vegetation, which was detectable from the air and identifiable in the photography, was not extensive. Damage to some Eastern white pine was severe, but it is not the major conifer growing in the test site. The symptoms found indicated oxidants as the cause, although sulfur dioxide may be a contributing factor. The damaging effect of coke-oven effluents on the nearby vegetation was easily detected in the aerial photographs. The major damage appeared to be localized to an area adjacent to the coke ovens.

EXAMINATION OF SPACE PHOTOGRAPHY

The space photography was obtained in the form of reels of 70-mm color transparencies from the Earth Resources Data Facility Index at the NASA Manned Spacecraft Center. It was analyzed by comparison with 1:125,000 scale topographical maps and Public Health Service maps of major point sources of air pollution, available for some areas.

Figure 6 is an Apollo 9 color infrared photograph of Arizona just east of Phoenix. This image is from the multispectral SO-65 experiment. A number of air pollution point sources, mainly copper smelters, can be located in this photograph. The most obvious plume is that from the smelting operation

at Hayden, Ariz., and is evidenced by a long wispy plume in the lower central portion of the figure. Some of the other smelting operations, at Superior (northeast of Hayden) and Globe-Miami (north of Hayden), can also be seen in this frame. In these cases, the plume is more of a greyish cloud rather than the continuous plume at Hayden. Figure 7 is an enlargement of the Hayden plume and demonstrates the effect of local topography on the dispersal of air pollution. The plume stays together for some time when leaving the stack, but it apparently begins to disperse when reaching the first string of mountains to the north. Other photographs (figures not shown) that show air pollution sources include Gemini VII S-65-64053 (forest fire plumes in Florida), Gemini XII S-66-63031 (industrial air pollution on the Texas Coast), Apollo 7-8-1918 (industrial air pollution on the Alabama Coast), and Apollo 7-11-2022 (smog over Los Angeles, Calif.).

A Gemini XII photograph (S-66-62796) of northern Arizona and New Mexico has been the subject of some recent controversy. A long plume that crosses the upper portion of the photograph has been interpreted by a number of people as the smoke plume from the Four Corners power plant near Farmington, N. Mex.^{4/}. The plume seems to start near Tuba City, Ariz., and to end near Alamosa, N. Mex. A detailed meteorological study of the photograph, done under contract to a local utility, has indicated that the plume is from an accumulation of jet contrails^{5/}. The line of the plume is coincident with a well-traveled jet aircraft route. Additional evidence that the plume is not from the Four Corners plant is that Farmington lies approximately midway between either end of the plume. The presence of a wind condition to produce a plume going in both directions is improbable.

Gemini and Apollo photography demonstrates the detection of major air-pollution sources dramatically. The chief advantage of such photography is the synoptic quality of such imagery, allowing the interpreter to "track" the plume from its origin to the point at which it is completely dispersed.

Future work will be devoted to refining photographic detection techniques and to applying EROS data to the measurement of particulate air pollution.

REFERENCES

1. Hindawi, I. J. Air Pollution Injury to Vegetation. National Air Pollution Control Administration Publication No. AP-71, 1970.
2. Fritz, N. L. Optimum Methods For Using Infrared Sensitive Color Films presented at the Annual Convention of the Amer. Soc. of Photogram., Washington, D. C., 1967.
3. Smith, G. L., and B. Linsky. Air Pollution Control of Beehive Coke Ovens. Paper No. 71-90 presented at the 64th Annual Meeting of the Air Pollution Control Association, Atlantic City, N. J., June 27-July 2, 1971.
4. United States Senate Hearings before the Committee on Interior and Insular Affairs, Ninety-Second Congress, Albuquerque, N. Mex., May 24, 1971, Part I, pp 5, 81. U. S. Government Printing Office 1971.
5. Ibid p. 124.

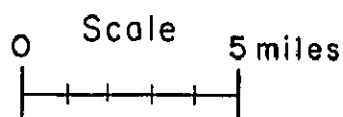
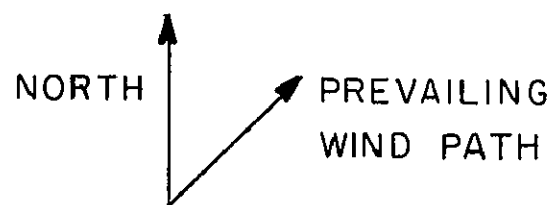
FIGURES

1. Air pollution sources in the test area.
2. Aerial color photograph of stressed Eastern white pine.
3. Color infrared analog of figure 2.
4. Aerial color photograph of coke oven complex.
5. Color infrared analog of figure 4.
6. Apollo 9 color infrared photograph showing air pollution sources in Arizona.
7. Enlargement of a portion of figure 6 showing plume from Hayden smelter.

POWER PLANT (1) ● 1800 MEGAWATTS, 650 TONS PER HOUR

▲ BEEHIVE COKE OVEN COMPLEX, 120 UNITS

POWER PLANT (2) ● 1200 MEGAWATTS, 440 TONS PER HOUR



POWER PLANT (3) ● 1800 MEGAWATTS
650 TONS PER HOUR

Figure 1- Air pollution sources in test area.



FIGURE 2. - Aerial color photograph of stressed Eastern white pine.

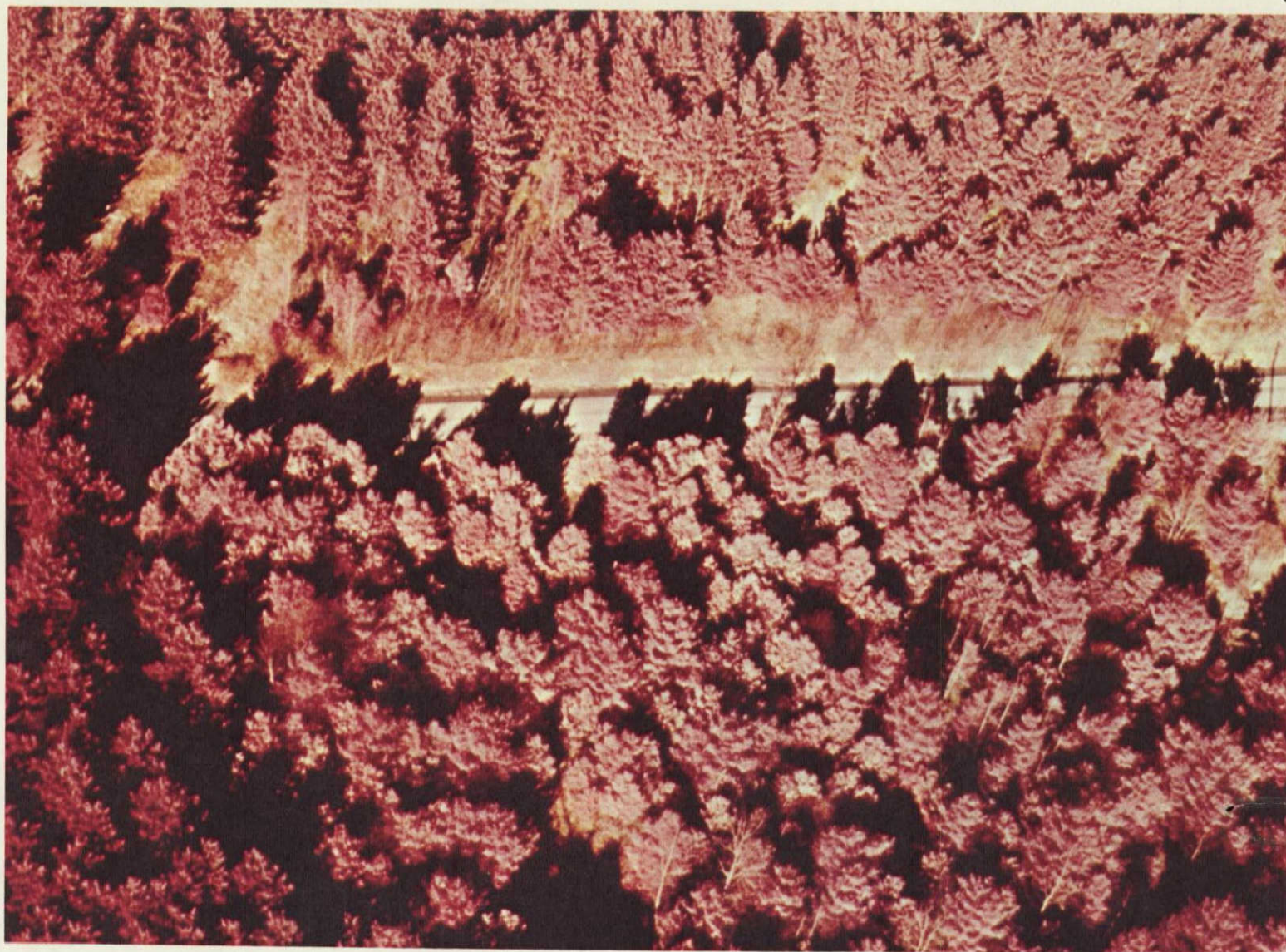


FIGURE 3. - Color infrared analog of figure 2.



FIGURE 4. - Aerial color photograph of coke oven complex.



FIGURE 5. - Color infrared analog of figure 4.



FIGURE 6. - Apollo 9 color infrared photograph showing air pollution sources in Arizona.

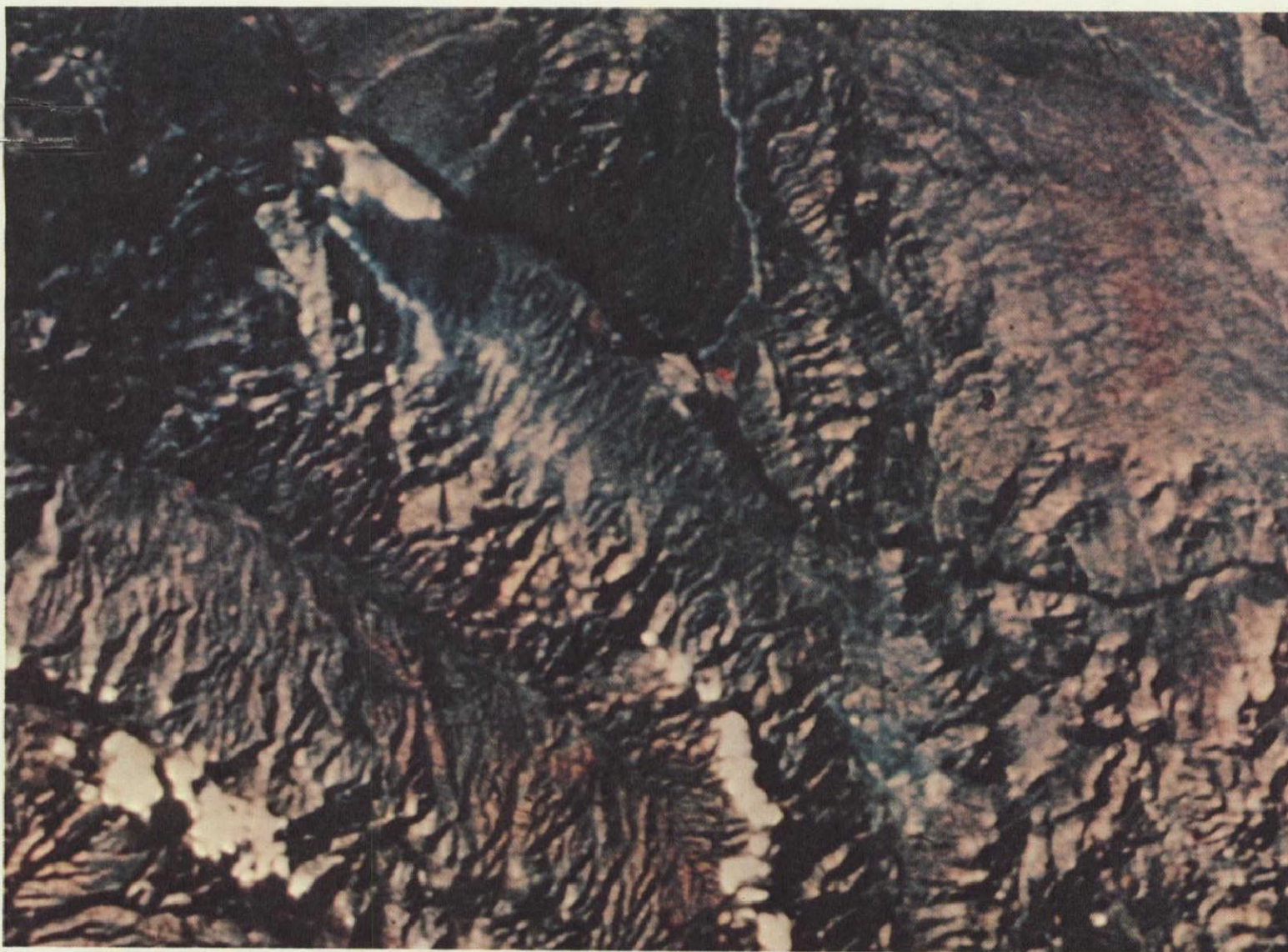


FIGURE 7. - Enlargement of a portion of figure 6 showing plume from Hayden smelter.

N72-29364

SECTION 66

REMOTE SENSING OF WET LANDS

IN IRRIGATED AREAS

by

Herbert H. Ham
Bureau of Reclamation
Denver, Colorado

INTRODUCTION

Irrigation of agricultural lands alters the ground-water regimen and usually produces a rising water table. If ground water invades the root zone, crop growth is adversely affected by the presence of excessive moisture. Furthermore, in arid climates, soluble salts present in the irrigation water, soil, and ground water tend to concentrate at the soil surface and in the root zone and alter the osmotic salt balance, to the detriment or preclusion of normal crop growth. The net result is waterlogged and salinized soils, commonly referred to as a subsurface drainage condition or wet land. Associated unfavorable conditions include cold and unworkable ground, restricted equipment accessibility, accelerated weed growth, and flooding of subsurface structures. Widespread occurrence of wet lands often has serious economic consequences. Locally, it may mean the difference between success and failure for the individual farmer.

The susceptibility of an irrigated area to development of wet lands depends on several factors including: water use, topography, infiltration rate, surface drainage, natural ground-water levels, and most importantly, subsurface hydraulic conditions. Subsurface conditions generally are so complex, however, as to preclude precise estimates of drainage requirements or location and design of facilities prior to irrigation. Provision of subsurface drainage facilities, especially in arid lands, must therefore await the development or threat of wet land before precise remedial action can be prescribed.

The only practical solution to a subsurface drainage condition, if the land is to be retained for permanent agricultural use, is the

removal of excessive ground water and salinity by deep drains or wells. The provision of effective and permanent drainage facilities requires extensive and time-consuming field investigations, precise design requirements, and careful construction.

Drainage problem areas are usually anticipated or identified by on-site observation by the affected landowner, through inspection of long-term ground-water hydrographs, and/or by surface or airborne visual or photographic observation. In addition to detection of newly wet areas, periodic surveys are made to assess previously wet areas and to evaluate the status and effectiveness of the drainage program.

The task of detecting wet lands may become extensive, especially on large projects that have acute and progressive drainage requirements. New and improved methods are constantly being sought and evaluated. The objectives of this study were to determine the usefulness of airborne remote sensing for: (1) detection of drainage problem areas; (2) delineation of the problem in terms of areal extent, depth to the water table and presence of excessive salinity; and (3) evaluation of the effectiveness of existing subsurface drainage facilities. This paper represents an appraisal of remote sensing techniques as alternatives to presently used methods.

This study was supported by the Department of the Interior's Earth Resources Observation Systems Program under National Aeronautics and Space Administration Task No. 160-75-73-01-01 and was administered under Bureau of Reclamation Contract No. 14-06-D-6840 (Solicitation No. DS-6768).

Appreciation is extended to Messrs. Jack N. Christopher, Loren D. Hampton, George E. Neff, H. Dan Neumann, and W. Oliver Watson of the Bureau of Reclamation for their participation in the planning, operation, and evaluation of this study and assistance in the preparation of this paper.

LOCATION AND DESCRIPTION OF STUDY AREA

Personnel from the University of Michigan gathered airborne remote sensing data of areas affected by drainage conditions on the Columbia Basin Project, Washington. This project, shown in Figure 1, contains about one-half million acres of irrigated land and has developed extensive arid-type wet lands. The areas surveyed ranged topographically from level to steep and rough and had diverse sources

of moisture, complex crop patterns, and variable soil conditions. Investigations for and construction of drainage facilities have been in progress for more than a decade under the guidance of a professional staff of drainage engineers, soil scientists, and other technical personnel.

PROCEDURE

Remote sensing data collected during this study included color and color infrared photography and optical-mechanical scanner imagery in several bands ranging from 0.4 to 13.5 microns. Flights were made principally at 2,000 feet at four diurnal intervals during late October, 1969. Field data, including ground-water levels, soil and salinity conditions, and crop cover, were acquired by project personnel simultaneously with collection of remote sensing data. Engineering data on project facilities, topography, and other features were also provided.

Although the season was not ideal for maximum day-night and air-soil thermal differentials, the selection was made to take advantage of normally favorable weather conditions and to coincide with the highest ground-water levels and most severe drainage conditions.

RESULTS AND DISCUSSION

The study yielded interesting and outwardly useful examples of detection of wet lands and associated conditions and facilities by remote sensing.

Figure 2 shows a pronounced thermal anomaly that coincides with a known wet area. Approximate depth to the water table in feet is shown by contour lines. Despite the apparent correlation, the thermal pattern is not believed to be directly related to water table depth. The principal factor is probably soil moisture resulting from capillarity. This wet area would be obvious in the field to even the casual observer. The circle marks a major canal; irrigated land lies to the left, and dry land to the right.

The anomalous diagonal pattern marked by arrows in the center portion of Figure 3 coincides with a system of deep (8 feet) sub-surface drains. The pattern is thermally reversed, however, with

drain alignments appearing cold, thus wet. This is believed to result from surface manifestations of the effects of drain construction activities on soil properties and crop growth. In this figure the circle indicates a shallow, open drain.

Figure 4 shows a complex area of drained land and minor wet land. However, because of the complexities related to distribution of vegetation and other features, correlation with known conditions could not be made. The circle indicates a major canal but the dark irregular feature marked by the arrow could not be identified.

In Figure 5 the thermal pattern, while outwardly associated with vegetation, is so complex that significant correlation could not be made. Part of one area, outlined at the lower left, is known to be wet. The circle indicates a canal of moderate capacity.

These illustrations have been included to demonstrate two overriding factors: (1) where drainage conditions are simple and pronounced, remote sensing does not display an appreciable advantage over present methods; and (2) where conditions are complex and subtle, remote sensing is inadequate. This applies to photography as well as imagery.

Burge, Prentice, and Thomson (1970, p. 34) in their preliminary report on this study conclude that "depth to the water table cannot be directly sensed from a knowledge of soil surface temperature."

Myers (1970, p. 10) in his study of shallow aquifers in glacial drift of eastern South Dakota, reports that depth to ground water is not significant in defining aquifers by thermal imagery.

Conversely, Abdel-Hady and Karbs (1971) report that under laboratory conditions, depth to the water table in the range 0 to 4 feet in two uniform soils, is detectable by thermal imagery. Based on experiences as outlined here, however, it is suspected that application of the techniques reported by Abdel-Hady and Karbs would be limited to field areas that simulate their controlled laboratory conditions. Such uniform conditions are infrequent in nature, especially where altered by vegetation cover, extraneous sources of moisture, cultural activities, and other similar conditions.

CONCLUDING REMARKS

In considering the performance and the results of this remote sensing operation and experience by others in attempting to determine subsurface hydrologic conditions by remote sensing, it can be concluded that:

Remote sensing, as demonstrated in this study and as presently constituted and priced, does not represent a practical alternative as a management tool to presently used visual and conventional photographic methods in the systematic and repetitive detection and delineation of wet lands and evaluation of the effectiveness of drainage facilities on a complex major irrigation project such as the Columbia Basin Project. Principal adverse factors contributing to this conclusion are:

1. Complex environmental conditions, including uneven topography, diverse vegetation, extraneous sources of moisture, and variable soil conditions, tend to mask the presence of high ground water and concentrations of excessive salinity and make interpretation difficult to impossible.
2. The inability of any field-demonstrated remote sensing technique to "penetrate" earth materials, especially in the presence of soil moisture, restricts usefulness in this area.
3. The intrinsic characteristics of remote sensing equipment, which require optimum weather and other operating conditions, would limit systematic and repetitive coverage in areas subject to variable conditions.
4. The often ill-defined and transient nature of surface and ground water and salinity tend to make collection and application of correlative field data difficult to impossible.
5. The anticipated high costs of systematic and repetitive coverage by remote sensing methods would be unrealistic when balanced against the expected results.

This is not an attempt to discredit remote sensing as a useful tool in the investigation, development, and management of land and other natural resources. In the correct application, the potential is appreciable. In the field of drainage and ground water, such applications might include:

1. Reconnaissance level delineation of shallow aquifers or high water tables in environmentally simple areas
2. Detection of leaky reaches of canals and aqueducts
3. Identification of crops that exhibit spectrally detectable response to presence of excessive moisture or salinity

The task described here, however, is not believed to be at this time a valid or practical application.

REFERENCES

1. Burge, W., Prentice, V., and Thomson, F., "Multispectral Data Processing of Moses Lake, Washington Data." The University of Michigan, unpublished report, 36 pp.
2. Myers, Victor I., "Remote Sensing for Defining Aquifers in Glacial Drift," NASA Third Annual Earth Resources Program Review, Volume III - Hydrology and Hydrography. December 1970, pp 48-1 to 48-20.
3. Abdel-Hady, Mohamed, and Karbs, Harlan, H., "Depth to Ground-Water Table by Remote Sensing," Journal of the Irrigation and Drainage Division, ASCE, Vol. 97, No. IR3, Proc. Paper 8360, September 1971, pp 355-367.

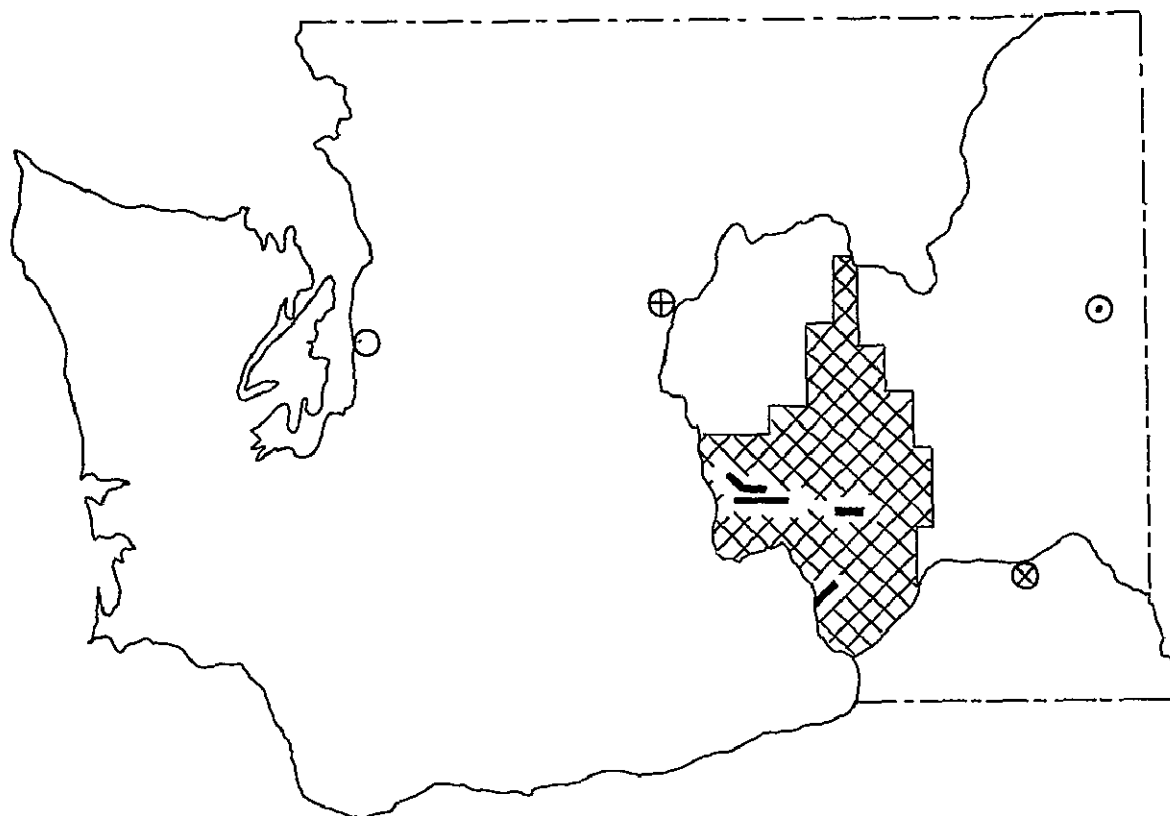


Figure 1.- Location map of Washington showing the Columbia Basin Project (cross hatched) and study areas (heavy lines).

- | | | | |
|---|---------|---|----------------|
| ○ | Seattle | ⊕ | Columbia River |
| ● | Spokane | ⊗ | SNAKE RIVER |

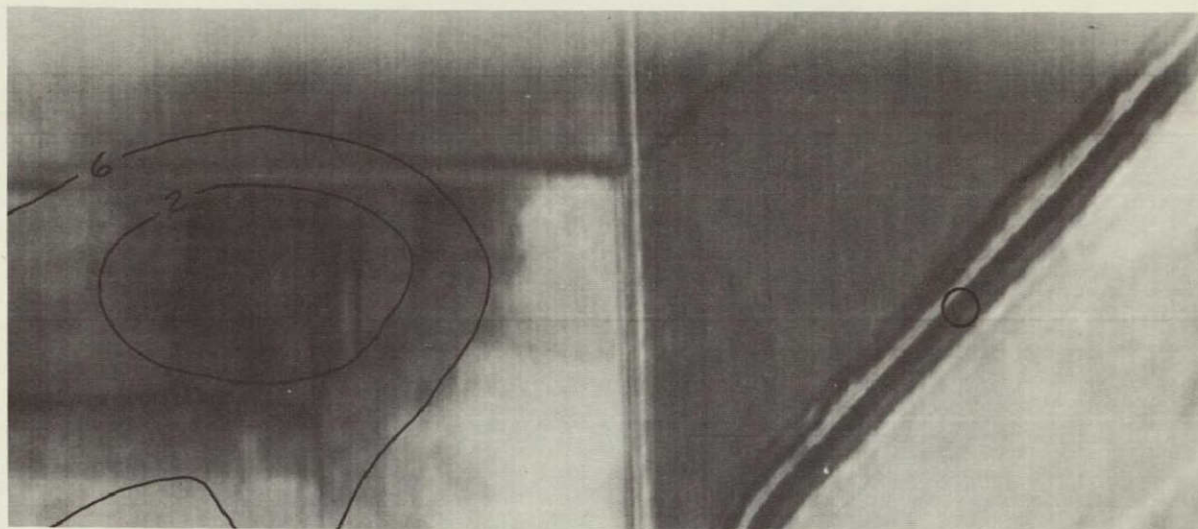


Figure 2.- CBP, Block 46, Farm Units 15 and 16. Forenoon thermal image of wet land (dark, irregular feature at left). Dark is cool. Imaged area is about 2,000 x 4,500 feet. North is up.

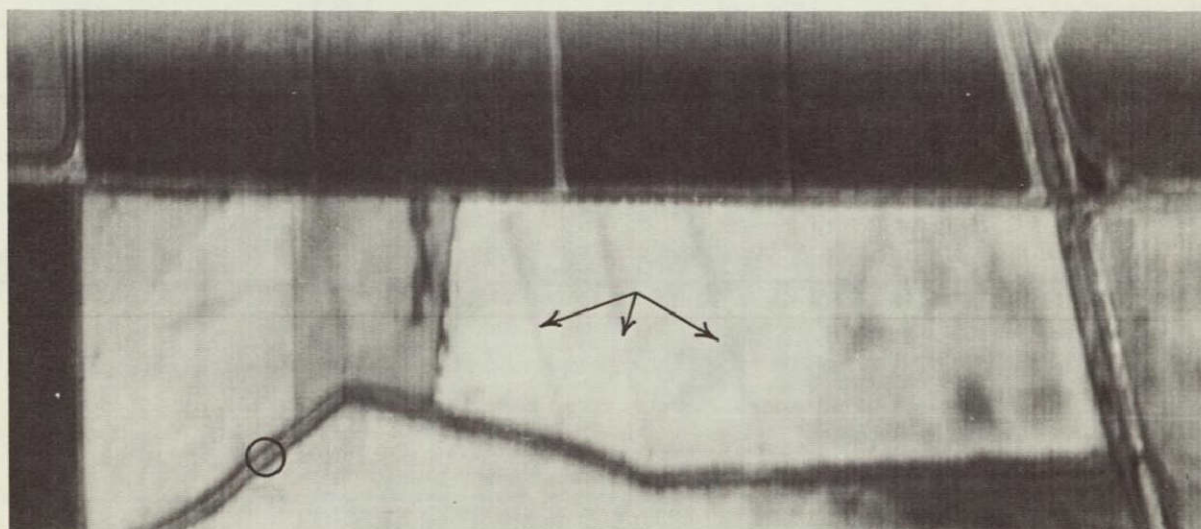


Figure 3.- CBP, Block 46, Farm Unit 20. Thermal image of diagonal system of subsurface drains (arrows). Time, scale, direction, and gray scale-heat relationship are similar to Figure 2.

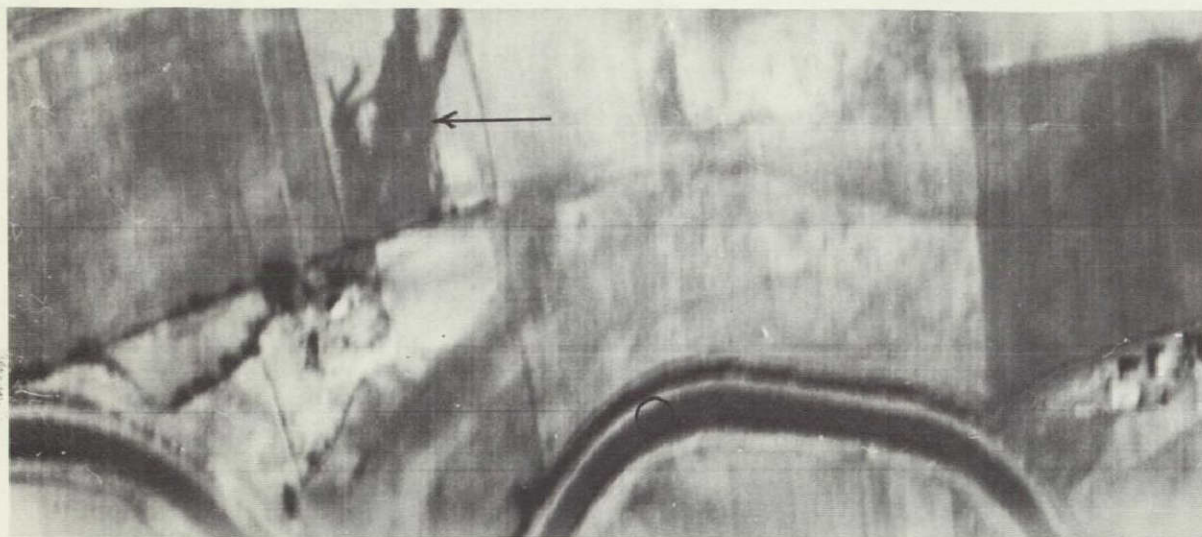


Figure 4.- CBP, Block 78, Farm Units 95 and 97. Thermal image of drained land with minor wet land. Time, scale, direction, and gray scale-heat relationship are similar to Figure 2.

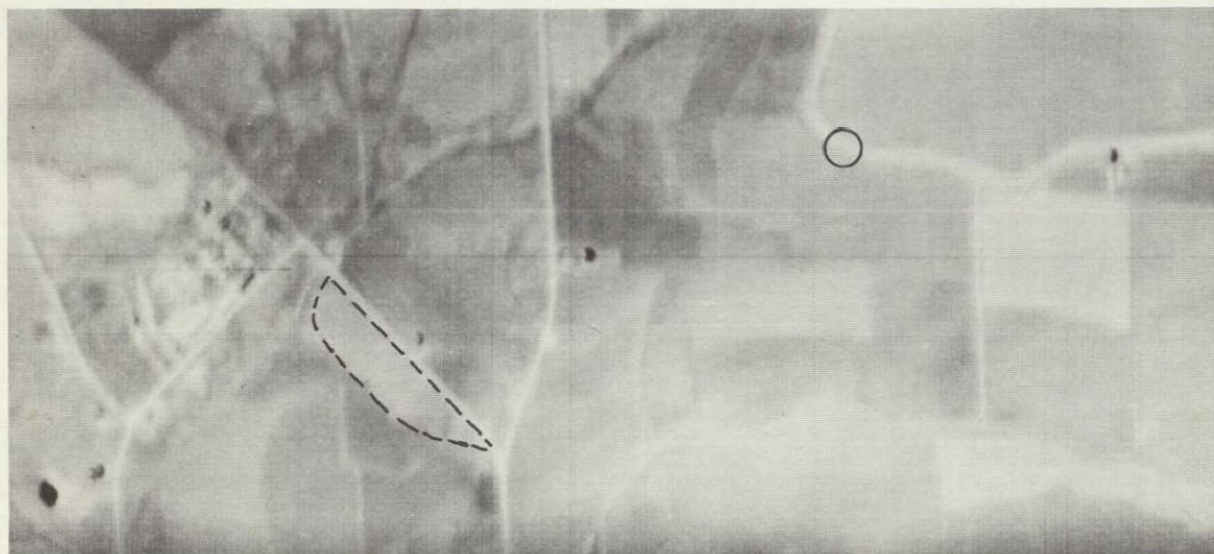


Figure 5.- CBP, Block 87, Royal Camp area. Post-sunset thermal image of mixed undrained, drained, and wet land. Dark is cool. Imaged area is about 5,000 x 11,500 feet. North is up.

This page is reproduced again at the back of this report by a different reproduction method so as to furnish the best possible detail to the user.

SHORT PULSE RADAR MEASUREMENTS OF
LAYERED ICE AND SNOW.*

R. S. VICKERS and G. C. ROSE
Department of Electrical Engineering
Colorado State University
Fort Collins, Colorado

I. INTRODUCTION AND BACKGROUND

Techniques for the remote measurement of snow and ice thickness have been studied for a number of years. They range from infrared and microwave multichannel radiometers (1,2) and gamma ray absorption spectrometers (3) to a wide variety of active radar techniques (4,5,6). All the methods except those involving radar signals rely on the natural absorption and emission from the ice or snow subsurface, a process which is uncontrolled and dependent upon many parameters. Similarly, radar techniques have their drawbacks, particularly when the target temperatures allow a large free water content in the pack. Nevertheless, radar methods provide the most direct approach to the measurement of layer thickness in ice and snow, and in some circumstances can also provide data on the water equivalent of the snow, as will be shown later.

In this paper, the development of a high resolution system for the remote measurement of layer thickness is described. The system has been designed for eventual incorporation into a light aircraft, although the study reported here only includes measurements taken a few feet off the ground. The system has a vertical resolution of less than 3".

II. MICROWAVE PROPERTIES OF SNOW AND ICE

The attenuation of a microwave signal propagating through frozen water in its various forms is well reported in the literature (7,8). Using the data shown in Figure 1, it can be seen that there exists a range of frequencies between 1 GHz and 3 GHz for which the attenuation is low, and does not change drastically with frequency. Within this range, the wavelengths are sufficiently short to allow a theoretical resolution (half a wavelength) of a few centimeters. Figures 2 and 3 show the variation in dielectric constant and loss tangent of snow as a function of snow density and temperature from 3.2 cm radiation. It can be seen that the worst losses will occur in the case of high density snow which is approaching the melting point, for example, ice at 0°C has a loss tangent of 2.6×10^{-3} at 10 GHz and 4.6×10^{-4} at 2 GHz.

These figures indicate that radiation in the 2 to 4 GHz band should be able to penetrate layers of ice and snow with acceptable losses. The penetration depth can be calculated from the dielectric approximation to the skin depth formula:

* This work was performed under funds from the U.S. Bureau of Reclamation, contract number 14-06-D-7159.

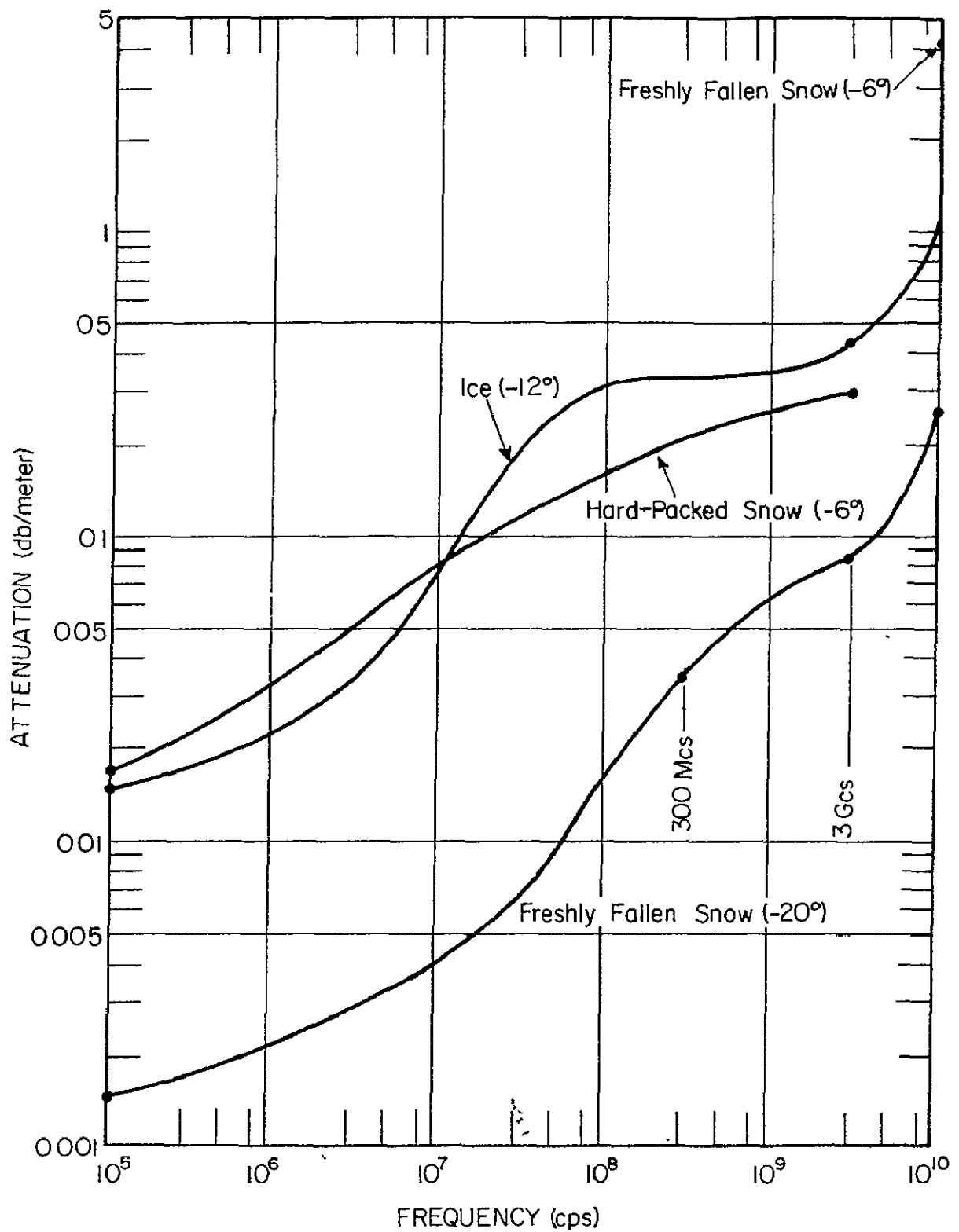


FIGURE 1 ATTENUATION OF ELECTROMAGNETIC WAVES BY ICE AND SNOW vs FREQUENCY

$$\text{Skin Depth } \delta = \frac{2}{\sigma} \sqrt{\frac{\epsilon}{\mu}}$$

where σ = conductivity (mhos/m)

ϵ = permittivity of the medium

μ = permeability of the medium

For a loss tangent of 2×10^{-3} and $f = 2$ GHz; $\delta = 40$ m. The velocity of propagation of an E-M wave in a dielectric is given by

$$v = c \left(\frac{1}{\sqrt{\epsilon}} \right)$$

and the time for a pulse to propagate through a layer 'h' meters thick is

$$t = \frac{h \sqrt{\epsilon_r}}{c} \text{ secs.}$$

Where $c = 3 \times 10^8$ m/sec

h = thickness in meters

ϵ_r = relative dielectric constant

Therefore, when using the short pulse technique to measure layer thickness a knowledge of ϵ_r must be assumed. If 't' is plotted as a function of snow density however, the graph shown in Figure 4 results. If this graph is used for a measurement in which the layer thickness is known, the density of the layer can be found, and hence the water content of the pack. Thus, in a practical survey, at least one calibration point is required before the results can be interpreted. In cases where the snow density is known to say $\pm 20\%$, a linear approximation could be drawn through the graph for that region, in which case the expression for the two way pulse transit time would take on the form:

$$t = 2 \left(k_1 h + \int_0^h k_2 \rho(h) dh \right)$$

where k_1 and k_2 are constants

The integral $\int_0^h \rho(h) dh$ is the water equivalent of the layer.

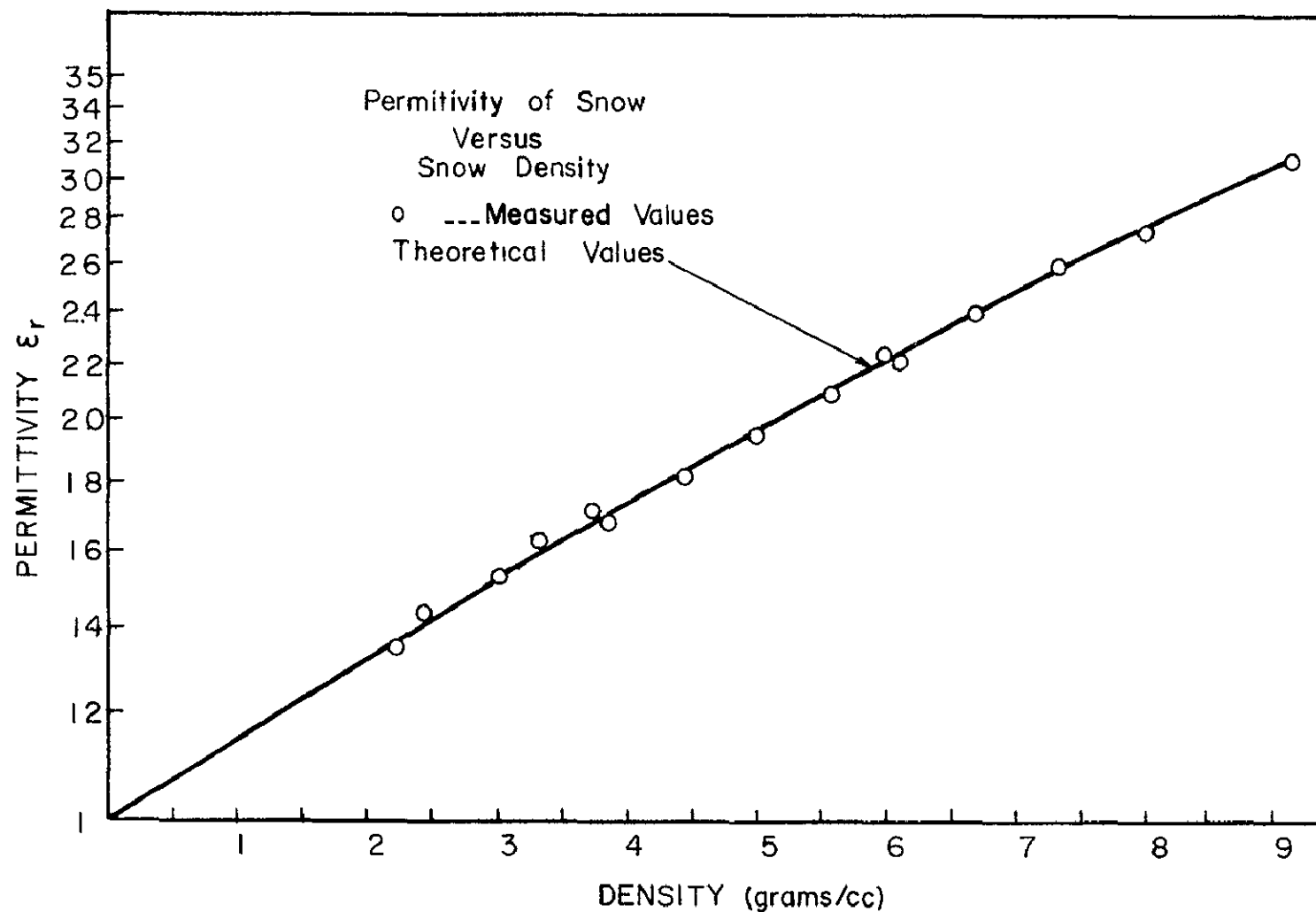


Figure 2 Permittivity of Snow as a Function of Density (After Cumming)

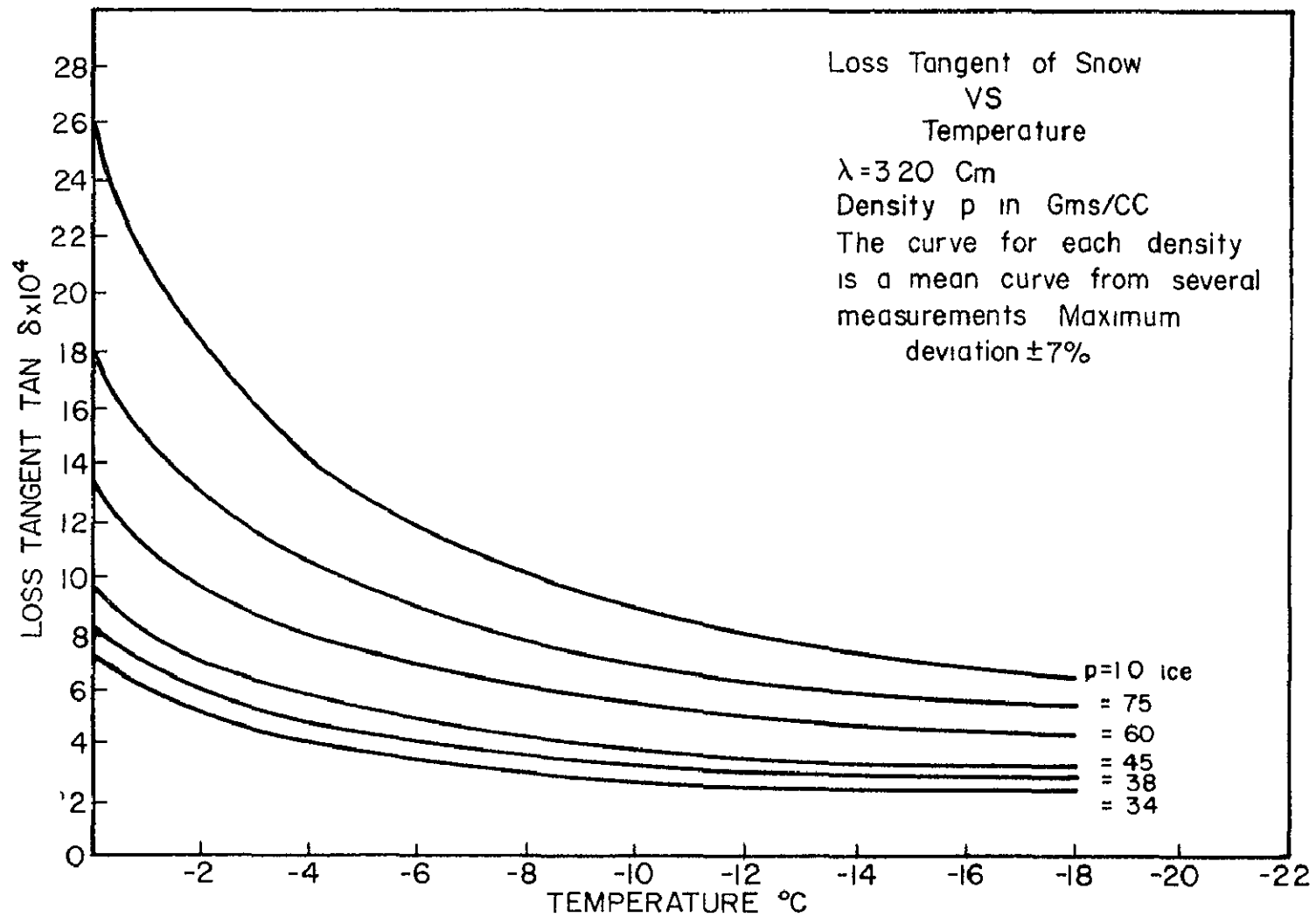


Figure 3 The Variation of Loss Tangent of Snow With Temperature (After Cumming)

Reflection Coefficients - Assuming that the snow is a dielectric, the reflection coefficient between two layers of permittivity ϵ_1 and ϵ_2 is given by

$$R = \frac{\sqrt{\epsilon_2} - \sqrt{\epsilon_1}}{\sqrt{\epsilon_2} + \sqrt{\epsilon_1}}$$

Table I shows the range of values in ϵ_r which can be expected for ice and snow layers. It has been shown (8) that these values do not vary appreciably with temperature.

Consider now a layer of snow ($\epsilon_r = 1.4$) with the lower surface in contact with the ground which is not frozen ($\epsilon_r = 81$). The reflection coefficient from the upper surface will be 8.4% and from the lower surface will be close to 70% (as seen by the radar antenna). Even a snow/ice interface would have an effective coefficient of 13%, thereby indicating that the most difficult boundary to observe will not be the snow/ground interface as one might first expect, but the snow/air interface. This prediction is verified in practice. Measurements on fresh snowfall at -1°C indicated a surface reflection of 4 to 6% at the time of settling, and a lower boundary reflection of approximately 60%. More measurements are necessary before the variations in microwave reflectivity can be predicted for a variety of air temperature and sunlight conditions. Reflections can be expected from internal structure of the snowpack (if any) due to changes in the dielectric constant. Clear boundaries have been detected for changes in ϵ_r of about 0.5 with the system described in this report.

In summary, the microwave properties of snow are compatible with the short pulse radar approach to snow thickness measurements. However, the case where the snowpack contains quantities of distributed free water has not been analyzed. It is hoped that the forthcoming snow season will yield enough data to allow the effects of free water to be determined experimentally.

III. SYSTEM DESIGN

A diagram of the system design appears in Figure 5. The S-Band source for the research instrument is a frequency generator capable of being tuned from 2 to 4 GHz. The frequencies of interest lie within a narrow range from 2.5 to 2.9 GHz and an operational system would therefore be best designed with a solid state or klystron source. The CW signal from the source is modulated by a double balanced mixer to produce a pulse of duration 10^{-9} seconds. The switching drive for the mixer is generated by a pair of suitable driven step recovery diodes.

TABLE I. ELECTROMAGNETIC WAVE ATTENUATION BY SNOW AND ICE

	Frequency (cps)	Dielectric- Loss Tangent	Relative Dielectric Constant (ϵ'/ϵ_0)	Attenuation (db/meter)
Freshly Fallen Snow (-20°C)	10^3	0.4920	3.33	$7.9414(10^{-5})$
	10^4	0.3420	1.82	$4.1378(10^{-4})$
	10^5	0.1400	1.24	$1.4144(10^{-3})$
	10^6	0.0215	1.20	$2.1422(10^{-3})$
	10^7	0.0040	1.20	$3.9856(10^{-3})$
	$3(10^8)$	0.0012	1.20	$3.5870(10^{-2})$
	$3(10^9)$	0.00029	1.20	$6.6688(10^{-2})$
	* 10^{10}	0.00042	1.26	4.2882
Hard Packed Snow (-6°C)	10^5	1.5300	1.90	$1.6130(10^{-2})$
	10^6	0.2900	1.55	$3.2503(10^{-2})$
	$3(10^9)$	0.0009	1.50	$3.0078(10^{-1})$
	10^5	0.8000	4.80	$1.4927(10^{-2})$
	10^6	0.1200	4.15	$2.2193(10^{-2})$
Ice (-12°C)	10^8	0.0180	3.70	$3.1493(10^{-1})$
	$3(10^9)$	0.0009	3.20	$4.3932(10^{-1})$
	10^{10}	0.0007	3.17	1.1336

* At -6°C.

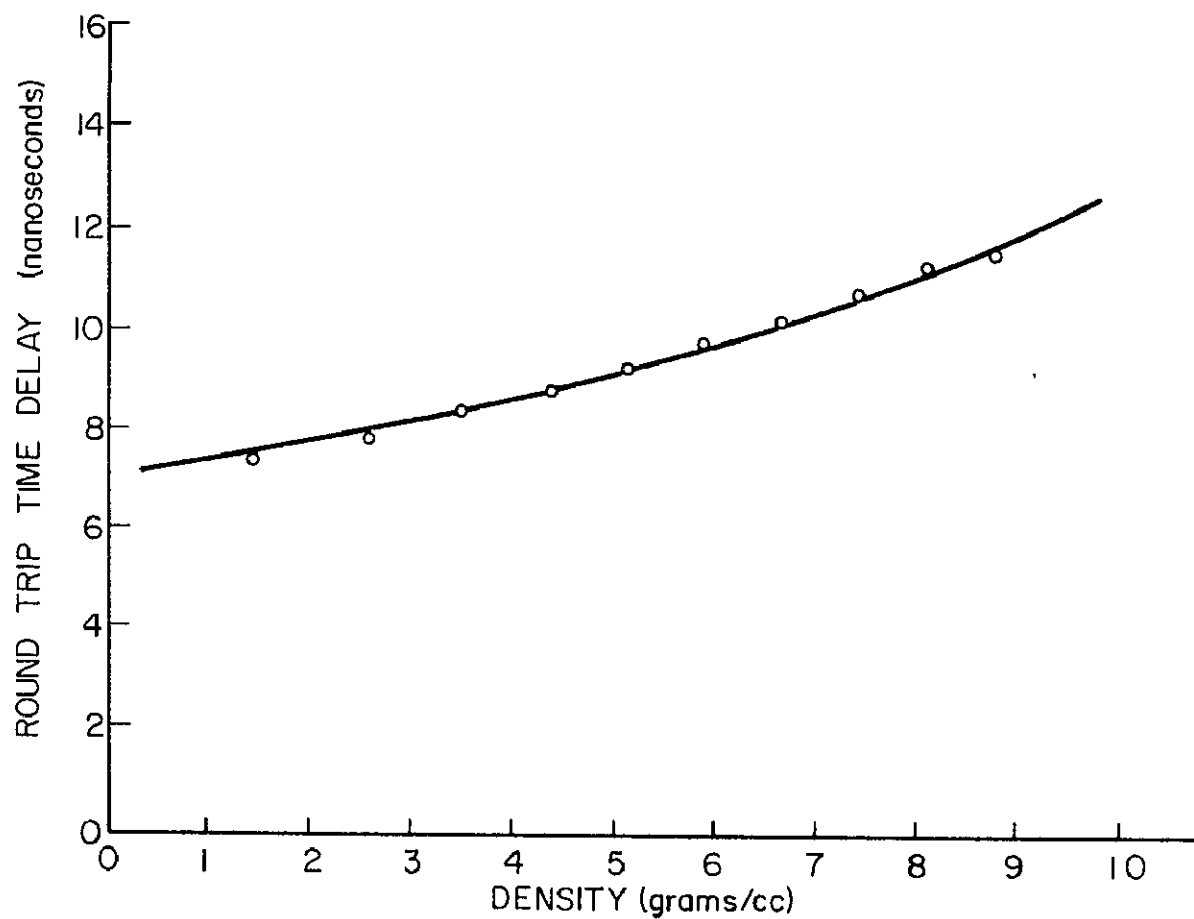


FIGURE 4. TRAVEL TIME OF A MONOCYCLE PULSE THROUGH 1 METRE OF SNOW AS A FUNCTION OF SNOW DENSITY (grams/cc)

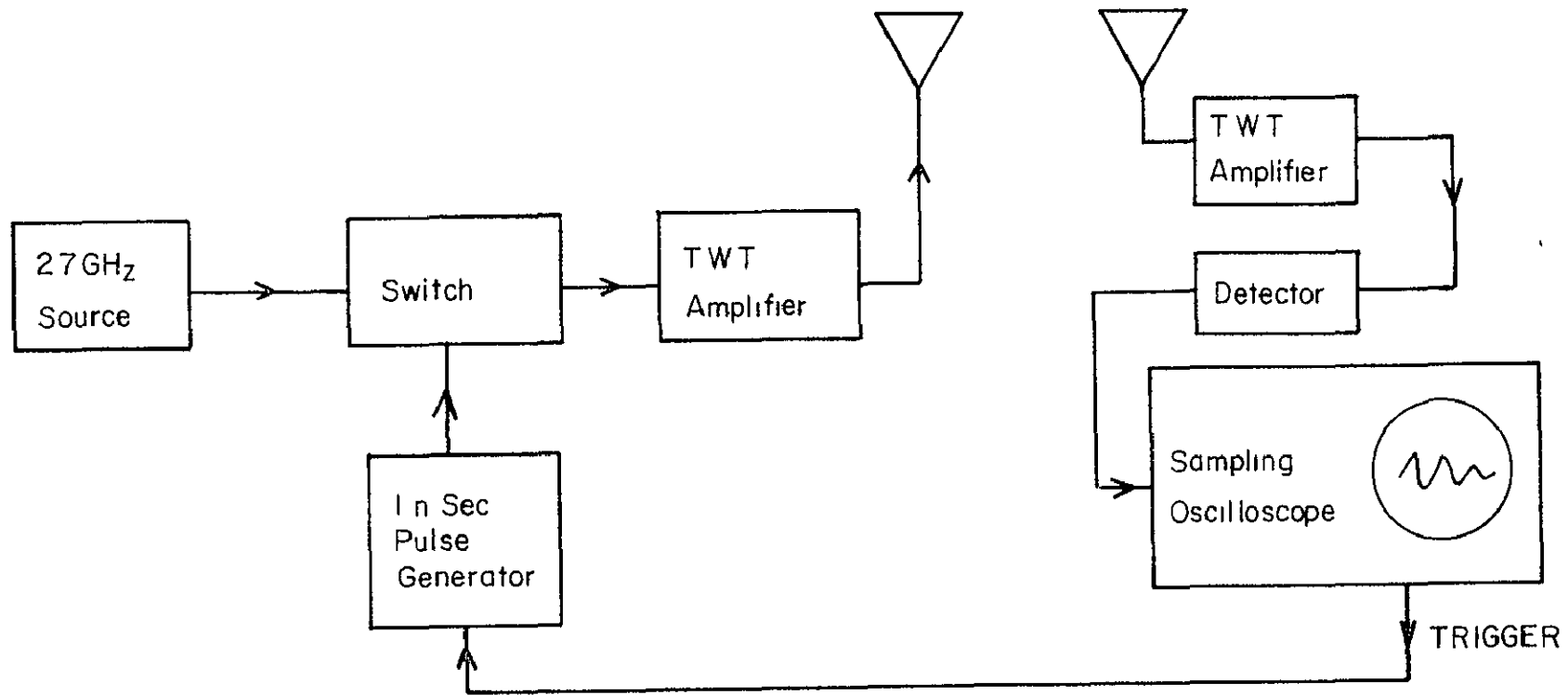


Figure 5 Short Pulse Radar System

The signal strength at this point is only a few milliwatts, and it is therefore passed to a Traveling Wave Tube (TWT) amplifier to produce a peak output power of 1 watt into the transmitting antenna. In the low sensitivity version of the radar, the return signal is simply detected at the antenna and displayed on a sampling oscilloscope, as discussed in the following section. For higher sensitivity a second TWT can be included in the receiver. Initial experiments with this latter configuration indicate a usable range of 40-50 feet.

The two key problems in the design of the radar system were the generation of a short, high power pulse and the design of an antenna to propagate it. Several designs were evaluated for the pulse generator including avalanche transistor generators, mercury wetted switches, and designs involving shorted transmission lines. All suffered from spurious reflections after the main pulse had been generated, and all but the transmission line system produced pulses longer than the one nanosecond design goal. The limitations of the design presently in use is that the peak power from the generator is only a milliwatt or so, and therefore substantial amplification is required in the transmitter.

A number of possible antenna designs were investigated during the study. The desired criteria for the antenna response vary with the bandwidth and phase characteristics of the pulse being transmitted, and consequently no decision could be taken on the antennas until the pulse generation problem had been solved. The desired parameters of the antenna are high directivity (i.e., high gain), and good impulse response, resulting in a minimum stretching of the input pulse length. Initially discone antennas were used and proved effective, although their directivity pattern was very poor (omnidirectional) in one dimension.

Further work has concentrated on different varieties of horn antenna, the present design being capable of transmitting pulses approximately 1.4 nsec in length at 2.7 GHz.

IV. EXPERIMENTAL RESULTS

Initial system tests were performed on snow close to the laboratory in October. Due to the small quantities of snow available, measurements on the natural snowfall were not possible, and the snow was therefore shovelled into a pack 39" high and 36" long, which was then used to obtain experimental data. During the construction of this snowpack a layered discontinuity in the snow density was introduced accidentally. This layer was later observed on the radar return. Figure 6 shows the radar data from those first experiments.

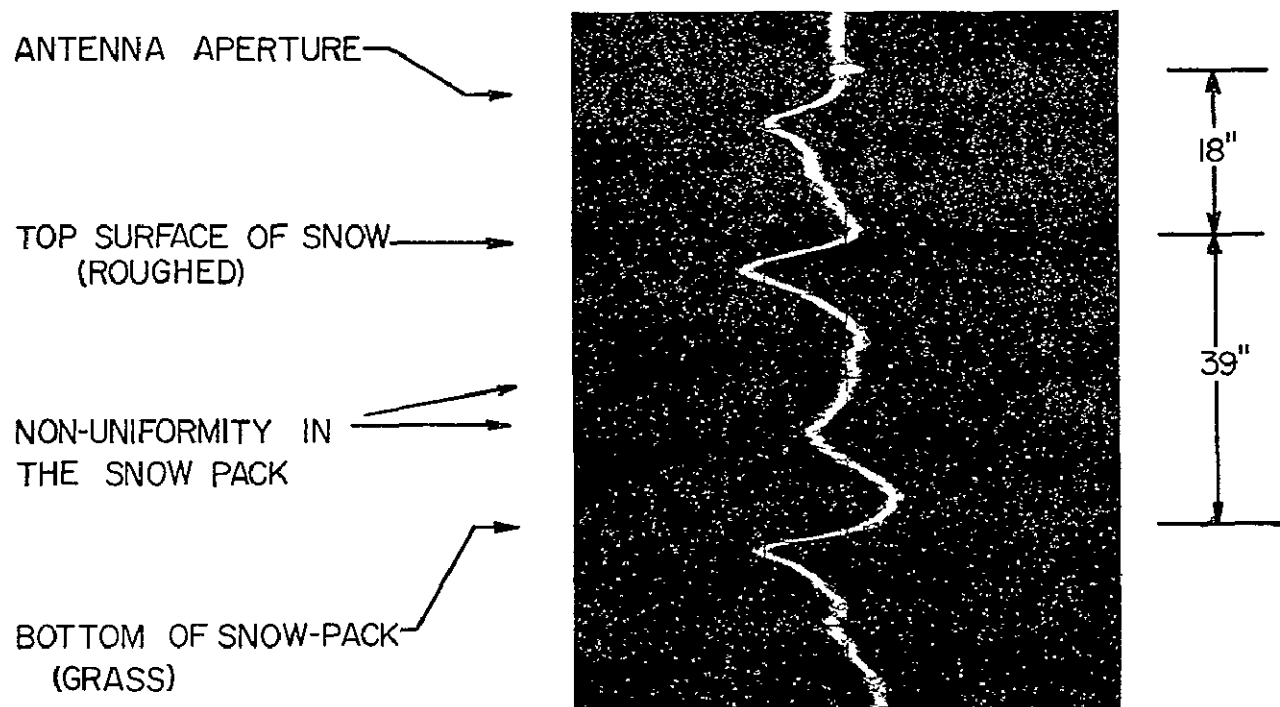


Figure 6. DATA FROM A TRAVERSE OVER SNOW 39 INCHES DEEP AT $-\frac{1}{2}^{\circ}\text{C}$
USING A SHORT PULSE RADAR OPERATING AT 2 GHz

In this figure, the first reflection results from a direct path from the transmitting to the receiving antenna, the second from the top surface of the snow and the third from the snow/ground interface. This data agrees well with the predicted waveforms (Figure 7) and the earlier computer simulation by Cook (4). In all experimental data in this report the received signal is rectified and therefore unipolar in character. It will be noticed that there is a reflection from within the snowpack due to density changes. This effect was verified in later experiments by taking core samples. The data shown in this figure corresponds to a density of 50% for a depth of 39".

To illustrate a second type of data presentation a limited traverse was made over the snowpack. The return signal was used to intensity modulate an oscilloscope, while simultaneously applying a ramp voltage to the vertical deflection amplifier. The result is shown in Figure 8. In the figure the dark bands are due to the reflection from the top and bottom of the snowpack. Some layering can also be observed within the snow and is again attributed to changes in density.

In an attempt to find greater quantities of snow preferably in an undisturbed state, a field trip was made to Berthoud Pass, Colorado, where a recent snowfall of 15" was available. Some older snow was also present which had been stacked by snowplough to a depth of about 30" and in one area, the new snow overlaid older metamorphosed snow. This latter snow was in the form of tightly packed ice pellets of about 0.2 cm diameter. Figure 9 shows the radar return from this area. The direct antenna feed-through has been suppressed on all the data from this field trip, thus the first reflection is from the top of the snowpack, and the second from the snow/ground interface. In between these can clearly be seen a third smaller reflection which was verified to be due to the boundary between the old snow and new snow. Core samples were taken with a Rosemont Snow Tube and the density calculated from the core weight and volume. Table II shows the comparison between the snow density as measured by the short pulse radar system and by the snow tube. It is felt that errors could easily be introduced into the gauge measurements by the nature of the experimental technique. Similarly, with the low power and resolution of the radar system accurate measurements of pulse travel time were difficult. Consequently, no further discussion is offered on the discrepancies shown in Table II. In general, the agreement is good. The low number of measurements was due to extreme difficulty in maneuvering the radar system on its sled from site to site. Considerable redesign has taken place in the light of the experience gained on this field trip. Figure 10 shows the return from packed snow, 28" deep, and is typical of the remainder of the measurements.

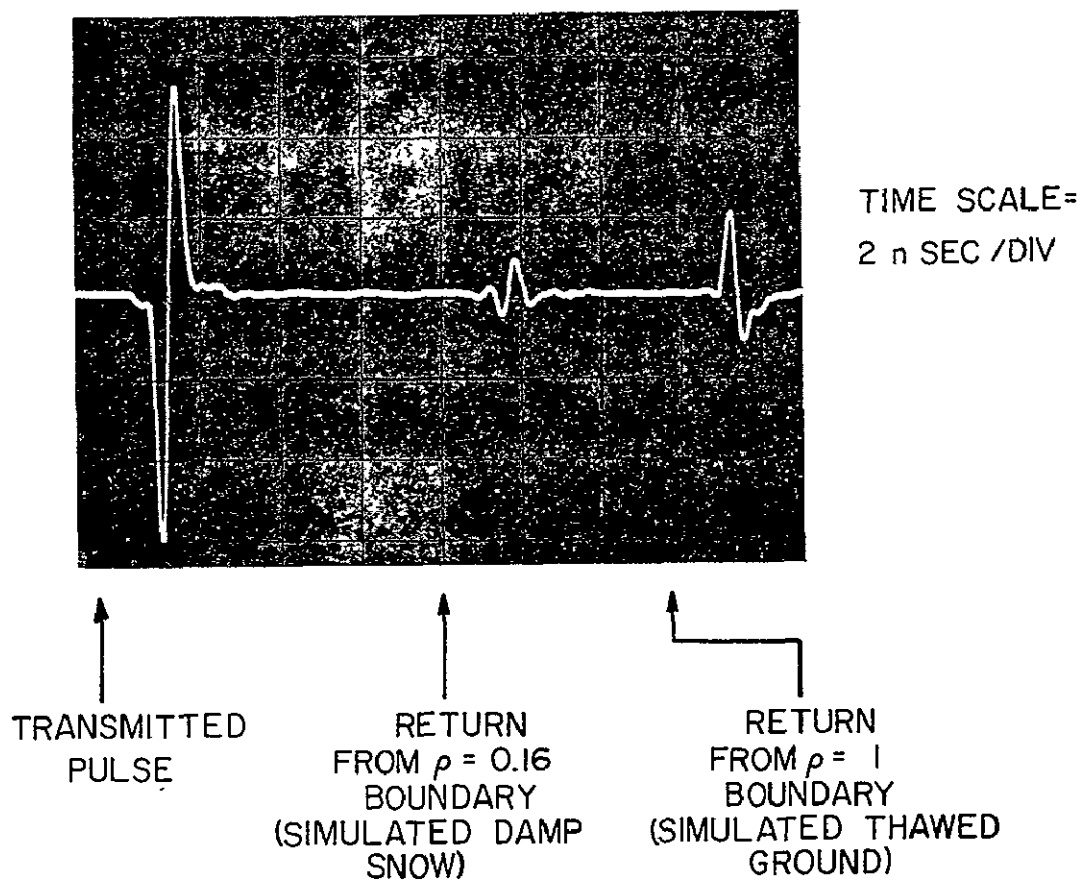


FIGURE 7. PREDICTED WAVEFORM FROM A MONOCYCLE PULSE PROPAGATED THROUGH A LAYERED SNOW.

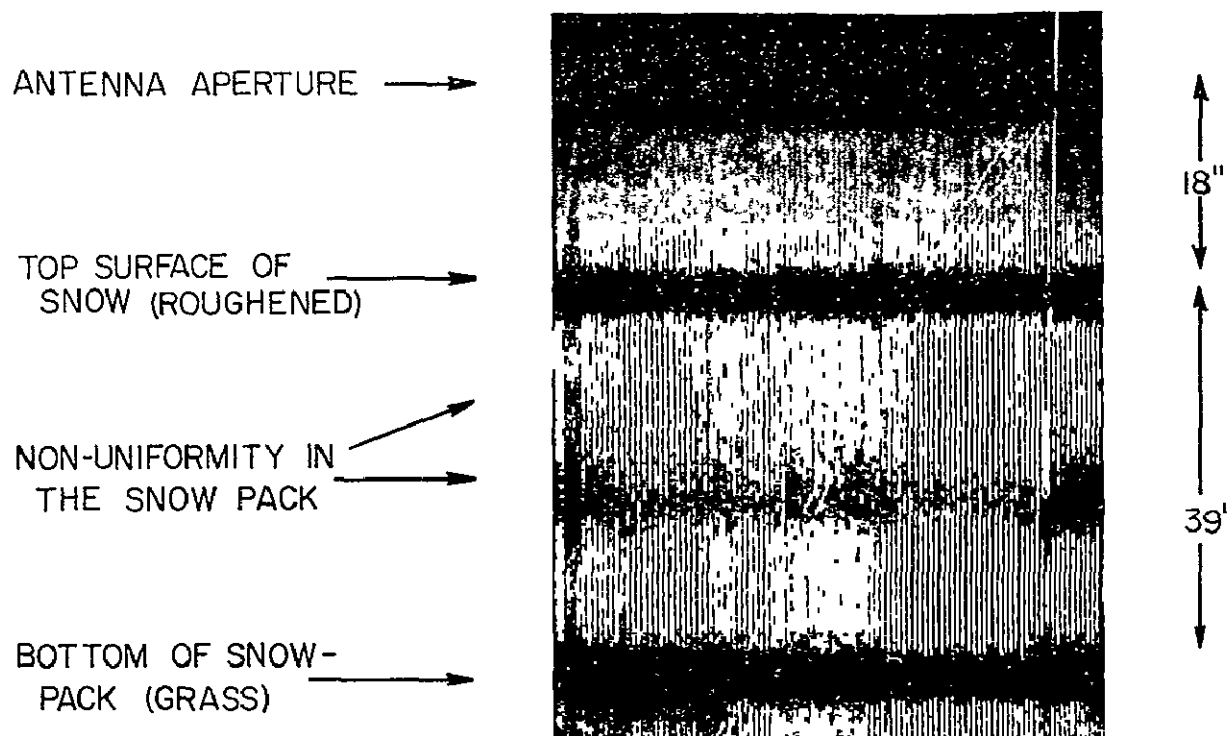


Figure 8. DATA FROM A TRAVERSE OVER 39 INCHES DEEP AT $\frac{1}{2}^{\circ}\text{C}$
 USING A SHORT PULSE RADAR OPERATING AT 2 GHz

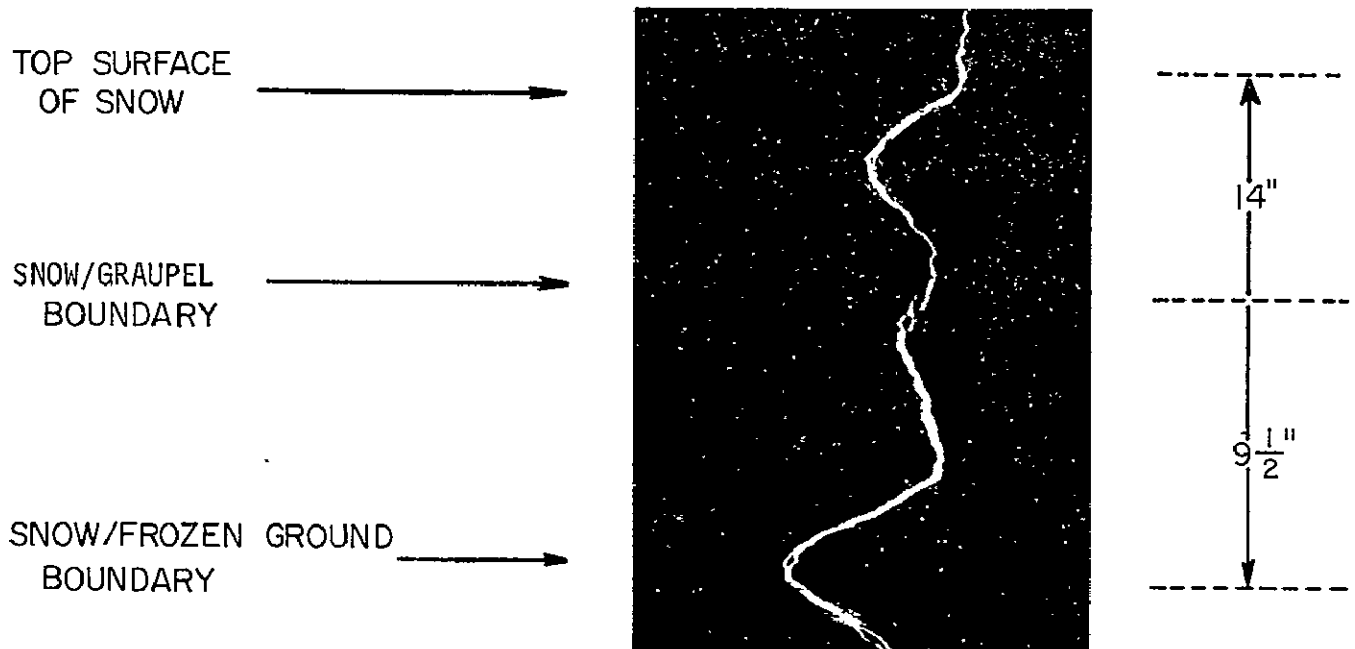


FIGURE 9. RADAR RETURN FROM METAMORPHISED SNOW OVERLAIN BY FRESH SNOW.

TABLE II. DATA FROM BERTHOUD PASS FIELD TEST

SNOW DEPTH (Rosemont Gauge)	SNOW DENSITY		WATER EQUIVALENT	
	Gauge	Radar	Gauge	Radar
14.5" (compacted)	45%	55%	6.5"	8"
14" fresh snow on top of 9 1/2" metamorphosed snow	-	19.7%	-	2.75"
	-	100%	-	9.5 "
TOTAL 23 1/2"	50%	42%	11.7"	12.25"
28" (compacted)	47%	44%	13.2"	12.3"
26" (compacted)	48%	42%	12.5"	10.9"
15" (fresh)	22%	19.5%	3.3"	2.9"

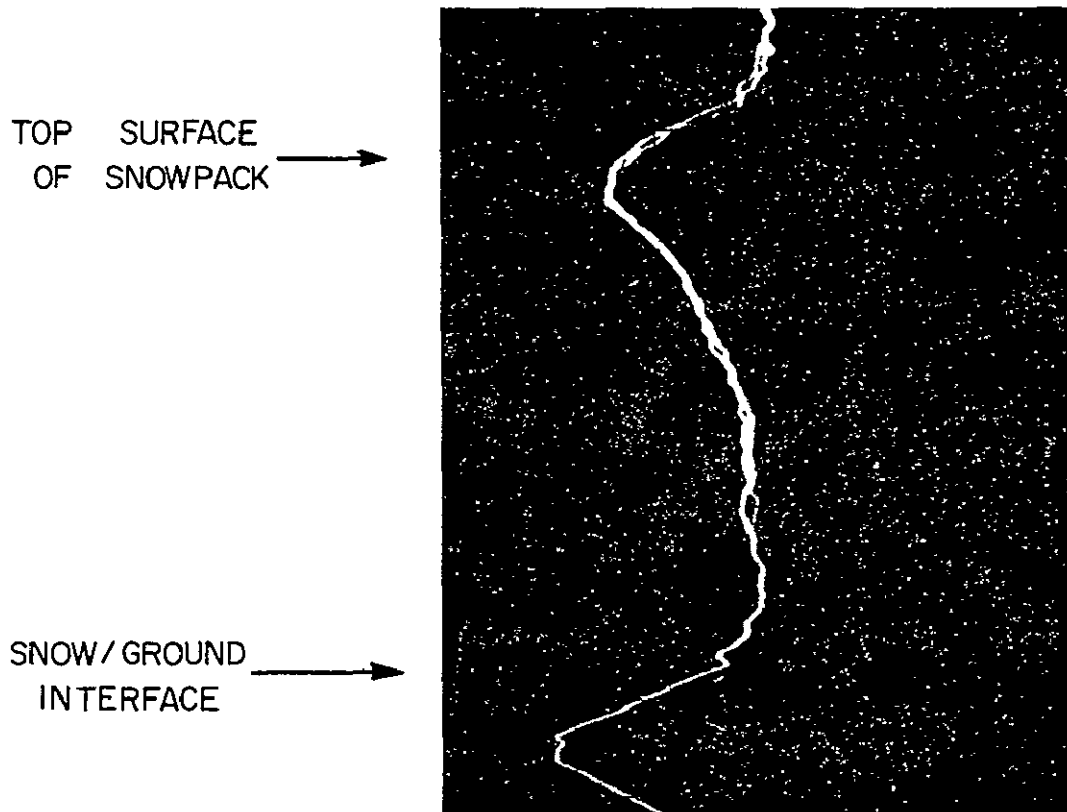


FIGURE 10. RADAR RETURN FROM COMPACTED SNOW
(depth = 28") AT BERTHOUD PASS, COLORADO
SNOW TEMPERATURE = -6° C

V. FUTURE POTENTIAL OF THE SHORT PULSE RADAR SYSTEM

a. System Accuracy - The accuracy of the snow density or snow depth measurements is limited primarily by the transmitted pulse length. Presently the pulse length is 1.9 nsec due to a combination of poor antenna characteristics and the limited bandwidth of the TWT's being used. It is anticipated that significant improvements in the antenna impulse response could be achieved with further study. Transmitted pulse lengths of 0.8 nsec would allow a resolution of roughly 6 cms in free space, which should be more than adequate for the snow and ice measurements presently envisaged. The limitations in TWT performance can be overcome by acquiring more sophisticated equipment.

The fact that short pulse lengths are important can be seen by inspecting the expression developed earlier for pulse propagation time, i.e.,

$$t = 2 \left(k_1 h + \int_0^h k_2 \rho(h) dh \right)$$

The first term gives the time taken by the pulse to travel a distance 'h' *in vacuo*, while the second gives the time increment due to the presence of the snow. A calibration point is required in order to derive the snow density from this equation, and a suitable calibration would be one that gives the value of h. From this measurement, $k_1 h$ can be calculated, allowing the value of ρ to be then derived.

The measurement of ρ therefore involves taking the difference between two nearly equal quantities, t and $k_1 h$, and is thus very sensitive to the accuracy with which either can be measured. For example, a 1 meter layer of snow of density 0.5 ($\epsilon_r = 1.9$) would give a value of $(t - 2k_1 h)$ of

$$\begin{aligned} \left(t - 2k_1 h \right) &= \frac{2h}{c} \left(\sqrt{\epsilon_r} - 1 \right) \\ &= 2.6 \text{ nsec} \end{aligned}$$

Therefore, if we assume that the position of the received pulse can be measured in time to one quarter of the pulse length, a 2 nsec pulse would give a value of $(t - t_0)$ and hence the water equivalent to $\pm 10\%$. This situation improves linearly with increasing snow depth and decreasing pulse width. The other extreme would be a 1 nsec pulse passing through 5 meters of snow, in which case the value of $(t - t_0)$ would be accurate to $\pm 1\%$.

It is perhaps more meaningful to consider the converse case, where a measurement of snow density is used as a calibration point, and values of 'h' are calculated from the radar return. In the second mode, the radar system could be used to estimate the total moisture content of a given snowfield using the assumption that the density of the snow is constant over the field.

b. System Sensitivity - The system reported here used a single TWT with a gain of 30 db. The effective range of the radar was about 8 feet. Since that time, a second TWT has been added, allowing measurements to be made at ranges of up to 50 feet. This modified system is still seven orders of magnitude less sensitive than could be built using standard equipment.

CONCLUSIONS

Using a radar system with high range resolution, it has been shown that measurements of snow and ice thickness are feasible with an accuracy of better than 3". In addition, the water equivalent of the snowpack can be estimated, given a single surface measurement of the snow depth.

Discontinuities in density have also been detected and their location determined by inspection of the radar returns.

The potential of the radar to evolve into an airborne, operational system is considered good, even with the constraint of using standard commercial components, and experiments will be conducted in the coming year to perform measurements from an altitude of 1,000 feet above terrain.

REFERENCES

- 1) Meier, M. F. and Edgerton, A. T., "Microwave Emission from Snow," Proc. 7th Symp. on Remote Sensing, University of Michigan, 1971.
- 2) Kennedy, J. M. and Sokamoto, R. T., "Passive Microwave Determinations of Snow Wetness," Proc. 4th Symp. on Remote Sensing, University of Michigan, 1966.
- 3) Deal, L. J. et al, "Environmental Radiation Surveys and Snow Mass Predictions from Aircraft," Proc. 7th Symp. on Remote Sensing, University of Michigan, 1971.
- 4) Cook, J. C., 1960, "Proposed Monocycle - Pulse V.H.F. Radar for Airborne Ice and Snow Measurements," Trans. A.I.E.E., November 1960.
- 5) Meyer, M. P., 1966, "Remote Sensing of Ice and Snow Thickness," Proc. 4th Symp. of Remote Sensing, University of Michigan Press, April 1966.
- 6) Barringer, A. R., 1965, "Recent Progress in Remote Sensing with Audio and Radio Frequency Pulses," Proc. 3rd Symp. of Remote Sensing, November 1965.
- 7) Evans, S., "Dielectric Properties of Ice and Snow," J. Glaciology 5, 42, 773-792, 1965.
- 8) Cumming, W. A., "The Dielectric Properties of Ice and Snow at 3.2 cms.," J. App. Phys. 23, 7, July 1952.
- 9) Casey, K., "Propagation Effects of Soil Using a 300 MHz Monocycle Radar," Master's Thesis, San Diego State 1969.

N72-29366

68-1

SECTION 68

EARTH RESOURCES CARTOGRAPHY PROGRAM

by

Alden P. Colvocoresses
U.S. Geological Survey
Washington, D.C. 20242

ORIGINAL CONTAINS

INTRODUCTION

COLOR ILLUSTRATIONS

Progress on our cartographic projects is described in our annual report to NASA and the program objective and tasks for fiscal 1973 are listed in table I. Our major effort is now directed to the task of developing an operational system for isolating specified themes from imagery. Dean Edson of the Geological Survey will report on this task later at this meeting. I will briefly cover the other tasks.

DEFINING AND EVALUATING MODES AND SENSORS

We feel that in remote sensing cartographic spatial requirements are the most stringent, and in this light we must take a critical view of all defined earth-imaging systems. The film-return mode is the one we consistently champion for basic mapping, and, until electronic data-transmission systems have comparable geometry and throughput, we will continue in this vein. Even the Hasselblad cameras carried on Apollo 9 demonstrated the enormous cartographic potential of the film-return mode. Figure 1 shows the relationship between an Apollo photo and what was considered to be a good 1:250,000-scale map. The photo showed significant error in the map, which was consequently corrected. If a non-metric camera of 3-inch focal length can do this, just think what a precise calibrated camera of 12-inch focal length, such as we have proposed, would accomplish.

However, we are well aware that film-return systems have distinct limitations, particularly with respect to recording time-variant phenomena. We are actively supporting ERTS by subjecting each of its RBV cameras to a precise geometric calibration. We also have proposals accepted by NASA, to analyze the geometry of the multispectral scanner (MSS) imagery and to prepare a wide variety of cartographic products from ERTS data. In fact we have agreed to scientifically monitor and evaluate all cartographic experiments involving ERTS data. We have proposed a similar range of activities for Skylab.

In 1969 we proposed an earth-sensing geosynchronous satellite, and we still believe in this concept, because it is the only space mode that

offers true selectivity with respect to both area and time. In addition, it has some unique cartographic capabilities, which we plan to investigate through research at Ohio State University.

We believe that the full potential of the aircraft mode is yet to be developed and that, even as we move into space, aircraft programs cannot be neglected. As an indication of our interest, we have loaned both a 6-inch and 12-inch mapping camera to NASA for experimental use in U-2 flights. We are just as interested in using high-altitude photographs for mapping operations as we are in using them for providing a correlation medium for space imagery.

In addition to sensor geometry, we are concerned with photometry and resolution. With respect to photometry, we can only define our requirements and ask NASA for meaningful photometric calibration, as we have little in-house capability in this field. We do have, however, a NASA-funded task to examine the resolution of RBV imagery. This is of paramount importance since the term resolution has several meanings which have caused a good deal of confusion. We accept the photographic criterion of resolution as defined by bar targets. It is essential to compare the resolution of TV and scanner systems with photography, and that is what we hope to do. Based on existing data, we accept $2\sqrt{2}$ TV lines as being capable of resolving a high-contrast bar target pair and about 4 lines for a low-contrast pair. We believe a similar relationship should hold for the instantaneous field of view of a scanner, but empirical testing of all new TV and scanner systems is obviously required. To insure objectivity we suggest that such testing be accomplished by those not concerned with contractual specifications. We now predict the resolution of selected ERTS and Skylab sensors to be as shown in table II.

TRANSFORMATION TO DEFINED REFERENCE SYSTEMS

Both theoretical modeling and actual transformation are involved in placing imagery or graphic detail on a defined reference system. Fortunately, we have agreed on the Universal Transverse Mercator (UTM) as the standard projection and grid for the EROS program. By combining the thematic isolation techniques with the processing of rectified photoimages, we believe that the production of meaningful color photomaps is only a year or so off. Figures 2 and 3 illustrate our approach to color photomapping from high-altitude photographs. The color photograph in figure 2 has been filtered into separate bands, each of which has been passed through a rectifier with identical settings. The color IR photograph in figure 3 has been transformed through the rectifier in one step but onto a color-sensitive base. We still have not carried such products through a lithographic press but hope to do so during 1972.

A most significant development is illustrated in figure 4. It indicates that a 1:50,000-scale orthophotoquad can be made from U-2 photographs to meet the horizontal ground accuracy standards for a 1:24,000-scale line map. Since an orthophotoquad can be made in a fraction of the time and cost of a line map, this could mean a real breakthrough towards map revision. We consider the orthophotoquad and line map complementary rather than competitive. Note that all our new products have a fine-line UTM grid to expedite precise digitizing of map data, by any map user. We have developed coordinate readers for quick referencing of points on gridded maps. We are, of course, looking for constructive criticism and comment on all these new products.

USER RESEARCH FACILITIES

As a byproduct of NASA and EROS cartography programs, we are gradually building a user research facility in the Washington, D.C., area. Equipment is now divided between our McLean, Va., and Silver Spring, Md., offices. Before long we will move our research effort to Reston, Va., and, of course, the Sioux Falls Data Center will also have facilities to aid the researcher.

CONCLUSION

We believe that real progress is being made in the cartographic applications of imagery obtained from space vehicles and high-altitude aircraft. We also believe that this work is of value to all who would monitor earth resources and our environment.

TABLE I.--EROS CARTOGRAPHY PROGRAM FOR FY 73

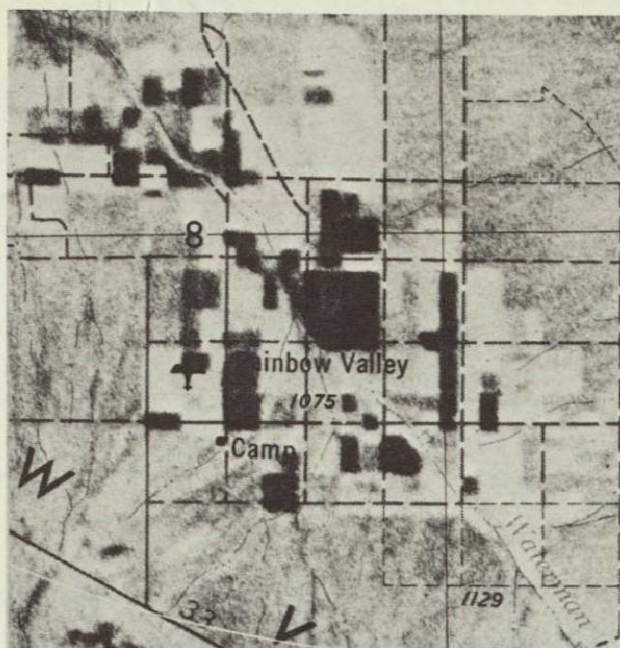
Objective

To prepare cartographic products depicting Earth surface data

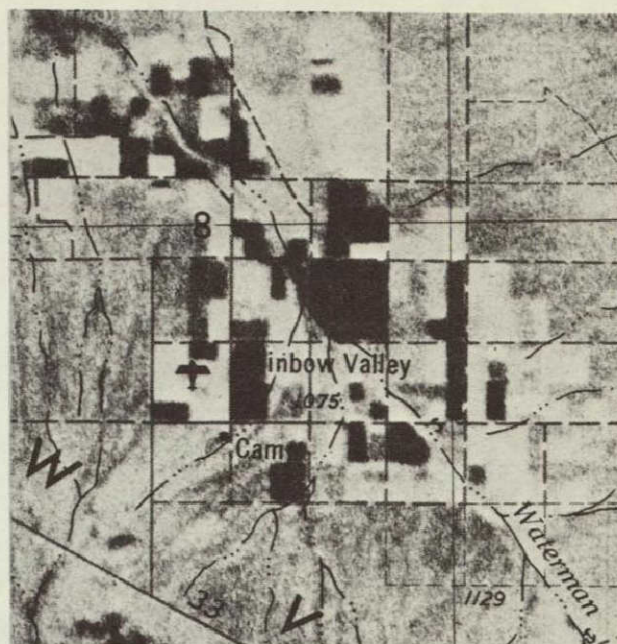
- In support of defined resource requirements
- At appropriate scales and forms
- On defined reference systems
- As functions of spectral energy reflected or emitted from the Earth
- At infrequent intervals for fixed features
- At frequent intervals for specified time-variant thematic phenomena

Tasks

- Defining and evaluating acquisition modes and sensors that satisfy the cartographic objective
- Developing procedures for transforming sensor outputs to the defined reference systems and cartographic forms
- Developing procedures for isolating specified themes
- Developing procedures for disseminating cartographic data
- Preparing a series of prototype products
- Obtaining and evaluating user responses to prototype products
- Providing user-oriented cartographic research facilities



Original Map



Corrected Map

Figure 1.--Map detail (planimetry) was moved about 1 mm (0.04") on this 1:250,000-scale map (Phoenix) to conform with the detail on the space photo (Apollo 9). The photo was found to be correct.

TABLE II.--PREDICTED RESOLUTION (PHOTOGRAPHIC CRITERION) OF EARTH-SENSING SPACE SYSTEMS FOR TYPICAL LOW-CONTRAST EARTH SCENES.

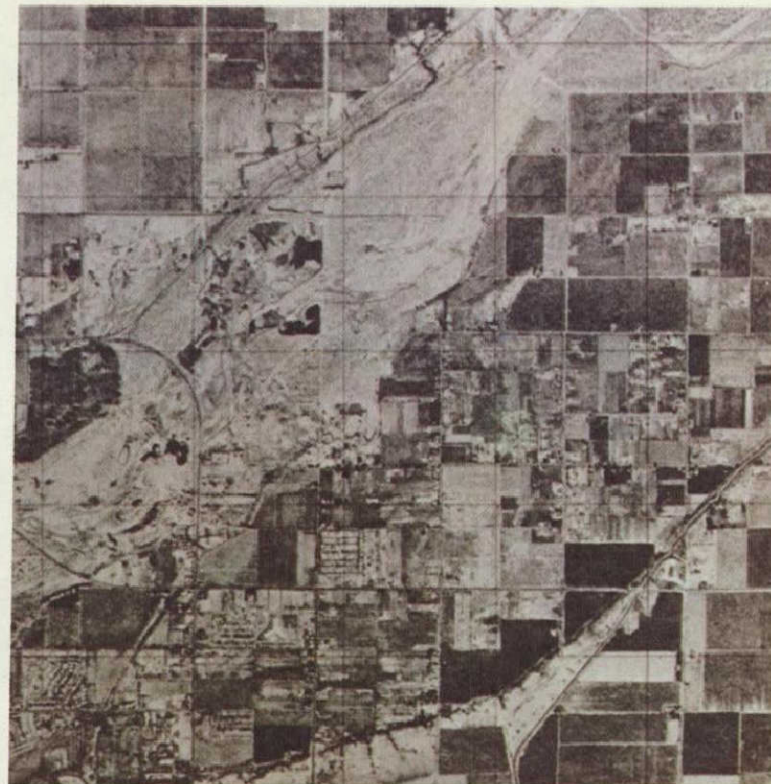
Program Sensors	As recorded by the sensor, lp/mm	In terms of meters on the ground	As normalized to a typical Gemini/Apollo photo (80 mm f.l. camera from 230 km)
Gemini/Apollo Hasselblad	30	97	1.0
ERTS RBV's (average of three cameras)	35	212	2.2
MSS	23	316	3.3
Skylab S190 (mean)	42	68	0.70
Hycon ETC (average of B&W, color, and color IR film)	40	24	0.25



Figure 3.--Comparison of line map and rectified color IR photograph. Camera focal length 12 in.; flight height 60,000 ft. (Sugarloaf Key, Fla.)



1:24,000-scale topographic line map



1:50,000-scale orthophotoquad
made from U-2 photograph(s)

Figure 4.--The line map and orthophotoquad are complementary map products: both have equivalent horizontal ground accuracy; the orthophotoquad updates the line map.

N 72-29367

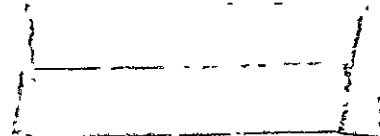
69-1

SECTION 69

AUTOMATIC THEMATIC MAPPING IN THE EROS PROGRAM

by

Dean T. Edson
U.S. Geological Survey
Topographic Division
McLean, Virginia



INTRODUCTION

During the last 12 months the Topographic Division, U.S. Geological Survey, has been responsible for defining and implementing an Automatic Thematic Mapping system which is to be operational by the time ERTS-A flies. The basic system design features utilization of state-of-the-art image processing and high productivity. A throughput of 45 continuous-tone images, constituting 15 multispectral scenes, was set as a desirable goal. On this basis the following design criteria were specified:

1. The system must be capable of accepting a wide variety of input mediums and formats.
2. The system must include preprocessing to normalize input, thus providing maximum hardware throughput at minimum initial investment. Preprocessing includes but is not limited to analog image scaling, geometric and radiometric rectification, and image conversion to digital mode when required.
3. The system must provide real-time evaluation of thematic content on which instructions for photomechanical theme-extraction processing are based.
4. The system must provide state-of-the-art equidensitometric photochemical processing according to detailed standard instructions generated in the theme evaluation phase under rigid quality control.
5. The system must finally be capable of relating highly reliable theme data to a ground reference system by means of ground truth and of providing a wide variety of map-formatted data in both graphical and digital form.

In the context of the EROS program the term "Automatic Thematic Mapping" designates a specific approach to the automatic extraction and cartographic presentation of thematic data contained in multispectral photographic images obtained from a wide variety of sources. First experimental efforts are concentrated on the mapping of four basic themes,

- Open water
- Snow and ice
- Infrared-reflective vegetation
- Massed works of man.

The system described is by no means limited to these themes, but they are considered typical user requirements. In final form, extracted data will be referenced to the real world by means of a suitable grid and scale. The grid system adopted for this purpose is the UTM.

Prior art in extracting themes from remote-sensed imagery has used three equidensitometric methods--digital, video (analog), and photomechanical (analog). As a basis for theme extraction in the new system, we assume that each mappable phenomenon has a distinct spectral signature. We further assume that the spectral signature called a density ratio signature, can be defined in terms of recorded densities related to the response of an individual sensor.

Among the serious problems in extracting and quantizing specific thematic data, not the least are related to metrically incorrect images. We are assuming that every image selected as input to the system has errors due to such causes as attenuation of light through the atmosphere, anomalies in the electronic and optical elements of the sensor system, and imperfect processing of telemetered data into a suitable analog image.

As indicated in figure 1, the first step in Automatic Thematic Mapping is density rectification of each photographic image to be processed for theme extraction. This rectification produces the equivalent of an ideally illuminated scene, a combination of the original image and a continuous-tone density correction mask generated by computer.

The second major function is the Multichannel Image Analysis Subsystem (MIAS), which enables a trained operator to determine the specific theme content of a set of spectral response images. MIAS essentially duplicates the photographic process in a video electronic real-time mode. The three or more images constituting a scene are scanned and stored in geometric register on a video disk recorder. The images can then be combined electronically in the same way that images are combined in the photographic laboratory, but with lower resolution.

The final major step in theme extraction is photomechanical processing of images according to instructions generated in the analysis phase. This processing combines all the original images with all the correction masks, which are in analog form (written on film) and geometrically registered to their corresponding original images.

SYSTEM DEFINITION

The image format for input to thematic extraction is based on 70-mm nominal size. We plan to concentrate on using, but not limit ourselves to, ERTS A bulk imagery. The system will provide means of using just about any size and type of photographic image that might be available and of scientific interest. As shown in figure 2, the original image is transferred to a film chip based on the standard 4- x 5-inch size of cut film. The image is positioned on the chip in such a way as to provide the necessary geometric register accuracy and for the required radiometric auxiliary data, such as density step wedges. The precise placement of the image on the film chip establishes the single image coordinate system required to maintain geometric register throughout the theme-extracting process.

The functions of image preparation are also shown in figure 2. The first converts the image to digital form by means of an image digitizer. The digitized data are then analyzed by computer programs that generate the necessary radiometric corrections. The third function reconstitutes the images into analog form as a continuous-tone film print. Three products result from preparation processing. The most important is the density correction mask, which is the analog version of radiometric correction for any given image. Placed in combination with the original, it provides an evenly illuminated scene. The other two analog masks (fig. 2) are the rejection mask, which eliminates unwanted imagery that may result in the processing of spurious data, and the high-frequency noise mask, only used with electronically constituted image data.

All three correction masks are generated in precisely the same coordinate system that was established with the input image. When the masks are combined with the originals in correct geometric register, they constitute the first major goal of a corrected image.

SYSTEM IMPLEMENTATION

The major hardware components in the Automatic Thematic Mapping system are (1) the density manipulation subsystem, which is the only digital processing component; (2) the Multichannel Image Analysis Subsystem, which provides an analog electronic simulation of the entire photomechanical process; and (3) the photomechanical process, which is photolab work. Figure 3 diagrams the configuration of digital hardware for the density manipulation subsystem, under the control of a PDP 11 computer with 12k 16-bit words of core storage. A data link is provided to several on-line devices by means of the PDP Unibus and interfaces. Three of the devices shown at the bottom of figure 3 operate on-line with the PDP 11 to select density correction control points. The image clipping and platforming unit provides a means of rapidly generating a rejection mask by threshold filtering of digital density levels. The fifth unit is the image recorder, which can reconstitute digital image data in analog form. The system has two mass storage units, a disk drive unit with 5 million words random access and a magnetic tape drive with controller for nearly unlimited additional serial storage. The TTY and paper-tape reader are system support and operator control devices.

In figure 4 the hardware configuration for digital processing is schematically laid out. The coordinate Entry Unit contains a joystick control so that the operator can control a computer-generated cursor which appears on the interactive display screen. The continuous-tone image being examined, which appears on the interactive display, is generated by the Dicomed digitizer. The digitizer scans the image and writes it on the storage tube at a resolution of 2048 lines. When the cursor mark is aligned with a suitable density control point, the position of the point is then transferred to the PDP 11 under operator control and stored on the disk. A maximum of 25 density control points are required to adequately control and statistically evaluate each radiometric correction mask. As indicated in the center and lower portion of figure 4, the selection of density control is based on density samples of common features. If, as an example, we want to map open water, we select those control points that we can interpret positively as open water. The size of the density sample, or cluster of pixels which indicate each control point, is variable under operator control from a 2-by-2 array to as large as an 8-by-8 array. For each density control point we record the x and y and the mean density. The generation of the density correction function is based on approximately half of the density control points selected according to their even spacial distribution, and the remaining half are used to evaluate the performance of the density correction algorithm. A statistical report of this analysis is printed out after each

correction function is generated. Once an acceptable density correction is generated, the results are printed on film by the image recorder.

MIAS permits a rapid evaluation of theme extraction from the multiple images of a multispectral scene. Figure 5 is a diagram of the MIAS function. On the left are the input images and the registered radiometric correction and rejection masks. MIAS is based entirely on analog electronic scanning and signal processing. The hardware permits as many as 70 images to be scanned together with their companion correction masks and stored on a video disk. The orientation of each of the input images which will eventually form a multispectral scene are referenced, by means of the original coordinate system, to the image-scanner film stage. The operator controls geometric image register by recording the first image in the scene as a reference and then combining subsequent images as observed on a real-time CRT display. The operator can offset subsequent images from the original coordinate system to obtain exact image alignment. As soon as the second image is registered to the first, it is stored on the video disk. The third and any subsequent images are recorded similarly so that all can appear in register with the first or reference input image. MIAS is based on low-resolution video processing (525 lines) but can be converted to medium-resolution processing by simply updating the scanner tube and display devices. The image combiner (fig. 5) is an electronic processor which permits any or all of the stored images to be combined in any desired grouping, in negative or positive form, and displayed either in black and white or in density-coding color. The image combiner is an electronic equivalent of the photographic process. Once the proper combination of image and image sense is determined, it is recorded in terms of detailed instructions for the photographic laboratory.

The low-resolution theme-extracted product may be of great value to the time-critical user. An auxiliary investigation is underway to investigate the feasibility of transmitting this processed scene over voice-grade telephone lines to a remote user terminal. We think that the low-resolution image can be transmitted economically.

The photographic laboratory is more or less conventional. The major pieces of equipment are a precision copy camera and an array of precision contact printing equipment. No color processing is expected, but color-keyed products will probably be used. The laboratory will produce high-resolution theme extracted products from specified combinations of registered images.

The final step in automatic thematic mapping is map grid generation and formatting, whereby the binary theme-extracted images are related to ground control. The result is a geometrically precise map product which can be reproduced for distribution as either a conventional map or a photomap. Both types of product will contain the same primary reference such as scale and grid, which permits direct correlation with the real world.

A validation test of the system will be based on a clear-field-view RBV image obtained from an evenly illuminated RBV scan recorded in the laboratory and processed through the Ground Data Handling System. This clear-view image contains most of the systematic errors that will appear in live ERTS A RBV images. The test is underway and should be completed within 60 days.

PRODUCTS

Figures 6 and 7 are representative examples of automatic thematic mapping products. Both were based on tripac color originals that were subsequently color separated into three bands for theme extraction. Figure 6 shows extraction of open-water areas in the Chesapeake Bay. Figure 7 shows IR-reflective vegetation in the Florida Keys. Both samples are formatted to the image boundary rather than a map boundary; and the reference grid is the UTM.

OPERATIONAL TESTING

All major components of the automatic thematic mapping system are scheduled to be delivered and in operation by early spring 1972. All major contracts and in-house efforts contributing to this system are on time, and we expect to complete the operational tests well in advance of the flight of ERTS A. Additional information and progress reports on this project can be obtained by contacting the U.S. Geological Survey, EROS Program Office in Washington, D.C.

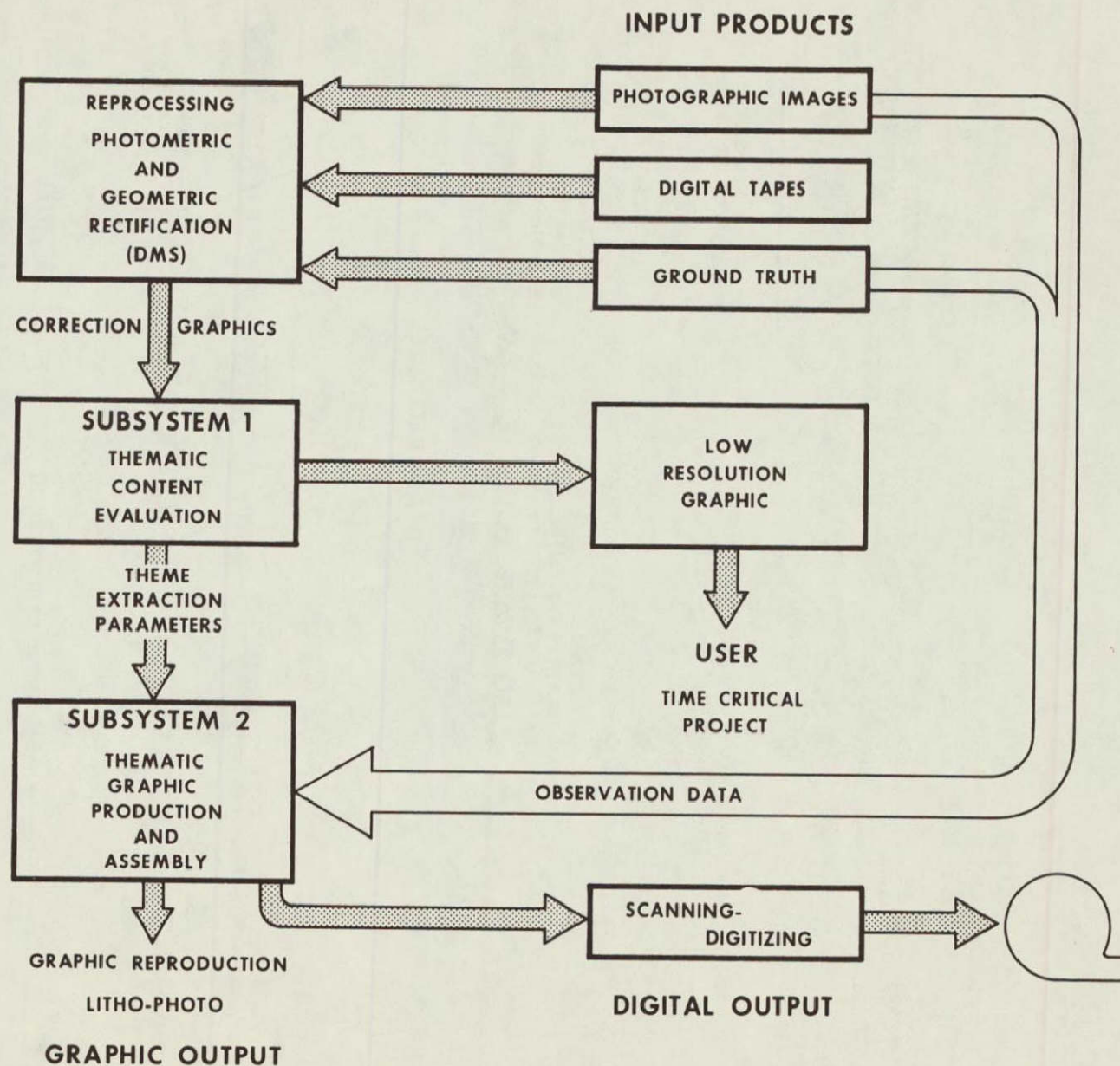


Figure 1.--Thematic mapping system.

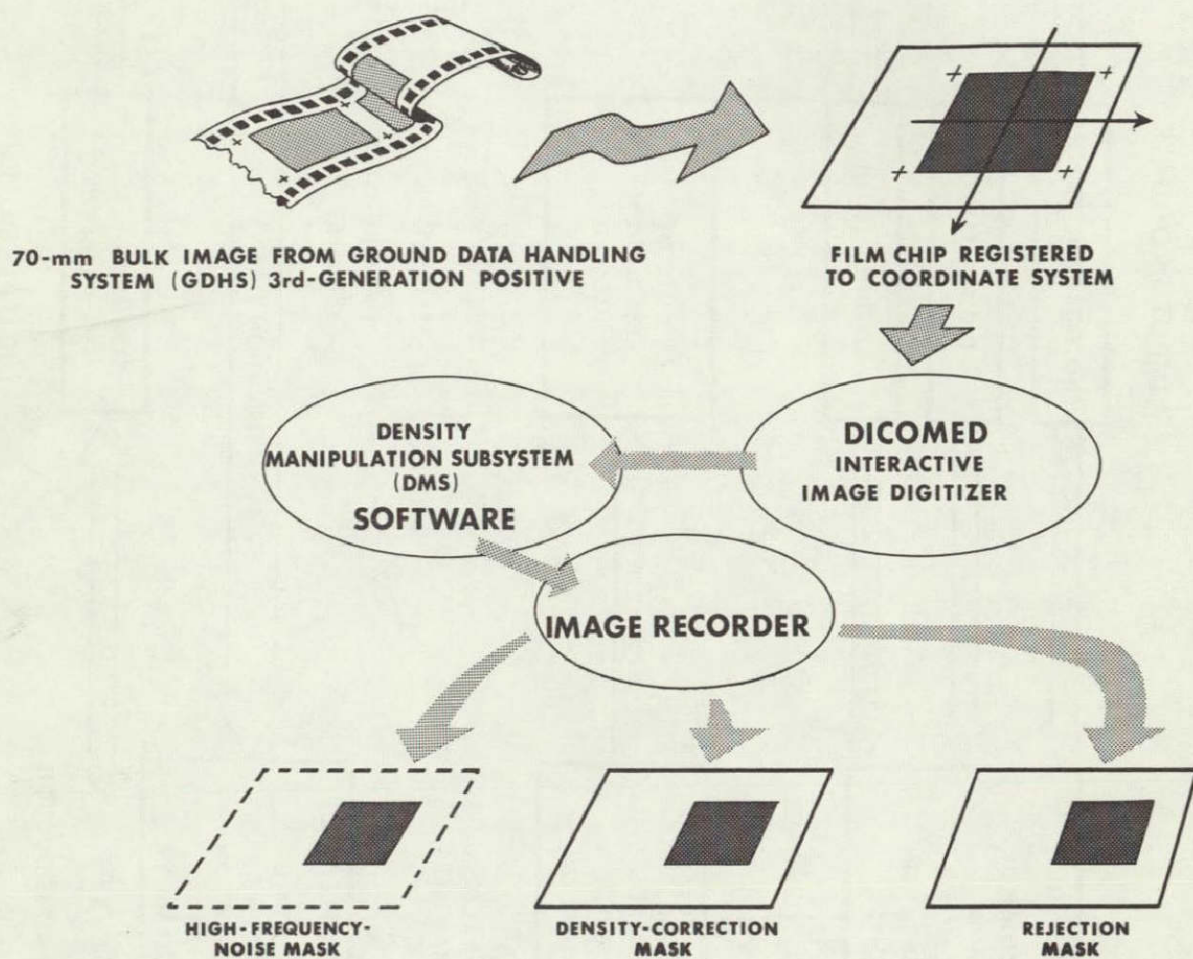


Figure 2.--Image preparation for thematic mapping system (TMS).

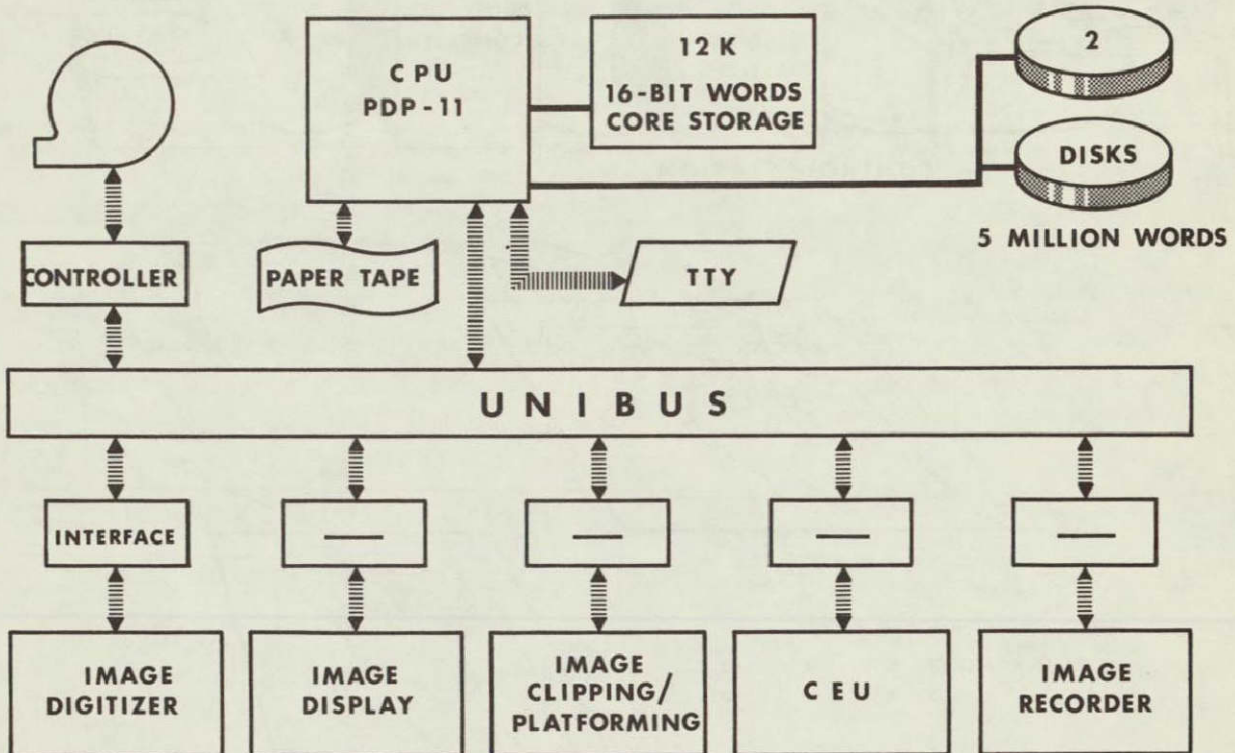


Figure 3.--Thematic mapping computer hardware configuration.

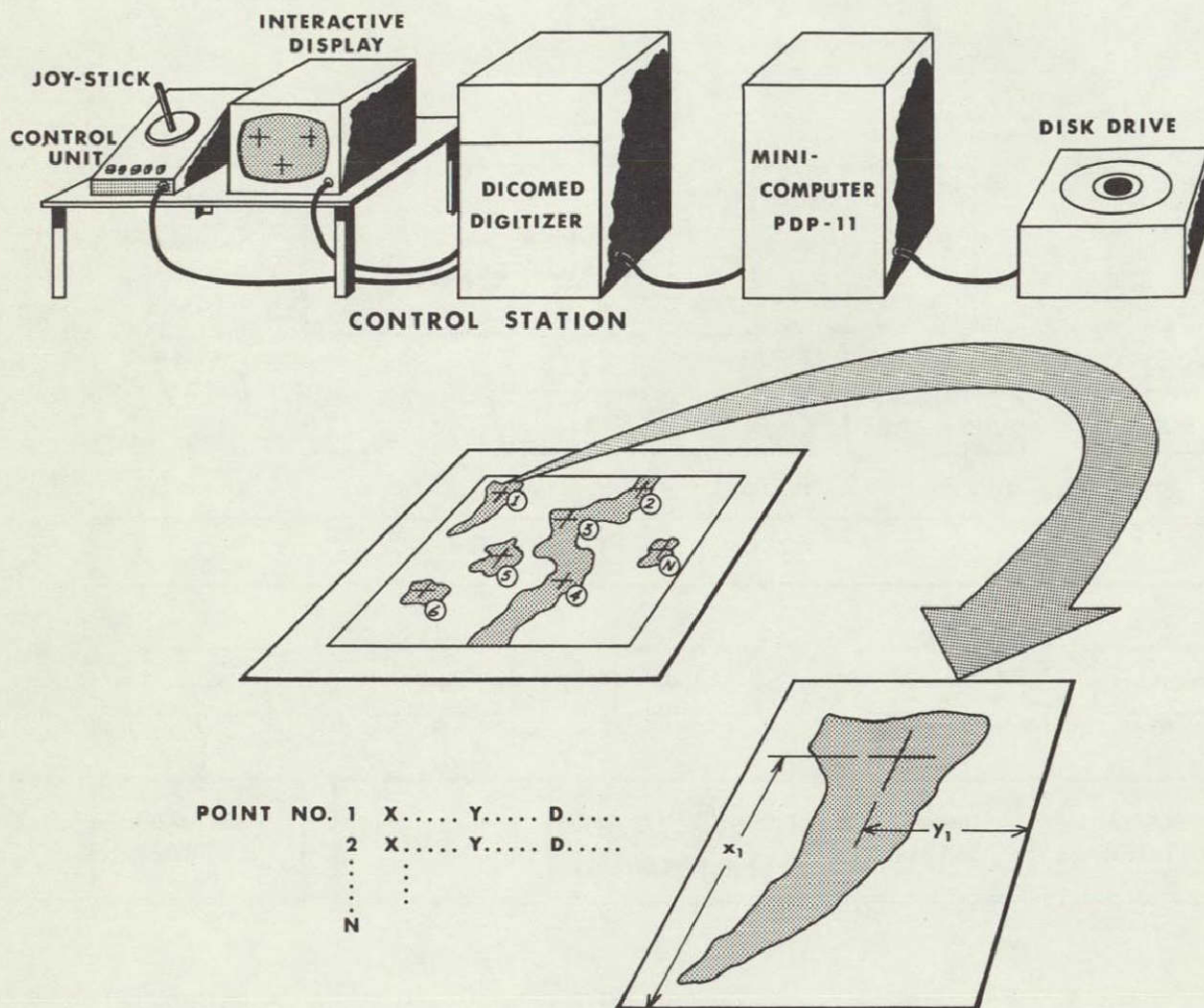


Figure 4.--Density control point generation.

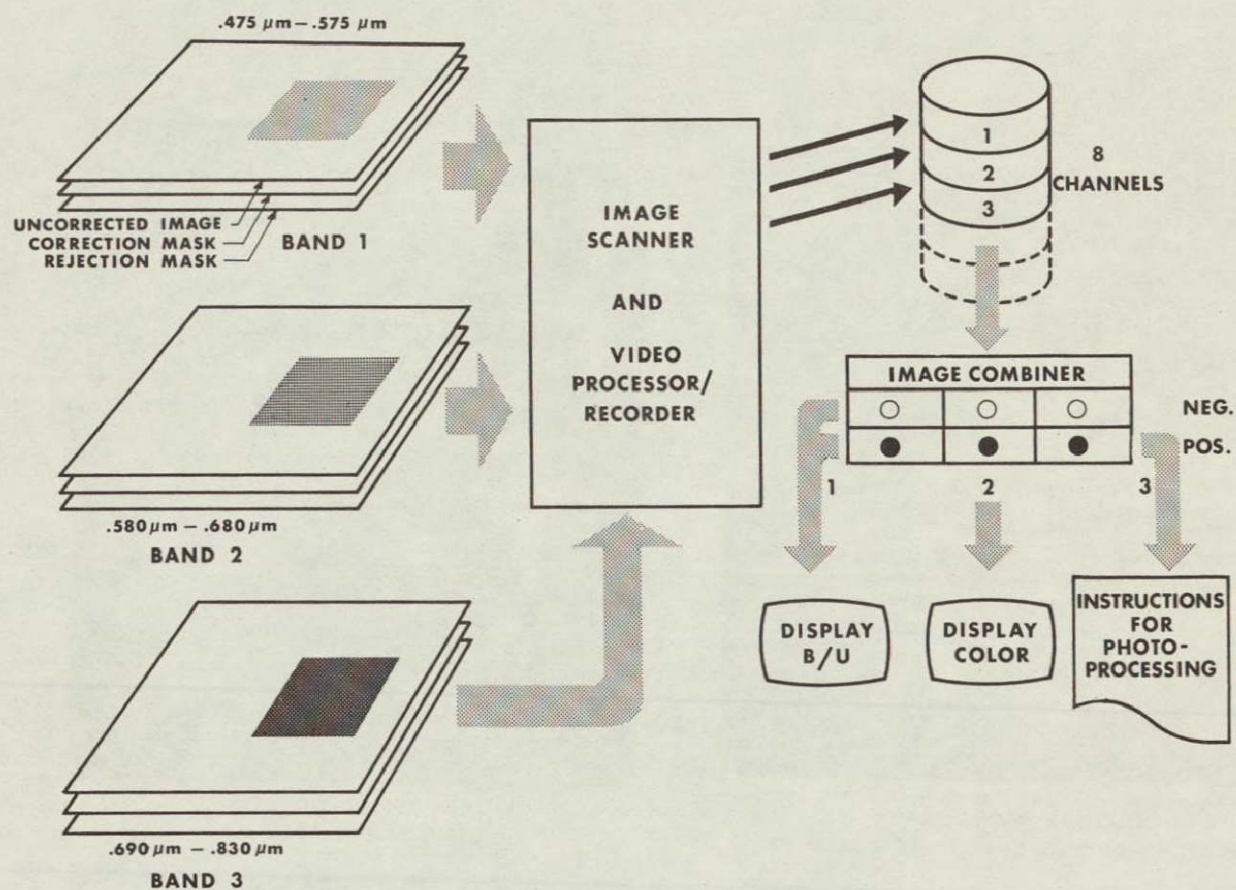
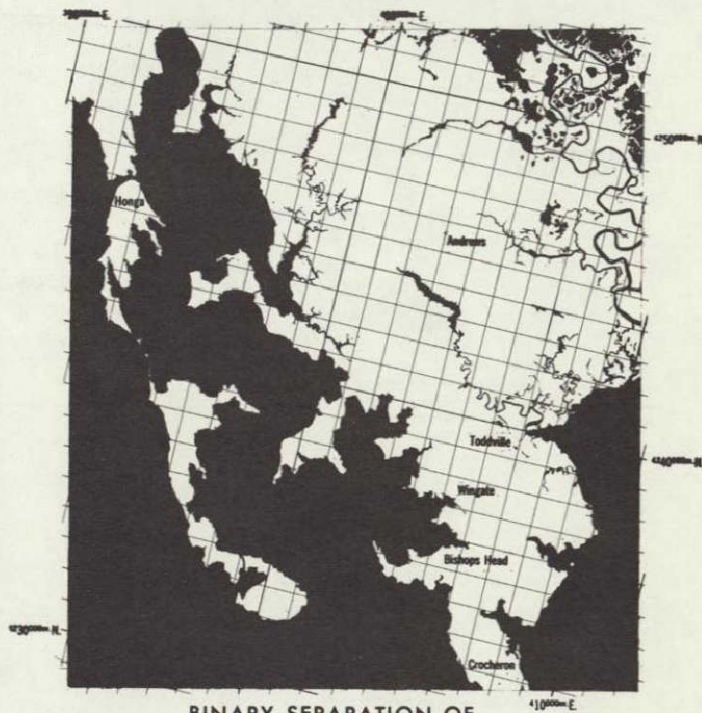


Figure 5.--Multichannel Image Analysis Subsystem (MIAS).



COLOR IR PHOTOGRAPH
6-INCH MAPPING CAMERA AT 60,000 FT.



**BINARY SEPARATION OF
LAND AND WATER**

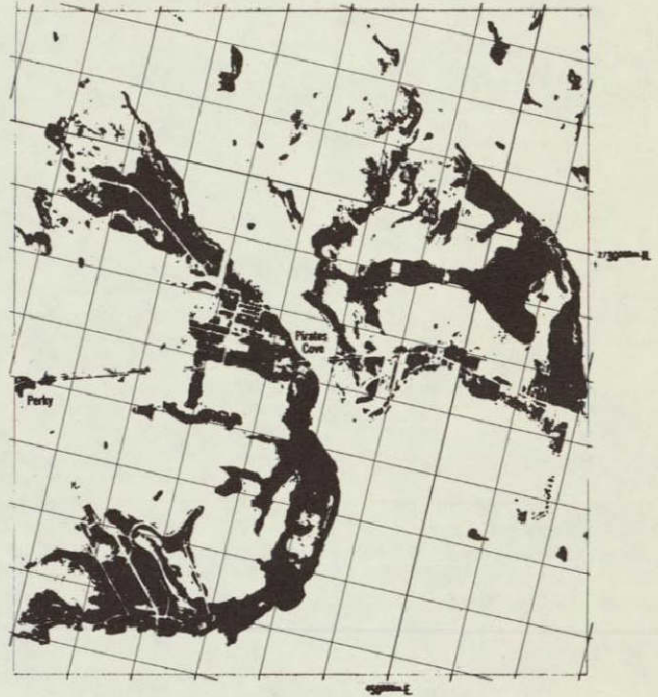
Example of density slicing by Philco-Ford under contract to USGS; NASA photograph.



Figure 6.--Thematic mapping of water (Chesapeake Bay area).



COLOR IR PHOTOGRAPH
12-INCH MAPPING CAMERA AT 60,000 FT.



BINARY ISOLATION OF VEGETATION

Example of density slicing by Philco-Ford under contract to USGS; NASA photograph.



Figure 7.--Thematic mapping of vegetation (Florida Keys).

THE GEOGRAPHY AND HUMAN-CULTURAL RESOURCES
WORKING GROUP OF THE EROS PROGRAM

by

Arch C. Gerlach
Chief Geographer
U.S. Geological Survey
Washington, D.C.

INTRODUCTION

The Geography and Human-Cultural Resources Working Group of the EROS Program serves primarily to bridge a gap between the remote sensing experiments of physical scientists and the needs of socio-economic and culturally oriented planners, policy makers, administrators and other user groups. With that objective in view, the Working Group has been instrumental, through its representatives from various Bureaus of the Department of the Interior, in formulating and activating experimental projects for the application of remote sensing technology and data to problems and operations of those Bureaus. The Deputy Chairman of the Working Group, George Loelkes, will report on the nature, status, and achievements of projects in the Bureaus of Indian Affairs, Land Management, Outdoor Recreation, and the National Park Service, and in other agencies such as the Ozark Commission in the Department of Commerce, the TVA, and State agencies in Oklahoma and Washington.

Within the U.S. Geological Survey, the primary contributor to the field of interest of the Geography and Human-Cultural Resources Working Group is the Geographic Applications Program in the Office of the Director of the Survey. The principal focus of the Geographic Applications Program is on land use analysis and mapping, and on the creation of an operational automated information system which will be receptive to land use and environmental data, which will effectively update and process those data and output information in cartographic, computergraphic, tabular, or textual format. The information system must be effective in identifying changes and trends, and in predicting the reciprocal impact of modifications on land use or on the environmental complex.

THE USGS GEOGRAPHIC APPLICATIONS PROGRAM

The Geographic Applications Program is most closely associated with a USGS plan for the assessment of land resources and environmental conditions. As funds become available the Geographic Applications Program will use data from satellites and high altitude aircraft to create national overview maps at small scales (1:5,000,000-

1:7,500,000) for a folio of special subject maps carefully selected to provide information about land use, resources, and environmental factors to aid in national land use policy development.

Beginning with ERTS-A data, the Geographic Applications Program expects to produce within four years a delineation of current land cover and land use for the entire country at a scale of 1:250,000 which can be used as a base for national and regional planning, for monitoring and measuring trends, and hopefully for predicting and evaluating desirable modes of future land use.

The land resource analysis component of the USGS program will concentrate more intensive efforts on the Nation's most critical areas--those to be most severely impacted by national growth. Consequently, the Geographic Applications Program's Atlas of Urban and Regional Change will constitute a significant contribution to the overall effort, as will also multidisciplinary studies of critical regions such as the Central Atlantic Regional Ecological Test Site.

Noteworthy progress is also being made, in cooperation with the EROS Program, the Computer Center Division, and the Topographic Division, toward creating a geographic information system which will utilize computerized data storage, processing, and print-out technology. Such a system is needed to expedite the geographic projects mentioned above, but it must have sufficient flexibility to fit and function within the broader scope of a gradually developing automated information system for the Survey, and possibly the Department of the Interior as a whole.

User Conferences

In order to relate projects of the Geographic Applications Program more intimately to user needs, three types of user conferences were held during the past year. One was a three-day National Conference on Land Use Information and Classification which was attended by approximately 200 officially designated representatives of national, regional, state, and local agencies concerned with land use planning, taxation, parcel records, zoning, etc. The conference was planned by a Steering Committee under my chairmanship, with representatives from NASA, the USGS Geographic Applications Program, the Soil Conservation Service, Cornell University, the Association of American Geographers, the International Geographical Union, and the Canadian Land Use Survey. The conference was sponsored by the U.S. Geological Survey and NASA. After hearing five invited papers and completing seven discussion sessions, the conference participants accepted in principle, at its closing session, a nested scheme for land use classification with four levels of detail to be defined in more detail by the Conference Steering Committee which is still active.

TENTATIVE LAND USE CLASSIFICATION SCHEME

<u>Level I</u>	<u>Level II</u>	<u>Level I Key (Digit)</u>	<u>Level II Key (Digit)</u>
I. Urban and Built-up	A. Residential	1	1
	B. Commercial & Services		2
	C. Primary Industry		3
	D. Extractive		4
	E. Major Transport Route & Areas		5
	F. Public & Institutional		6
	G. Open Land		7
.....		
II. Agricultural	A. Cropland/Pasture	2	8
	B. Orchards, Vineyards, Groves, Bushfruit, including horticultural areas		9
	C. Feeding Operations		10
	D. Other Agricultural Land		11
.....		
III. Rangeland	A. Rangeland	3	12
.....		
IV. Forestland	A. Forest (Solid crown)	4	13
	B. Aforesting brushland (intermittent crown)		14
	C. Arid Woodland		15
	D. Tree Plantations		16
.....		
V. Water	A. Streams & canals	5	17
	B. Lakes		18
	C. Reservoir		19
	D. Coastal & Estuary Waters		20
.....		
VI. Non-forested Wetland	A. Vegetated	6	21
	B. Bare		22
.....		
VII. Tundra	A. Tundra	7	23
.....		
VIII. Bareland	A. Beaches	8	24
	B. Exposed Rock		25
	C. Tailings, abandoned pits, strip mines & quarries		26
	D. Salt Flats & playas		27
	E. Lava Flows		28
	F. Sand (other than beach), including dunes		29
	G. Other		30
.....		
IX. Permanent Snow & Ice Fields	A. Permanent Snow & Ice Fields	9	31

Figure 1.

As Figure 1 illustrates, there are nine very broad categories of land use at the first level that can be reliably identified from Apollo quality satellite photography. At the second level are 31 categories of land use which can be reliably identified from high altitude aircraft photography. Both of these levels are suitable for mapping at 1:250,000 and smaller scales for national, regional, and possibly state overviews. The third and fourth levels of the classification scheme were left open-ended for development in detail by local agencies to meet their specialized needs. Those levels will be largely dependent on low altitude aerial photography and field investigations respectively, but will relate closely to the Standard Land Use Coding Manual and other widely used classifications that aggregate upward into broader categories at the second and first levels for regional and national use.

A second user conference of primarily regional significance was the CARETS Conference planned by the Geographic Applications Program and sponsored by the COSPEAR Committee of the National Academy of Sciences. It was attended by some 200 representatives of national, regional, state, and local agencies in the Central Atlantic Regional Ecological Test Site area, and channels of communication were established between them and staff members of the CARETS project which have become increasingly effective during the ensuing months.

This leads to the third type of user conference--personal interviews by staff members and contractors. They are being carried on continually throughout our test site projects, and are very rewarding.

Introduction of Subsequent Speakers

I am now going to call upon the senior geographers in charge respectively of the Phoenix Pilot Project, the CARETS regional ecological project, and our urban projects to present their own summaries of achievements. The Deputy Chairman of the Geography and Human-Cultural Resources Working Group will then review progress on remote sensing projects in other Bureaus and agencies which are co-operating with this Working Group.

The next speaker will be Dr. John Place, who will review the Phoenix Pilot Project for Land Use Mapping and Data Processing.

* * *

AN AUTOMATED MAP AND MODEL OF LAND USE IN THE
PHOENIX QUADRANGLE

by

John L. Place
Geographic Applications Program
U.S. Geological Survey
Washington, D. C.

INTRODUCTION

Planners and resource managers have long had a need for up-to-date land use maps of the United States. Very few maps of nationwide land use have been prepared, and they were highly generalized in addition to being out of date, because they required several years to compile and publish. Furthermore, such maps represent situations that existed over a range of dates in the past rather than at one given time. With the advent of the earth resources satellites, it has become feasible to map large regions of the Nation and keep such maps up-to-date. In this way, trends in changing land use can be monitored.

Regional land use mapping should be a major component of effective regional analysis. Land use maps, topographic maps, and soils maps are principal tools in the planning process. Land use maps should be accurate as well as up-to-date, and should provide the appropriate information in a format most useable for planning purposes.

It is now anticipated that satellite imagery of the ERTS type will supplement existing sources of land use information, making it possible to monitor general trends, and very specifically point up problem areas in land use that require more detailed study with aircraft overflights and field surveys. The first step is mapping current land use and modeling it in a computer along with other environmental factors. An investigation of this procedure has been conducted during the past year and a half within the USGS Geographic Applications Program in Washington, D.C., with SR & T funds provided by NASA.

During the development of this program, we were greatly assisted by Prof. James R. Anderson of the University of Florida, who advises us on land use classification systems and on the need for land use information.

PROCEDURES

The most promising approach to accomplishing this mapping appears to be to use as a plotting base the standard 1:250,000 topographic maps, which constitute the largest scale coverage available for the entire country. Each quadrangle map could be overlain with transparent plastic and a land use map compiled upon it, using satellite and ultra high altitude imagery as the principal source of land use information.

For a pilot project, the Phoenix Quadrangle in Arizona was selected. A special topographic map had already been made for this quadrangle by the USGS which included, as background, a controlled mosaic made from two Apollo 9 photographs. This photo mosaic became a plotting base for a map of land use in the Phoenix Quadrangle.

As mentioned earlier, nationwide land use maps have been prepared in the past, but they required years to prepare. Figure 1 shows the most recent example which was prepared for the National Atlas of the United States, and published by the U.S. Geological Survey in 1970. It took two years to compile the map, and data for some parts of the country are as much as ten years old.

We believe that national coverage is now possible at the much larger scale of 1:250,000, which, as mentioned above, is the largest scale for which complete coverage in the United States exists.

Color infrared images obtained from orbit, such as shown in Figure 2, south central Arizona, make this possible.

As an experiment we prepared this land use map of the Phoenix Quadrangle (Figure 3). Information was obtained not only from satellite photos, but also from high altitude aerial photos of Phoenix and most of the irrigated areas. The standard topographic quadrangle provided both geometric precision and supplementary data.

Overlain upon the land use map was a matrix of grid intersections, spaced one kilometer apart, of which Figure 4 is an enlarged example. Actually, it takes over 20,000 kilometer squares to cover the entire quadrangle. The corners of the squares represent even thousands of meters on the Universal Transverse Mercator projection.

In order to make the computerized land use model more useful to planners and resource managers, data on other environmental factors were also recorded for each grid intersection. These factors included soils, drainage basin and land ownership, as well as locational identifiers for states, counties, and census tracts, and for the UTM,

geographic, and state plane coordinate grids. To record these new types of data, maps of land ownership from the Bureau of Land Management, maps of soils from the U.S. Department of Agriculture, and census tract maps from the Bureau of the Census were converted to the same scale (1:250,000) as the land use map. All of these data were read off onto computer cards and tapes using two different methods: 1) hand coding and key punching, and 2) automatic digitizing of the map data. The latter was done at the McLean office of the USGS Topographic Division. It was intended that these two methods be compared for efficiency and accuracy. The digitizing appeared to save considerable labor time. The accuracies have not yet been compared.

Precision

In regard to precision of the results, the standard unit of area measurement is the square kilometer which is well designed for inventory of large regions of the United States, such as the Rocky Mountain Region. However, for studies of individual urban areas, the kilometer cell matrix probably is too coarse for accurate mapping, although accurate enough for sampling urban land use.

Furthermore, studies of major urban areas are being conducted under a different program--our Census Cities experiment described by Mr. James Wray. When map data are read off by automatic digitizer, it will be just as easy to record urban use by hectare cells rather than kilometer cells, although storage capacity may become a problem. We plan to experiment also with polygon search techniques, rather than cellular search, when suitable computer programs become available through research by the Boeing Company, under a contract supported by the EROS Program in cooperation with the Bureaus of Land Management and Indian Affairs.

Results

We now have reached the point where automated output of both maps and statistical analysis are possible. It is our plan to publish the experimental maps in color, each general land use type being shown on a different color plate, with subdivisions in patterns.

The following series of figures shows the automated plots as color plates by land use category. The first is the cropland pattern in the Phoenix Quadrangle (Figure 5). It is an example of the automated output from our Calcomp plotter. Cropland is shown in green with different texture patterns for tree crops and non-tree crops.

Figure 6 shows the urban and built-up areas as sampled by our 20,000 grid points. This general category, shown here in a reddish-pink color, may eventually be shown in the salmon pink which is standard for urban areas on most USGS topographic maps. This has been divided into eight sub-categories by texture or symbols: small cities above and below 2,500 population, airports, quarry pits, industrial sites, and for the City of Phoenix, residential, commercial, and urban open land--the latter being the urban green areas easily seen on color infrared photographs.

Figure 7 shows the large park areas outside of Phoenix, divided by texture patterns into desert oriented recreation and water oriented recreation. These boundaries are obtained not from aerial photos, but from readily available maps, such as USGS topographic maps. Water areas will be shown in blue, but are essentially absent in the Phoenix Quadrangle.

Figure 8 shows the area within the quadrangle reserved for military use, primarily the Yuma Gunnery and Bombing Range, shown here as a red plate.

Most of the remaining land, approximately 85 percent of the quadrangle, is classed as range or potential grazing land, and will be shown (Figure 9) in some light color such as tan or yellow. We are combining all of these color plates to create a published map.

An experiment has been conducted to determine the best method for updating the automated land use maps. Figure 10 shows a map of detected change in land use as found in photo coverage of the quadrangle flown by a NASA U-2 aircraft in November 1970. This map represents the change over a period of eight months. The color shown indicates the new land use. This type of monitoring of change has been of particular interest to tax appraisers in various states.

Figure 11 shows the updated land use map, incorporating the changes shown on the previous map. The black plate of the standard 1:250,000 quadrangle map has been overlain on this to give the impression of what the final map should look like. We hope to print on the automated map, some parts of the black plate from the standard Phoenix Quadrangle, for example, the frame, grid, some place names, and some fixed lines.

Highway data, however, being subject to change, will be updated by automatic digitizer. We have the highway data already digitized, but still in the process of writing a computer program to plot it out. Eventually, it will constitute an additional overprint to the automated map.

In the case of changes, we keep a record in the computer data bank of both the new and old land uses, as well as the dates of the information. In this way, trends in changing inventories of land uses can be monitored and analyzed.

A basic problem underlying all of this work with satellite images and high altitude aircraft photographs is the question of how detailed a classification of land uses can be mapped and kept updated for large areas. Because of the relatively small scale necessary, the classification system must be general, yet it must meet the needs of users.

Figure 12 shows the classification system used with the Phoenix Quadrangle land use map. It depended upon aerial photographs to interpret the urban breakdown and to distinguish tree crops from non-tree crops. We could not have interpreted these from satellite pictures alone.

However, we hoped for a classification scheme which could utilize more fully the satellite images that would be forthcoming in 1972 and subsequent years. We envisioned a classification system consisting of four or more levels or digits. If the first level could represent a very generalized land use classification attainable using satellite imagery only, then subsequent levels could be developed to utilize other supplementary information.

As mentioned by Dr. Gerlach in the introductory presentation, we held a conference in Washington last June to discuss and develop such a land use scheme. In attendance were about 200 potential users from all parts of the country. A tentative first level classification was generally agreed upon at that meeting, plus some discussion of the second level, but those categories still require further definition and follow-up review by the conference steering committee.

The proposed scheme differs from the Phoenix classification shown in Figure 12 primarily in that Recreation and Military have been moved to a lower breakdown level. Henceforth, in the first level of classification, we will report Recreation and Military areas only by their cover type, i.e., forest, rangeland, or built-up, as seen in orbital images. We have added categories for tundra, bare ground, and permanent snow, none of which were found in the Phoenix Quadrangle. It is anticipated that this new classification will be used in any future quadrangles that we map.

In addition to automated maps produced by our Calcomp plotter, we also are turning out tabulations of inventories and analyses run on the computerized data bank.

The resultant printout presents first a matrix of an inventory of land use compared with soil types. For example, it reports the number of square kilometers of soils favorable to agriculture which are still being used only for rangeland. We can print out automatically a map of those specific soil areas.

A second matrix compares land use with land ownership, that is, land owned or administered by Government agencies or privately owned. For example, we can monitor the rate that land is being built upon under any of the ownership categories.

A third matrix shows land use in relation to river basins. With this model, we could inventory, for example, the amount of land converted from rangeland to cropland within the drainage area of Bouse Wash during an eight-month period, thus affecting the yield of sediment to be carried by the streams.

A fourth matrix compares land use with individual census tracts. This could facilitate comparison with data from the 1970 Census. Distribution of population is important to planners and managers, and our capability to relate land use to census data could be very helpful.

This supplementary information in the form of a computer model will be far more meaningful and useful when a large block of many adjacent quadrangles is completed. The data bank is open-ended so that other factors, such as slope, rainfall, or vegetation cover may be added later.

We have brought the development of the automated mapping to a point where the maps are being printed out by both drum and flat bed plotters. These are black-and-white plots, each plot representing a different land use. Each plot is being converted into a printing plate of a different color.

Information from the standard topographic quadrangle map is being used where possible, and some modification of the standard legend is being prepared. A printed color map should be completed in the next month or two. Black-and-white maps and computer runs resulting from analysis of the data bank are already available for use.

Discussion

All of this leads up to an ERTS-A experiment in which we are going to test the utility of ERTS images for updating land use maps of the Phoenix Quadrangle type. To prepare for that experiment, designated as SR-186, we have been testing change detection procedures

using the RB-57 aircraft photos, and soon will be using the U-2 ERTS-simulation photos taken over the Arizona Regional Ecological Test Site.

It is hoped that the techniques developed for monitoring regional land use change seen in ERTS images can be tested further using photographs from Skylab-EREP missions.

Next on our schedule of regional mapping in Arizona are the Mesa and Tucson Quadrangles, which we hope to do during this fiscal year as part of our cooperation with the ARETS effort, depending upon the availability of funds.

Conclusions

We are nearing completion of a semi-automated system for producing computer maps and computer models of land use and other environmental factors. Initially we have done this for the Phoenix (1:250,000 scale) Quadrangle and hope to move on to other quadrangles soon.

Perhaps our most important job in the next two months is working with planners and managers in Arizona to evaluate the usefulness of the Phoenix map and model and, hopefully, to determine how it could be improved. This survey of user reaction will include the responses to the proposed land use classification system designed for nationwide mapping.

After March 1, our primary activity will relate to our ERTS experiment, including tests of the ARETS ERTS-simulation photos. Next year, we hope to use Skylab-EREP photographs for regional land use study generally similar to that just described.

* * *



Figure 1. - The map of land use nationwide from the National Atlas of the United States of America, published by the U.S. Geological Survey in 1970. It is now possible to map and monitor nationwide land use on a much larger scale.

This page is reproduced again at the back of this report by a different reproduction method so as to furnish the best possible detail to the user.



Figure 2. - An example of a color infrared picture obtained from orbit. This one is Apollo 9, frame 3801, of south central Arizona. Such pictures will facilitate monitoring of general land use over large regions.

This page is reproduced again at the back of this report by a different reproduction method so as to furnish the best possible detail to the user.



Figure 3. - A colored map of land use in the Phoenix 1:250,000 quadrangle, produced by the Geographic Applications Program using two Apollo 9 photos, supplemented by high altitude aerial photographs, obtained in Feb. 1970.

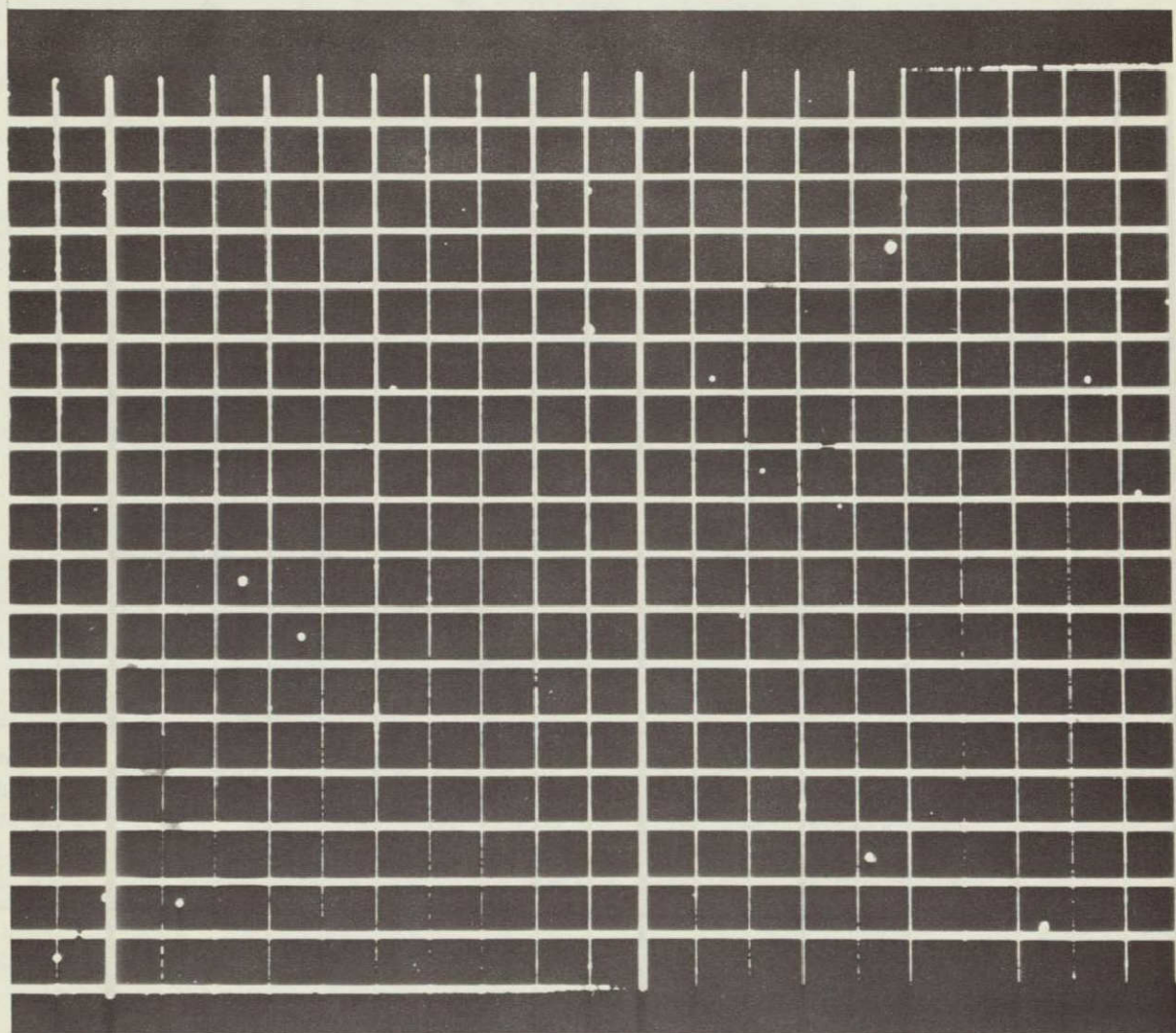


Figure 4. - An enlarged section of the kilometer grid used to read off into a computer several environmental factors, i.e.: land use, land ownership, soils, drainage basin and six types of locator codes.



Figure 5. - The automated plot of cropland in the Phoenix Quadrangle, to be shown in green on a composite map of land use.

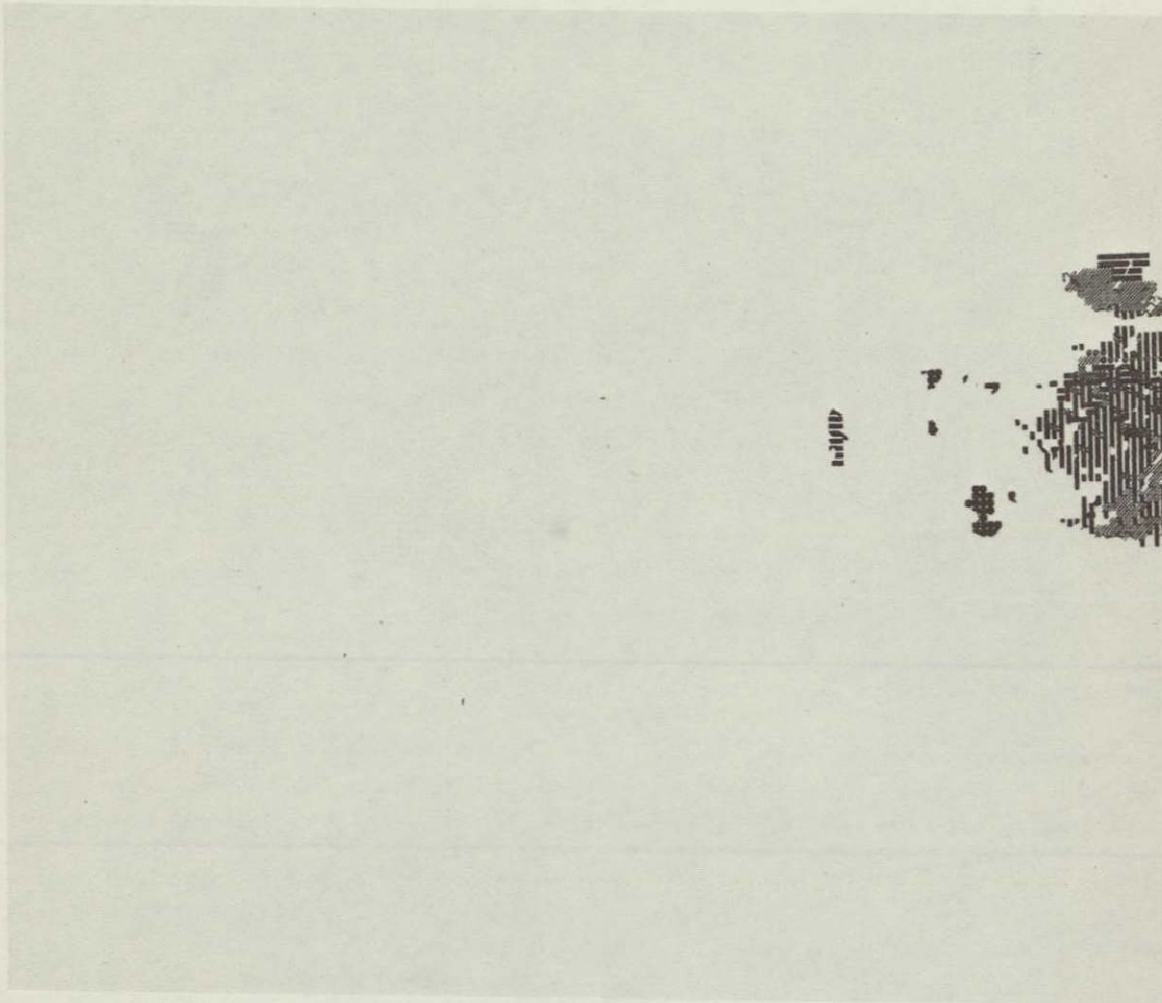


Figure 6. - The automated plot of the urban and built-up areas in the Phoenix Quadrangle, to be shown in red on a composite map of land use.

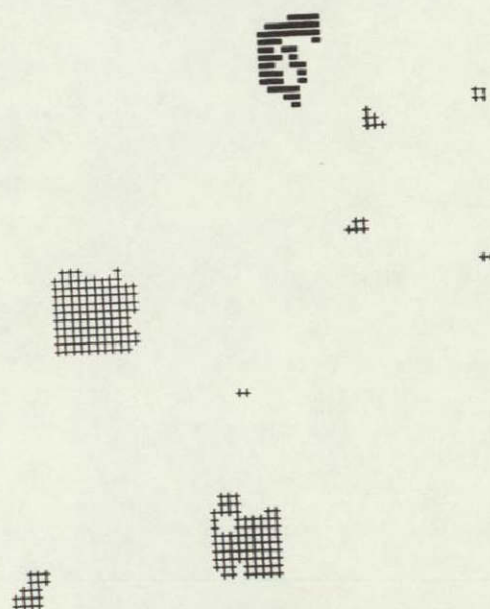


Figure 7. - The automated plot of the non-urban park areas in the Phoenix Quadrangle, to be shown in brown on a composite map of land use.

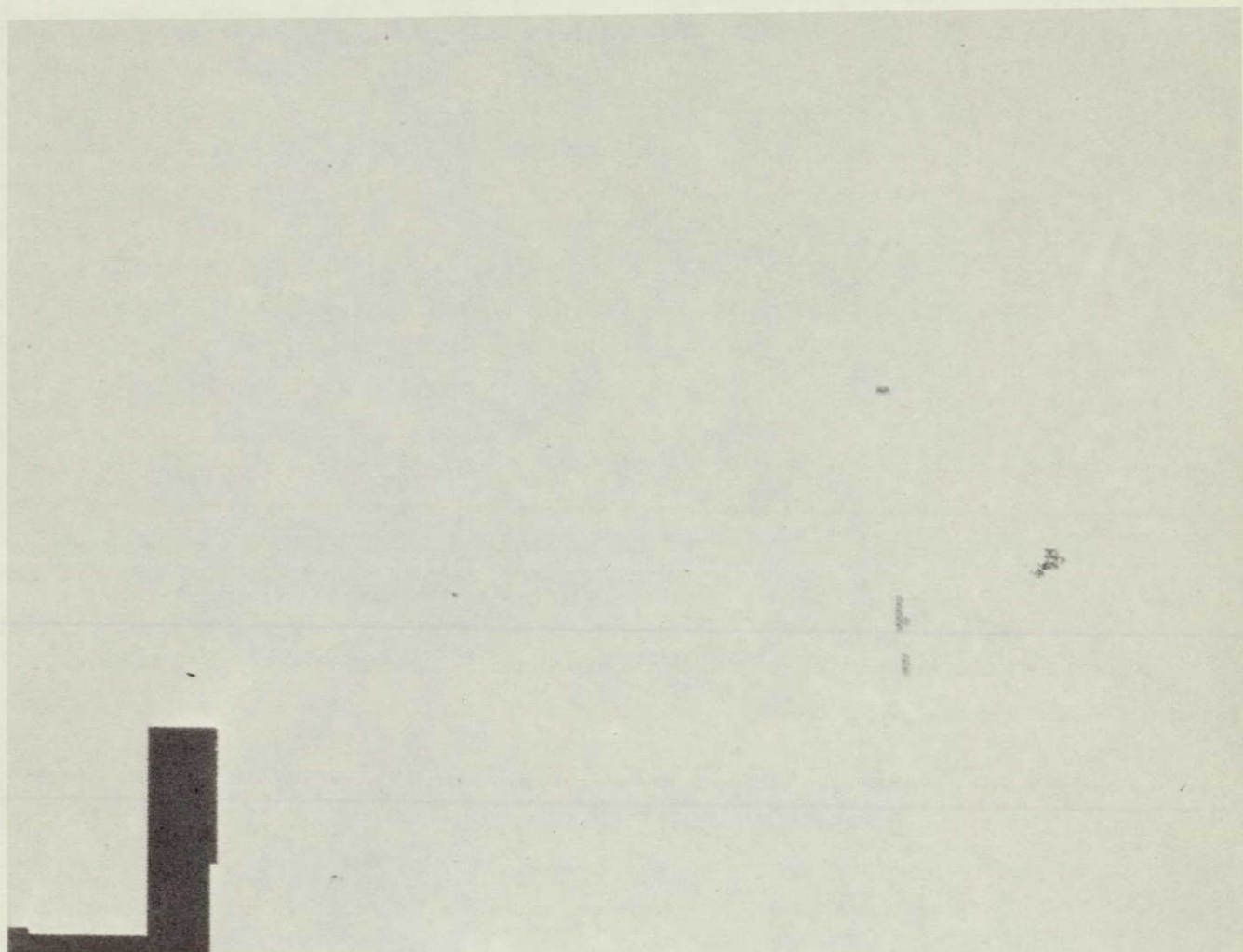


Figure 8. - The automated plot of areas of military use in the Phoenix Quadrangle, to be shown in purple on a composite map of land use.

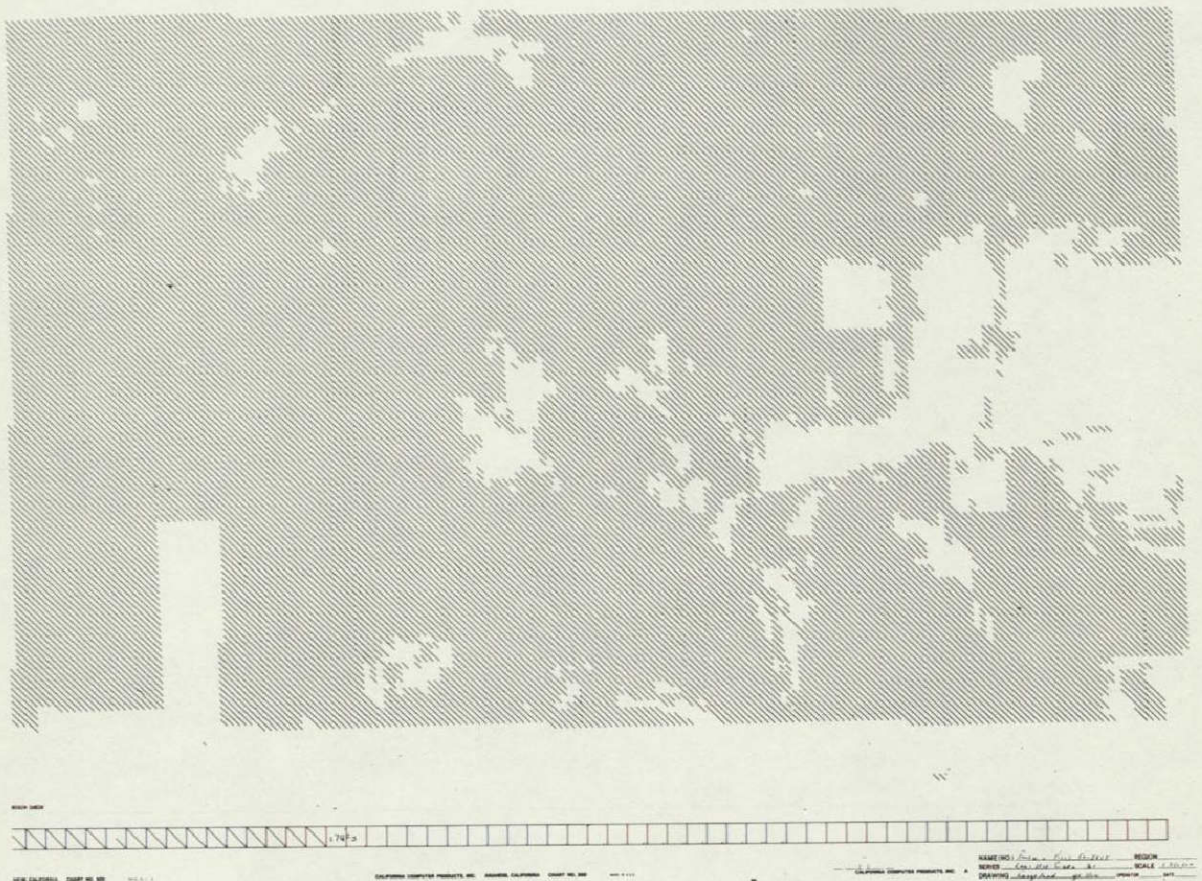


Figure 9. - The automated plot of areas of range or potential grazing land in the Phoenix Quadrangle, to be shown in light tan on a composite map of land use.

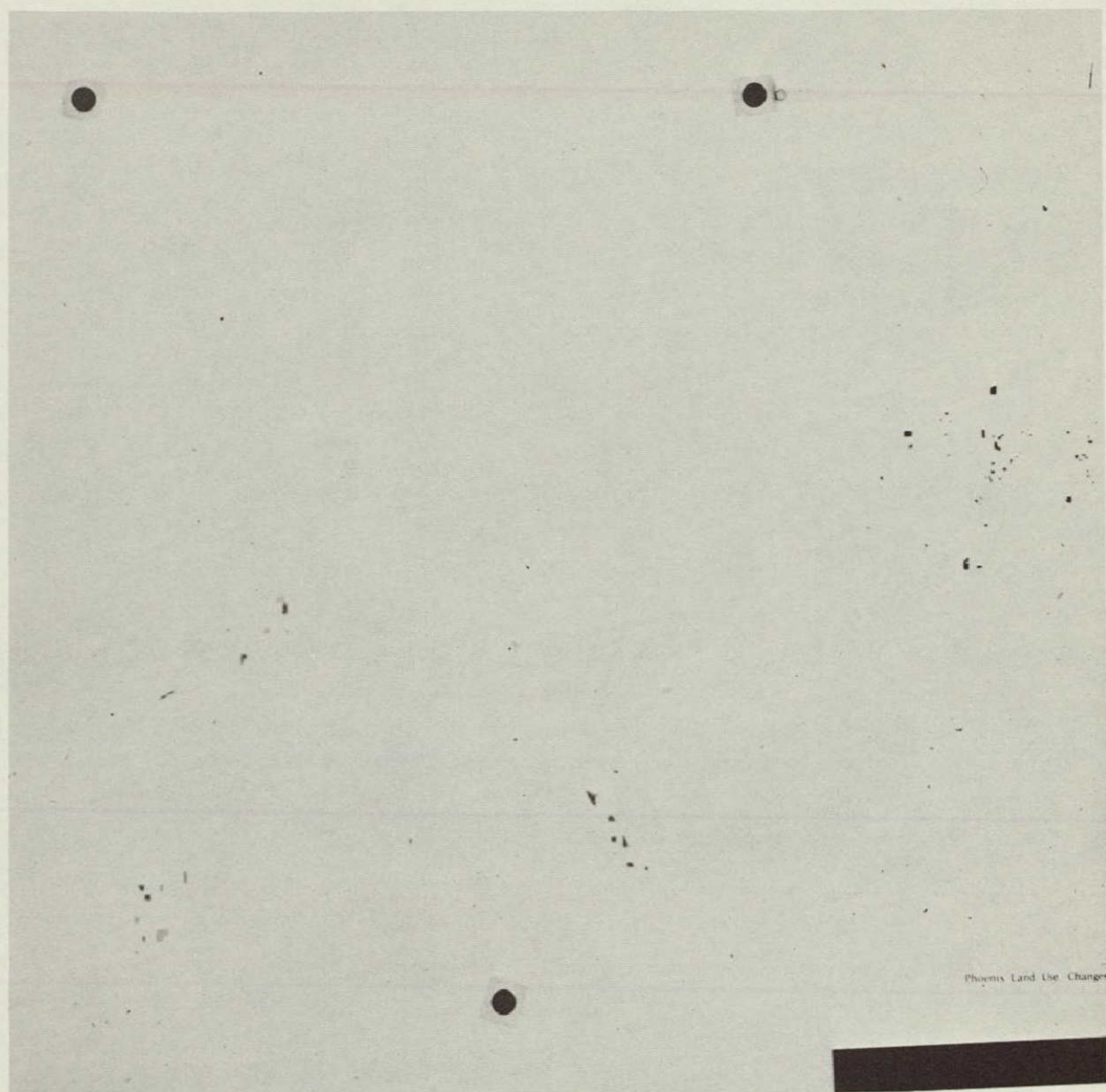


Figure 10. - A map of detected changes in land use in the Phoenix Quadrangle during an 8-month period in 1970.

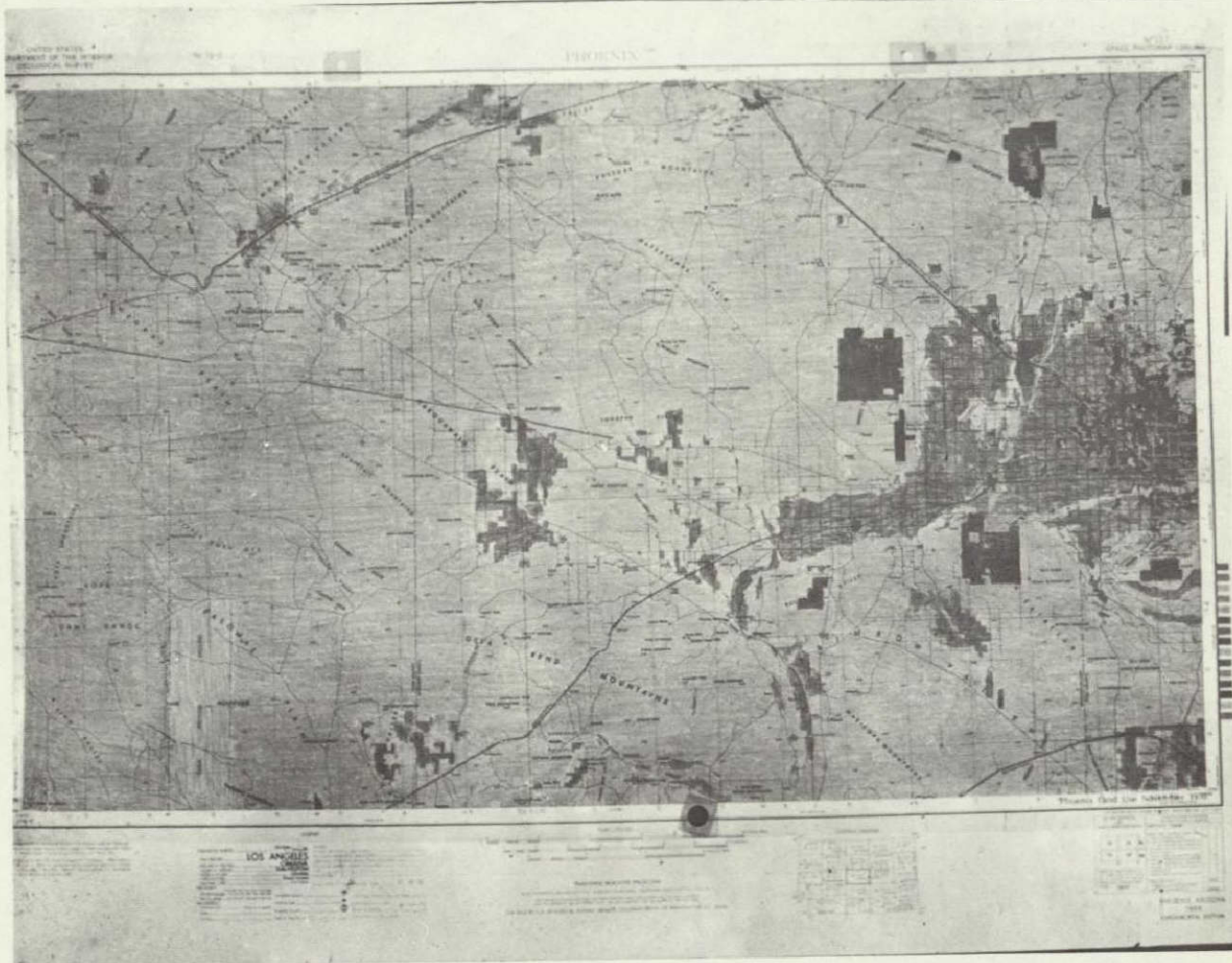


Figure 11. - The updated land use map incorporating the changes detected in photographs taken by a NASA U-2 aircraft in November 1970. The black plate from the standard Phoenix Quadrangle has been overlain.

This page is reproduced again at the back of this report by a different reproduction method so as to furnish the best possible detail to the user.

LAND USE TYPES (For Phoenix Quad)

1. CROPLAND
2. RANGE/GRAZING LAND
3. FOREST
4. MINING / QUARRYING
5. TRANSPORTATION
6. URBAN (6 types)
7. RECREATION-PARKS
8. MILITARY USE
9. WATER

Figure 12. - The classification system for land use utilized for the Phoenix Quadrangle. These categories are being modified to correspond with the land use classification scheme agreed upon in principle at the National Land Use Information and Classification Conference in June 1971.

N72-29370

CENTRAL ATLANTIC REGIONAL ECOLOGICAL TEST SITE

by

Robert H. Alexander
U.S. Geological Survey
Geographic Applications Program
Washington, D.C.

ORIGINAL CONTAINSBACKGROUND**COLOR ILLUSTRATIONS**

A jointly-sponsored USGS/NASA demonstration project is underway in the Central Atlantic Regional Ecological Test Site (CARETS) to test the hypothesis that data from the Earth Resources Technology Satellite (ERTS-A) can be made an integral part of a regional land resources information system, encompassing both inventory of the resource base and monitoring of changes, along with their effects on the quality of the environment. The demonstration project is being conducted as a prototype of a new land use and geographic analysis function within the USGS. The CARETS project is being carried out in cooperation with Federal, state, and local agencies having land resource planning and management responsibilities in the region.

In this paper the acronym "CARETS" refers to the specific USGS project described herein, as distinct from any other usage which has come into being in the past few months. We were asked to comment on the sources of funding for results reported here today. To do this for CARETS, it is necessary to go back to the Third Annual Earth Resources Program Review presentation summarizing the results of the USGS geography program.^{1/} At that time we reported the development of a new program concept in the USGS, taking advantage of the remote sensors' capability for monitoring and updating land use. Our central hypothesis was that the phenomenon we call land use, which can be measured from aerial and space photographs, is the surface expression or end product of a set of environmental processes, and these processes, acting over time, produce the pattern that is observable by remote sensors. Therefore, we regarded the monitoring of land use to be a method for integrating the contributions of various environmental-science disciplines. We had proposed a series of urban and regional test sites to test this concept.

Then came the NASA concept of ecological test sites, about a year ago. This concept was designed to do a number of things, one of which was to economize on pre-ERTS aircraft flights by concentrating on fewer regions and more interdisciplinary effort in each region. Another goal was to stress the inter-relationships among processes and

environmental subsystems in the test regions--hence NASA's use of the word "ecological."

One of the test sites proposed by NASA was in the Central Atlantic or Chesapeake Bay area. The USGS was asked by NASA to serve as a coordinator for some of the activities concerning this ecological test site. The proposal for the CARETS program resulted from that request. The work was handled internally by combining existing SR&T funds with USDI/EROS funds. The CARETS project was expedited by results already obtained from SR&T experiments under the titles of Regional Change Detection and Environmental Impact Studies in the previous fiscal year. In the ensuing months, the CARETS program evolved in close consultation with the National Academy of Sciences Committee on Space Programs for Earth Observations, advisory to the Department of the Interior.

PROGRESS TO DATE

THE CARETS CONCEPT

The first step was to establish a model which would essentially treat CARETS as a land resources information system, with the capability of adjusting to the environmental reality of the region. This "reality" is, briefly, that decisions which result in changing use of the land are inevitably linked to certain environmental consequences. Data on land use change, which can be obtained by remote sensors, must be made available to the user institutions in such a way that new land use decisions can be made with full knowledge of their probable environmental impact. The scheme for accomplishing this in the test region is called the CARETS concept, which is illustrated in Figure 1.

Data sets on land use and land use changes are derived from remote sensing data received from aircraft and spacecraft. These data sets are interpreted in terms of their mutual interaction with processes of the bio-physical environment. Products, including maps and land use data sets aggregated by both planning regions and environmental regions, are then channeled to a community of users through a regional information center. Evaluations in terms of regional priorities are then used to feed back revised requests for remote sensing data and land use analyses. Iteration of this process will result in an improvement of the ability of the CARETS apparatus to respond to regional information needs, thus providing a screening mechanism for guiding the use of remote sensing technology toward applications that result in improved management of land resources.

Priority attention will be given to areas that are defined by the

users as being of critical environmental concern. It is expected that CARETS may serve as a model for the development of remote-sensing based regional information systems elsewhere. In addition, valuable spin-off products and services will be produced, such as timely land use maps and area measurements of land use changes, aggregated or disaggregated as required by cities, counties, metropolitan areas, or regional planning districts. The objectives of the ERTS-A experiment are to determine the extent to which ERTS-A and correlative aircraft and ground data can be utilized to derive the required land use data sets, and to develop procedures for processing the resulting data quantitatively by geographic area as required by users. An arrow should connect the right-hand box in Figure 1 back to the remote-sensing input, illustrating feedback to the data-gathering part of the program. We stress that these are very real arrows; we are very conscious of the need to establish interaction among the various program elements, and are taking several steps to make sure that this interaction occurs.

REGIONAL BOUNDARIES

After consultation with state and Federal agencies, the boundary of the CARETS test region was delimited, and is indicated in Figure 2. In choosing the boundary consideration was given to: a) the extent of the urbanized hinterlands of the Chesapeake and Delaware Bay systems; b) the boundary of the Corps of Engineers' study area for their existing Chesapeake Bay project; c) the requirement for partitioning the area into sub-units compatible with census data and planning regions (hence county boundaries); and d) a reasonably-sized area for aircraft and spacecraft data collection.

PHOTOMOSAICS AND GRIDGING

As a base for mapping land use and for keying the regional data sets to precise locations on the Earth's surface, a rectified, UTM-gridded photomosaic for the entire region has been completed (except for small marginal areas) using RB-57, RC-8 photography from NASA/MSC Missions 144 and 145, October 1970 (Figure 3). The mosaic was prepared by the Topographic Division, USGS. The photography was obtained from an altitude of 60,000 feet, and the mosaic is at a scale of 1:100,000, with a kilometer-square grid overlay, keyed to the coordinates of UTM Zone 18. The numbers on the index sheet (Fig. 3) refer to UTM coordinates in kilometers, the origin being somewhere outside the lower left-hand corner. A pricing policy is now being developed by the Geological Survey to govern the release and sale of the mosaics.

LAND USE MAPPING

Using the first two levels of a land use classification scheme developed by the Steering Committee of the USGS/NASA Conference on Land Use Information and Classification, land use has been mapped for about one-fourth of CARETS. More detailed land use mapping of the Washington, D.C. metropolitan area has also been completed as part of the USGS Geographic Applications Program "Census Cities" project. These areas are delimited in Figure 4.

NORFOLK AREA EXAMPLE

At the extreme southeastern portion of CARETS is the Norfolk-Portsmouth Standard Metropolitan Statistical Area (SMSA). This SMSA has been selected as a sample sub-region of CARETS to test the model and work out the procedures for detailed application in the rest of the region. This SMSA was chosen as a microcosm of the principal kinds of land uses in CARETS, representing variations from the highly urbanized Norfolk and Portsmouth areas to coastal wetlands, and agricultural and forest lands.

A reduced example of the photomosaic for the Norfolk-Portsmouth SMSA is shown in Figure 5. An example of the Level II land use map (Norfolk-Portsmouth SMSA) is shown in Figure 6. Level II is the level of detail extractable from high altitude aerial photography, providing data suitable for mapping at a scale of 1:100,000. Level I is that classification expected to be derivable from ERTS-A; it represents a collapsing of the detailed Level II into 9 major types (not all of which are present in CARETS), and a link between aircraft and spacecraft data sets. An example of Level I is shown in Figure 7. Even though not all of the land use categories developed by the Conference are present in CARETS, we have included the whole legend to illustrate the point that this is a test of a nationwide mapping system.

The basic land use data sets for the Norfolk-Portsmouth SMSA have been field verified by a research team. Sample areas representative of the various land use categories were visited. Further verification was obtained by low altitude overflights.

To provide a test of the system's capabilities for assessing land use change, high altitude photography taken in 1959 was obtained for the Norfolk-Portsmouth SMSA. Using the Level I land use classification, data sets on change and area measurement were derived and compared with the 1970 data, making possible an assessment of the locations and categories of land use change that took place during the decade

corresponding to the decennial census. Changes in terms of the 1959 and 1970 land use categories, respectively, are shown in Figures 8 and 9. These maps show dramatic increase in urbanization at the expense of agriculture and forest. Structural components of the change for the whole SMSA are displayed in the transition matrix, Figure 10, showing the types and amounts of change, in Km^2 , both "out of" and "into" each Level I category. The matrix shows transitions among categories, with the diagonal representing land that did not change in this period. About 91 percent of the total land area is on that diagonal. That means that even in this rapidly changing, highly urbanized region, only 9 percent of the land area has changed categories in 11 years.

This suggests a number of hypotheses. One is that the ERTS-A category (Level I) may not be very sensitive to changes that are taking place in the region. Land use change at the detail of Level I would not necessarily show in Level I categories. But it also suggests that, even in fast-changing areas, the total land area involved in the critical environmental change may be relatively small. This experiment represents a chance to get some real data, some quantitative figures, on amounts of change relevant to an assessment of the environmental crisis. These data sets are helpful in pinpointing areas of expected change during the period of the ERTS-A experiment.

INFORMATION CENTER AND USER SERVICES

An experimental regional information center for CARETS has been established in the Geographic Applications Program Office of the USGS. Figure 11 is an illustration of the kinds of activities and products that we are building into the CARETS Information Center. The input into the information center will be a variety of remote sensing data from NASA and other sources appropriate to the analysis of problems of the region. There will also be maps, ground truth, and other kinds of information that would be necessary to help interpret remote sensing data. Later, the Center will contain analytical studies and user evaluations as well. Processing will include screening, indexing, and cataloging services to meet users' needs. Library facilities will be maintained to handle the film, the maps, and the reports. Viewing equipment, indexes, and a reference library are available. By cooperative arrangement with the USGS Map Information Office, a sales outlet for photos and other CARETS products is being provided to give assistance in imagery and analysis interpretation to the user representatives in the region.

A conference of potential users of CARETS products was held in Washington, D.C., June 11, 1971, under the joint auspices of NASA, the USGS, and the National Academy of Sciences Committee. About 200

representatives of agencies in the region attended, representing Federal, state, and local organizations involved in land planning, primarily with a focus on the kinds of agencies that are involved with data needed for making critical decisions (Figure 12). Background presentations were made on the potential of remote sensing for regional environmental analysis. A description of the CARETS project was presented, and a panel discussion period followed.

We have a somewhat selective approach to the users, concentrating on those who are most critically involved with land use decisions that our data may affect. Planning agencies in portions of the CARETS region have reviewed preliminary products and provided recommendations on how these products might be made more useful to them. These agencies include the Metropolitan Washington Council of Governments, Southeast Virginia Regional Planning District, City of Norfolk, and the Maryland State Planning Office. A design for systematically including other potential regional users in the evaluation process, making full use of the CARETS Information Center facilities, has been completed.

ENVIRONMENTAL IMPACT ASSESSMENT

Geological Assessment

By cooperative arrangement with the Geologic Division, USGS, a new compilation of geologic data, pertinent to the interpretation of present land use and assessment of potential land use in the CARETS region, has begun. First attention is being given to the Norfolk and Washington-Baltimore areas, where related work is underway. This will stress the relationships between rock types, topography, land stability, and changing patterns of land use.

Hydrology

An initial review of data needed for quantifying relationships between land use categories, precipitation, runoff, and accumulation rates has been completed. Coordination of CARETS activities with the Water Resources Division, USGS, has begun, with the first effort being to improve the delineation of wetlands boundaries.

Land Use/Environmental Impact Modeling

A preliminary land use/environmental impact model has been developed for the southern portion of the CARETS region.² The model provides a framework for relating changing land use and land surface

characteristics with the most critical elements of regional hydrology and climatology, so that water and air quality impacts of land use changes can be assessed. Substantial environmental and socio-economic data sets have been assembled and coded in preparation for testing the model, along with land use data sets to be derived from ERTS-A and correlative remote sensing data from aircraft.

Preservation of Environmental Values

An example of what we mean by the relationships between land use and environmental impact is illustrated in Figure 13, depicting the area of the Back Bay National Wildlife Refuge, located within the Norfolk test area. A preliminary evaluation has shown that rapid urban growth has led to significant environmental stress on the water system of the area. Severe pressure from several directions in the upper reaches of the Albemarle-Pamlico systems of North Carolina and Virginia provided an excellent problem for a specific case study. The basic model is changing land use (urbanization) which results in modified run-off, siltation, pollution, sedimentation, and water quality. These, in turn, greatly influence the ecological systems of the bays, which in turn affect the resource use; that is, recreation, commercial fishing, wildlife habitat, etc. The area has been subjected to a number of stresses as a result of the changing land use over the past 10 years.

One of the stresses is the stabilization of the coastal sand barrier as a result of the demands for recreational use of that land by the growing urban population. This means that the inlet from the sea to this former salt-water lagoon has been essentially cut off. The biotic community is being changed from a salt-water community to a fresh-water community, with deleterious effects on the plant life and wildlife refuge. Also, we have data on the deteriorating water quality in the water of Back Bay, which is very closely related not only to the growth of the urbanized and built-up area to the north, but also to the agricultural area, which is increasing the use of agricultural chemicals draining into this region.

Clearly, land use must be related to the urban growth, and agricultural land areas to the kinds of drainage and environmental factors that result from land use changes. We can not get all this information from remote sensors; we have to go into the field and obtain correlative data. Then the remote sensing data, by permitting monitoring the change in the land use, will provide a key to how these changes are affecting environmental quality. The steps involved in the analysis are: observe the present land use; monitor the change in land use over whatever time period appears to be critical; measure the relevant geologic, hydrologic, and other environmental factors; and integrate with population data and planning models.

The key to this is going to be the development of a spatial information system, an example of which John Place illustrated in the preceding paper. We are developing land use data sets to match census units as well as the yet-to-be-determined patterns from ERTS-A imagery.

SUMMARY

CARETS is proposed as a three-year demonstration project. At the end of that time it is expected that the functions, methods, and analytical procedures developed will be incorporated into appropriate operational activities, according to recommendations and evaluations that are developed. One of the objectives of CARETS is to determine scaling factors for developing land use information and regional analyses for regions of any given size. Therefore CARETS has been subdivided into modular sub-regions (Figure 14) to facilitate assignment of project resources on an orderly basis, in accordance with project priorities. Thus sub-region I a (Norfolk-Portsmouth SMSA) will be used as a stepping-stone toward analyzing all of CARETS, just as CARETS will be a prototype of a proposed land resources analysis scheme for larger regions and possibly the whole United States.

The results reported here have been made possible by a cooperative effort on the part of the Chief Geographer of the USGS, and the entire Geographic Applications Program staff. Particular thanks are due to William B. Mitchell, for overall coordination and development of user services; to Ivan Hardin, Peter DeForth, and Katherine Fitzpatrick for photointerpretation and land use mapping; to Susan Moorlag and Harry Lins, for establishment and operation of the CARETS Information Center; and to project consultants Edward A. Ackerman, Robert Dolan, and James R. Wray.

REFERENCES

- 1/ Alexander, Robert H. "Geography Program Design, Structure, and Operational Strategy," Third Annual Earth Resources Program Review, Vol. I, pp. 9-1 through 9-9.
- 2/ Goodell, H. G., et al, "The Richmond-Cape Henry Environmental Laboratory, Land Use and Environmental Impact: A Model," University of Virginia, 1972.

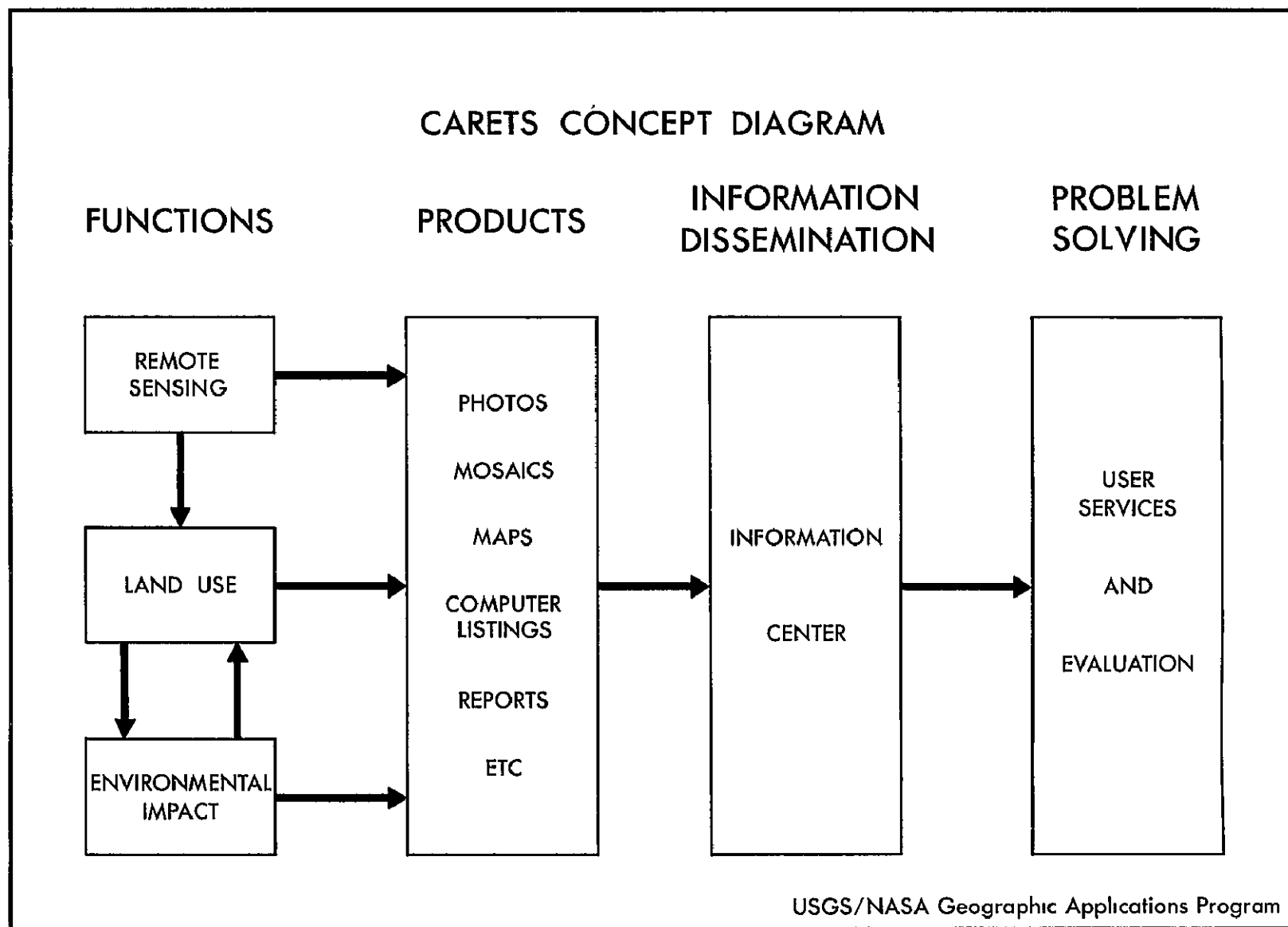


Figure 1.- CARETS Concept Diagram

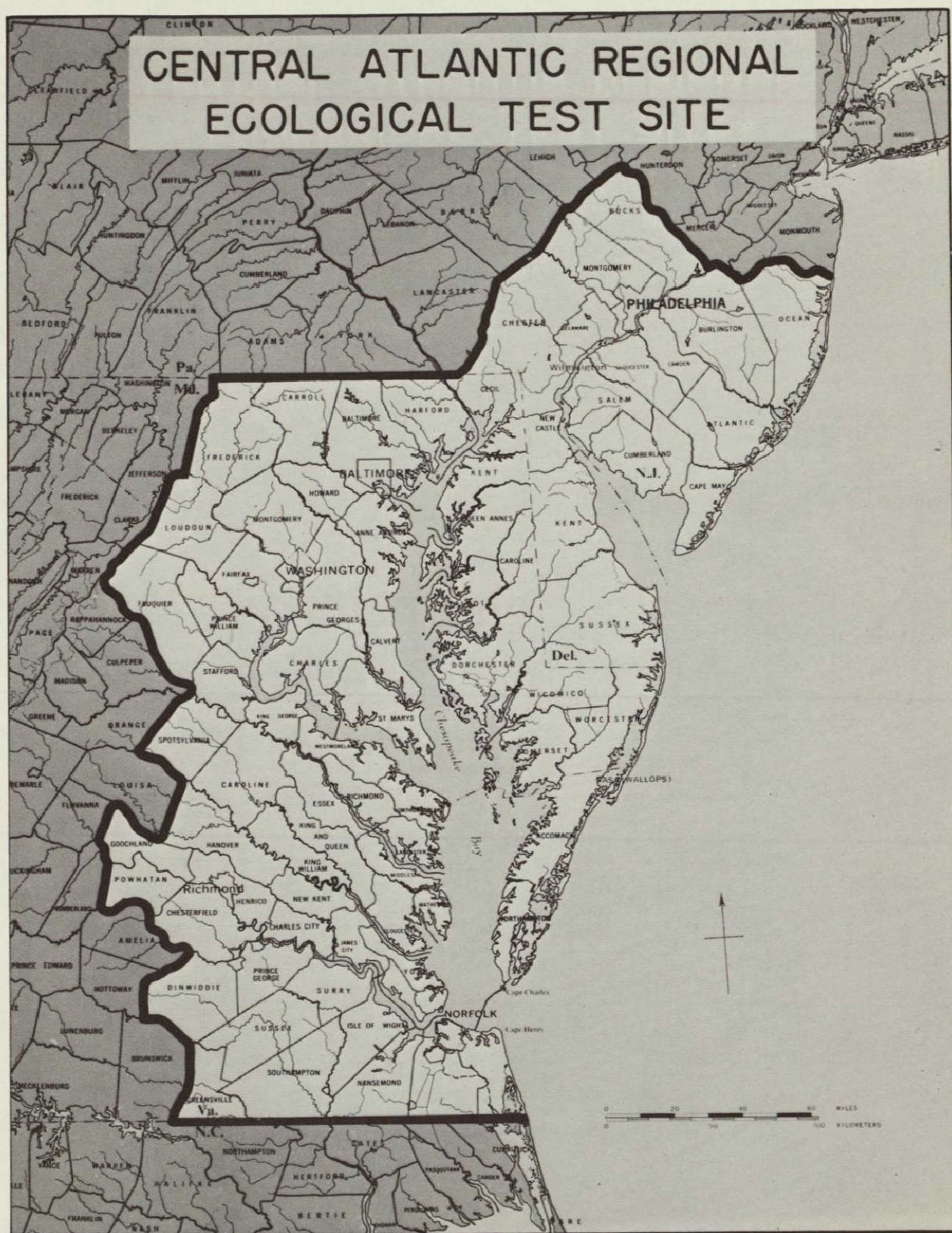
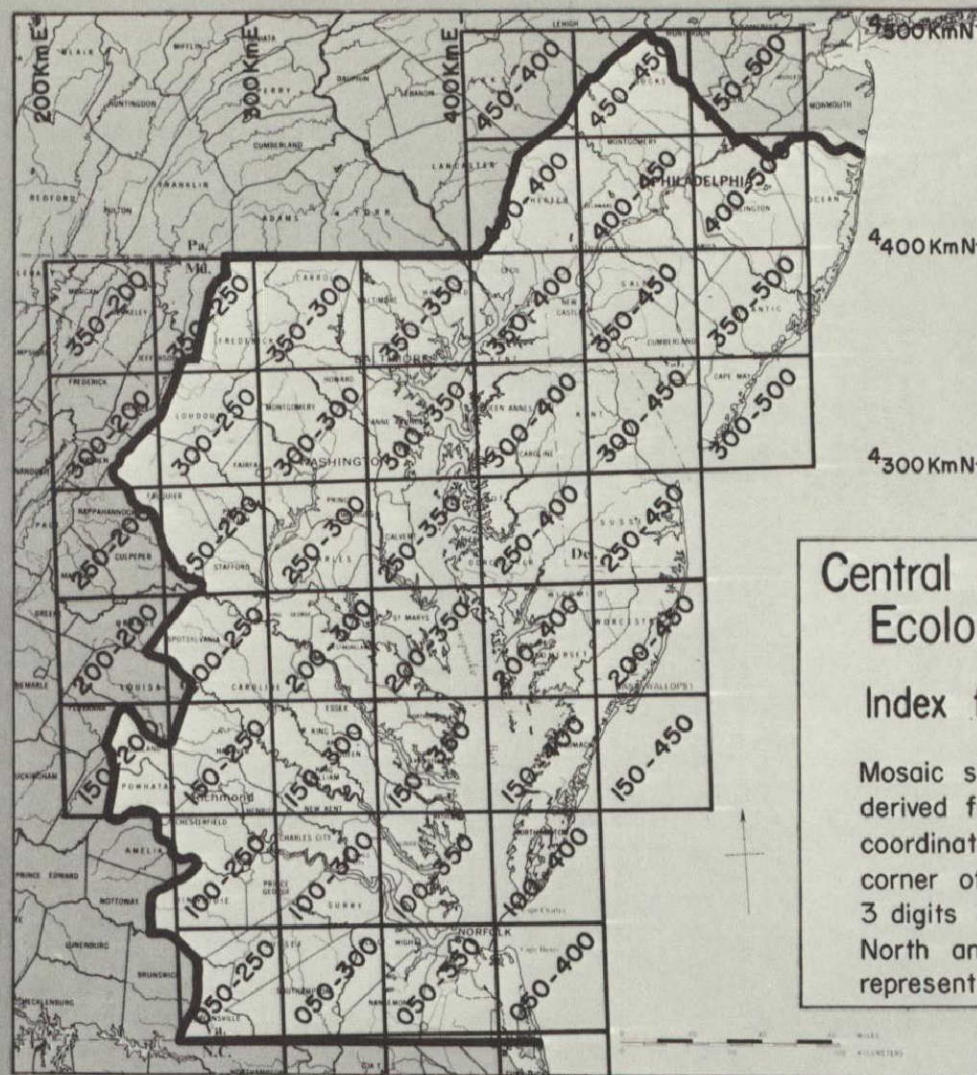


Figure 2.- CARETS Region Boundaries



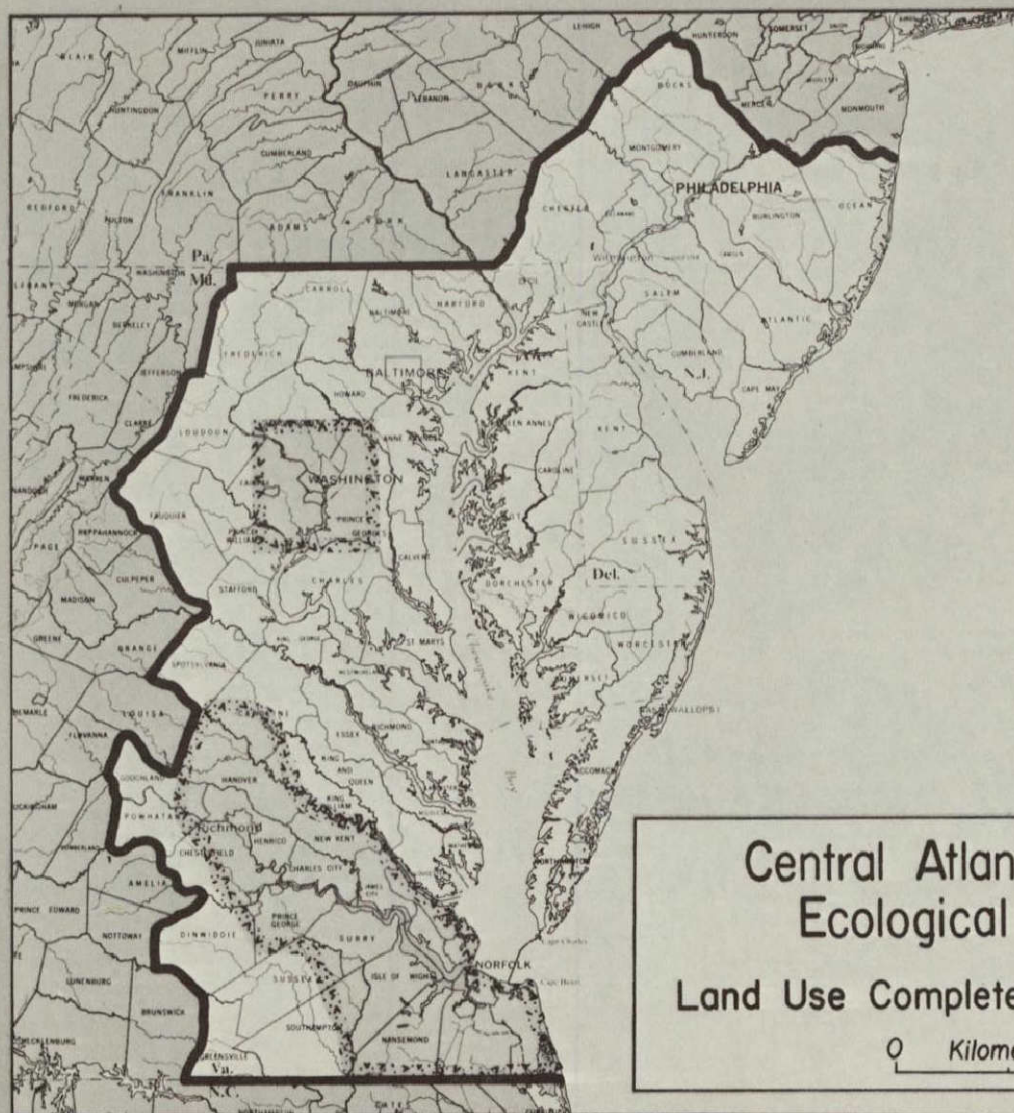
U.S. Geological Survey....
.....January 1972

Central Atlantic Regional Ecological Test Site

Index to Mosaic Sheets

Mosaic sheet numbers are derived from UTM (Zone 18) coordinates of the southwest corner of the sheet. The first 3 digits represent kilometers North and the second 3 digits represent kilometers East.

Figure 3.- Index to CARETS Photomosaic Sheets



U.S. Geological Survey....
.....January 1972

Central Atlantic Regional Ecological Test Site

Land Use Completed Jan.'72

0 Kilometers 100

Figure 4.- CARETS Land Use Mapping Completed, January 1972

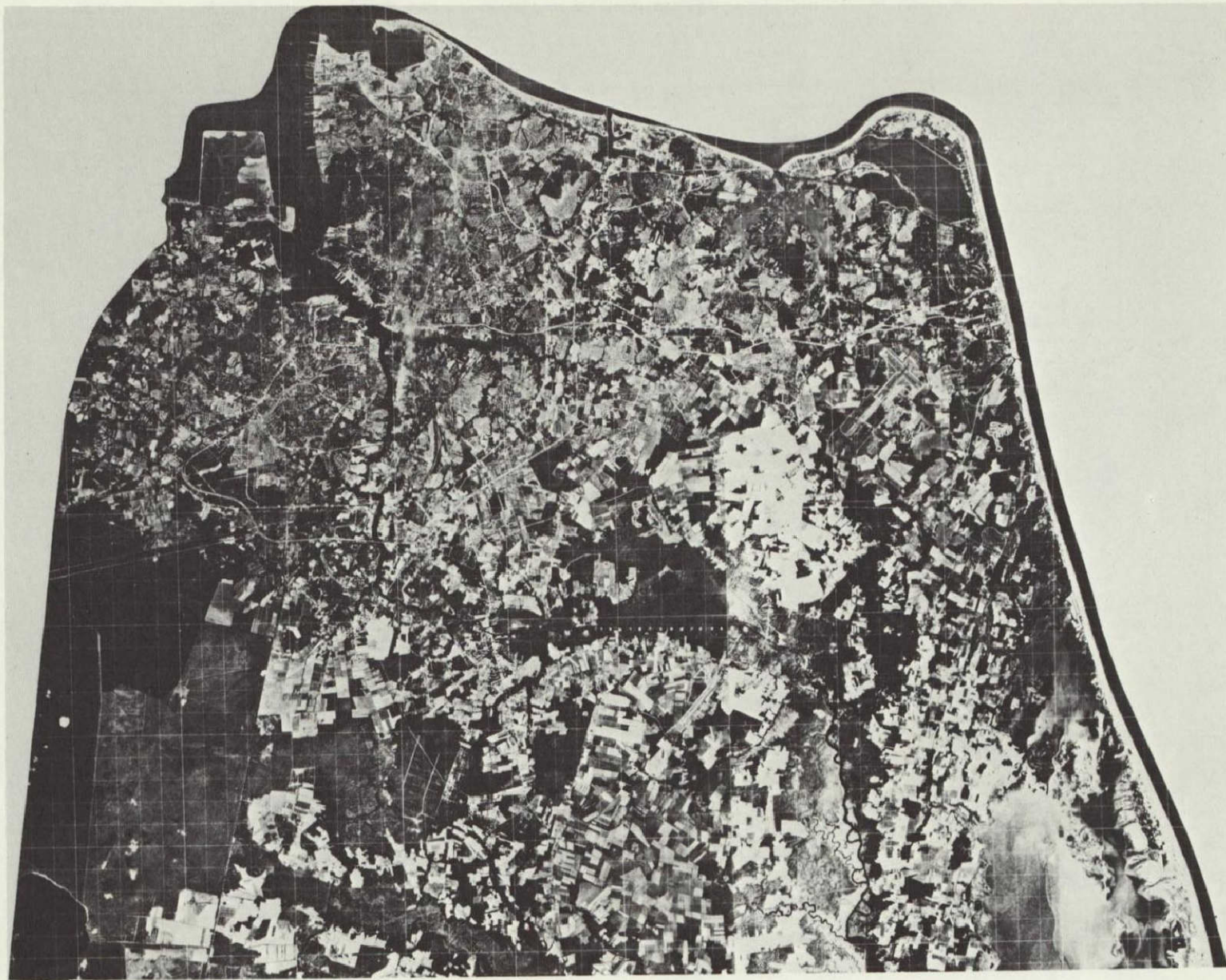


Figure 5.- Reduced Example of Photomosaic: Norfolk-Portsmouth SMSA
(Original at scale of 1:100,000)

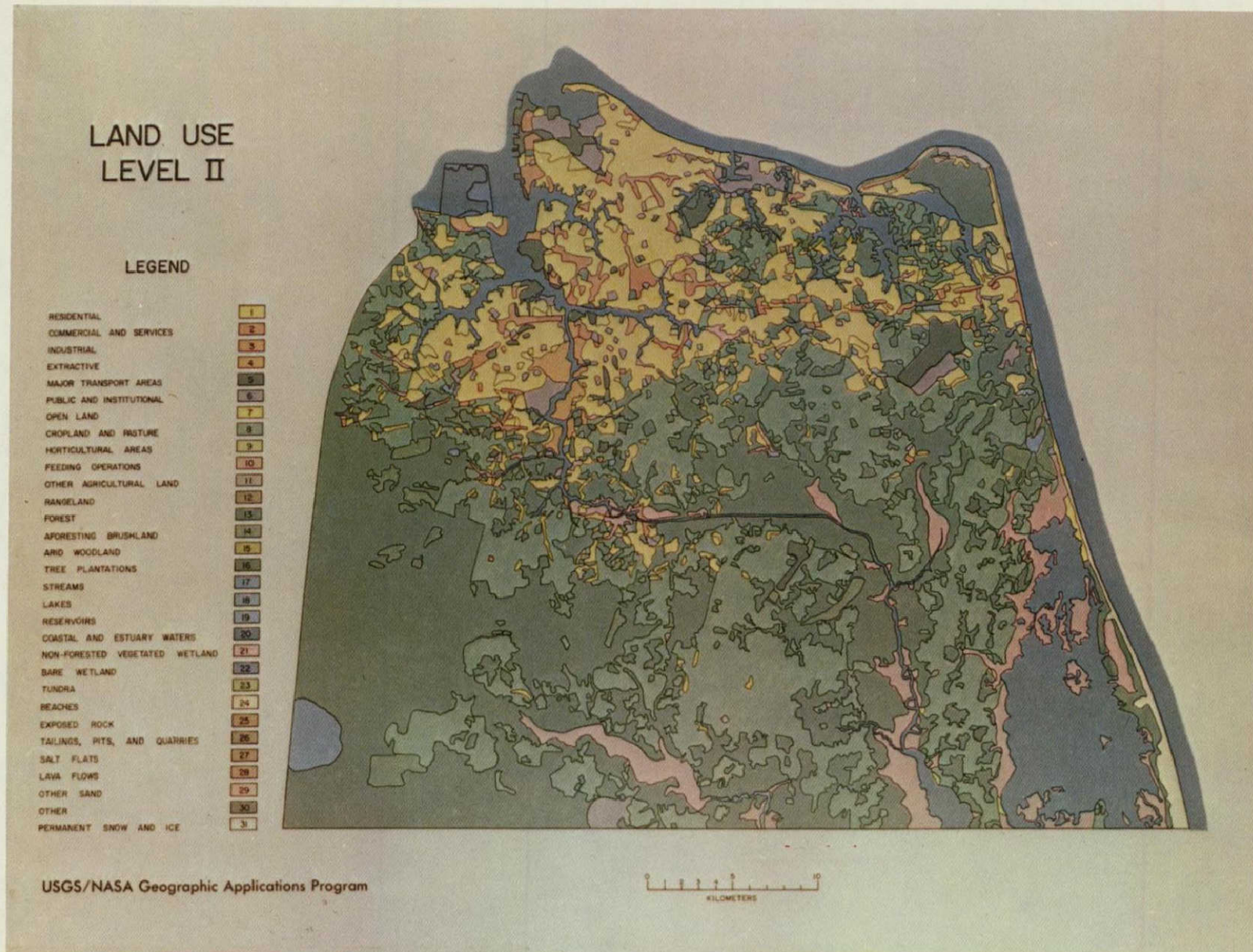


Figure 6.- Land Use Level II, Norfolk-Portsmouth SMSA, 1970

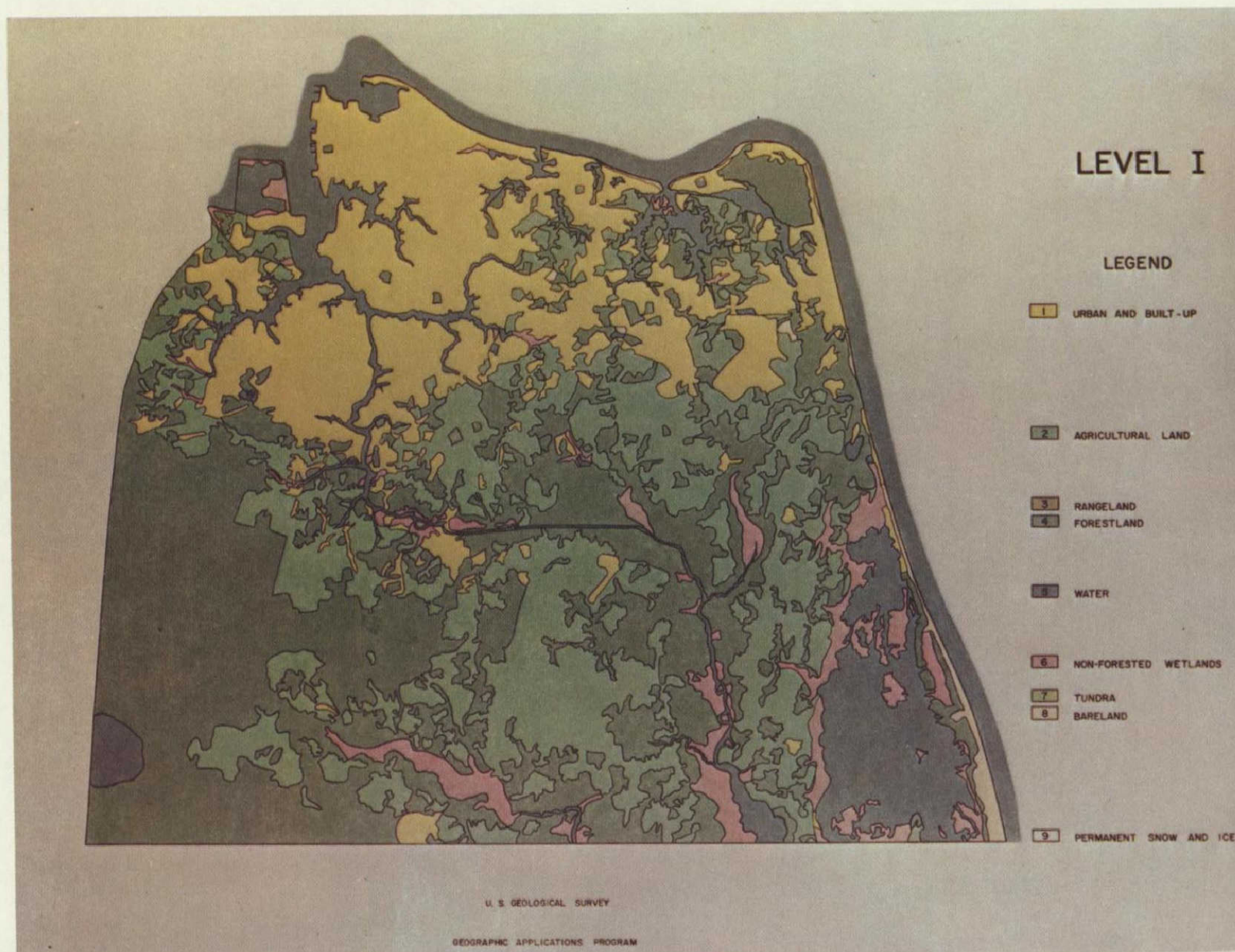


Figure 7.- Land Use Level I, Norfolk-Portsmouth SMSA, 1970

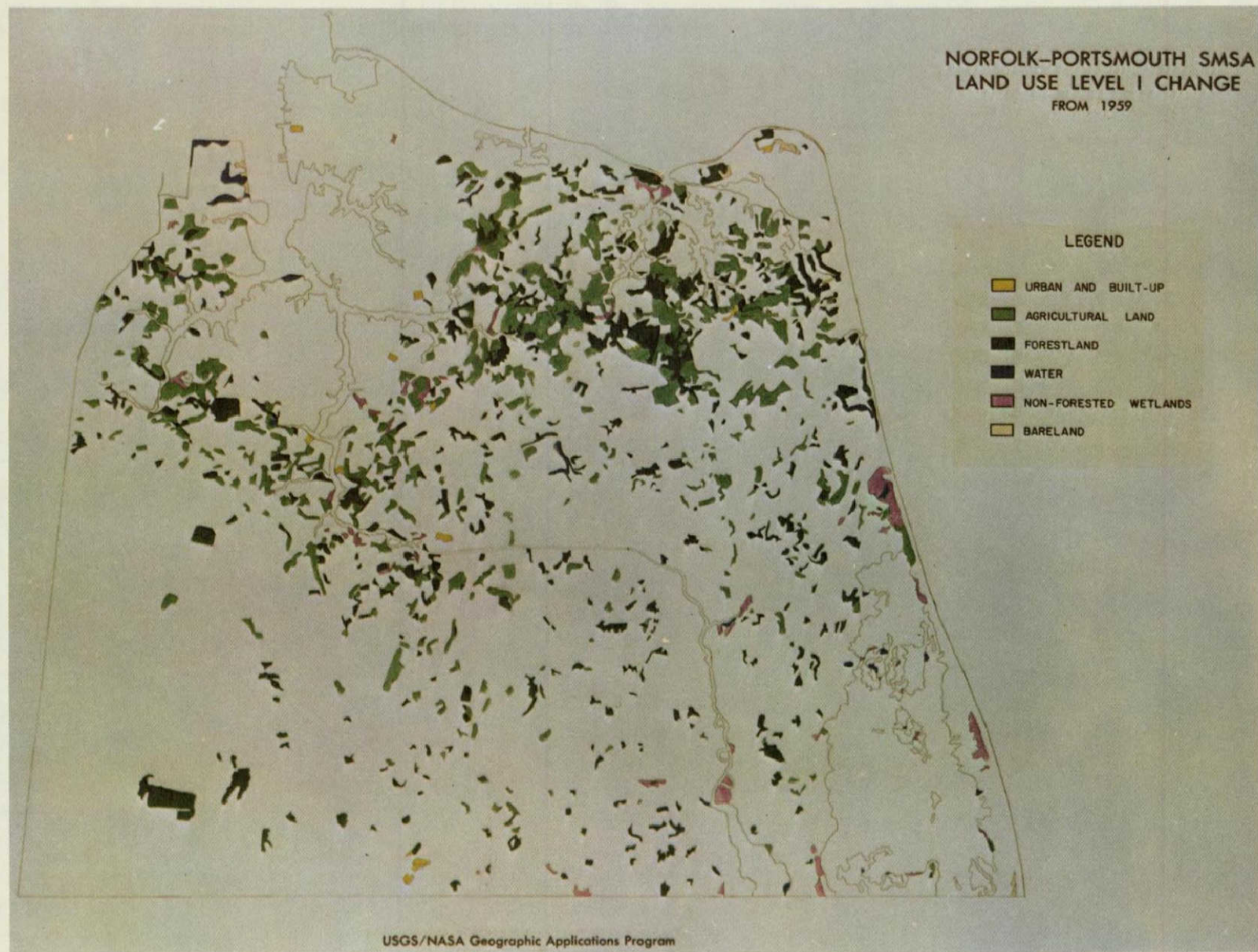


Figure 8.- Land Use Change, Norfolk-Portsmouth SMSA, 1959-1970 (1959 Land Use Categories)

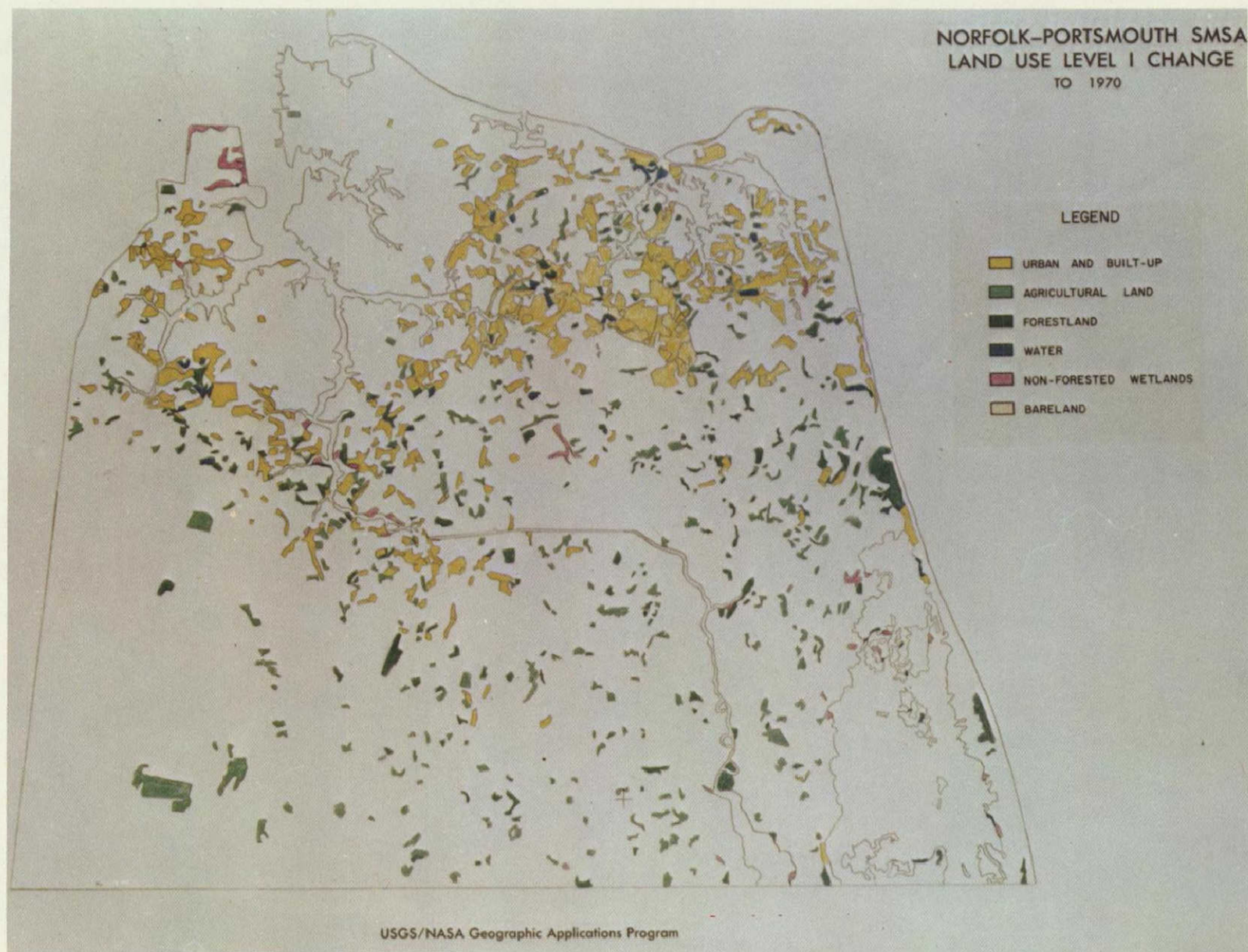


Figure 9.- Land Use Change, Norfolk-Portsmouth SMSA, 1959-1970 (1970 Land Use Categories)

		1970									
1959	TO FROM	1	2	3	4	5	6	7	8	9	Total 1959
	1	286	2		1	-	-				289
	2	80	549		19	1	-		-		650
	3										
	4	34	32		495	2	2		-		566
	5	-			-	244	3				244
	6	2	1		5		129				138
	7										
	8	-			-		-		24		24
	9										
Total 1970		402	584		520	247	134		24		1911

NORFOLK-PORTSMOUTH SMSA

LAND USE LEVEL I CHANGE MATRIX 1959-1970

In km²

USGS/NASA Geographic Applications Program

Figure 10.- Land Use Transition Matrix, Norfolk-Portsmouth SMSA, 1959-1970
(1=Urban; 2=Agriculture; 4=Forest; 5=Water; 6=Non-forested wetlands; 8=Bare Land)

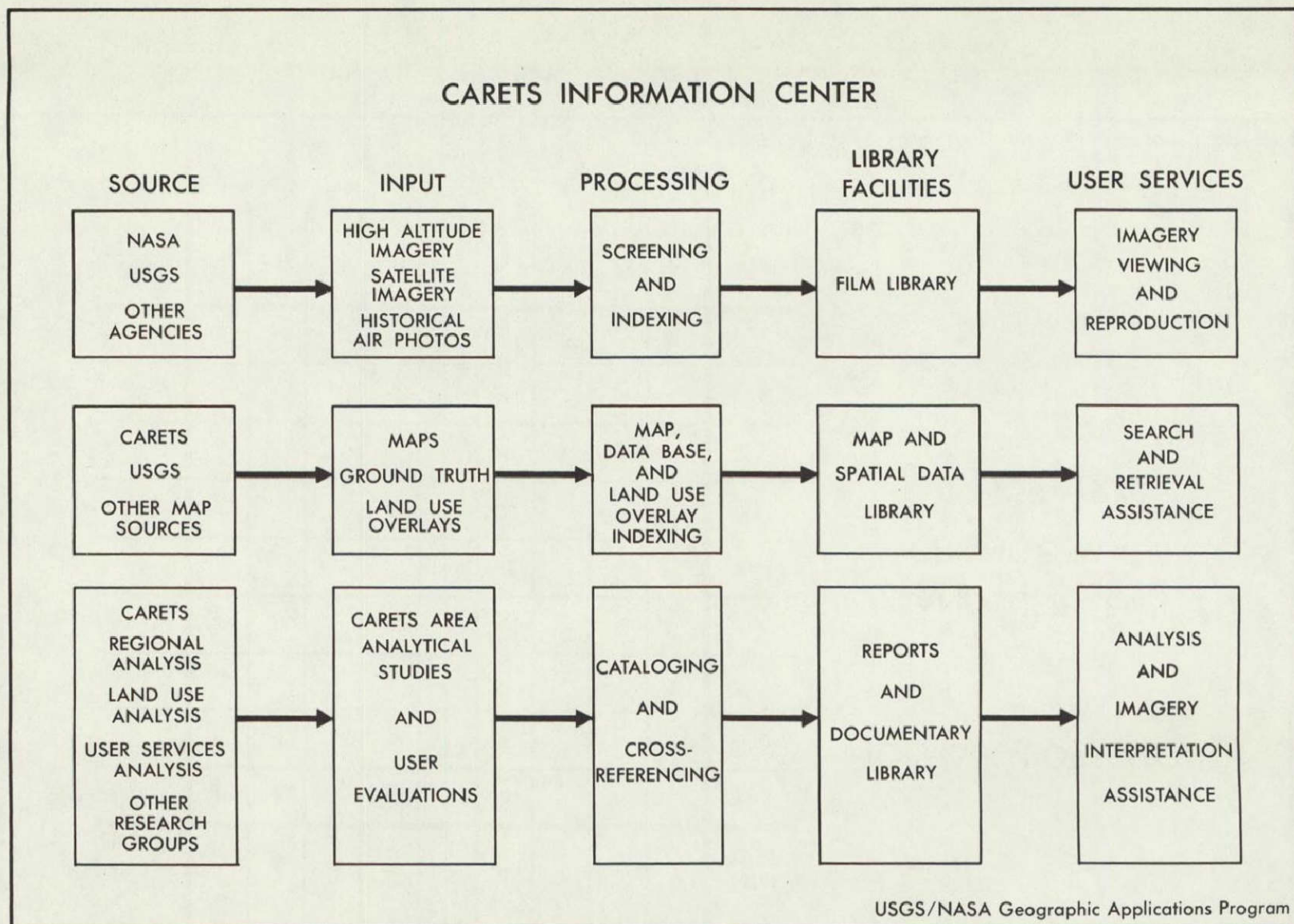


Figure 11.- CARETS Information Center Functions and Facilities

User Conference

CARETS--



Decision Inventory

Regional Organizations

Key State Agencies

Research Community

Key Federal Agencies

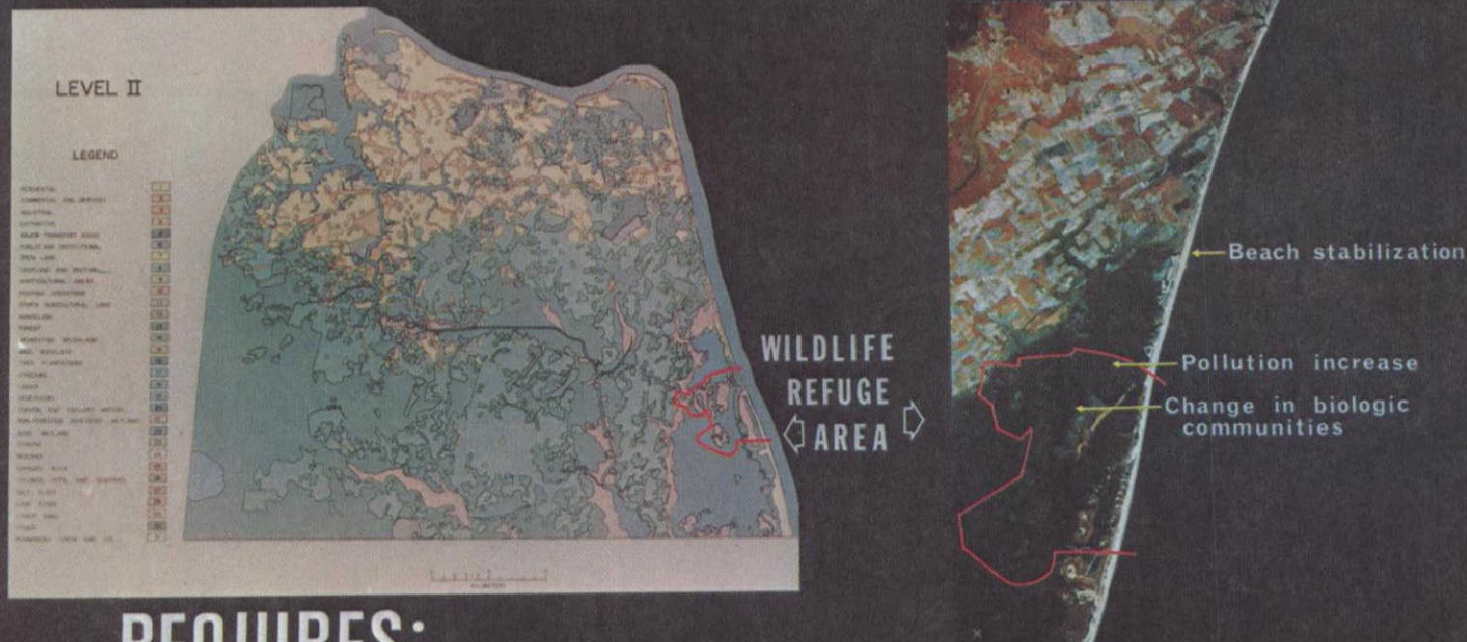
Private Sector

U.S. Geological Survey

Geographic Applications Program

Figure 12.- CARETS User Conference: June 11, 1971

PRESERVATION OF ENVIRONMENTAL VALUES in areas of urban growth...



REQUIRES:

- Observing present land use
- Monitoring land use change
- Measuring relevant geologic and hydrologic factors
- Integrating the above with population data and planning models

Figure 13.- Norfolk Area Growth and Environmental Impact Illustration: Back Bay National Wildlife Refuge Problems Resulting from Changing Use of Land

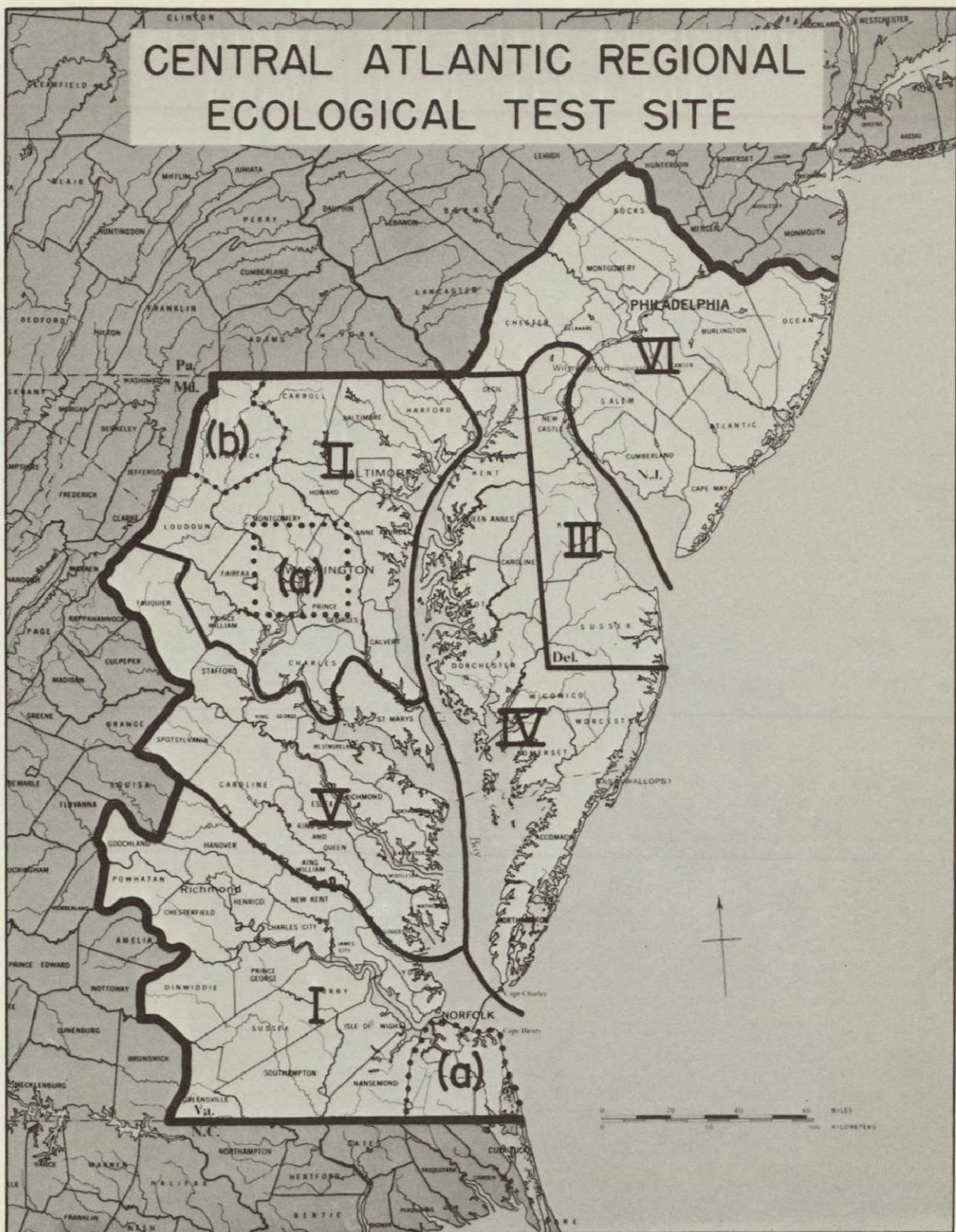


Figure 14.- CARETS Modular Subregions and Priorities

C.5

THE CENSUS CITIES PROJECT: A STATUS REPORT FOR 1971

by

James R. Wray
U.S. Geological Survey
Geographic Applications Program
Washington, D.C.

ORIGINAL CONTAINS
COLOR ILLUSTRATIONS

INTRODUCTION

At the Third Annual Earth Resources Program Review we described the research design of "The Census Cities Project." This is an experiment in urban change detection using remote sensors aboard high altitude aircraft and earth orbiting satellites. Multispectral photography acquired for a rank-size sample of U.S. urban areas at the time of the 1970 census was an essential part of the 'ground truth' phase. Similar photography requested in 1972 will provide a basis for analyzing gross change in land use and for assessing the utility of ERTS imagery for this purpose.

This experiment is part of the Department of the Interior's Earth Resources Observations Systems (EROS) Program. The work is also part of NASA's Earth Observations Program, whose Science, Research and Technology funds have been the principal support. Responsibility for conduct of the research rests in the Geographic Applications Program, a part of the Office of the Chief Geographer, U.S. Geological Survey.

Test Sites Under Study in 1971

During 1971, work was underway at eight of the urban test sites (Figure 1). Work on Boston and New Haven is under contract to Dartmouth College, Department of Geography, where Prof. Robert B. Simpson is the Principal Investigator. Analysis of Pontiac, Mich. is by the Oakland County Planning Commission, George N. Skrubb, Director. Analysis of Cedar Rapids is under contract to the University of Iowa, Institute of Urban and Regional Research, Prof. Frank E. Horton, Director. Analysis of Washington, D.C. is by USGS Geographic Applications Program personnel. Under a contract with the USGS/GAP, the Metropolitan Washington Council of Governments is auditing the potential role of remote sensors in fulfilling the operational needs of metropolitan regional planners. Harry J. Mallon is project director. Analysis of San Francisco, by far the largest

of the urban test sites, is by USGS personnel at Menlo Park and San José State College, assisted by a team of USGS geographer-cartographers at Silver Spring, Md. Work at Tucson and Phoenix is in the planning stage. For all of these test sites, the Geological Survey has prepared controlled and gridded photo mosaics. Depending on funding and cooperative agreements with local universities and user organizations, similar work is projected for Riverside-San Bernardino, Seattle, Salt Lake City, Denver, New Orleans, and Pittsburgh. Analyses of these and other urban areas are encouraged on a cooperative basis. The amount of urban land use actually classified in 1971 is about 11,000 square miles, an area roughly equivalent in size to the State of Maryland. A mosaic and analysis of 1970 land use in the Houston-Galveston area have been completed through a somewhat similar effort by the NASA Manned Spacecraft Center at Houston. This work is reported by Brian Erb.

The test site map also shows early Geography regional test sites. The encircled ones have subsequently been designated by NASA as Regional Ecological Test Sites. For these, pre-ERTS simulation photography is being acquired for ERTS-related multidiscipline remote sensing research. Note that five of the urban test sites lie in these regions. In Arizona (ARETS) and the Central Atlantic area (CARETS) the urban analyses are being coordinated with related research by John Place and Robert Alexander.

Photography Acquired in 1971

During 1971, high altitude aircraft overflights of urban test sites consisted of two kinds, each with a different purpose. For the first time for this research, multispectral metric camera coverage from the RB-57 aircraft was acquired for West Palm Beach (NASA Mission 157, February 1971), and for Midland-Odessa (NASA Mission 128e, January 1971). The sensor data are similar to those acquired for most other test sites at the time of the census, but the altitude was about 60,000 feet above terrain, not 50,000 feet. Seattle was overflown twice. In September, the P3-A aircraft acquired metric camera, color infrared coverage at 1:25,000 and 1:50,000, plus four band multispectral imagery with the I²S camera at a scale of about 1:100,000. In October, on NASA Mission 189, the RB-57 aircraft at 60,000 feet acquired the basic nine-camera multispectral coverage flown for the other test sites in 1970. For other research needs, Mission 189 imagery also provides new time series coverage for urban test sites at Phoenix and Denver. The San Francisco and Riverside-San Bernardino test sites were also covered by the RB-57 aircraft at 60,000 feet on NASA Mission 164 in March and April. This mission provides new multispectral

coverage of the California urban test sites eleven months after the census contemporaneous coverage acquired by NASA Mission 128a. A sample frame from Mission 164 (Figure 2) shows the newer type of Eastman color infrared 2443 film, also exposed through a minus blue filter. It appears less blue and red than the earlier film, but we have found little difference in its utility.

The second type of aircraft photography acquired by NASA in 1971 was the pre-ERTS simulation, small scale camera multispectral coverage from the U-2 aircraft over the regional ecological test sites. This provides fortuitous coverage of the urban test sites. This photography was just becoming available in 1971, so no substantive evaluation has been completed.

Atlas of Urban and Regional Change

Following procurement of the photography, two subsequent operations are performed, separately or in either order. One is the preparation of a controlled and gridded photo mosaic, and the other is the interpretation of land use and mapping of ground truth statistical areas. Both are ultimately combined as elements comprising a loose-leaf Atlas of Urban and Regional Change. This is a prototype, user-oriented, intermediate product. Its design is part of the experiment. It is too early to document any recommendations as to its operational application, but keen user interest encourages us to proceed as originally planned.

An Index to the Atlas sheets for the San Francisco urban test site illustrates the page format (Figure 3). As the sprocket holes suggest, the map page is one standard computer printout page size, 14.7 by 11 inches. The format accommodates many kinds of copy, i.e., photo mosaic, conventional map, computer printed map, computer tabulated data, and text in three columns with illustrations inserted where needed. Map copy is being prepared at a scale up to two times larger than publication scale. This is not because it cannot be prepared for reproduction at publication size, but because the accompanying area analysis is facilitated at the larger scale. Map pages will usually consist of a square neatframe, or map module, placed to the left of center. Title and legend panel at the right allows space for the user's legend also. Looseleaf pages may be bound at top or left. Individual pages may also be folded and tipped into technical reports, bound on the left, with page size 8 by 10.5 inches or 8.5 by 11 inches.

Scale of the Index map for San Francisco, at full page size, represents an area of 200 by 200 kilometers at 1:1,000,000.

The same publication space will cover areas 100 by 100 km at a scale of 1:500,000, or 50 by 50 km at 1:250,000, etc. The 44 squares shown on the Index map each cover 25 by 25 km at 1:125,000. The sheetlines are drawn on whole kilometer grid lines, using the Universal Transverse Mercator rectangular coordinate system, in this case for UTM grid zone 10. The sheet identification or page number consists of six digits which identify the location of the southwest corner of the sheet in whole kilometers north and east of an origin outside of the grid zone. We are listing the northing or latitude first (minus the prefix of 4,000 km); the last three numbers are the easting or longitude. This is not in keeping with current military practice, but it is in keeping with a longer geographic tradition and with a nationwide geo-coding precedent that adapts the UTM coordinate system for Standard Location Codes for centroids of census statistical areas. This sheet numbering system and the square map module not only facilitate mapping in a family of metric map scales, but also provide a logical page number for sheets to be added at a later time. The UTM grid on the base graphics and in the spatial data information system thus provides the locational control necessary for computer mapping. It also facilitates joint use of computer generated maps with map or mosaic underlays or overprints.

The gridded mosaic frame for San Francisco, Atlas page 150-575, shows the Hayward-Fremont urban corridor on the east side of San Francisco Bay (Figure 4). As in certain other frames to follow, the neatframe copy is genuine, if still unedited, while the marginalia are schematic and simulated. The full page publication scale covers an area 25 by 25 km at a scale of 1:125,000. At the same page size, the mosaic module for other urban test sites covers 20 by 20 km, at 1:100,000. At this scale, one centimeter on the map represents one kilometer on the ground. The San Francisco mosaic was made by the U.S. Geological Survey from its own 1970 photography acquired as part of the San Francisco Bay Region Environment and Resources Planning Study. This is a joint effort by USGS and the Department of Housing and Urban Development to demonstrate the performance and presentation of basic earth science environmental studies for direct inputs to the planning process for metropolitan regions. Because of the strong relief in the Bay Region, the mosaic was prepared by orthophotography. This is an advanced photogrammetric process which adjusts, digit-by-digit, for the displacement of photographic images due to differences in relief. This adjustment diminishes somewhat the pictorial quality of the mosaic, but it increases the accuracy of position locations, and thus the accuracy of measurements of distances, angles, and surface areas. In our land use analysis we do not depend on the degraded mosaic for image interpretation, but use it primarily as a place to record and measure what has been interpreted from the original imagery. It usually doesn't matter--as in this case--that the mosaic is made from imagery other than

that used for the land use interpretation. Accompanying the mosaic in the published version of the Atlas there will be an identification overprint which delineates and labels selected point and line features which are missed by, or which augment, the analysis of area features.

The San Francisco Atlas mosaic sheet 150-575 may be compared in simulated Atlas format with the corresponding portion of the new USGS topographic map at 1:125,000 (Figure 5). Also produced in 1971, this map is part of an impressive array of cartographic and earth science ground truth becoming available from the USGS/HUD San Francisco Bay Region Study. It is perhaps appropriate to recognize that the preparation of orthophoto maps and topographic maps by photogrammetric methods is an application of remote sensing of earth resources that has long been in an operational mode! Innovations in this particular map include the use of smaller scale photography for orthophotomapping at map accuracy standards, plus the mapping--even at this small scale--of all the street pattern appearing in the imagery. Streets and roads are shown in red ink. This accounts for the overall red appearance of the more urbanized areas without the addition of a screen tint customarily used on larger scale topographic maps produced by USGS.

Urban Area Analysis: How and Why

A preliminary, unedited land use map of the Hayward-Fremont area (Atlas sheet 150-575) represents an analysis of area features as distinguished from point and line features (Figure 6). For use as an operational working tool, for reporting changes from time to time, the land use map will be produced in monochrome with land use labels, statistical areas, and mosaic base printed in contrasting colors. The map with land use printed in colors is primarily for illustration and explanation. A very simplified, and still provisional, land use classification scheme appears in the legend panel. A more detailed legend, and a discussion of the urban land use mapping and change detection, appears among the invited papers at the National Land Use Information and Classification Conference, co-sponsored by the USGS, NASA, and the Soil Conservation Service held in Washington, D.C. in June 1971. Besides the land use categorization itself, it is important to keep in mind the minimum area size for recording land use. This is only partly a function of scale and resolution. In the Census Cities Project, the minimum area size is about 2.0 by 2.0 mm on the original color infrared photo transparency at 1:100,000 or 1:120,000. This area is about four hectares or ten acres. The RB-57 photography from the RC-8 metric camera has much better resolution than this, but the resolution of the ERTS imagery will be about the same as this minimum area size. It is easy to overlook what effect this has upon the definition of land use classes mappable at a given scale, and the relation of any of those classes to definition of classes for mapping land use at larger or smaller scales.

For subsequent area analysis and for the construction of an urban spatial model, the land use categories for urban analysis can be grouped under three headings: "Livelihood," "Residential," and "Other." A further interpretation for change detection and model building then delimits "Urban" from "Non-urban." Dr. Duilio Peruzzi is devising a technique for delimiting the San Francisco and San José urban areas and for monitoring changes on time series imagery. His method is a near-operational refinement of a similar one suggested by Robert Simpson for the Boston test site.

Recognizing that some users will not be satisfied with the land use category called "Commercial and Public and Private Services," Richard Ellefsen is devising a technique for breaking down this category into regional, community, and neighborhood shopping centers. In doing so, he has documented nearly a 10 percent increase in land in this category in the San José area during the 11 months between Mission 128a (May 1970) and Mission 164 (April 1971).

While the Hayward-Fremont mosaic, topographic map, and land use map are still in mind, it is useful to note the wide range in terrain and land use cover which is represented. The Bay border wetlands to the southwest are industrialized to the extent that they are farmed as salt evaporator ponds. The scrub vegetation on the ridges frame the northeastern corner of the sheet. Between these environmental extremes, and trending from northwest to southeast, is another environmental extreme, the East Bay corridor of transportation routes and urban sprawl, connecting or reaching to well defined urban nodes. Some agricultural land still lies between the Hayward node to the northwest and Fremont node to the south. Underneath much of this lies a seismic zone called the Hayward Fault. Throughout its length, 13 schools with 5,000 pupils lie astride this potential hazard. Here then, is a simplified approximation of a portion of the complex real world stage in which environmental stresses are present and for which management decisions must be made to find the best mix of societal goals, technology, and non-renewable resources. How can the monitoring of land use change by remote sensing aid the planning and decision making process? During a year of duty and dialogue we have identified a growing sample of potential applications and the user agencies concerned with them. Some of these applications are: a) calibrate a traffic flow model and estimate daytime distribution of population; b) estimate water use requirements; c) define "Open Space" land and assess environmental hazards affecting possible urban expansion; d) assess environmental hazards on land already urbanized; e) identify prime land which ought to be preserved for agriculture; f) identify open space land to be saved for recreation and "green" space; g) calibrate a waste management model for San Francisco Bay, and monitor possible changes in water quality; h) map susceptibility to land and air pollution; i) assess quality of residential environment; j) project future population densities, and estimate changes in population distribution between censuses; k) prepare for large scale emergencies resulting from

foreseeable hazards and for the assessment of environmental impact resulting from gradual as well as catastrophic changes. Many of these applications can be subdivided. For most, there are commercial or military counterparts. This list is a teaser and a challenge to document specific applications at an early date.

Part of the mechanism for making these applications possible is a systematic analysis of the area and a matching of sensor data--in time series--with data from the census and other 'ground truth.' The model building and predicting come later. After the land use mapping, the land use areas are measured and recorded by statistical area in a retrievable information system. We are using the 1970 census tract as a statistical area (Figure 7), although Prof. Frank Horton and associates at the University of Iowa find the census tract too coarse a unit for analyzing a smaller urban area such as Cedar Rapids. This device is a fairly primitive form of data reduction, but it does not preclude subsequent analysis by grid cell, land use polygon, or other, more sophisticated systems of data reduction and manipulation. Each census tract is identified by code which is matched to political jurisdictions at county and municipal levels or to other minor civil divisions. These are primary user jurisdictions for which management decisions affect land use policy and environmental quality. Beside each tract number is a cross symbol for the tract centroid. This is a somewhat arbitrarily selected point within the tract whose location is recorded in UTM coordinates. For tracts which happen to be in fragments, each fragment is treated as a separate tract and is assigned its own tract number and centroid. For one system of data reduction, the centroid becomes the address for all data for the statistical area insofar as computer manipulation of small area data location is concerned. Use of the UTM coordinates for this purpose makes it possible to compute distances and directions between centroids or other points even if the point-pairs are not located on the same mosaic sheet.

For the San Francisco urban test site, the 1970 land use compilation, covering all 44 Atlas pages and 7,000 square miles of land, was completed in 1971. The area analysis and the preparation of maps for publication are still to be done. Even so, the graphic inventory and mosaic record already completed provide a stage for evaluating the pre-ERTS simulation photography as well as the ERTS imagery itself. If it should happen to be centered on the Bay Region, one ERTS frame, 103 nautical miles on a side, could nearly contain the entire test site, and Sacramento, the state capital, might appear in the northeast corner (Figure 3).

A Metric Coordinate Reader, prepared by the USGS in 1971, is useful for reading UTM coordinates of tract centroids from gridded maps and mosaics at 1:24,000; 1:62,500; 1:125,000, or 1:250,000. An Area Measurement Grid, prepared at these scales (plus 1:100,000)

by the Geographic Applications Program, is useful for measuring areas of land uses. Since many of these are small they are subject to large error, so other area measurement techniques are also employed to maintain control for areas aggregated by census tracts.

Both the reading of UTM coordinates of centroids, or of land use boundary lines or nodes, and the measurement of areas are performed manually at present. It is painfully clear, however, that these operations will have to be mechanized if inventory and change detection are to be conducted on an operational basis. We have made an attempt to map land use by using a film densitometer and a data color analyzer. If this could be done, we then hoped to measure land use areas by accessory equipment that reads out the percentage of area scanned which is in any one of 32 density ranges. At present, there is too much 'noise' in the system for either task to be performed by such automation. We are continuing the performance of these tasks manually in order to produce a dependable prototype and to evaluate its promise. When this is confirmed, we will pursue semi-automation of the interpretative and measurement tasks.

Next, the locational data (including tract centroids), the land use data from the 1970 overflights, and selected population and housing data from the 1970 census are reported by census statistical area on an "Area Measurement Worksheet" prior to encoding and machine tabulation (Figure 8). Later, in one prototype change detection strategy, we anticipate creating a similar file for 1972 land use. Then we will program the computer to retrieve the 1970 and 1972 land use data by statistical areas and to tabulate differences which are indicators of change (Figure 8).

Prospect for Change Detection by Satellite

Preliminary work at the Phoenix urban test site analyzed gross urban land use by interpreting color infrared imagery from the Apollo IX mission in March 1969. Detectable in the space photo is a circular golf course, 1.5 miles in diameter at Sun City, a retirement community on the growing edge of metropolitan Phoenix. In the months before and after the Apollo mission, geographers at Northwestern University, in cooperation with the USGS Geographic Applications Program, documented some land use changes. They also analyzed the extent of land use data useful to planners which could be elicited from sensor imagery of varying resolutions (Figure 9). In the vicinity of the initial circular golf course at Sun City the very rapid expansion of residential land use is shown in a series of conventional black and white air photos taken six months apart. The expansion is providing a second circular golf course tangent to the east of the first one where a common clubhouse will serve both. Metric

camera photography flown from U-2 aircraft in November 1970 clearly shows the spread of housing and golf courses as of that date (Figure 10). We anticipate that such changes in the growing edge of urban areas may be monitored from ERTS-type imagery, and that changes in the rural-urban interface are indicative of other changes. We also anticipate that intercensal population estimates may be derived from an urban area once a model is established which expresses the relationship--for a given culture region--between a settlement's area size and its population size.

Digitizing the Boston Land Use Map

A manuscript map of 1970 land use in Boston and vicinity has been completed by Robert Simpson, David Lindgren, Robert Yuill, and Robert Yost at Dartmouth College (Figure 11). Prepared prior to the completion of the photo mosaic, this map was based on 35 USGS 7½-minute topographic quads, each fitted with a one-kilometer UTM grid and reduced to 1:62,500. The interpretation was done on colored pencil overlays at 1:120,000 or 1:100,000 contact scales of RB-57 aircraft color infrared photos from NASA Missions 103 and 128d, respectively. The colored pencil interpretations were then enlarged to 1:62,500 for area analyses by census statistical area and for preparation of Atlas drawings at that scale.

An experimental computer land use map by census tract was made by identifying and digitizing census tracts and land uses at grid cells 0.2 by 0.2 km (Figure 12). Derived from the UTM grids, these cells cover four hectares or about ten acres. A land use letter code is printed in each cell. By using the UTM grid in this manner, location control of the data is retained, and areas are measured by machine aggregation of cells in each land use category.

The Dartmouth research team has extended the digitization of land use data to the entire 93,000 grid cells (about 1400 square miles) at the Boston test site. A 'mosaic' of 25 computer printout pages, very much reduced in size, shows land and water cells (Figure 13). Similar maps show Multi-Family Residential land (4 percent of area total) and Single-Family Residential land (23 percent of area total) (Figures 14 and 15). Similar maps and measurements have been produced for other land use categories, and a similar analysis and digitization of 1970 land use in the New Haven test site are nearing completion at Dartmouth.

All land use categories comprising the "Built-up Area" at Boston occupy 40 percent of the total area (Figure 16). Since most of the non-built-up land is in forest (42 percent), the maps of Built-up Area and Forest are very nearly negative images of each other (Figure 17). If they were viewed at arm's length, through squinted

eyes and with the image width measuring two inches, the scale would simulate imagery at 1:1,000,000. Of course, the resolution cell is more coarse than that of the ERTS image. What doesn't appear as "urban" on the bands showing the Built-up Area will be reinforced by the infrared band which will enhance the Forest land, leaving as "urban" the balance of the image which is not water. As a result of the Boston analysis, moreover, we can account for the exact location and the land use category at each 'dot' comprising these simulated images. Any other mappable parameter, whether generated from remote sensors or not, can be stored and matched in this same manner.

* * *

List of Illustrations

Urban and Regional Test Sites	Figure 1
San Francisco, Mission 164 Color Infrared Photo	Figure 2
*San Francisco, Atlas Sheet Index	Figure 3
*San Francisco, Atlas Sheet 150-575, Photo Mosaic	Figure 4
*San Francisco, Atlas Sheet 150-575, Topographic Map..	Figure 5
*San Francisco, Atlas Sheet 150-575, 1970 Land Use ...	Figure 6
*San Francisco, Atlas Sheet 150-575, 1970 Census Areas	Figure 7
Area Analysis Worksheet	Figure 8
Image Scale as a Factor in Urban ... Change Detection	Figure 9
*Phoenix, Atlas Sheet 710-375, Photo Mosaic	Figure 10
*Boston, 1970 Land Use	Figure 11
Boston, Computer Land Use Map by Census Tract	Figure 12
Boston, 1970 Water Area, Computer Map by Grid Cell ..	Figure 13
Boston, 1970 Multi-Family Residence Land	Figure 14
Boston, 1970 Single-Family Residence Land	Figure 15
Boston, 1970 Built-up Area	Figure 16
Boston, 1970 Forest Land	Figure 17

*Not received at time of publication.

CENSUS CITIES EXPERIMENT Urban and Regional Ecological Test Sites

... Work in Progress, 1971

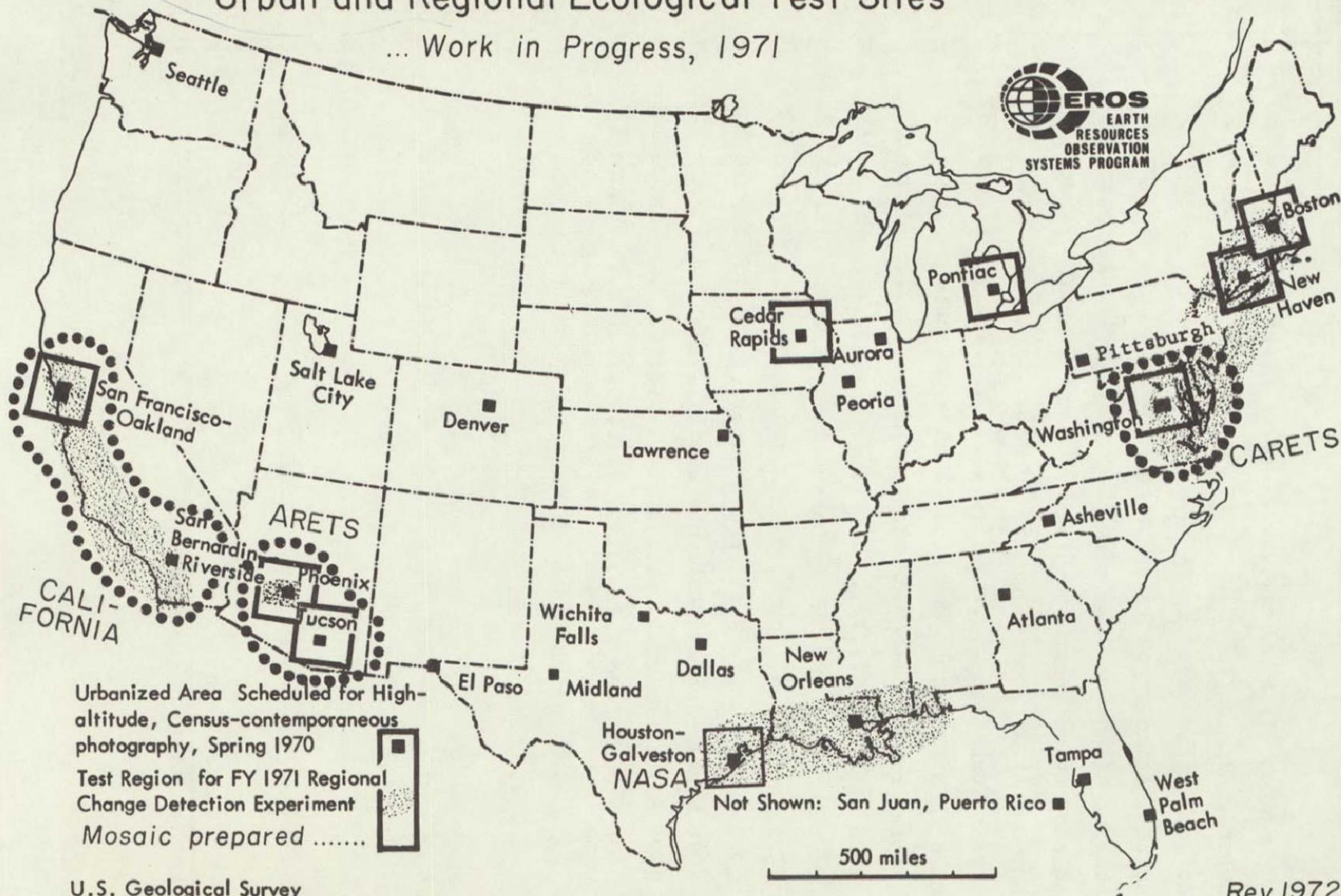


Figure 1.--Urban and Regional Ecological Test Sites



Figure 2.--Portion of color infrared photo, San Francisco, NASA Mission 164, April 1971.



Area Analysis, as of a given date

Time	Location descriptors								Area		Sensor data: Land Use																			Census data				Environ.
	tract		map	UTM coords.				hectares -totals		hectares by Land Use category																			Pop-ulation		Hous-ing			
1	2	3		5	7	8	9	10	11	12	13	14	15	16	17	18	19	20	21	22	23	24	25	26	27	28	29	31	32	34	35	37	38	
70	01	-	-	-	-	-	-	-	-	-	-	-	-	-	-	-	-	-	-	-	-	-	-	-	-	-	-	-	-	-	-	-		
70	02	-	-	-	-	-	-	-	-	-	-	-	-	-	-	-	-	-	-	-	-	-	-	-	-	-	-	-	-	-	-	-		
70	03	-	-	-	-	-	-	-	-	-	-	-	-	-	-	-	-	-	-	-	-	-	-	-	-	-	-	-	-	-	-	-		
70	04	-	-	-	-	-	-	-	-	-	-	-	-	-	-	-	-	-	-	-	-	-	-	-	-	-	-	-	-	-	-	-		
70	05	-	-	-	-	-	-	-	-	-	-	-	-	-	-	-	-	-	-	-	-	-	-	-	-	-	-	-	-	-	-	-		

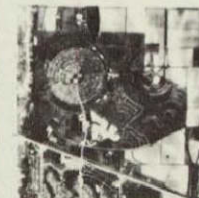
Area Change Detection, between two given dates

Time	tract	map	UTM coords.		Area		Sensor data: Land Use																									
1	2	3	5	7	8	9	10	11	12	13	14	15	16	17	18	19	20	21	22	23	24	25	26	27	28	29	31	32	34	35	57	58
72	03	-	-	-	-	-	-	-	-	-	-	-	-	-	-	-	-	-	-	-	-	-	-	-	-	-	-	-	-	-	-	-
70	03	-	-	-	-	-	-	-	-	-	-	-	-	-	-	-	-	-	-	-	-	-	-	-	-	-	-	-	-	-	-	-
Ch	03	-	-	-	-	-	-	-	-	-	●	●	x	x	-	-	x	-	●	●	●	●	●	●	●	●	●	●	●	●	●	●

Figure 8.--Area analysis worksheet.



Image Scale as a Factor in Urban and Regional Change Detection



February, 1970
(NASA)

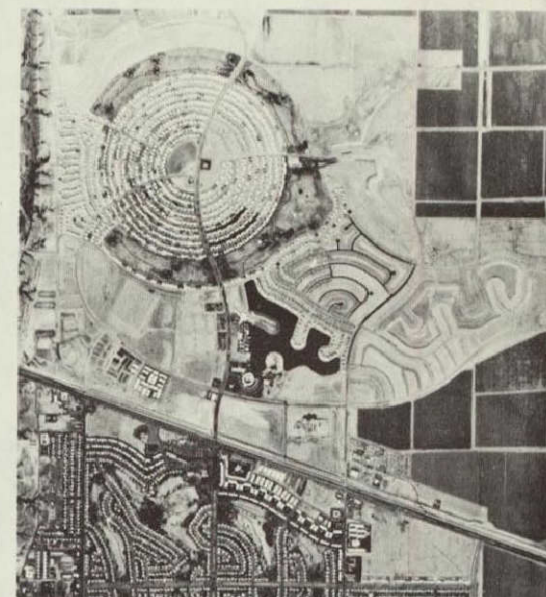
Sun City, Arizona



January, 1969



June, 1969



January, 1970
(Landis Aerial Surveys)

0 Statute Miles 3

Based on research at Northwestern University. . .

. . . as part of the USGS/NASA Geographic Applications Program

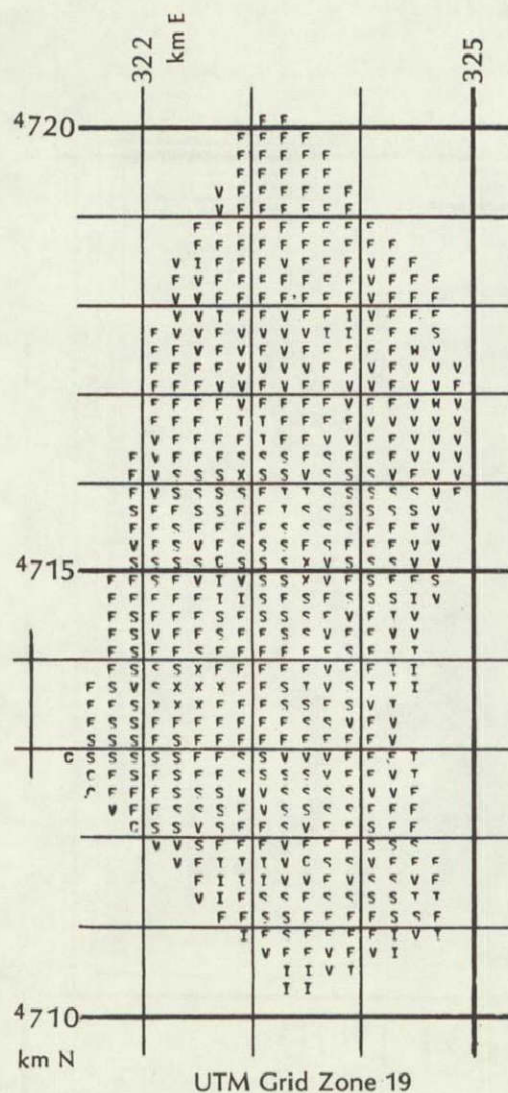
Figure 9.--Image scale as a factor in urban and regional change detection.





Computer Map of Land Use by Census Tract

Boston Land Use Study
Dartmouth Project in Remote Sensing
Wilmington, Massachusetts 7-1/2 Minute Quad.
Census Tract No. 3311, 1970

USGS Geographic Applications Program



LAND USE	PERCENT OF AREA
FCREST	47.8
SINGLE FAMILY RESIDENTIAL	22.8
VACANT	19.2
INDUSTRIAL	5.1
TRANSPORTATION - UTILITIES	2.2
INSTITUTIONAL	1.6
COMMERCIAL	1.0
WATER	0.3
TOTAL AREA = 25.5 SQ. KM.	

SCALE.....HORIZONTAL  = 1.0 KM.
VERTICAL  = 1.2 KM.

Sample computer-printed land use map for one census tract at the Boston Test Site. Note relation of digits to UTM grid, for location control. Each digit is four hectares.

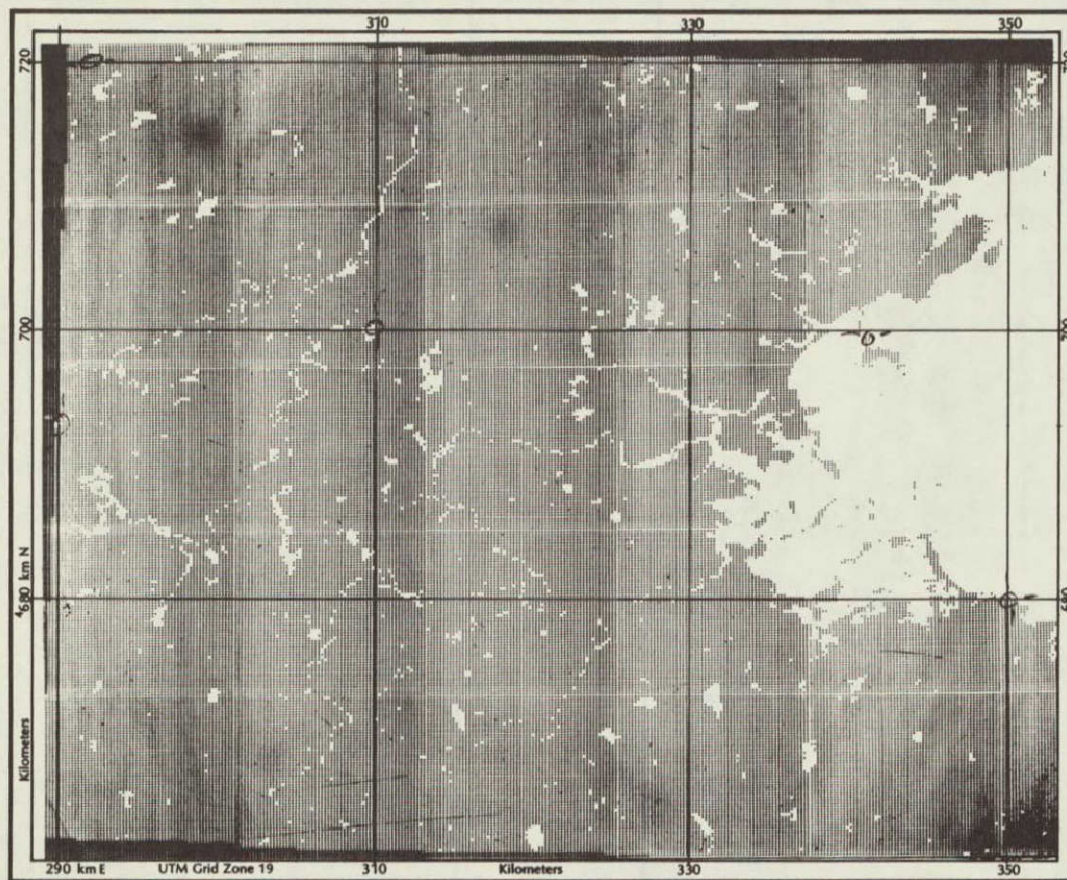
May, 1971

Figure 12.--Computer map of land use by census tract, 1970, Boston test site.



Boston

Water
1970



Based on research at Dartmouth College .. as part of the USGS/NASA Geographic Applications Program

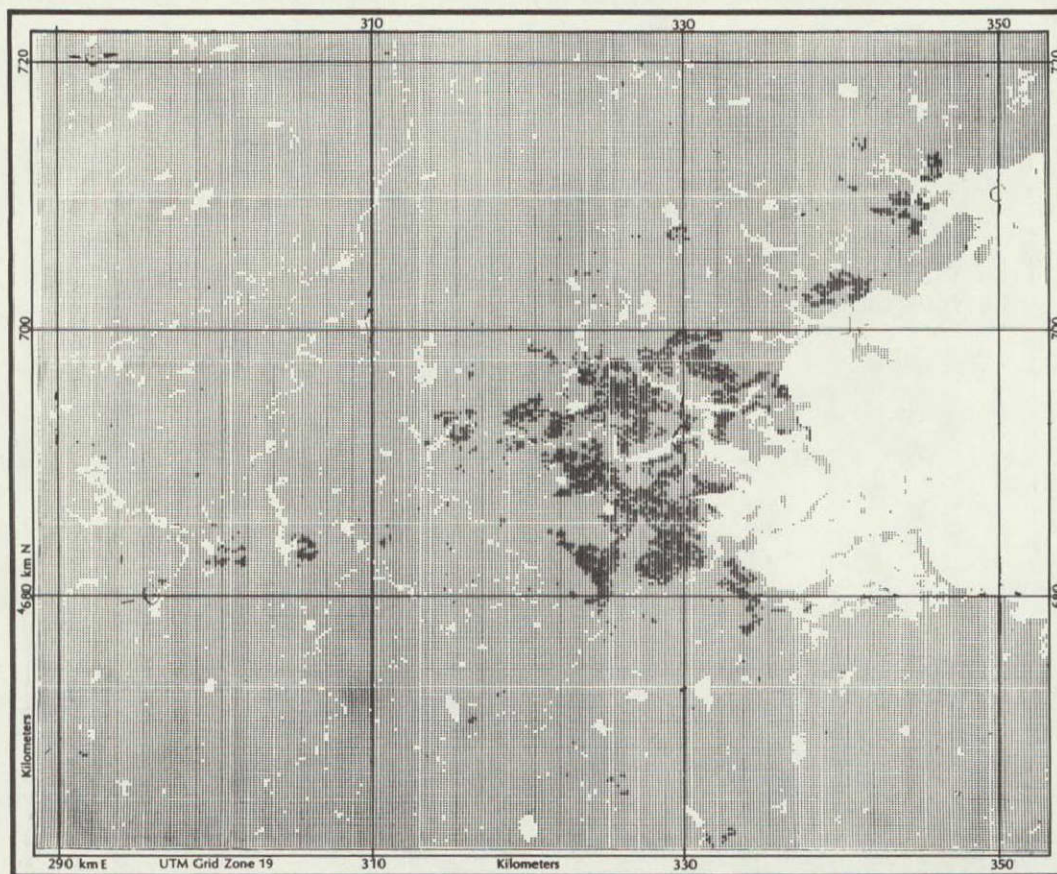
Figure 13.--Boston, 1970 water area, computer map by grid cell.

ATLAS OF URBAN AND REGIONAL CHANGE

CENSUS CITIES EXPERIMENT



Boston
Multi-Family
1970

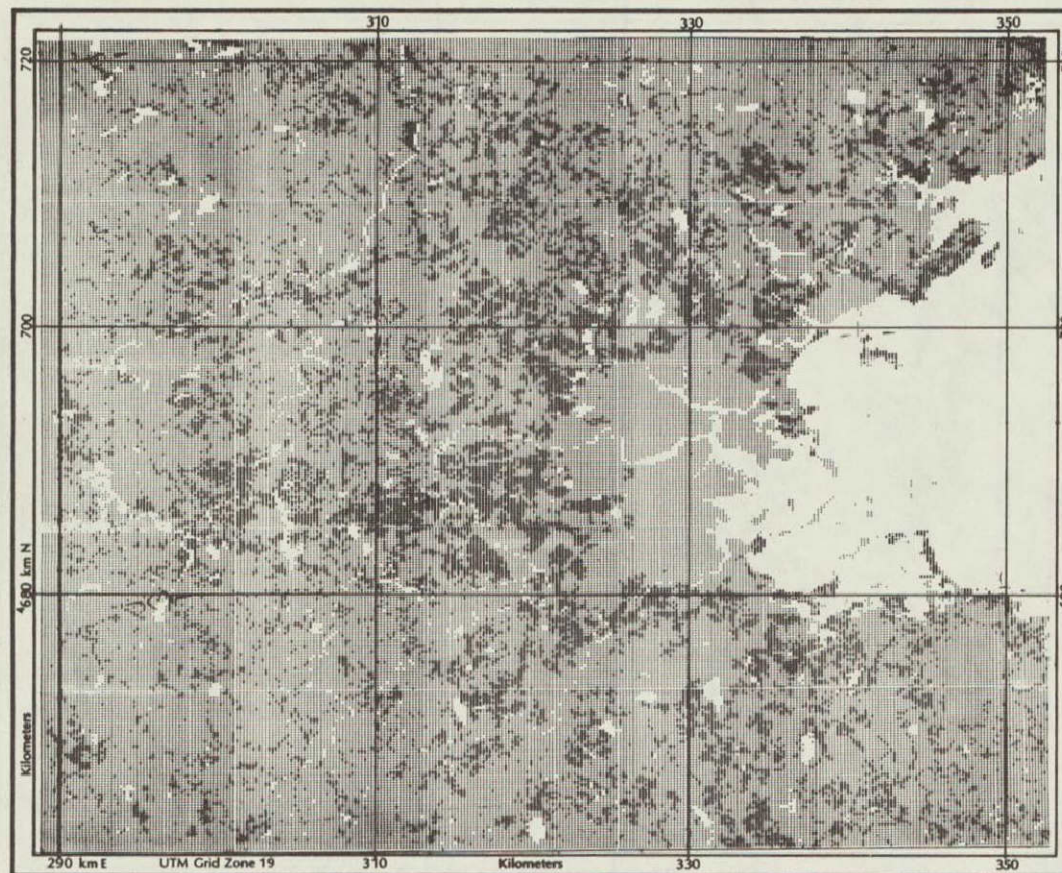


Based on research at Dartmouth College ... as part of the USGS/NASA Geographic Applications Program

Figure 14.--Boston, 1970 multi-family residence land.



Boston
Single-Family
1970



Based on research at Dartmouth College ... as part of the USGS/NASA Geographic Applications Program

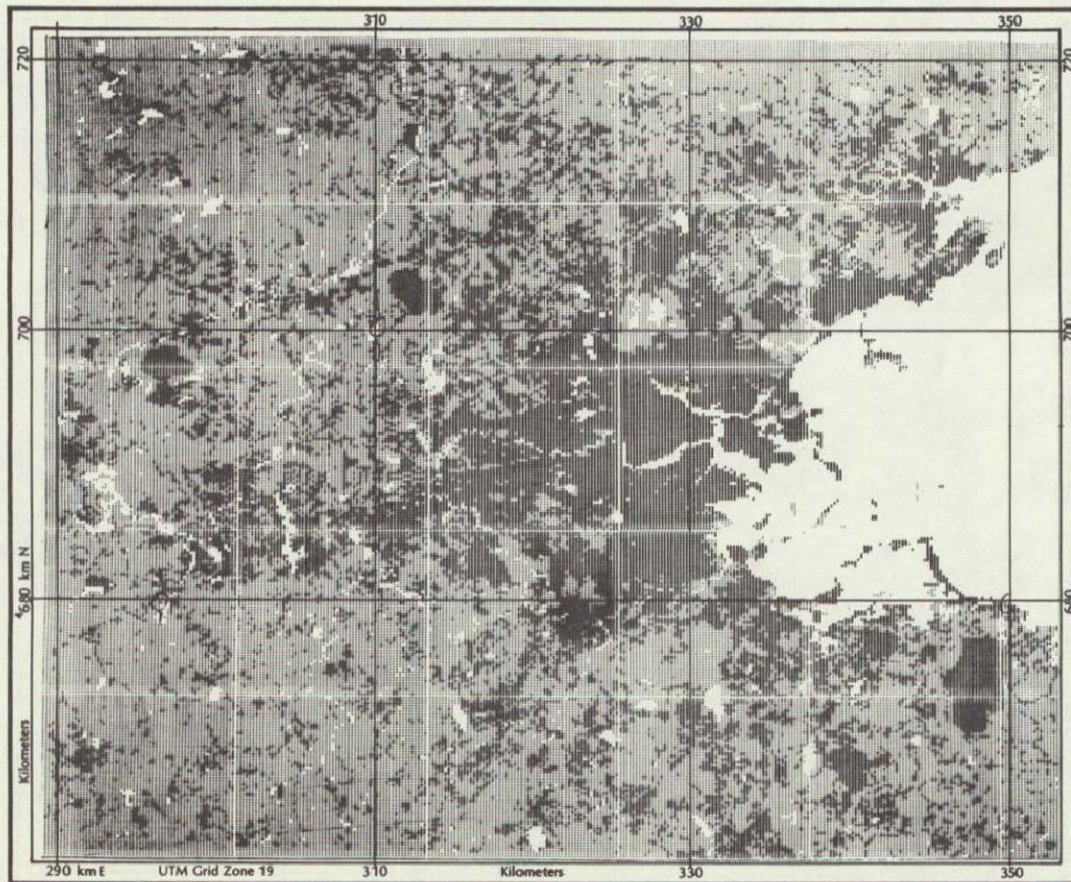
Figure 15.--Boston, 1970 single-family residence land.

ATLAS OF URBAN AND REGIONAL CHANGE

CENSUS CITIES EXPERIMENT



Boston

Built-up
1970

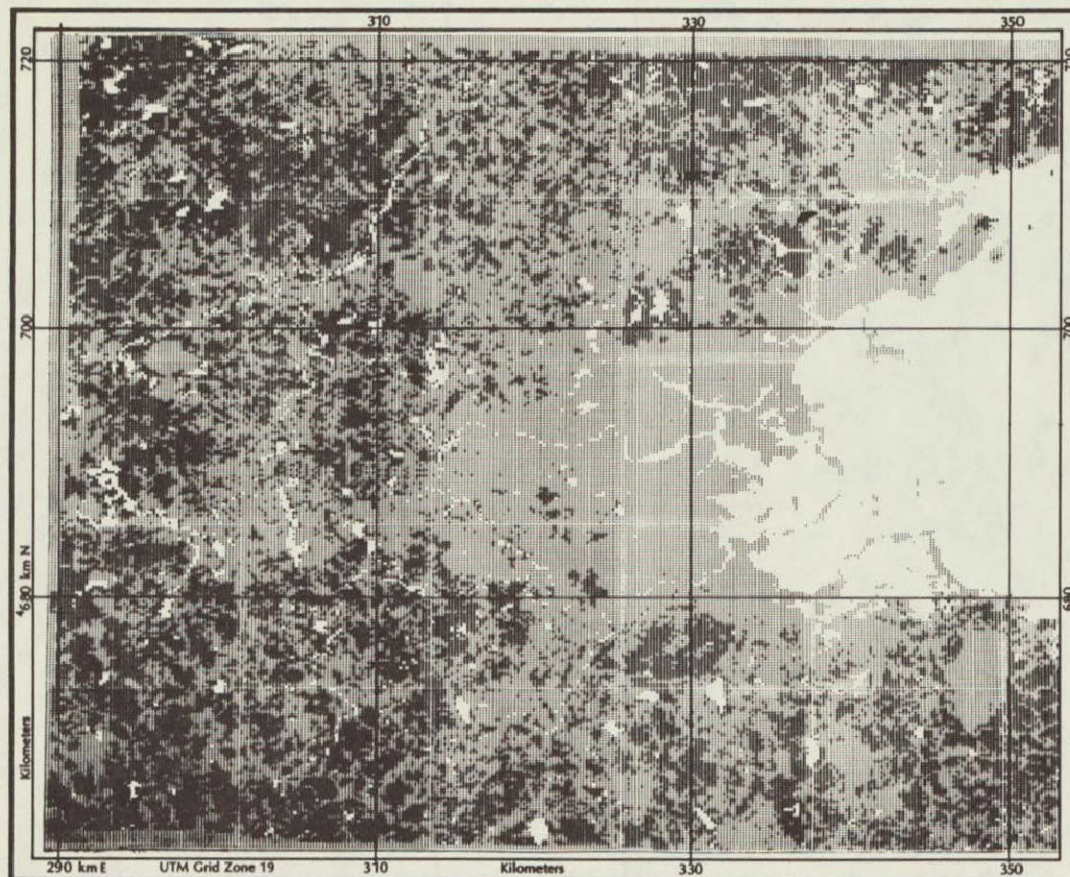
Based on research at Dartmouth College .. as part of the USGS/NASA Geographic Applications Program

Figure 16.--Boston, 1970 built-up area, a partial ERTS-simulation.



Boston

Forest
1970



Based on research at Dartmouth College ... as part of the USGS/NASA Geographic Applications Program

Figure 17.--Boston, 1970 forest land, a partial ERTS-simulation.

SECTION 74

BUREAU AND AGENCY REPORTS

by

George L. Loelkes
U.S. Geological Survey
Geographical Applications Program
Washington, D. C.

INTRODUCTION

As was indicated in Dr. Gerlach's introductory remarks on the Geography and Human-Cultural Resources Working Group, the Group serves as a bridge between 'the remote sensing experiments of physical scientists and the needs of the socio-economic and culturally oriented planners and policy makers.' To accomplish this aim, the Working Group, which is composed of representatives from various Bureaus of the Department of the Interior, meets periodically to generate ideas which subsequently are developed into research proposals to apply remote sensing technology and data to Bureau problems and operations. These research proposals, when converted into projects, are monitored by the Working Group to achieve maximum results from the investment of time and money.

This paper constitutes a summary of work accomplished during the past year through the auspices of the Geography and Human-Cultural Resources Working Group. Projects were monitored by the Working Group for the Bureau of Outdoor Recreation and the National Park Service, and in addition, technical advisory assistance was provided for two research projects managed by the EROS Program staff, i.e.: one with the University of Washington and the other jointly with the Association of American Geographers, the Tennessee Valley Authority and East Tennessee State University.

New projects for the coming year involve four Interior Bureaus, i.e., the Bureaus of Outdoor Recreation, Land Management, and Indian Affairs, and the National Park Service. In addition, liaison has been established with the Ozark Regional Commission of the Department of Commerce, which has resulted in a pilot project to prepare a computerized land use map of the Ozark Region beginning with four specially selected quadrangles.

The first section of this report will cover on-going projects, and the second section will deal with proposed projects, all of which use remote sensing data, mainly from NASA sources.

ON-GOING PROJECTS

The projects described in this section were approved by the Geography and Human-Cultural Resources Working Group as part of the EROS Resources Management Program, financed by either NASA or EROS SIR funds, or a combination of the two, and based largely upon high altitude aircraft or satellite data provided by NASA.

BUREAU OF OUTDOOR RECREATION

A contract was negotiated between the Bureau of Outdoor Recreation and the University of Virginia's Department of Environmental Sciences for research on "Remote Sensing Applications in the Outdoor Recreation Planning Process."

The Bureau of Outdoor Recreation is responsible for the coordination of recreation planning at all levels of Government. The comprehensive outdoor recreation planning process endeavors to identify the full range of public and private goals for the provision of recreation opportunities, and justify plans and programs to achieve these goals for the full range of public and private decision makers. In recent years, opportunities to expand the types of data collected and to speed up the process of collection and analysis have come from new environmental monitoring systems, including remote sensing and mathematical modeling. The Bureau of Outdoor Recreation proposed this study to determine the range of possible applications of remote sensing technology as a source of data for outdoor recreation planning. It became clear that specific data needed by outdoor recreation planners can be satisfied by remote sensing technology.

Approach. - The approach was first to determine the type of data needed to support the comprehensive outdoor recreation planning process. To accomplish this, an extensive literature search was undertaken to determine: 1) the steps in the process; 2) the agencies and decision makers involved; 3) the activities they perform; 4) the types of analyses supporting these activities; 5) the data types required by these analyses, and 6) the specific characteristics of the data used.

Results. - In systematically tracing through the outdoor recreation planning and decision making process, this project has identified a set of data for which remote sensors can provide an alternative or unique data source. These data include: 1) landscape descriptors including topography, standing, ground and flowing water, soils, land uses such as agriculture, forests, mines, transportation networks, urban and non-urban delimitations; 2) population characteristics and place of residence; 3) biological characteristics including vegetation and animals; 4) atmospheric variables; 5) air and water quality; 6) air, water, land, and noise pollution; and 7) special characteristics such as location of resources in relation to needs or demands, present recreational facilities, and development constraints or benefits.

The project alerts planners to the opportunities of incorporating remote sensing imagery and centrally interpreted remote sensing data into their on-going data collection programs. Current and potential sources of imagery and interpretation programs are identified for the planner, and the potential for using remote sensing based data in more detailed analyses of the environmental conditions of site and surrounding areas are indicated.

Conclusion. - Clearly outdoor recreation planners could make extensive use of imagery from a wide range of sensors, take advantage of centralized interpretation services, and engage in a more detailed level of environmental analysis and planning than is now being done.

NATIONAL PARK SERVICE

Archeological Sites

Under a contract with the National Park Service, the New Mexico Archeological Center, University of New Mexico, undertook a study of "Remote Sensing of Archeological Sites in the Chaco Canyon Region of New Mexico." The following is a summary of activities during the past year, provided by the Principal Investigator, Prof. Thomas Lyons.

The New Mexico Archeological Center has been working on analysis of aerial photography of the Chaco Canyon Region, New Mexico that was flown in the 1930's and the 1960's. Emphasis has been upon developing facility in the detection and recognition of relevant phenomena, as well as upon establishing a base for the development of differential spectral signatures for environmental zones and various forms of human modification of the natural landscape. We foresee a long range program of remote sensing investigations and the application of the techniques involved to environmental studies, along with archeological analyses. It is anticipated that our studies will develop models applicable to other target areas in the American Southwest and elsewhere and thus be of service to both scientific research and resource management.

Problems. - There are two specific research problems in terms of the application of remote sensing to archeology which have been studied by this center. These problems are:

- 1) Although aerial photography has been used in archeology in England since before the turn of the century, relatively few substantive analyses of aerial photographs have been made in North America. Consequently, the initial problem can be stated as one of imagery interpretation for the detection and identification of archeological anomalies not readily discernable from ground station vantage points.

Specifically we are attempting in the Chaco Canyon environs to identify and map what are here referred to as echo lines. Such features appear to be prehistoric roads or causeways, and their occurrence in the region has been known for some time. Our work has identified a significantly large number of these linear features, and initial analysis indicates that their occurrence was patterned according to some plan or design, and formed a possible system or network of routes for human passage. One of these features has been traced from a major site, Pueblo Alto, to a point 15 miles north. Continuing work suggests that it extends even further. This particular echo line passes immediately to the east of a mound which was recorded as an unexcavated Pueblo III ruin. This association of ruin and "roadway" observed on the aerial photography was field checked and verified, thus providing a site which may serve to test hypotheses designed to explain the function of these enigmatic linear features. The full extent of these systems has not yet been determined. Consequently their function and significance in the prehistoric setting is currently a matter of hypothesis only.

- 2) The second problem is related to data manipulation techniques. The aim of this research is the differentiation of data with prehistoric relevance which is inherent in remote sensor imagery but not detectable by the unaided human eye.

Equipment. - We have in our laboratory a capability for analysis of multiband photography flown with a compatible camera or with a bank of bore sighted cameras. Since this equipment is capable of selectively accentuating or isolating variable densities, it has the potential for discriminating modifications of the natural environment due to human activities and other factors. Microdensitometry equipment is also available for our use and like the color additive viewer has the potential for feature discrimination.

Multiband photography, color photography, and thermal infrared imagery of selected flight lines in the study area are being acquired through a combination of data already available from NASA and some low altitude, instrumented overflights by the USGS and commercial aircraft.

Marine Archeological Surveys

The National Park Service funded research by the Earth Satellite Corporation for "A Feasibility Demonstration of Aerial Photographic Support for Marine Archeological Surveys."

Procedure. - A feasibility demonstration was undertaken over Loggerhead Reef in Fort Jefferson National Monument to determine the

utility of aerial photography in support of marine archeological surveys. Photography was obtained through a contract with the Earth Satellite Corp. on a 70 mm format using five film/filter combinations. The five combinations evaluated were conventional color, both haze filtered and unfiltered, false color infrared with Wratten 15 filter, blue insensitive color with Wratten 15 filter, and panchromatic with Wratten 12 filter.

Results. - The results show that in the clear waters predominating in the national monument, conventional color provides ample depth penetration. However, both minus-blue filtered color films showed potentially greater depth penetration capability for turbid water conditions. Several sites containing significant remains were identified, including one previously unlocated site containing perhaps the most important remains in the national monument. Coordinated use of both large and small scale photography proved particularly useful for precisely locating newly identified sites, and for providing the capability to relocate previously identified sites. This latter capability is particularly noteworthy in that existing charts contain numerous errors which complicate the task of relocating a site.

Conclusions. - Aerial techniques should be used in concert with more conventional survey techniques, especially since aerial techniques are presently unmatched in the dimension they provide for precise location of sites. Furthermore, interpretation of photography obtained prior to ground survey should occur simultaneously with ground survey procedures in order to increase the likelihood of convergent evidence providing identification and location of unknown sites.

UNIVERSITY OF WASHINGTON

Procedure and Analysis. - In the absence of NASA overflights during the early stage of the project, a review of pertinent literature was undertaken. It was completed in August 1971. A review of existing historical photography from traditional sources (Dept. of Agriculture, U.S. Geological Survey, and state agencies) was then undertaken and copies of the photography acquired. Liaison was established with planning agencies to ascertain their needs for data. Test sites were selected and documented, and ground truth acquisition was initiated.

In October, overflights by the NASA NP3A and RB-57F aircraft were made, but the RB-57F photography, desired for a basic mosaic, has not yet been received. Subsequently, the data analysis phase

was initiated, using the small scale multispectral photography as well as the larger scale CIR photos from Mission 184. Arrangements were made to use an I²S Mini Addcol viewer acquired by the Engineering Department under a sister contract with the EROS Program. Study was focused upon specific functional applications--one of the first being to airport system planning. The categorization and delineation of land use data follow closely the specifications for the Census Cities Project:

- a. Major boundaries of physiographic units, land-water edges, and flood plain escarpments.
- b. Major regional transportation arteries which serve as significant linkages.
- c. Boundaries of built-up land (urban--non-urban interfaces).
- d. Various types of non-urban land, agriculture, rural residential.
- e. Vacant land within urban areas.
- f. Retail commercial, public, and public services.
- g. Commercial strip development.
- h. Wholesale commercial.
- i. Heavy industry.
- j. Port facilities, airports, and other major transportation centers.
- k. Single family residential, multifamily, and mixed.

This interpretation process will be evaluated by comparison with the same area interpretation of RC-8 color IR photography viewed stereographically and supplemented with mapped land use information from local agencies.

Department of Engineering

Procedure and Analysis. - Research under this contract has been preparatory in nature. Equipment has been acquired and evaluated, including the International Image System I²S Mark I, multi-lens camera Model 500. This camera proved to be the principal research tool for this project. The equipment obtained will be also used for important

phases of the contract on urban planning at the University of Washington. The I²S Mini-Addcol Additive Color Viewer, Model 600, was also acquired for viewing the I²S films.

Discussions have been held with staff personnel from the University's Departments of Geography, Urban Planning, and Natural Resources, and the State Department of Natural Resources in Olympia. The discussions were for the purpose of identifying areas of high interest within the various departments visited. The result provided 13 sites for study, and these were photographed.

A parallel investigation under development in connection with this project is the technical requirements and procedures for color calibration of the multiband cameras. The objective is to determine the spectral modification of light passing through the camera system at various angles of incidence. To accomplish this, targets of known reflectance will be photographed for analysis. The targets have been completed and reflectance measurements begun. There have been no published results to date.

The ground truth information for the 13 test sites will be obtained by a close range, 35 mm camera, utilizing the same film-filter combination as the aerial camera system. Field trips have been initiated to the 13 test sites, and documentation of ground truth for each site begun.

ASSOCIATION OF AMERICAN GEOGRAPHERS

The EROS Program contracted jointly with the Association of American Geographers, the Tennessee Valley Authority, and East Tennessee State University to perform research on selected spatial problems. Efforts to date have focused mainly on basic data needs within the TVA, with respect to levels of information which can be obtained from high altitude aircraft and ERTS-A imagery. The research has been financed with EROS SIR funds, and the photography has been provided mainly by NASA.

Procedure and Analysis. - To determine basic data needs within the TVA, two sets of interviews were conducted. First, a joint session with TVA personnel representing the following 11 divisions or branches was held at Chattanooga in May 1971.

Computer Center
Forestry, Fisheries, and Wildlife Research
Geologic Branch
Hydraulic Data Branch
Maps and Surveys

Navigation Development and Regional Studies
 Regional Planning Staff
 Recreation Resources Branch
 Soils and Fertilizer Research Branch
 Agricultural Resources Development Branch
 Transportation Planning and Engineering

The second stage of interviews involved meeting with individual TVA representatives to obtain specific data requirements in line with availability of data from high altitude aircraft and satellite imagery. Questions for these interviews were particularly keyed to:

1. The types of information needed.
2. The variation of scales between high altitude and satellite maps.
3. Temporal considerations as they apply to repetitive coverage.

Ten individuals from six TVA branches were interviewed.

Results. - Results to date include the completion of Parts A & B of Phase I, and Phase II. Dr. Nelson Nunnally of the University of Oklahoma has completed the literature search and an annotated bibliography has been typed in final form. The second portion of the first phase of the project--the delineation of informational requirements for a regional organization--has also been completed. This information will be used as a basis for the development of the third part of the first phase--interpretation of imagery. Phase II, concerned with the identification of planning regions, has been completed and field work to test the utility of high altitude photography from the RB-57 aircraft accomplished.

PLANNED PROJECTS

Much effort by the Geography and Human-Cultural Resources Working Group during Fiscal Year 1972 has been devoted to planning project for FY 1973. The more important of these are summarized below in order to demonstrate that Bureaus of the Department of the Interior have awakened to the value of using remote sensing technology and data to solve current problems and expedite operations.

BUREAU OF INDIAN AFFAIRS

The Bureau of Indian Affairs, with assistance from the Geography and Human-Cultural Resources Working Group, has progressed far toward

the development of a project for "Regional Planning and Monitoring of the Phoenix Area Indian Reservations." This project will demonstrate the feasibility of using high altitude and satellite photographic imagery, obtained repetitively, as a basis for developing and implementing regional comprehensive planning and in monitoring changes in natural conditions in Indian Reservations (Salt and Gila Rivers) bordering the Phoenix metropolitan area. It will provide training for Indians in the use of remote sensing data in maintaining a continuous planning effort. Finally, this project by using BIA/BLM Natural Resources Management Information System will combine information obtained with previously gathered data to develop a data base from which data can be synthesized to provide inputs for comprehensive planning.

The approach for this project is to utilize the remote sensor data in preparation of base maps and thematic map overlays in order to show land use, soils, hydrology, etc. The resultant maps and overlays will provide aid to Indians in preparing comprehensive plans for the Gila River Reservation, and to illustrate to the Salt River Indians how their comprehensive planning documents relate to the physical environment. Training programs will provide both academic (through special remote sensor courses offered by universities) and on-the-job training.

GEOGRAPHIC APPLICATIONS PROGRAM

With seed money from the EROS SIR funds the Geography and Human-Cultural Resources Working Group is preparing a pilot land use map at 1:250,000 to demonstrate to the Ozark Regional Commission of the Department of Commerce and officials in the four states adjacent to the Ozark Region the potentials for "Automated Land Use Mapping in the Ozark Region." This work is being done as the result of a request from the Ozark Regional Commission and state authorities in that area for assistance in planning a land use analysis project for the entire region next year.

The Ozark Regional Commission now has an operational data bank containing social and economic data in the form of community profiles and work is underway to incorporate into the data bank from the latest census those data. They also would like to include land use information and geographically oriented data. Based on this requirement, the Geography and Human-Cultural Resources Working Group has initiated a feasibility study to demonstrate the way in which geographical data can be incorporated with social-economic information.

Approach. - A sample land use map, at the scale of 1:250,000, utilizing the categories from the land use classification scheme developed at the June 1971 National Conference on Land Use Information and Classification is being prepared using as a base the USGS standard topographic quadrangle map. This pilot map will include not only land use data but also information such as town references, soils, geology, etc., and is scheduled for completion some time in February 1972.

BUREAU OF LAND MANAGEMENT

The Bureau of Land Management proposed a project in FY 1972 for research on "The Regional Impact on Environmental Conditions in the Lower Colorado River Basin." The desired data were obtained from NASA overflight photography, but funds were not available in FY 1972 for the analysis of this data and the achievement of conclusions. Preliminary studies revealed that the annual visitor use of public domain land in the deserts adjacent to, and in the immediate vicinity of, the lower Colorado River, has increased five times over the national trend. The fact that this area lies within a few hours' drive of approximately 32 million people, has many facilities for water sports, and a large acreage of open public lands makes the area an ideal recreation site.

This project seeks to demonstrate that remote sensing interpretation techniques can show the impact on the desert ecology of expanded recreational and residential use. Recreational resources include wildlife, desert vegetation, geology, archeological and paleontological sites, historical sites, and open space. The relationship of urban development to land designated for public use, and its orientation to the river will be considered.

Secondly, the project hopes to demonstrate that land pollution (i.e., garbage dumps, landfills, and unauthorized dumps) can be detected by remote sensors and that water pollution, as detected by remote sensors, is a direct result of recreation and urban development.

Finally, a standard matrix to be used with ERTS imagery will be developed. It is anticipated that analysis of the data and demonstration of the first two objectives will provide a basis for using ERTS-type data to monitor conditions in the desert. Preliminary studies now underway in the Bureau of Land Management (BLM) indicate that remote sensing will provide more pertinent resource information, using fewer men, at a lower cost, and in a shorter time period. The data obtained by remote sensing techniques should provide a valid base for BLM to use ERTS satellite data on land use, recreation, and natural resources to achieve a fuller understanding of desert ecological problems.

Approach. - The approach will combine a graphic display of major changes in the area in regard to vegetation, roads and trails, lot plans and urban areas, and in water and agricultural areas, with statistical data available from many sources. The statistical data will include a visitor/day listing, plus the permanent residents, obtained through concessionaires. One overflight by NASA, yielding multispectral, thermal infrared, and metric camera imagery has been completed. It is hoped that this imagery will illustrate present data conditions as related to past overflight photography. The area of interest covers about 20,000 square miles, fifty miles on either side of the Colorado River from the Mexican-Arizona border to Bullhead City, Arizona.

A graphic display denoting changes of certain representative areas only will be made with a Cedartron printer. In the event the Cedartron will not take the available negative-positive film composites, films will be printed for the graphic display.

The correlation of the graphic and statistical data should lead to development of matrixes for projecting visitor/day use of areas, and the analysis and prediction of urban change.

NATIONAL PARK SERVICE

The National Park Service has proposed a major project for "Monitoring Vegetation Vigor in the Washington, D.C. Area," and has recommended that the research be performed by Ecology and Environment, Inc.

This project seeks to develop the input necessary to establish the reflective properties of plant materials in both urban and non-urban areas and under known ecological conditions. Special multispectral photography of the Mall and Rock Creek Parkway areas in Washington, D.C. will be used. Once the photography has been obtained, the contractor will use enhanced photographs to analyze tree vigor and disease.

In FY 1971, the National Park Service obtained a spectrophotometer to measure spectral reflectance of vegetation in the ultraviolet visible and near infrared spectral regions. This equipment will be used for the analyses required in this project.

BUREAU OF OUTDOOR RECREATION

The Bureau of Outdoor Recreation has proposed and developed a plan for research on "The Application of Remote Sensing to the

Optimization of Outdoor Recreation Projects." It is proposed that the research be carried out by the Environmental Awareness Center of the University of Wisconsin, with Professor Philip Lewis as the Principal Investigator.

This proposed project is an experimental application of remote sensing and computerized decision making techniques in outdoor recreation resource planning and development in conjunction with a planned major interstate highway. The specific purpose of the project is to develop the methodology and capability for utilizing data acquired by remote sensing techniques in multi-disciplinary planning programs.

The Bureau of Outdoor Recreation has also proposed a study on "The Evaluation of High Altitude Photography for Recreational Area Planning," to be carried out under a contract with the Pennsylvania State University, with Prof. Robert Douglass as Principal Investigator. The primary objectives of the study are: 1) investigate the use of ultra-high altitude imagery for predicting potential intensive use of recreational development sites; 2) evaluate high altitude imagery for use in recreation resource inventory including the forest lands and associated waters; 3) study the feasibility of classification of land and natural resources from ultra-high altitude imagery; and 4) determine signatures of stressed vegetation in and around intensively developed and heavily used recreation areas.

High altitude, multispectral photography for both of these projects has already been obtained.

* * *

(PAPER NOT SUBMITTED FOR PUBLICATION)

SECTION 75

HYDROLOGIC APPLICATIONS PROGRAM SUMMARY

by Morris Deutsch

ABSTRACT

(Not available)

texture, color, and depth, that have a major effect on the imagery. Regional scale influences of ground parameters have been calculated using trend surface models of the properties isolated in laboratory work.

For the Lake Ontario work the best data received was that of the July 6, 1970 mission. Surface indications of internal waves present on the imagery have had a useful input into the CCIW Internal Wave Program. Measurements from the imagery show that the apparent wavelength of these features lies in the range 400 to 1700 meters. This range of wavelength indicates that this important dynamic phenomenon should be observable from ERTS imagery and shows that the repetitive nature of ERTS data would be of particular value in this instance. The quasi-synoptic RB-57 photography over Lake Ontario demonstrates the importance of synoptic ERTS coverage as applied to observations of turbulent effluents, e.g., the Niagara River plumes, and their relation to lake circulation. Other applications are the observation of surface contamination e.g., water quality, and sediment transport in coastal areas.

SECTION 76

SIMULATION STUDIES OF ERTS-A&B DATA FOR
HYDROLOGIC STUDIES IN THE LAKE ONTARIO BASIN

by

Joseph MacDowall
Canadian Centre for Inland Waters
Burlington, Ontario, Canada

Allan Falconer
University of Guelph
Guelph, Ontario, Canada

and

Keith P. B. Thomson
McMaster University
Hamilton, Ontario, Canada

ABSTRACT

In the Lake Ontario basin remote-sensing research is oriented directly toward attainment of IFYGL objectives using ERTS simulation data, and falls into three project areas:

1. Calibration of ERTS imagery so that the sequential photography will yield consistently usable measurement of surface reflectance. This can be achieved by utilizing high and medium altitude photography over the area equivalent to one frame of ERTS imagery. All the individual photographs must be corrected for instrument distortion and influence of sun angle, etc., to give consistent readings. Integrating these for a completely automated correction of the block of photography has not yet been achieved but is in progress.

2. RB-57 photography over the land was studied to evaluate the use of ERTS data for a quantitative assessment of important hydrological parameters, such as soil moisture, aquifer and land-use boundaries, etc.

3. Laboratory and field studies have been carried out to determine those physical parameters, including soil

SECTION 77

COURT PRECEDENT FOR ACCEPTANCE IN EVIDENCE OF
REMOTELY-SENSED DATA AND THEIR
INTERPRETATION, CROSS-FLORIDA BARGE CANAL

by

Aaron L. Higer
and
Milton C. Kolipinski
U.S. Geological Survey
Miami, Florida

and

Eldon Lucas
U.S. Forest Service
Tallahassee, Florida

ABSTRACT

A legal precedent was set by the acceptance of remotely-sensed data without ground truth by the photo-interpreter as evidence in a Federal court.

Remote sensing data concerning the Oklawaha reservoir of the Cross-Florida Barge Canal were submitted as testimony in Federal court in Jacksonville, Florida, on September 8, 1971. The hearing was to consider the lowering of Oklawaha reservoir formed behind Rodman dam from its present level of 18 feet mean sea level to 13 feet mean sea level. The Federal government contended that the drawdown of the reservoir would save hundreds of acres of trees. The Florida Canal Authority, plaintiff, claimed that the lowering of the reservoir would wreck the recreational areas visited by nearly half a million people since it opened in 1969.

The trees, as interpreted from the color infrared photographs and ground truth collected by the U.S. Forest Service, were under stress that did not appear in the areas above Eureka lock or below Rodman dam. The stress was progressively more pronounced and severe proceeding from Eureka lock toward Rodman dam as the trees were more deeply inundated.

The remote sensing testimony was challenged by the plaintiff on the basis that the photo-interpreter had not been on the site. However, the judge overruled the objection, deciding that it was unnecessary to have been on the site to interpret color infrared photographs. This decision was based on the fact that color infrared photography was developed for the military for camouflage detection in areas where ground truth was unavailable to the photo-interpreter.

The judge ruled that the reservoir should be maintained at 18 feet mean sea level. He based his decision on the fact that at the time of the hearing the growing season for the trees had passed. He stated he would reopen the hearing at the next growing season to reconsider the lowering of the reservoir.

SECTION 78

WETLANDS DELINEATION BY SPECTRAL SIGNATURE

ANALYSIS AND LEGAL IMPLICATIONS

by

Dr. Richard R. Anderson
Chairman, Department of Biology
The American University
Washington, D.C. 20016

and

Virginia Carter
Office of Remote Sensing
U.S. Geological Survey
Washington, D.C. 20242

INTRODUCTION

This paper presents progress on research conducted in the laboratories of The American University as funded by the Office of Remote Sensing, U.S.G.S. During the period since the last Aircraft Review Meeting, one flight (Mission 166, May 16 and 18, 1971) was obtained over Test Site 168, the Patuxent River - Chesapeake Bay. These data were the best obtained over this test site since high altitude flights began in 1969.

Research has proceeded along three lines, each unique but related to the general effort of attempting to analyze wetland resources from high altitude and using this information in an operational mode to address specific problems of wetland preservation at the state level. These areas of research are:

- a. Continue to expand data bank on spectral reflectance of wetland plant species and associated shallow water areas (Carter);
- b. Visual enhancement techniques whereby high altitude imagery may be used to define and analyze wetland resources (Carter and Anderson);
- c. Application of experience gained in four years association with NASA Earth Resources Program and U.S.G.S. to a specific wetland problem in the state of New Jersey (Anderson).

RESULTS

A. SPECTRAL REFLECTANCE DATA

There are several problems associated with the interpretation of remotely sensed data from wetlands. Among these are seasonal changes in the reflectance of plant species and their distribution, shifts in plant orientation, and certain natural environmental complications. Knowledge of the spectral characteristics of important marsh species and of typical wetland components such as mud flats and salt pans are providing solutions to some of these problems.

Field "in situ" spectral radiometric measurements are being collected for 19 marsh species (6 have been completed) since field conditions cannot be simulated in the laboratory. Plants such as smooth cordgrass (Spartina alterniflora Loisel), cattail (Typha sp.), sweet flag (Acorus calamus L.), and arrow arum (Peltandra virginica Schott and Endl.), have vertically oriented leaves which may expose a large percentage of background soil or water. This is particularly true in low-vigor forms of Spartina alterniflora. For this reason, laboratory measurements of the spectral reflectance of wetland plants are of questionable value in predicting or interpreting photographic tones or multispectral response.

Field spectral reflectance are being collected by using an ISCO Spectroradiometer equipped with a fiber optic remote probe.

Summary of Work to This Point on Spectral Reflectance of Wetland Environments

1. Small changes or differences in red reflectance of typical plant species around 0.675 μ m have a relatively large effect upon the color or tone of the resulting image on color IR photographs. Increases in red reflectance caused by changes in leaf or plant orientation result in a lighter tone. This is largely a result of density changes in the magenta layer of the film.
2. Vertically oriented leaves of marsh plants, such as Typha sp., Acorus calamus, and Peltandra virginica, exhibit low reflectance in the visible spectral range. Reflectance in the near IR is high, regardless of orientation. The low visible reflectance results in a dark-red tone on infrared photographs.
3. The lodging, or flattening, of plants such as Spartina patens and Acorus calamus greatly increases the reflectance of all wavelengths,

giving these plants a light tone where lodged and a darker tone where upright. These two conditions may exist simultaneously with a transitional zone in between.

4. The spectral reflectance of plants such as Spartina patens changes over the growing season. As a result of an increase in reflectance at all wavelengths from May to August, Spartina patens may appear darker in tone than Spartina alterniflora in May and June and lighter in July and August.

Spectral reflectance data collected in selected wetland areas are useful for interpretation of aerial color IR photographs and a better understanding of the dynamic wetlands ecosystem. Application to interpretation of multiband photography has already begun and its usefulness in interpreting multispectral scanner data from wetlands will be investigated shortly. Of particular importance is the eventual application of these data to automatic mapping of wetland ecosystems.

B. HIGH ALTITUDE IDENTIFICATION OF WETLAND PHENOMENA (18 KM, NASA RB57)

It is currently possible to use high altitude, small scale data for the following wetland and coastal phenomena: (1) delineation and mapping of wetlands plant communities and boundaries of the wetlands ecosystem; (2) monitoring wetlands on a regular basis for protection from man-made and natural reductions in wetlands productivity; (3) monitoring of tidal and offshore marine currents for placement of erosion-control structures such as groins, bulkheads, and jetties; and (4) dredge site and disposal planning.

Wetland Boundary Definition

(1) Fig. 1 shows some boundaries associated with wetlands which may be defined using high altitude photography. It can be noted that in most cases, boundary definition in wetlands may be interpreted through spectral reflectance data. The most difficult and potentially the most significant boundary to define is the mean high tide line. Currently the authors are using vegetative indicators (i.e., differentiating between species which typically grow above the mean high water line and those which require daily tidal inundation during the growing season to survive). If this method passes a court test and is accepted as a meaningful substitute for the physical mean high water line, then state riparian property may be defined wherever viable wetlands occur.

BOUNDARIES ASSOCIATED WITH WETLANDS	PHYSICAL PHENOMENA WHICH ESTABLISH, MAINTAIN A CHANGE BOUNDARY	PHYSICAL PHENOMENA WHICH CONTROL DEFINITION OF BOUNDARY BY REMOTE SENSING TECHNIQUES	REMOTE SENSING TECHNIQUES
1. Land-water interfaces	1.(a) Wetland drainage patterns (b) Sediment deposition in wetlands (c) Man-made disturbances in wetlands (ditching, filling, etc.) (d) Tidal hydraulics	1.(a) Spectral reflectance differences between land phenomena (soil, vegetation, etc.) and contiguous water body (b) Tidal stage (c) Water quality (sediment, content, etc.) as it affects contrast between water and land	1.(a) Color/Color IR photography (b) Black and white IR (c) Thermal IR
2. Mean high water boundary	2.(a) Land subsidence or change in mean sea level (b) Topography (slope, etc.) (c) Natural or man-made disturbances such as filling, berm formation, etc.	2.(a) Spectral reflectance differences of plant communities (i.e., those that typically grow above or below mean high water) (b) Spectral difference between land and water (if recorded at mean high water)	2.(a) Color/Color IR photography (most widely used) vegetation boundaries
3. Upper wetland boundary	3.(a) Topography; elevation above mean sea level and related soil moisture (b) Sediment and organic depositions on wetlands which dictates rate of natural successional trend to dry land environment	3.(a) Spectral reflectance differences between wetland and dryland plant species at the boundary	3.(a) Color/Color IR photography (most widely used) (b) Black and white IR photography (high potential for use at high alt.)

Figure 1. Shows boundaries associated with wetlands, physical phenomena which identify them and remote sensing techniques.

(1) Wetland monitoring for natural and man-made changes in productivity: The wetland habitat is a dynamic one since it is transitional between an open water habitat undergoing natural succession to high ground, regional climax vegetation. Natural succession occurs over an extended period of time. Succession is accelerated by activities of man such as ditching, draining, diking and filling, in or near wetlands. The following dynamic conditions are being monitored with high altitude photography.

(a) Successional Rates: Successional trends are most obvious near the upper (inland) wetlands boundary. This boundary is clearly identified on high altitude photography (particularly B&W IR). Subtle tonal shifts from what is clearly wetland to clearly upland, indicates that the transitional zone is uniquely recorded on film and may be studied as an independent feature in wetlands. Changes in size or position may be determined.

Fig. 2 shows B&W IR high altitude prints (enlarged from 1/240,000 scale transparencies) of the upper wetland boundary. The transition zone is clearly shown as is the sharp interface between wetland and dryland.

(b) Ecological Changes Due to Disturbances by Man: Man has had great impact on coastal wetlands through various activities, the most important being ditching for mosquito control (wetland drainage), stream channelization (wetlands drainage and erosion) and diking for agricultural purposes. The amount of disturbed wetland in the Chesapeake Bay area is being ascertained and the rates at which these areas are changing ecologically to non-wetland environments. High altitude repetitive, multispectral data are being used for defining past and current activities detrimental to wetlands and ecological impact over periods of time.

Fig. 3 is black and white prints from color IR transparencies showing an area which has been mosquito ditched, next to one that has not been disturbed. Plant species change from wetland to dryland types is apparent from tonal differences between the two areas. Mosquito ditching typically results in wetland drainage and reduction in soil moisture. Also shown is the usefulness of high altitude photography in ascertaining the amount of wetland development.

C. WETLANDS MAPPING IN NEW JERSEY

The New Jersey Wetlands Act of 1970 required mapping and inventory of wetlands along the marine coastal zone and tidally-influenced estuaries. A prime requirement was that map products have validity

which could withstand the challenge of litigation. Color infrared aerial photography at a scale of 1:12,000 was used for mapping. Principal participants were the U.S. Geological Survey, National Ocean Survey, Earth Satellite Corporation, and The American University. Mark Hurd Aerial Surveys is providing photography and map products.

Final map products meeting National Map Accuracy Standards were prepared which contained: (a) the upper wetlands boundary; (b) the line of biological mean high water to establish state riparian lands; and (c) delineation of major plant species associations of five acres or larger in size.

In addition to the legal basis for protecting the state's wetlands, as provided by the Act, state riparian rights can provide a basis for protecting tidal lands. Delineation of riparian lands requires determination of a line of mean high water, lands seaward of which are owned by the state. Twenty-one maps have been completed and field checked for accuracy by the state of New Jersey. A state-wide mapping program is now underway. This state-wide wetlands mapping effort will be one of the largest operational remote sensing projects ever conducted. The methods developed, ecological data collected, and products prepared will have far reaching effects on future coastal zone programs. A suit by developers in the state (by this summer) will provide the first court test on whether remotely sensed data may be used to map wetlands and delineate privately owned from state owned wetlands.

Fig. 4 is a photograph of one of the maps being produced in New Jersey.

CONCLUSIONS

Three years in the NASA Earth Resources Program by The American University and U.S.G.S. has provided: (1) expertise whereby large scale color IR photography may be used operationally in a state wetlands mapping program; (2) high altitude photography from which considerable information on wetlands ecology may be obtained; (3) provided spectral data whereby photography may be more accurately analyzed visually and (4) spectral data whereby the first attempt at automated mapping of wetlands will be undertaken this year.

Research next year:

- (1) Attempt to complete data bank of spectral reflectances of major wetland features;
- (2) Apply spectral information to enhancement and automated techniques for wetland mapping at high altitude.

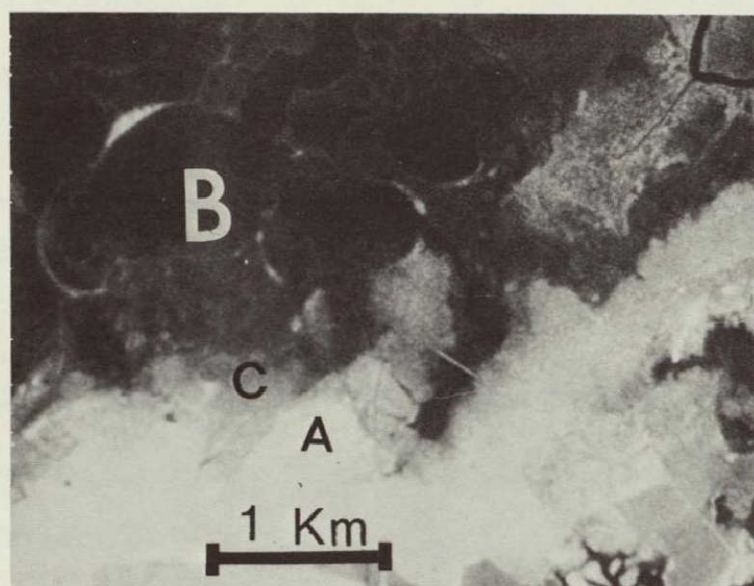
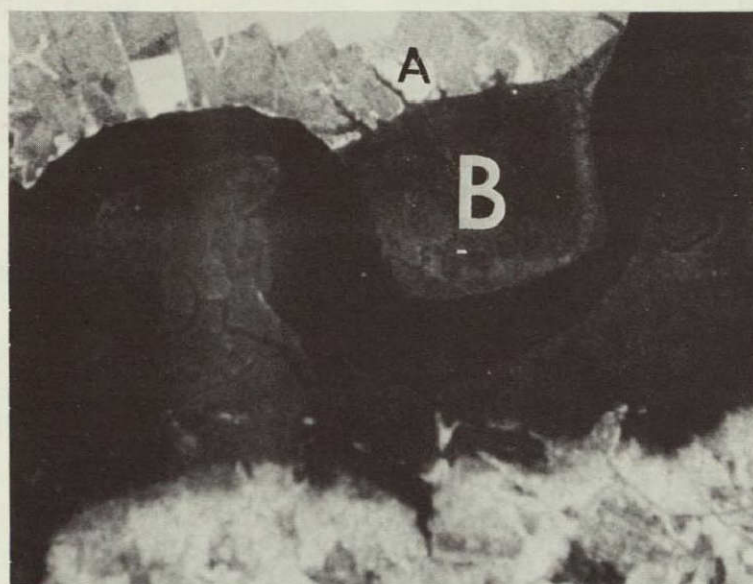


Fig. 2. Black and white infrared photographs showing wetland boundaries. Upper photo shows sharp boundary between dryland (A) and wetland (B). Lower photo shows gradual change or transition zone (C) between dryland (A) and wetland (B). Scale in both photographs is the same.

This page is reproduced again at the back of this report by a different reproduction method so as to furnish the best possible detail to the user.

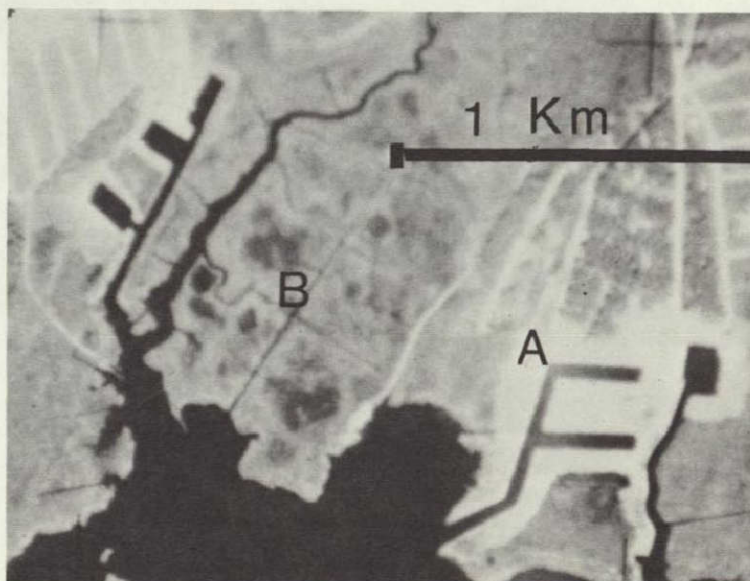
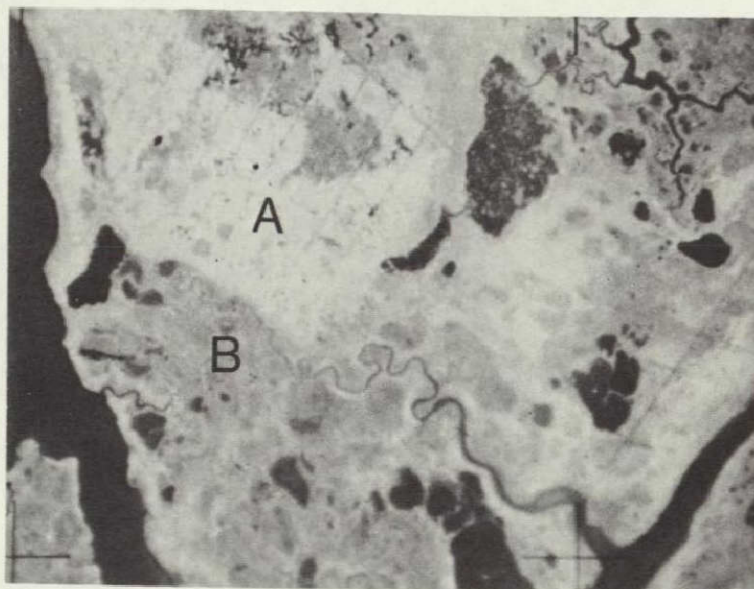


Fig. 3. Black and white prints from 1/60,000 scale color IR transparencies. Upper photo shows species change in ditched area (A) compared to more desirable species composition in non-ditched area (B). Lower photo shows wetland development (A) and ditching for mosquito control (B) which follows housing placement near wetlands.



Fig. 4. Photograph of one of the maps being produced in the New Jersey Wetland Mapping Program. Note development in the area which is endangering many coastal wetlands.

This page is reproduced again at the back of this report by a different reproduction method so as to furnish the best possible detail to the user.

N72-29374

79-1

SECTION 79

ORIGINAL CONTAINS

DISCRIMINATION OF FLUORIDE AND PHOSPHATE CONTAMINATION IN CO² ILLUSTRATIONS
CENTRAL FLORIDA FOR ANALYSES OF ENVIRONMENTAL EFFECTS^{1/}

by

ORIGINAL CONTAINS

A. E. Coker^{2/}, R. Marshall, and F. Thomson^{3/}

ORIGINAL CONTAINS

One of the most serious environmental problems in central Florida arises from the mining and processing of phosphate ores. The land area involved in mining extends over about 2,000 square miles and is in many places relatively inaccessible. The chemical effluents from the processing operations, which are acid and contain high concentrations of fluoride and phosphate, are ponded in large lagoons behind earthen dikes. Some of these lagoons, covering as much as 500 acres, appear to leak and hence permit toxic leachates to seep into the ground. Ruptures of the earthen dikes have occurred in the past and mining and processing wastes have spilled from the lagoons into the Alafia and Peace Rivers to flow into the Gulf of Mexico.

Remote sensing provides a tool for appraisal of environmental conditions and potential hazards.

This study deals with the spatial registration of fluoride and phosphate-pollution parameters by utilizing remote-sensing techniques. Multispectral remote-sensing data were collected over the area in 1969 and processed on the

1/ For presentation at the National Aeronautics and Space Administration 1971 Aircraft program review, NASA, MSC, Houston, Texas, January 1972.

2/ Hydrologist, U. S. Geological Survey, Tampa, Florida.

3/ Infrared and Optics Laboratory, University of Michigan, Ann Arbor, Michigan.

University of Michigan's spectral analysis and recognition computer to produce multispectral recognition maps. These processed data were used to map land areas and waters containing concentrations of fluoride and phosphate. Maps showing distribution of affected and unaffected vegetation were produced. In addition, the multispectral data were processed by single-band radiometric slicing to produce radiometric maps used to delineate areas of high ultra-violet radiance, which indicates high fluoride concentrations. The multispectral parameter maps and radiometric maps in combination showed distinctive patterns, which are correlatable with areas known to be affected by fluoride and phosphate contamination. These remote-sensing techniques have the potential for regional use to assess the environmental impact of fluoride and phosphate wastes in central Florida.

Processing Techniques

The techniques employed in processing this data were basically three: 1) single-band radiometric slicing, 2) multispectral recognition and 3) multispectral parameter mapping. The first two have been commonly employed in the past. Parameter mapping was developed for this application and seems not to have been used previously.

In single-band radiometric slicing a single spectral band of a scanner is analyzed by generating a series of strip film maps which are black wherever the scene has a radiance lying between two arbitrarily specified radiances. These are usually copied in color and superimposed to produce a color coded radiometric map in which a specific color indicates a particular temperature band.

Multispectral recognition is performed by continuously recognizing a specific object by its multivariate structure using likelihood ratio techniques for as many as 12 dimensions. In this case recognition was used to map water with specific chemistries, evaporate deposits, and three species of vegetation; a sedge grass, palmetto and salt bush. The recognition was performed using the Michigan SPARC (Spectral Analysis and Recognition Computer) and employed 6 dimensions (spectral bands).

Multispectral parameter mapping is a new technique which involves recognizing a specific object, determining how "far" it is from normal and then, using a quantitative estimate of the relation between the "distance" from normal and concentration of a chemical affecting the

object, making a map of the inferred concentration of the chemical. The chemical is treated as a parameter affecting the object (three plant species, in this case) which thus becomes an indicator of the parameter. In this case three such maps were made, one each for palmetto, grass and saltbush. Each map, by its photographic density at each point in the scene, indicates the concentration of the chemical affecting the plant. These maps were then superimposed to show the chemical concentration at all points in the scene where any one of these three plant species occur. Since the parameter affecting the plant species is mapped instead of the plants themselves, the term "multispectral parameter mapping" has been chosen to describe the technique.

This mapping was performed using a slight modification of the SPARC process and also used six dimensions (spectral bands). The process can be visualized as shown in the two dimensional diagram and block diagram of Figure 4. Suppose all samples of a species of plant as observed by a multispectral scanner have a radiance distribution in two spectral bands (λ_1, λ_2) as shown in Figure 5 and the normal plant is distributed as a sub-set in the space with a mean, $\bar{P}_N(\lambda_1, \lambda_2)$. Another species of plant is similar and is shown as a possible interfering background distribution. The object decision bound is determined by a likelihood ratio function of the two distributions. A distance $(D(P(\lambda_1, \lambda_2)))$ is continuously calculated for each point $(P(\lambda_1, \lambda_2))$ and is defined as the sum of squared distances from the mean,

$$\sum_{i=1}^k (P(\lambda_i) - \bar{P}_N(\lambda_i))^2.$$

If $P(\lambda_1, \lambda_2)$ is classified as a member of the object set, the distance is printed on a CRO film printer with an intensity proportional to the distance as shown in Figure 5. The printing process proceeds at a real-time rate, about 10^5 elements per second and provides a map of the parameter.

The technique of parameter mapping should prove useful in processing a variety of data involving the mapping of effects of various substances on plants. Among these are the effects of water privation, soil salinity, chemical pollutants and diseases affecting several species or maturities of plants.

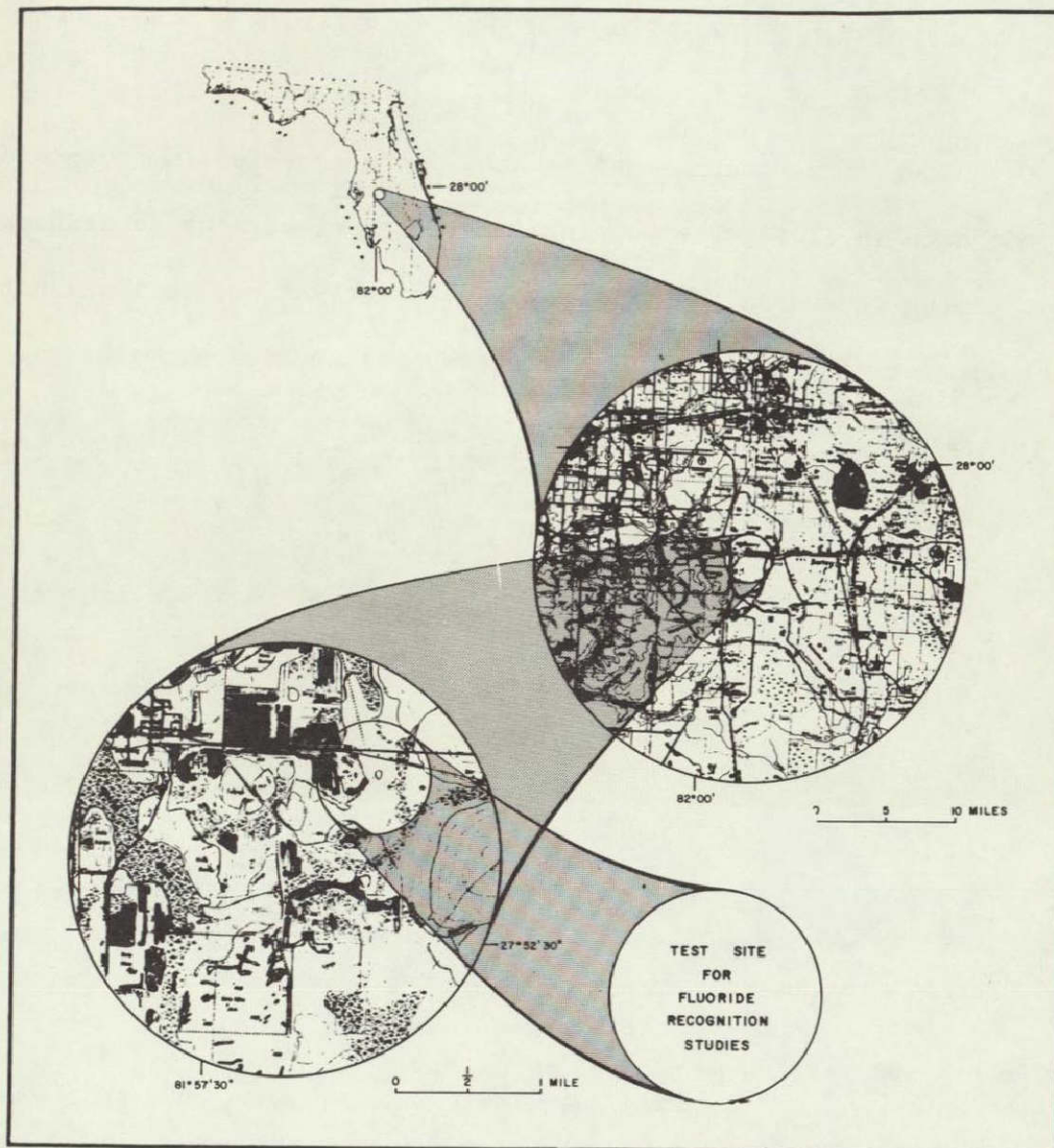


Figure 1. Location of study area.

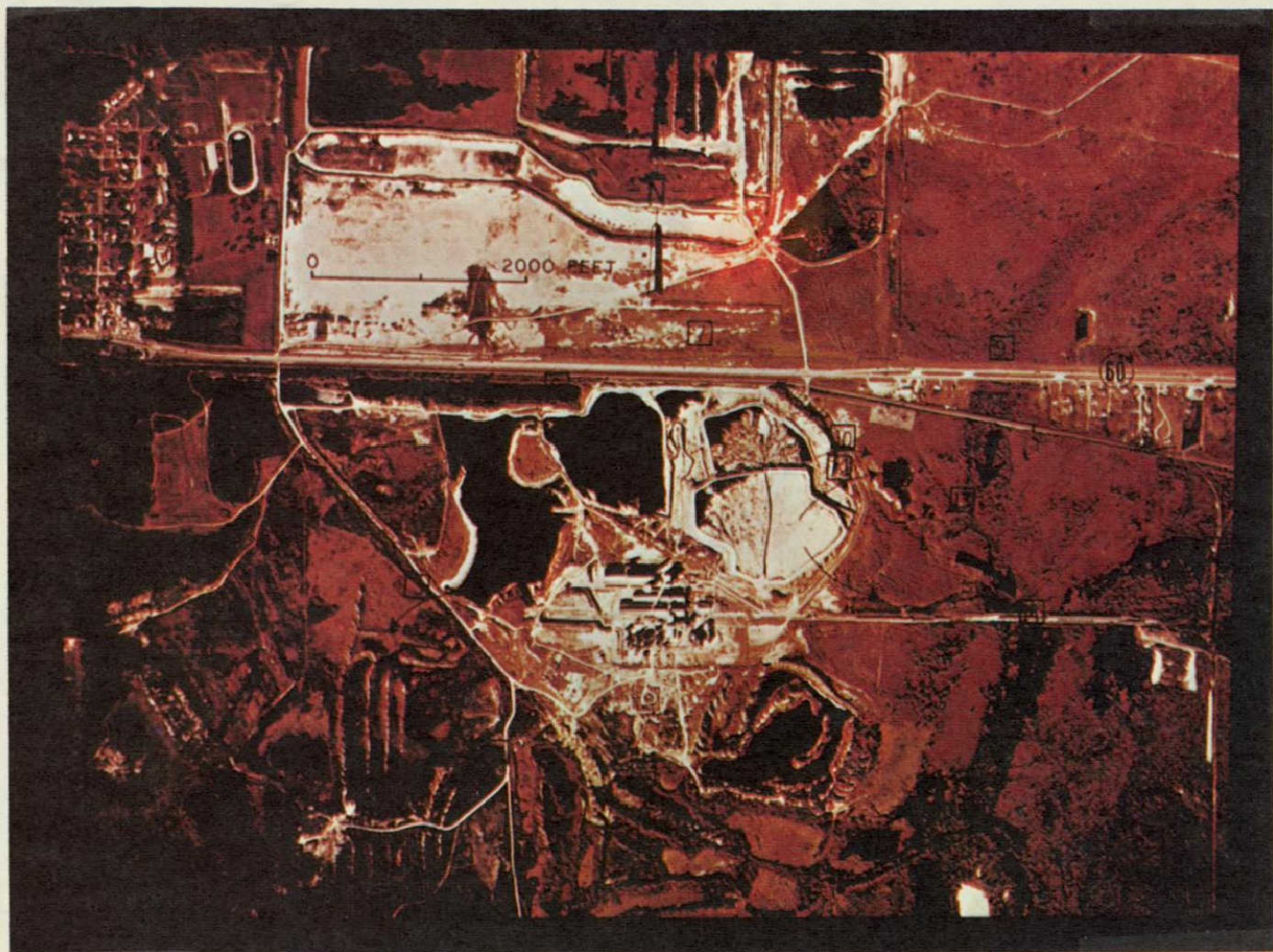


Figure 2. Photograph showing test site used to define effects on vegetation of water containing high fluoride concentrations near Mulberry, Florida.



Figure 3. Photograph showing effects on vegetation of water containing high fluoride concentrations near Mulberry, Florida.

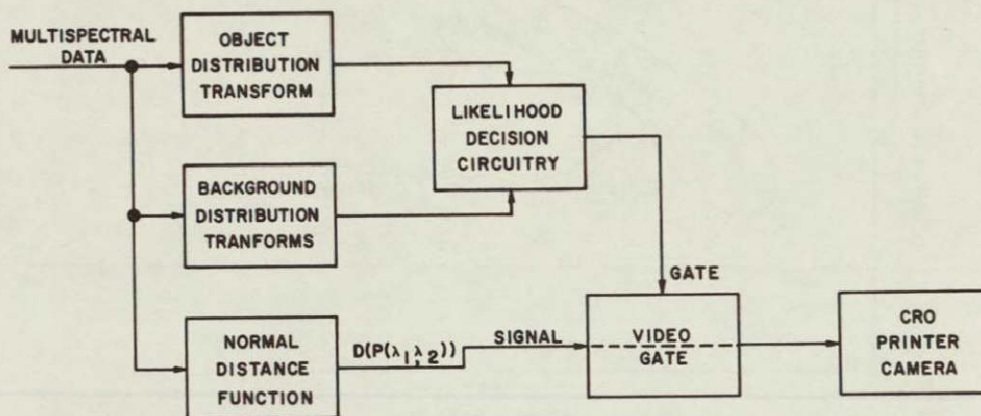


Figure 4. Simplified block diagram of SPARC configuration.

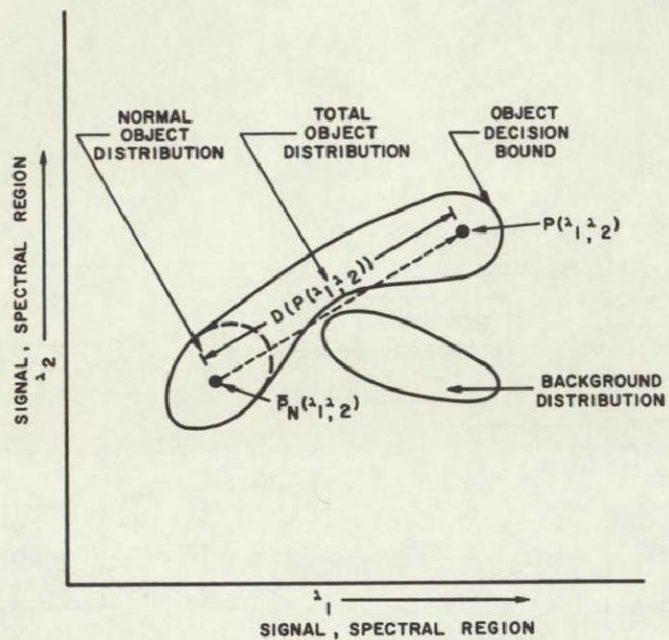


Figure 5. Two dimensional illustration of multi-spectral parameter computation.

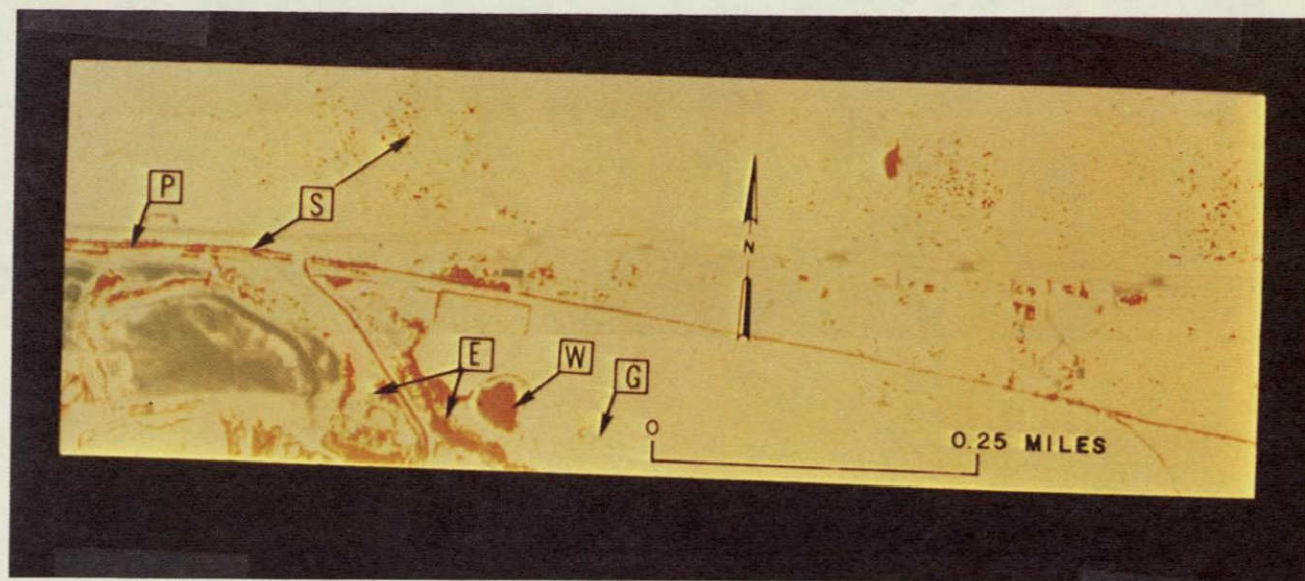


Figure 6. Map distribution of parameters for recognition of fluoride contamination. G = grass, P = palmetto, S = shrub; exposed to fluoride contamination: W = water contaminated with fluoride; E = evaporite, areas of fluoride seepage from gypsum settling lagoons.



Figure 7. Color coded ultraviolet map of phosphate mining and processing area. Red = high reflectance, high concentrations of fluoride and phosphate salts; yellow, green, and blue = moderate to low to very low reflectance respectively.

C.6.

SECTION 80

RELAY OF QUANTITATIVE RESOURCES

DATA BY ERTS-A

by

James F. Daniel
U.S. Geological Survey
St. Louis, Missouri

ABSTRACT

Experiments involving relay of quantitative ground data are typified by work planned in the Delaware River basin. In cooperation with the Delaware River Basin Commission, transmitters will be installed on river-level, ground-water level, and water-quality monitors to test feasibility of using a variety of real-time data in basin management.

Actual use of real-time data relay in problems related to ground water depends upon spatial and temporal requirements and is probably restricted to low-flow forecasting and to monitoring pollution of alluvial aquifers from stream sources. RBV and MSS imagery will be used in conjunction with the relayed monitor data from ground stations to provide spatial resolution. Sequential imagery will provide the spatial data needed to assess change. The potential for use in broader scale hydrologic problems is controlled by the economics of satellite vs land-oriented acquisition methods.

N72-29375

81-1

SECTION 81

APPLICATIONS OF SPECTROSCOPY TO REMOTE

DETERMINATION OF WATER QUALITY

by

Marvin C. Goldberg
U.S. Geological Survey
Water Resources Division
Denver, Colorado

and

Eugene R. Weiner
University of Denver
Department of Chemistry
Denver, Colorado

INTRODUCTION

The measurement of water quality entails definition of a state or condition of a body of water for a particular use. At present and in the foreseeable future there is a great demand for techniques that rapidly monitor the water quality of large areas. This need specifies the employment of a remote sensor.

Spectroscopy, means the taking of spectra, which are the recorded measurements of electromagnetic radiation, separated or arranged in the order of some variable characteristic such as wavelength, mass or energy. The most common form of spectroscopic application to remote sensing has been aerial reconnaissance using multispectral band photography and radar.

The use of remote sensing to determine water quality in large bodies of water, such as oceans, lakes, and rivers, makes use of the properties of emission, absorption, reflectance and scattering of electromagnetic radiation by the water and adjacent terrain. Emitted energy in the infra-red region, 4 to 14 microns, is useful for temperature mapping. Measurements of absorbed, reflected and scattered energy, use either the sun or some airborne generator as the source of incident radiation.

Water quality measurements should determine the physical (temperature, density, color, viscosity, shape, etc.), chemical (dissolved elements and compounds, acidity etc.) and biological properties (bacteria, algae, fish, dissolved oxygen, etc.). The most difficult parameters to sense remotely appear to be the chemical properties.

MULTI SPECTRAL IMAGERY

Multi spectral imagery has been taken and analyzed in two fashions,

1. An array of several cameras can be used to take simultaneous pictures of the same area. Each camera is made sensitive to a different band of spectral radiation by an appropriate combination of film and filter. Several investigators [Mallila, William; Photogram. (4) Eng. 34, 556, June 1968; Colwell, R.N., 4th Univ. of Michigan Symposium on Remote Sensing of the Environment, April 12-14, 1966] have described the applications of such systems. Since different materials have individual patterns of spectral absorption and reflection, they will have a characteristic film density in each of the spectral bands recorded. This is a "fingerprinting" technique, very similar to ordinary very-low resolution spectroscopy. One of the significant drawbacks of this method is the tedious analysis required (4). The wave-band-density pattern of each item of interest on the photos must be compared with the standards for that class of item. Although the information content of the images increases with more wave-band ranges, the difficulty of analysis increases also. The (information)/(analysis effort) ratio seems to be a maximum somewhere between 4 and 9 bands, depending on specific needs, at our present stage of technology. Computer analysis seems necessary if the number of bands exceeds 4. As many as 20 different bands have been used in a single instrument, extending from the ultra-violet to the near infra-red.

A method of constructing a single image from all of the different band-restricted images, using a color box which allows the color and intensity of each band range to be varied independently, speeds the overall evaluation of the photos (2). However, this essentially destroys the spectrographic information (intensity of detected radiation as a function of wave length), at least as the method is currently employed.

Since any two-dimensional density pattern can be converted to a one-dimensional sequence of densities by means of a scanning device, it should be possible to digitize the information on multi-spectral photos and analyze them by computer. It appears that such systems are being developed along the lines of the scanning photodensitometer described in the next section. A scanning multi-channel radiometer has been described (3) for geologic uses which might be useful for water quality measurements also. A wider frequency range and narrower bands are possible with this instrument and the data are obtained directly in linear digital form.

Multi-spectral imagery has proven to be quite sensitive in distinguishing certain types of vegetation and camouflage, but will detect only gross variations in water compositions and the observable contaminants are quite limited.

2. Amplification of density and color variations. The information collected by any photographic method ultimately is stored as density and color variations on film. It has been demonstrated that present black and white films can resolve density differences much smaller than detectable by eye. Color films are even more sensitive to tone. In ordinary spectroscopy, where the information is presented in one dimension, it is common practice to measure line densities electronically with a photodensitometer which scans the record along a very narrow line and displays the amplified density variations on a strip chart or digital print-out.

This approach could be used on a film image, which presents its information in 2 dimensions, by using a scanning raster, as in a television tube. To obtain a spectral fingerprint of objects in the image, a separate scan is necessary for each of the spectral bands recorded and then, corresponding sections of the scans must be compared. If the scans are spatially synchronized, they could be analyzed automatically by a computer which identifies the possible sources of the reflection "fingerprints" continuously along the records.

This approach has not been used extensively as yet, perhaps because of its complexity. The problem of a common calibration for each of the separate filter-film pairs used might be the most formidable obstacle to developing this method into a routine technique. It would seem, however, that nearly every image would contain several easily identifiable objects, such as concrete roads, certain types of foilage, tar roofs, etc. which could serve as standards in calibrating the different band-limited images.

A more qualitative but very sensitive and useful approach has been developed (5). Photographic techniques are used to isolate, on a single film, the portions of the image lying within a narrow density range. Superposition of a complete set of these density "slices" reconstructs the original image. By assigning arbitrary colors to each density slice, the image can be reconstructed so that extremely small differences in density are printed in contrasting colors. This makes the informational detail inherent in the image much more easily detected. This approach, however, does not use the spectrographic information potentially available in multi-spectral imagery.

MOLECULAR SPECTROSCOPY

It appears that the most promising methods for remote sensing of water quality must be adaptations of molecular spectroscopy.

Reflectance spectroscopy would seem well suited for this purpose but has not yet been made very sensitive. To detect most materials in water solution by attenuated total reflectance spectroscopy in the laboratory, they must be present in minimum concentrations of around one percent. Ordinary reflectance spectroscopy is generally even less sensitive and also involves angle-dependent reflectance effects.

Scherz and co-workers (6) have recently made laboratory spectral reflectance measurements to help evaluate the usefulness of different aerial photography film-filter combinations for distinguishing between various gases and compounds in water solution. The incident light was from a tungsten-quartz lamp which simulated the sun and the reflected energy was measured with a Beckman DU-2 spectrophotometer over the range 0.2 to 1.2 microns. They could detect no reflectivity differences between distilled water and water samples containing dissolved O_2 , N_2 , $NaCl$, Na_2SO_4 and $Na_3PO_4 \cdot H_2O$. The concentrations of the solutes were not given. Water from different lakes in the Madison, Wisconsin area showed reflectivity differences, but after the algae and other suspended matter were filtered out, the different lake water samples appeared identical. Certain samples of paper mill waste showed high reflectance in the infra-red and were found to be easily detected in infra-red aerial photos, but only in the immediate region of discharge into the stream. Although Scherz did not give the concentrations he used, his report does not make standard sunlight-reflectance spectroscopy look encouraging for sensitive contamination measurements.

Because the solute concentrations involved in water quality measurements are low (1-100 mg/l, usually) sensitivity of detection becomes a prime factor. Also if the instrument is to be a truly remote sensor, absorption spectroscopy is ruled out because a detector or mirror must be on the other side of the sample, away from the light source. Reflectance spectroscopy, using sunlight as the source, is insensitive and lacks control due to the variable intensity of the light source.

LASER RAMAN SPECTROSCOPY

Raman spectroscopy is uniquely suited to remote sensing. A suitable instrument configuration is shown in Figure 1. The light source and detector are both on the same side of the sample being measured, making the instrument single-ended. Since the Raman wavelength shifts arise from vibrational and rotational transitions, the Raman method has the same ability to identify specific molecules as

does infrared spectroscopy. The strongest Raman lines are due to symmetric vibrations and are both sharp and polarized (Sloane, 1971). This is helpful in separating them from noise, background and other interference. The intensity of a Raman line is proportional to the number of scattering molecules over a wide range of concentrations and is not affected by the presence of large concentrations of other molecules. If the laser is pulsed, the distance to the sample can be measured and it might be possible to selectively sample the water at specific depths. References to the theory and practice of Raman spectroscopy include Herzberg (1945), Szymanski (1967), and Gilson and Hendra (1970).

A minimum useful range of a few hundred feet would be necessary if the sensor were operated from an airplane or helicopter. A shorter range could be tolerated for certain fixed station uses, such as from a bridge. Remote Raman sensors of this type have been used for the detection of atmospheric gases. (Cooney, 1968; Cooney, 1969; Derr and Little, 1970; Inaba and Kobayashi, 1969; Kobayashi and Inaba, 1970; Leonard, 1967). The nitrogen, oxygen and water vapor balance can be determined to heights of several kilometers from the Raman back-scatter. Air pollutants, such as SO_2 , present at partial pressures of 15-20 torr can also be identified and the technique looks promising for air pollution measurements.

In trying to evaluate this technique for water quality measurements, we are concerned with the following:

1. How much Raman energy is available from the molecules of interest?
2. What interference may be expected from the water background?
3. Will the final signal-to-noise ratio allow reasonable measurement times?
4. Can the individual components of solute mixtures be quantitatively analyzed?

Using a laser light source, there is probably enough available Raman energy. In equation 1, the intensity of the Raman scattered energy is expressed in terms of a molar scattering cross-section σ .

The intensity of vibrational Raman Stokes lines is given by the equation $I_R = I_o M \sigma$ [1]

where,

$$\sigma = f \quad \alpha, \nu_R^4, \quad \frac{\nu_e^2 + \nu_o^2}{(\nu_e^2 - \nu_o^2)^4}$$

ν_R = $(\nu_0 - \nu_{vib})$
 I = intensity of incident radiation,
 M^0 = molar concentration of scattering species,
 σ = molar Raman scattering cross-section,
 ν_R = frequency of Raman line,
 ν_0 = frequency of incident radiation,
 ν_{vib} = frequency of vibrational mode being excited,
 ν_e = frequency of an electronic absorption of the scattering species, and
 α = molecular polarizability.

This equation indicates that as ν_0 increases, with $\nu_0 \ll \nu_e$, then σ increases as ν_0^4 . Resonance effects can greatly enhance σ as ν_0 approaches ν_e .

If $\nu_0 \ll \nu_e$ and is in the visible region, then

$$\sigma \approx 10^{-30} \text{ cm}^2 \text{ sr}^{-1} \text{ molecule}^{-1}.$$

This cross-section includes the dependency on the incident light frequency and the relevant molecular parameters such as polarizability.

Because the cross-section varies as the fourth power of ν_0 , it is advantageous to use as high a frequency as possible. Detection sensitivity also increases at higher frequencies because of photomultiplier characteristics. A resonance effect is observed if a value for ν_0 is chosen which lies close to an electronic absorption band of the scattering molecule. Under these conditions, the term $(\nu_e^2 + \nu_0^2) / (\nu_e^2 - \nu_0^2)^4$ becomes very large and σ can increase as much as 10^6 or 10^7 times.

The choice of ν_0 for water quality measurements is probably limited to the most light-transparent region of water, which is the 4800-5200Å region. This is certainly true if it is necessary to range the equipment and analyze at specific depths. Since most of the solutes of interest have electronic absorptions in the ultraviolet, the resonance Raman effect will not be of immediate value for routine work. It may be employed for special cases.

Specifying $\sigma \approx 10^{-30} \text{ cm}^2 \text{ sr}^{-1} \text{ molecule}^{-1}$, a calculation was made of the performance of a practical remote Raman system, consisting of a commercially available laser, photon counting electronics and a 92 cm diameter telescope coupled to a double monochromator. The system specified will generate a signal of around 100 counts per second at a range of a few hundred feet for a 1 mg/l concentration of phosphate anion.

The ability to detect this signal, however, depends on the noise and interference level. Unfortunately, the Raman scattering from water contributes a significant background over most of the spectral region of interest. Figure 2 shows the Raman spectrum of pure water along

with the vibrational assignments given by Walrafen (1962). The strong interactions among water molecules results in a broad and diffuse spectrum. The large band around 3400 cm^{-1} makes this region useless for measuring solute concentrations. Fortunately, the species of most interest have their strongest lines in the region of weaker water scattering. The absolute value of the Raman signal from a solute is less important than the relative signal intensities from the solute and from water. Figure 3 shows the strong 1050 cm^{-1} line of NO_3^- from a 1.1 M solution of NaNO_3 in water measured on a laboratory analytical laser Raman spectrometer. Figure 4 shows the same 1050 cm^{-1} line of NO_3^- from a measurement on a 50 mg/l solution of NO_3^- in water. The nitrate line was scanned at 0.05 cm^{-1} per sec. The background is due to Raman scattering from water which limits the detection sensitivity rather than the sensitivity limit being set by the instrument noise level. To detect lower concentrations, it will be necessary to increase the nitrate-signal to water-signal ratio, and this will require a longer measuring time. Insofar as the instrumental noise level can be reduced, smaller nitrate-to-water ratios can be resolved in shorter time and it will be important to use lasers and detectors with as low a noise level as possible.

The ability to scan back and forth between the nitrate and adjacent water signals would be a very useful feature. For the purpose of separating solute signal from solvent signal, it is unfortunate that Raman spectroscopy is basically a single-beam technique (Sloane, 1971).

Special photomultipliers, called "image dissectors", scan their window surface at high frequencies, observing only a small region at a time and these might prove useful in approximating a double-beam method. Another technique for rapid scanning over a small spectral region uses a refractor plate behind the entrance slit repetitively turned through a small angle by a piezo crystal. The fact that the strong Raman lines are narrow while the water signal is very broad makes these methods appear feasible. Solute lines can be as narrow as 0.2 cm^{-1} , being limited mainly by the width of the exciting laser line (Sloane, 1971). Linewidths of 2 cm^{-1} to 5 cm^{-1} , however, are more common. The narrowness of the solute lines not only makes a short range repetitive scan practical, it makes identification of the components of a mixture much easier.

The strongest Raman lines are also strongly polarized, while the water background is not. This fact should be useful in increasing the solute signal to water signal ratio. A rotating polarizer might perform the same function as a rapid scan technique at low solute concentrations.

Conclusions

The best method of water quality measurement via spectroscopic means seems to be molecular spectroscopy. Within this domain, Laser-Raman is the best suited by present state of the art information. To use Laser-Raman Spectroscopy as a remote sensor the solute-signal to water-signal must be enhanced. There are several techniques to achieve a larger solute signal-to-background ratio; the ones of choice are signal averaging and pseudo double beam compensation through use of a beam chopping technique accomplished with a piezo crystal. If the background can be lowered 3 orders of magnitude below the level shown in Figure 3, which seems likely, then sufficient sensitivity is available to make water quality measurements.

Bibliography

1. Strandberg, C. M. et. al, 1967, Photogrammetric Engineering 33.
2. Yost E. and Wenderoth S., 1967, Photogrammetric Engineering, 33 p. 1020.
3. Mallila, W., 1968, loc. cit., 34, 566.
4. Colwell, R. N., 1966, 4th Univ. of Mich. Symposium on Remote Sensing of the environment.
5. Ross, D. S., 1969, Image Tone Enhancement, 1969, Annual Meeting of the American Congress of Surveying and Mapping, Washington, D.C.
6. Scherz, J. P., Graff, D. R. and Boyle, W. C., 1969, Photogrammetric Engineering, 35, 38.
7. Cooney, J., 1968, Measurements on the Raman component of laser atmospheric backscatter: App. Phys. Lett., v. 12, p. 40-42.
8. Cooney, J., Orr, J. and Tomasetti, C., 1969, Measurements separating the gaseous and aerosol components of laser atmospheric backscatter: Nature, v. 224, p. 1098-1099.
9. Derr, V. and Little, C. G., 1970, A comparison of remote sensing of the clear atmosphere by optical, radio and acoustic radar techniques: App. Optics, v. 9, p. 1976-1992.
10. Gilson T. and Hendra P., 1970, Laser Raman Spectroscopy: Wiley-Interscience, Ltd., New York.
11. Herzberg G., 1945, Infra-red and Raman spectra: Van Nostrand Co. Inc., Princeton, New Jersey.
12. Inaba H. and Kobayashi T., 1969, Laser-Raman radar for chemical analysis of pollution air: Nature, v. 224, p. 170-172.
13. Kobayashi, Takao and Inaba, Humio, 1970, Laser-Raman radar for air pollution probe: Proc. of the IEEE, v. 58, p. 1568-1571.
14. Leonard, Donald A., 1967, Observation of Raman scattering from the atmosphere using a pulsed nitrogen ultraviolet laser: Nature, v. 216, p. 142-143.

15. Sloane, Howard J., 1971, The technique of Raman Spectroscopy, v. 25, p. 430-439.
16. Szymanski H., ed., 1967, Raman Spectroscopy, theory and practice: Plenum Press, New York.
17. Walrafen G. E., 1962, Raman spectral studies of the effects of electrolytes on water: Jour. Chem. Phys., v. 36, p. 1035-1042.

COMPONENTS OF A REMOTE LASER-RAMAN SENSOR

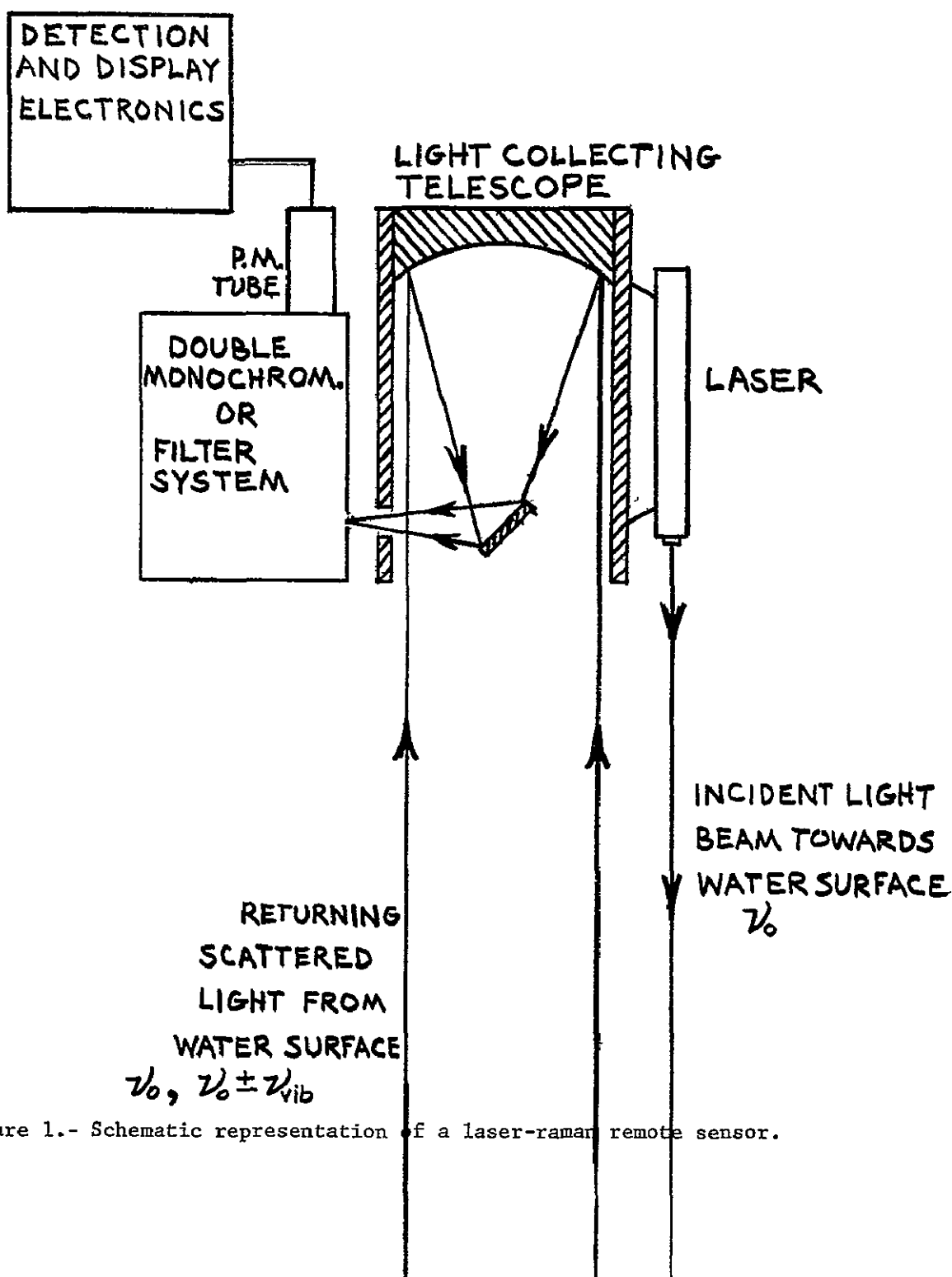


Figure 1.- Schematic representation of a laser-Raman remote sensor.

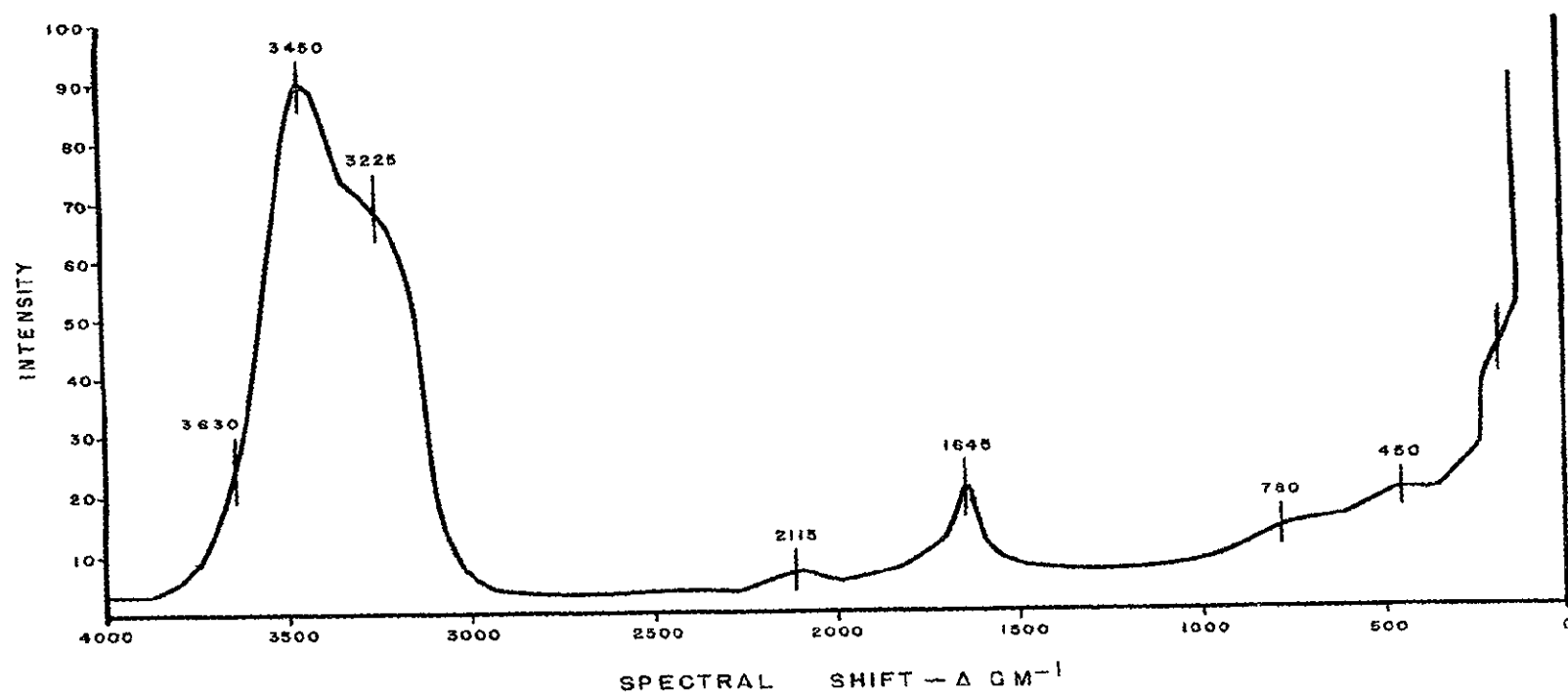


Figure 2.- Raman spectrum of water at 40°C centigrade. The vertical bars show the band centers.

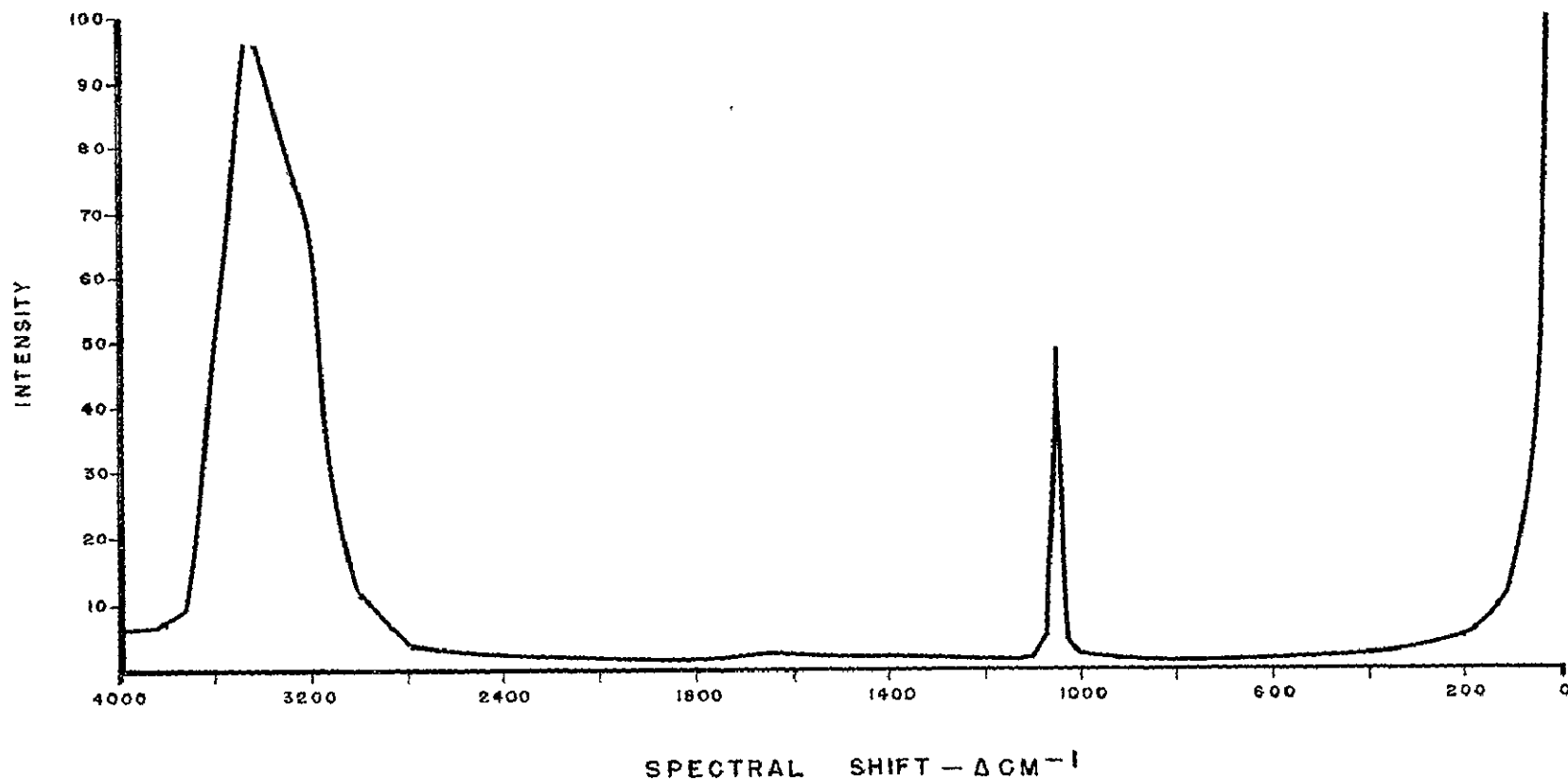


Figure 3.- Raman spectrum of nitrate in water at a one percent sodium nitrate concentration. The nitrate peaks occur at 720, 1050 and 1390 wave numbers (CM^{-1}). Note the intense peak at 1050 cm^{-1} .

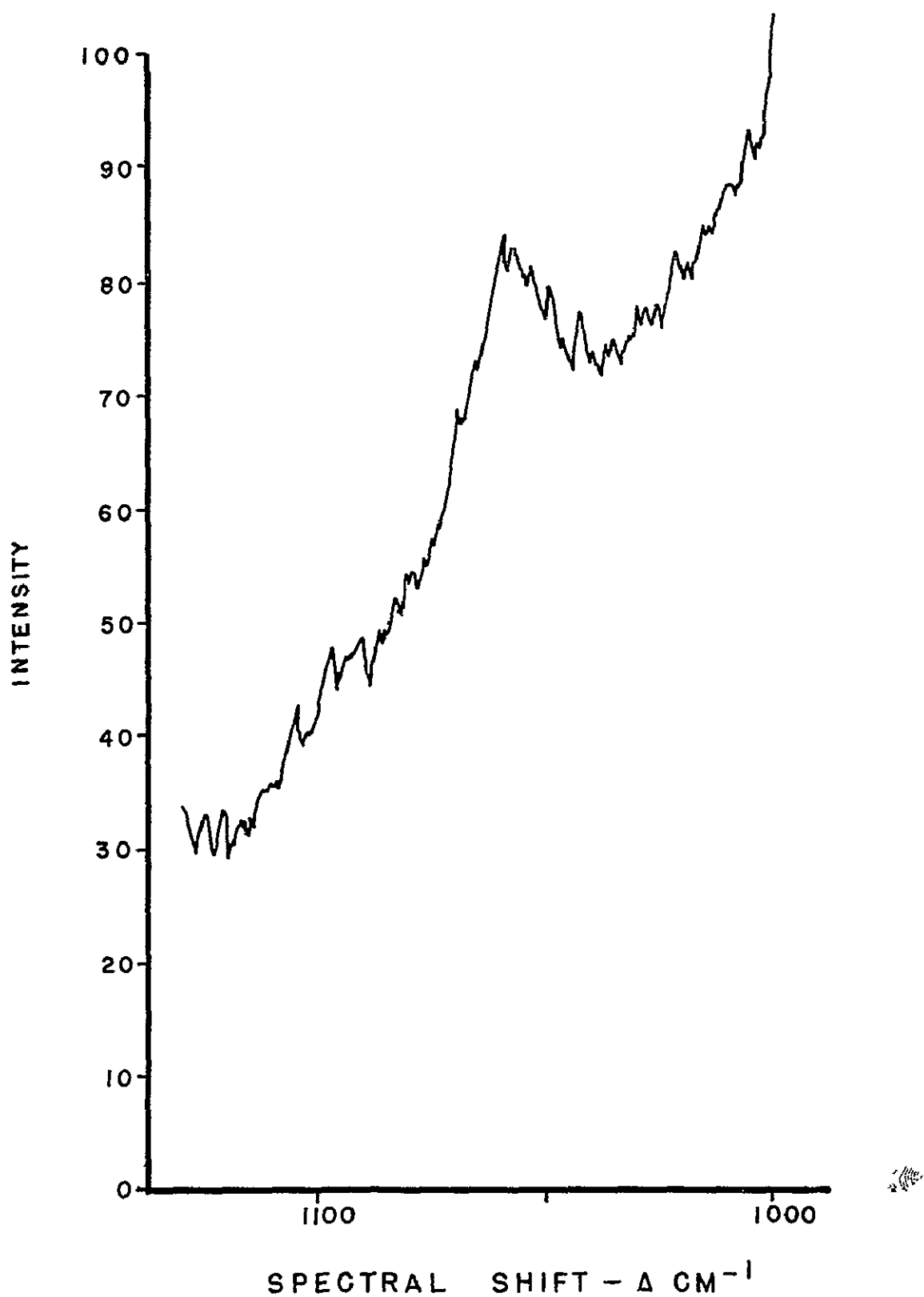


Figure 4.- Raman spectrum of nitrate in a water solution.
The concentration is 50 mg/l.

N 72-29376

SECTION 82

SPECTRAL REFLECTANCE OF SELECTED AQUEOUS SOLUTIONS
FOR WATER QUALITY APPLICATIONS*

M.R. Querry, R.C. Waring, W.E. Holland, W. Nijm, G.M. Hale
Department of Physics
University of Missouri - Kansas City

ABSTRACT

The relative, specular reflectances of individual aqueous solutions having salt content of 1M, 3M, and 5M NaCl, 0.5M NaNO₃, 0.5M NH₄H₂PO₄, and 0.5M K₂SO₄ were measured in the 2 μ m to 20 μ m region of the infrared for the component of radiant flux with the electric vector linearly polarized perpendicular to the plane of incidence. Distilled water was the reflectance standard. The angle of incidence was $70.03^\circ \pm 0.23^\circ$. Absolute reflectances of the solutions for the same polarization and angle of incidence were computed by use of the measured relative reflectances, one of the Fresnel equations, and the optical constants of distilled water. Phase-shift and phase-difference spectra were obtained by respectively applying a Kramers-Kronig dispersion analysis to the absolute and relative reflectance spectra. The optical constants of the solutions were determined by algorithms commonly associated with the Kramers-Kronig analysis. Spectral signatures that qualitatively and quantitatively characterize the solute and that show structure of the infrared bands of water were noted in the phase-difference spectra. The relative and absolute reflectances, the phase-shift and phase-difference spectra and the optical constants are presented in graphical form. Application of these results to remote sensing of the chemical quality of natural waters are discussed briefly.

* Supported in part by the U.S. Department of Interior, Geological Survey through Contract 14-08-0001-12636 with the University of Missouri.

Measurements in the 2-12 μ m region supported in part by the Missouri Water Resources Research Center (OWRR).

INTRODUCTION

The N.A.S.A. 24-channel multispectral scanner and data system, the E.R.T.S. multispectral scanner, and multispectral scanner for the skylab are optical instruments proposed for future remote sensing applications. Such instruments will be mounted in aircraft or satellites and typically will sense radiant flux as reflected or emitted from an area of the earth's surface. Future analysis of data from these instruments for purposes of qualitatively and quantitatively identifying the chemical constituents of natural waters ultimately must be based on a knowledge of the characteristic reflectance and emittance spectra of laboratory aqueous solutions and of natural water samples. To our knowledge, however, there are no published reports of careful, extensive investigations of the reflectance of aqueous solutions. This paper is a review of our recent measurements of the relative, specular, reflectance and subsequent computations of the optical constants in the 2-20 μm wavelength region of the infrared for aqueous solutions of NaCl , K_2SO_4 , and $\text{NH}_4\text{H}_2\text{PO}_4$ prepared in the laboratory. These investigations of the basic optical properties of aqueous solutions for remote sensing applications were contracted by Mr. Morris Deutsch, Hydrology Coordinator, E.R.O.S. Program, Geological Survey, U.S. Department of the Interior.

The measurements of relative reflectance recently have been extended to the near infrared and visible regions of the spectrum and to natural water samples. Analyses of data from these recent experiments are incomplete and results from those experiments are therefore reserved for a later report.

DESCRIPTION OF APPARATUS

A diagram of the reflectometer-spectrophotometer system is shown in Figure 1; the system was described in more detail in two previous publications.^{1,2} Radiant flux from a glower G was chopped at 13cps at C and was then collected and collimated by a Cassegrain unit consisting of spherical mirrors M1 and M2. A nearly collimated beam of radiant flux then passed horizontally to mirror M3, was directed to the sample at angle of incidence θ , was partially reflected to mirror M4, and then entered a Cassegrain condenser unit consisting of mirrors M5 and M6. From the condenser unit a convergent cone of radiant flux, with apex angle of about 75 mrad at the entrance slit of the monochromator, passed through a transmission polarizer consisting of twelve silver-chloride plates positioned at the Brewster's angle relative to the central ray of the convergent cone of radiant-flux. The polarizer passed about 0.1 percent of the undesired polarization component. The monochromator was a double-pass grating instrument of the Ebert design. The detector was a thermopile with a CsI window. And optical filter placed between the exit slit and the detector prevented over-

lapping diffraction orders and scattered radiant-flux from reaching the detector. The monochromator, chopper, detector assembly, amplifier, strip chart recorder, and scan control were components of a Perkin-Elmer E-system. A cathetometer with a protractor ocular was used to measure θ to ± 4 mrad ($\pm 0.23^\circ$) for the central ray of the slightly divergent pencil of radiant flux.

In the present work we measured the relative, specular reflectance R_{\perp} of the aqueous solutions for radiant flux plane polarized perpendicular to the plane of incidence. Distilled water was the reflectance standard. R_{\perp} was obtained by

$$R_{\perp} = \frac{R_{\perp s}}{R_{\perp w}} = \frac{N_s}{N_w}, \quad (1)$$

where s and w respectively denotes aqueous solution and distilled water, \perp denotes the polarization, and N denotes readings from the strip charts. Zero references were recorded periodically on the charts of N_w and N_s by scanning the monochromator while the radiant source was located several centimeters from the optic axis of the Cassegrain collimator. The spectral resolution $\lambda/\Delta\lambda$ was maintained at about 200; λ is the wavelength and $\Delta\lambda$ the spectral width of the exit slit of the monochromator. The salts were analytical grade. The temperature was about 27°C .

The relative reflectance spectra for aqueous solutions with 1M, 3M, and 5M NaCl, 0.5M K_2SO_4 , and 0.5 M $\text{NH}_4\text{H}_2\text{PO}_4$ are shown in the lower panels of Figures 2-4. The wavelength region was 2 μm to 20 μm : The angle θ was $70.03 \pm 0.23^\circ$. Each spectrum represents the average of three independent measurements of R_{\perp} . Averages R_{\perp} were determined at consecutive 0.05 μm intervals throughout the 2 μm to 20 μm region. The standard deviations for R_{\perp} were about $\pm 0.01R_{\perp}$ except in the central regions of the infrared bands for water vapor at 2.75 μm and 6 μm and the CO_2 band at 4.3 μm where the standard deviation was about $\pm 0.03R_{\perp}$. The absolute specular reflectances $R_{\perp s}$ of the aqueous solutions then were computed by use of equation (1) with measured values for R_{\perp} and with values for $R_{\perp w}$ computed from the optical constants for water^{3/} and one of the generalized Fresnel reflectance equations. Absolute reflectance spectra for the aqueous solutions are shown in the upper panels of Figures 2-4. Ignoring any uncertainty in the optical constants of water, the proportional standard deviations for the absolute reflectances are the same as those for the relative reflectance.

OPTICAL CONSTANTS

The optical constants n and k , which are the real and imaginary parts of the complex refractive index, were computed by use of an algorithm similar to the one developed by Roessler^{4/}:

$$n = \frac{(Q^2 - P^2 + \sin^2\theta) + [(Q^2 - P^2 + \sin^2\theta)^2 + 4Q^2P^2]^{\frac{1}{2}}}{2} \quad (2)$$

$$k = PQ/n \quad (3)$$

The parameters P and Q were given by

$$Q = \frac{(1 - R_{1s}) \cos\theta}{1 + R_{1s} - R_{1s}^{\frac{1}{2}} \cos\phi_{1s}} \quad (4)$$

$$P = \frac{2R_s \sin\phi_{1s} \cos\theta}{1 + R_{1s} - R_{1s}^{\frac{1}{2}} \cos\phi_{1s}} \quad (5)$$

where the Kramers-Kronig analysis was used to determine

$$\phi_{1s} = \text{Prin.} \left[\frac{\lambda_o}{\pi} \int_0^{\infty} \frac{\ln R(\lambda)_{1s}}{\lambda_o^2 - \lambda^2} d\lambda \right] \quad (6)$$

Integration of (6) was accomplished by numerical Simpson's rule techniques. For the integrations in the regions $\lambda > 20 \mu\text{m}$ and $\lambda < 2 \mu\text{m}$, we created nominal reflectance spectra for the aqueous solutions by use of the optical constants for distilled water^{3,5/}, one of the Fresnel equations, and the relative reflectance as measured at $\lambda = 20 \mu\text{m}$ and $\lambda = 2 \mu\text{m}$. A much more detailed description of the methods^{2/} used for these particular computations was presented in a previous paper.^{2/}

The optical constants for aqueous solutions of 1M, 3M, and 5M NaCl, 0.5M K_2SO_4 , and 0.5M $\text{NH}_4\text{H}_2\text{PO}_4$ are presented in Figures 5-7. The uncertainties for the index of refraction n and the extinction coefficient k were determined by considering the standard deviation for the absolute reflectances, which were $\pm 0.01R_{1s}$ to $\pm 0.03R_{1s}$, and for θ which was $\pm 0.23^\circ$. By randomly varying R_{1s} during numerical integrations of (6), and from observations of small-in-magnitude, nonphysical, negative values of ϕ_{1s} , which sometimes appeared in the KK analyses in wavelength regions where k was very small, we estimated the standard deviation for ϕ_{1s} was $\pm 0.003\text{-rad}$. Based on subsequent careful numerical analyses of (2) - (5) in which R_{1s} , θ , and ϕ_{1s} were varied in accordance with their standard deviations, the uncertainties for n were estimated as $\pm 0.01n$ except at the central position of the water vapor and CO_2 infrared bands where $\pm 0.02n$ was a better estimate. Similarly, the uncertainties for k were $\pm 0.05k$ at both $2.90 \mu\text{m}$ ($\approx 3440\text{-cm}^{-1}$) and $6.10 \mu\text{m}$ ($\approx 1640\text{-cm}^{-1}$), $\pm 0.03k$ at $18.85 \mu\text{m}$ ($\approx 530\text{-cm}^{-1}$), $\pm 0.12k$ at $8.00 \mu\text{m}$ ($\approx 1250\text{-cm}^{-1}$), $\pm 0.7k$ in wavelength regions where $k \approx 0.01$, and in excess of $\pm k$ in regions where $k \leq 0.005$. The largest magnitude of a nonphysical negative k was 0.006 in the $2.1 \mu\text{m}$ region for the 1M NaCl

solution. When plotting k we did not allow this quantity to be less than zero.

DISCUSSION OF RESULTS

For brevity, the following discussion is limited to the analysis of the aqueous solutions with NaCl. Similar analyses can be made for the other solutes. First we present a critique of the observed effects of NaCl on the water substance. Second, we discuss future computer simulations that will be needed to test the feasibility of applying remote sensing techniques to monitoring the chemical quality of natural waters.

NaCl AQUEOUS SOLUTIONS

The central positions of some of the infrared bands of water changed when the NaCl content was changed. Water has infrared bands centered at 2.75 μm , 6.1 μm , and 14.6 μm . These bands respectively are attributed to the ν_1 , ν_3 , and $2\nu_2$; ν_2 ; and ν_L vibration and libration modes of the water molecule. The presence of the Na^+ and Cl^- monotomic ions had significant, measurable effects on the relative reflectance in the wavelength regions of these bands as shown in Figure 2A. The changes in the reflectance spectra, which became more obvious with increasing salt content, are attributable in part to spectral shifts of the central positions of the infrared bands of water. By taking the positions at which the extinction coefficient k was a maximum to indicate the band center, similar computations in wavenumber-space ($\nu = 1/\lambda$) showed the water band centered at 3380-cm^{-1} was shifted to 3390-cm^{-1} for both the 1M and 3M solutions and to 3410-cm^{-1} for the 5M solution. The 10-cm^{-1} shift, which we observed for the 3M solution, compares well with the approximately 7-cm^{-1} band shift observed by Williams and Millett for aqueous solutions of 2.5M NaCl content. The 6.1 μm band center did not shift. The position of the 14.6 μm band center was indeterminate by observing positions of maximum k because the shifts are large, the maximum k occurs at about $3/570\text{-cm}^{-1}$, and our data extended only to 500-cm^{-1} . However, wavenumber positions at which n was a minimum indicated the band shifted about -10-cm^{-1} per mole of NaCl; this compares favorably with the -4-cm^{-1} shift observed by Friedman ^{7/} for synthetic ocean water composed primarily of 0.51 mole of chloride salts per liter of water. Friedman has attributed differences between the optical constants of water and those for synthetic ocean water in the 9 μm to 15 μm region mostly to the solute shifting the libration band. We were unable to accurately predict these differences for the 1M, 3M, and 5M NaCl solutions by only applying spectral shifts to the optical constants of water.

Some of the well known structure of the infrared bands of water are revealed in the phase-shift spectra shown in Figure 8. For example, the

asymmetrical shape of the 2.75 μm band which is characteristic of the ν_1 , ν_3 , $2\nu_2$ modes. There is a slight asymmetry in the phase-shift spectra in the region of the ν_2 -band. The libration band is a prominent feature in the 10 μm to 20 μm region. The band shifts listed in the preceeding paragraph could also be determined by examining tabulated phase-shifts. A Kramers-Kronig analysis of the relative reflectance spectra phase-difference spectra ϕ that is very interesting, but which is not yet understood in terms of interactions of electromagnetic waves with ions and molecules of the aqueous solutions. The phase difference spectra is shown in Figure 8. Some insight, however, is provided by further examination of Equation (6) applied to the relative reflectance. Integrating by parts gives the phase-difference as

$$\phi_{\perp} = \phi_{\perp s} - \phi_{\perp w} = \frac{1}{2\pi} \int_0^{\infty} \frac{d}{d\lambda} [\ln R(\lambda)_{\perp}] \ln \left| \frac{\lambda_0 - \lambda}{\lambda_0 + \lambda} \right| d\lambda. \quad (7)$$

The phase-difference spectra therefore will have the most significant structure in wavelength regions where the solutes cause the magnitude of the derivative of the logarithm of the relative reflectance to be large. There are two or more components to the phase-difference spectra in the wavelength regions of both the 2.75 μm and 6.1 μm infrared bands of water. The shifts of the infrared bands for water form only a partial, superficial explanation for the shape of the phase-difference spectra.

QUANTITATIVE ANALYSIS

Changes in either reflectance or phase-shifts caused by varying the NaCl content of the solutions are of possible interest for remote sensing applications; provided the changes occur in spectral regions where the atmosphere is transparent to radiant flux. In search of a basis for such applications, we investigated the influence of NaCl content on the product

$$C_{ws} \int_{9 \mu\text{m}}^{\lambda_0} \phi(\lambda)_{\perp} d\lambda, \quad (8)$$

where C_{ws} is the ratio of the mass of water to the mass of NaCl in the aqueous solution, $\phi(\lambda)_{\perp}$ is the phase-difference at wavelength λ as shown in Figure 8, and λ_0 is the wavelength position at which $\phi(\lambda_0)_{\perp} = 0$; e.g. $\lambda_0 = 13.57 \mu\text{m}$ for the 5M solution. The integral of (8) was evaluated by manually planimentering the designated areas. The products (8) in units of $\mu\text{m-rad}$ for the 1M, 3M, and 5M solutions respectively were -1.52 ± 0.09 , -1.50 ± 0.06 , and -1.42 ± 0.05 . The product is not a constant. However for NaCl concentrations below 3M, it seems the mass of NaCl relative to

that of water C_{sw} is closely approximated by

$$C_{sw} = \frac{-2}{3} \int_{9 \mu m}^{\lambda_0} \phi(\lambda) d\lambda, \quad (9)$$

where the integral is to be evaluated in μm -rad.

REMOTE SENSING

The feasibility of applying multispectral scanners to monitoring the chemical quality of natural water's can soon be tested by computer simulations of remote sensing experiments. Actual field applications would be based on the outcome of the computer simulations. The signal $S(\delta\lambda)$ produced by a single channel of the scanner system could be represented by extending the equations of Kriegler et al.^{8/} or Crane^{9/} to include both polarization components of the radiant flux and also radiant flux emitted by the water surface. We have

$$\begin{aligned} s(\delta\lambda) = & m A \cos\theta \frac{d\Omega}{\pi} \int \sigma(\lambda) \tau(\lambda, \theta) \left\{ E(\lambda)_{\perp} [R(\lambda, \theta)_{\perp} k(\lambda)_{\perp} + \left(\frac{1+p}{1-p} \right) R(\lambda, \theta)_{\parallel} k(\lambda)_{\parallel}] \right. \\ & \left. + \frac{P(\lambda, T)}{2} [\epsilon(\lambda, \theta)_{\perp} k(\lambda)_{\perp} + \epsilon(\lambda, \theta)_{\parallel} k(\lambda)_{\parallel}] \right\} d\lambda \\ & + m a \int \sigma(\lambda) [E(\lambda, \theta)_{\perp}^s k(\lambda)_{\perp} + E(\lambda, \theta)_{\parallel}^s k(\lambda)_{\parallel}] d\lambda + \text{noise}. \end{aligned} \quad (10)$$

The symbols in Equation (10) are defined as follows: m is a constant characteristic of gain of the amplifier (or integrator) - data storage system, A is the area of the water surface viewed by the detector system, θ is the angle of incidence, $d\Omega$ is the solid angle subtended by the detector whose surface area is a , π is a normalization factor, $\sigma(\lambda)$ is the spectral sensitivity of the detector, $\tau(\lambda, \theta)$ is the spectral, atmospheric transmittance, $E(\lambda)$ is the irradiance of the water surface, \parallel and \perp denote plane polarization parallel and perpendicular to the plane of incidence respectively, $R(\lambda, \theta)$ is the specular reflectance for radiant flux of wavelength λ incident and reflected at angle θ , $k(\lambda)$ denotes reflectance and transmittance of optical filters or other components of the sensor system, p is the degree of polarization of radiant flux incident on the water surface. $P(\lambda, T)$ denotes the Planck equation for the spectral radiance of a blackbody of absolute temperature T , and $\epsilon(\lambda, \theta)$ is the monochromatic spectral emittance at angle θ for the water surface; in the infrared for water

$$\varepsilon(\lambda, \theta) = 1 - R(\lambda, \theta). \quad (11)$$

$E(\lambda, \theta)^S$ is the irradiance of the detector surface by radiant flux scattered into the sensor system. The integration is over the spectral width $\delta\lambda$ of the single channel. The optical constants n and k as reported in this paper now form a preliminary basis for computing the optical properties $R(\lambda, \theta)$ and $\varepsilon(\lambda, \theta)$ that are needed in Equation (10). As the N.A.S.A. multi-spectral scanner are further developed and tested, a knowledge of instrument parameters such as m , σ , k , and noise finally will emerge. At the same time our continued investigation of reflectance and the optical constants for laboratory aqueous solutions and for natural water samples will form a firm basis for the future computer simulations of remote sensing applications, and also hopefully will form a basis for ultimate successful field applications of remote sensing of water quality.

REFERENCES

1. "Specular Reflectance of Aqueous Solutions", M.R. Querry, R.C. Waring, W.E. Holland, and G.R. Mansell, Proceedings of the Seventh International Symposium on the Remote Sensing of Environment Vol. 2, pp 1053-1069, (University of Michigan, Ann Arbor 1971).
2. "Optical Constants in the Infrared for Aqueous Solutions of NaCl", M.R. Querry, R.C. Waring, W.E. Holland, G.M. Hale, W. Nijm, J. Opt. Soc. Am. 62, (1972) Accepted for publication.
3. "Optical Constants of Water in the Infrared", A.N. Rusk, D. Williams, and M.R. Querry, J. Opt. Soc. Am. 61, 895 (1971).
4. "Kramers-Kronig Analysis of non-normal incidence Reflection", D.M. Roessler, Brit. J. Appl. Phys. 16, 1359 (1965).
5. "Dispersion and Absorption of Water in the Infrared and Radio Regions of the Spectrum", J.M. Zolotarev, B.A. Mikhailov, L.I. Aperovich, and S.I. Popov, Opt. Spektrosk. 27, 790 (1969) [Opt. Spectrosc. 27, 430 (1969)].
6. "The Effects of Various Ions on the Infrared Absorption of Water", D. Williams and W. Millett, Phys. Rev. 66, 6 (1944).
7. "Infrared Characteristics of Ocean Water (1.5 - 15 μ m)", D. Friedman, Appl. Optics 8, 2073 (1969).
8. "Preprocessing Transformations and Their Effects on Multispectral Recognition", F.J. Kriegler, W.A. Malila, R.F. Nalepka, W. Richardson, Proceedings of the Sixth International Symposium on Remote Sensing of Environment Vol. 1, p. 97 (University of Michigan, Ann Arbor, Oct. 1969).
9. "Preprocessing Techniques to Reduce Atmospheric and Sensor Variability in Multispectral Scanner Data", R.B. Crane, Proceedings of the Seventh International Symposium on the Remote Sensing of Environment Vol. 2, p. 1345 (University of Michigan, Ann Arbor, 1971).

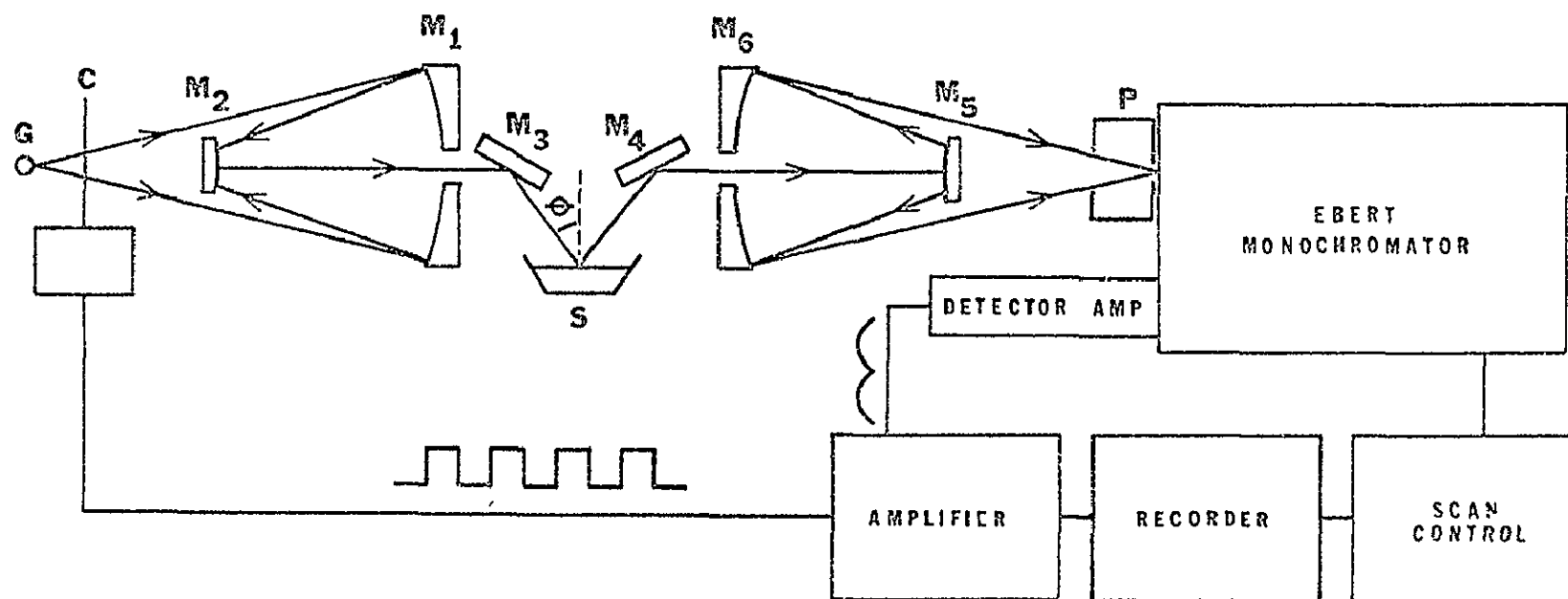


Figure 1.- Reflectometer-Spectrophotometer System, University of Missouri-Kansas City. The components are a source G, chopper C, Cassegrain Collimator unit M1 and M2, plane mirrors M3 and M4, sample S, Cassegrain Condenser unit M5 and M6, polarizer P, and Perkin-Elmer E-system spectrophotometer. The angle of incidence is shown as θ .

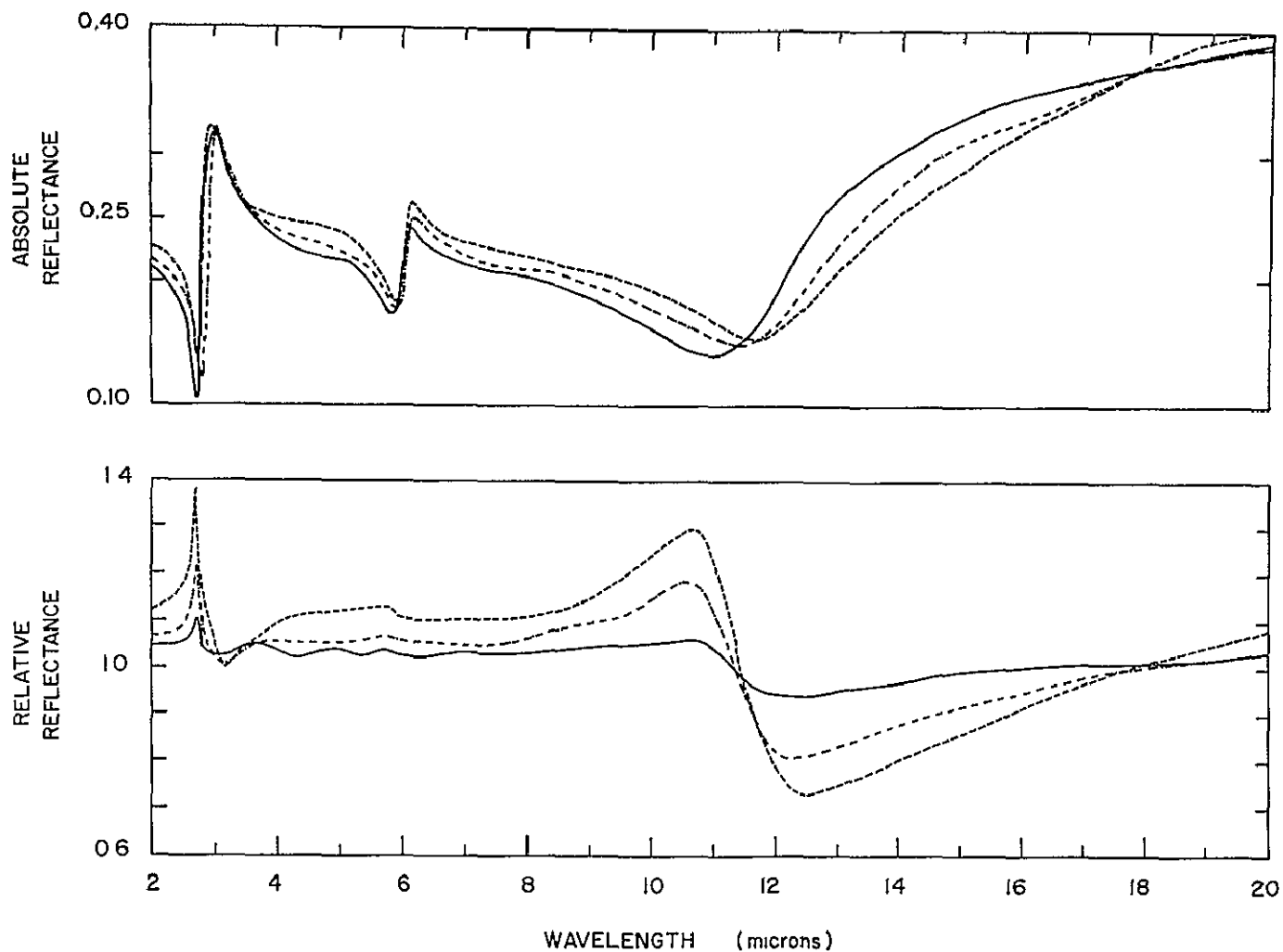


Figure 2.- Measured relative, specular reflectances (lower) and compute absolute reflectances (upper) in the 2 μ m to 20 μ m wavelength region for aqueous solutions of 1M —, 3M — . —, and 5M — — — NaCl content. The angle of incidence was $70.03^\circ \pm 0.23^\circ$. Distilled water was the reflectance standard; its relative reflectance is 1.0 at all wavelengths. The radiant flux was plane polarized perpendicular to the plane of incidence.

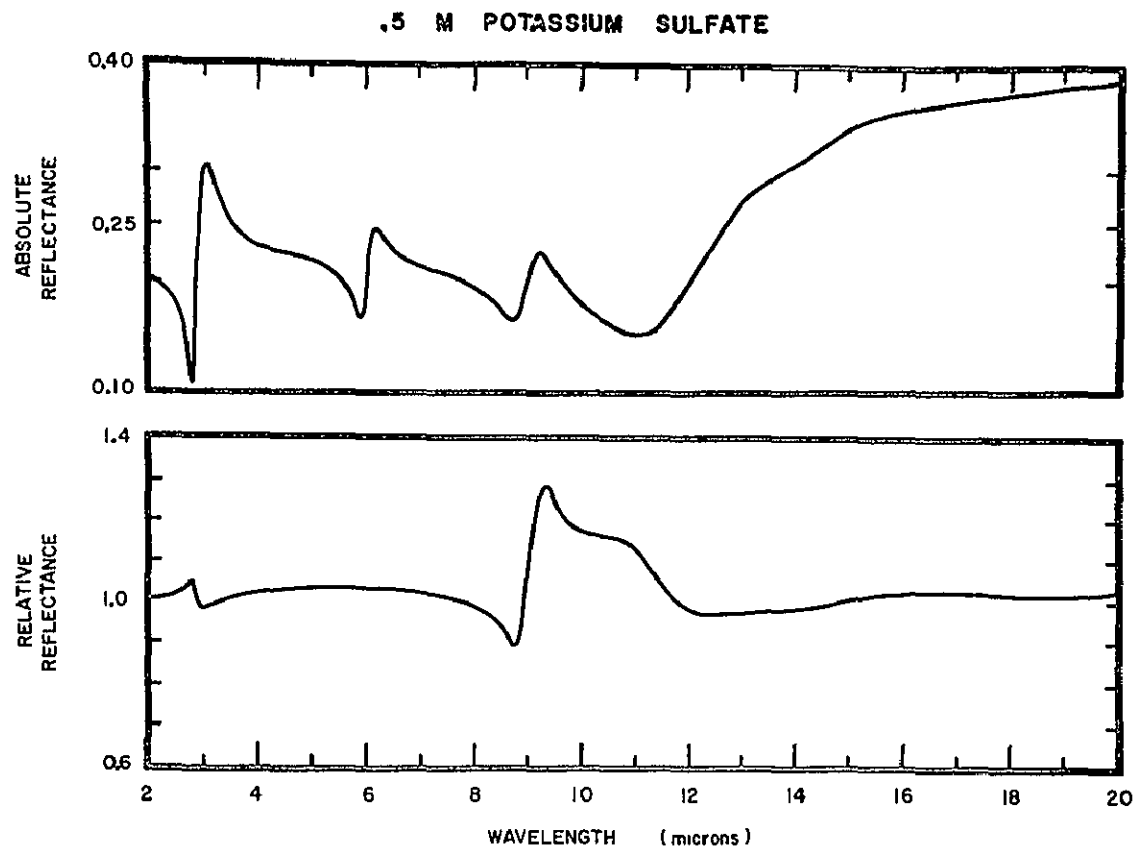


Figure 3.- Measured relative, specular reflectance (lower) and computed absolute reflectance (upper) in the 2 μ m to 20 μ m wavelength region for an aqueous solution of 0.5M K_2SO_4 . The angle of incidence was $70.03^\circ \pm 0.23^\circ$. Distilled water was the reflectance standard; its relative reflectance is 1.0 at all wavelengths. The radiant flux was plane polarized perpendicular to the plane of incidence.

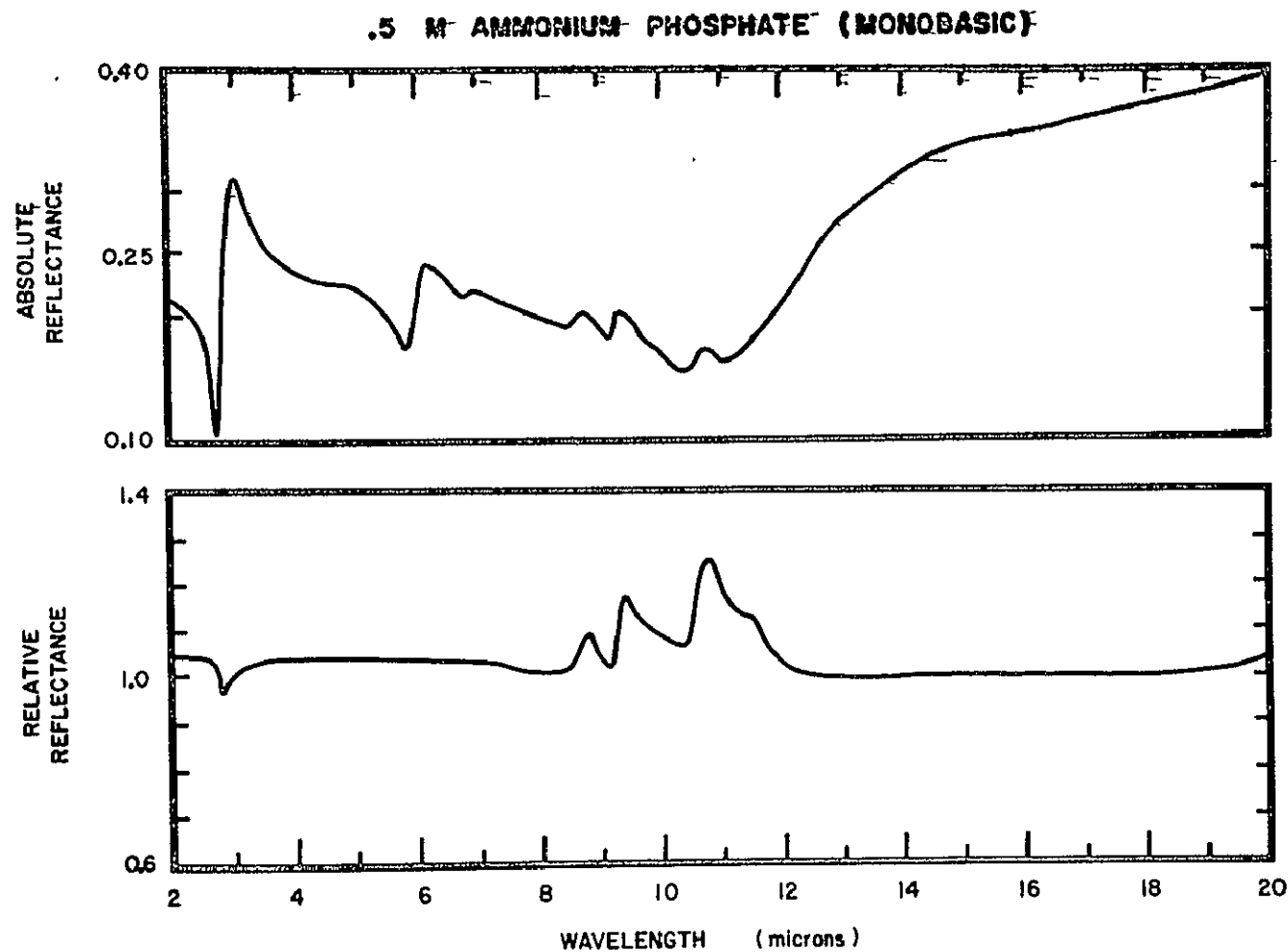


Figure 4.- Measured relative, specular reflectance (lower) and computed absolute reflectance (upper) in the 2 μ m to 20 μ m wavelength region for an aqueous solution of 0.5M $\text{NH}_4\text{H}_2\text{PO}_4$. The angle of incidence was $70.03^\circ \pm 0.23^\circ$. Distilled water was the reflectance standard; its relative reflectance is 1.0 at all wavelengths. The radiant flux was plane polarized perpendicular to the plane of incidence.

U.M.K.C. Optical Physics Laboratory

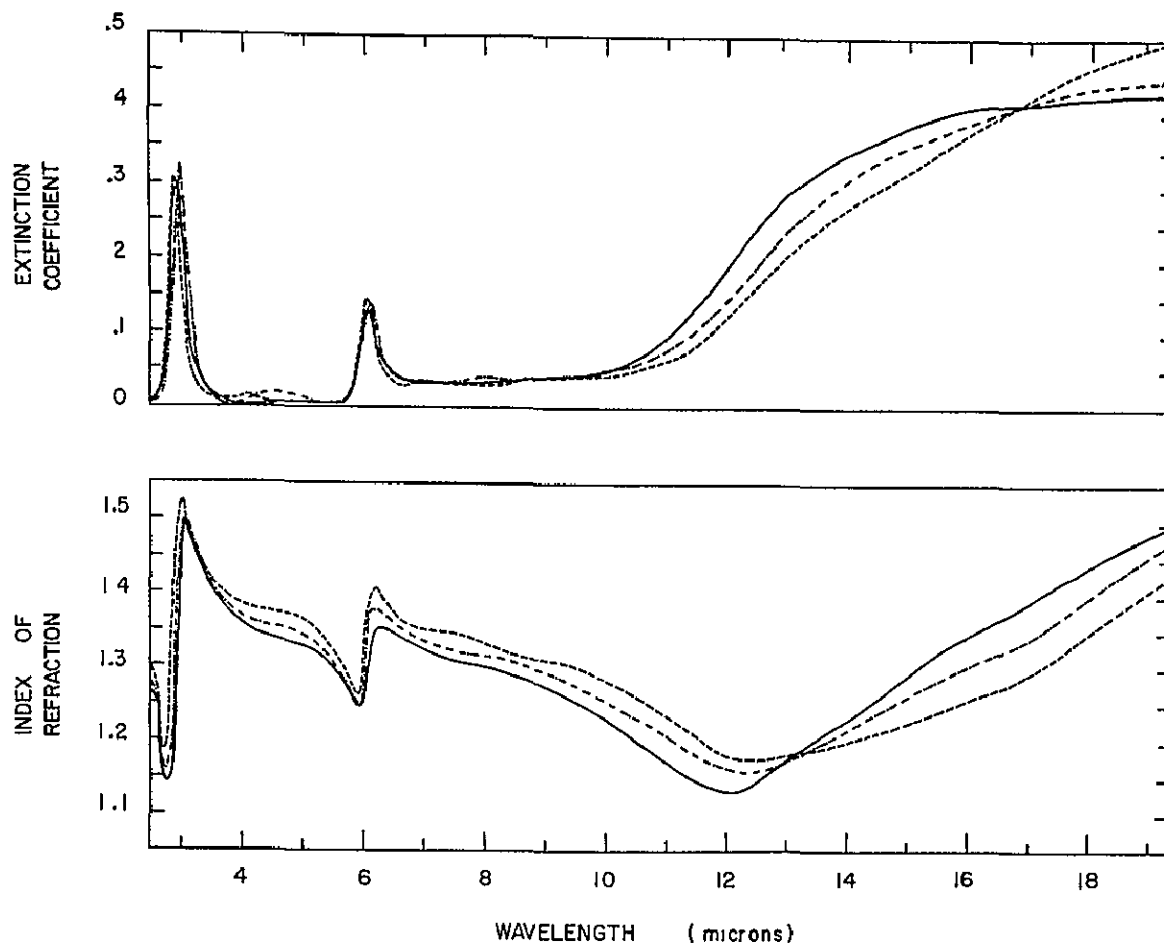


Figure 5.- The optical constants in the infrared for 1M —, 3M — —, and 5M — — — aqueous solutions of NaCl.

U.M.K.C. Optical Physics Laboratory

0.5 M POTASSIUM SULFATE

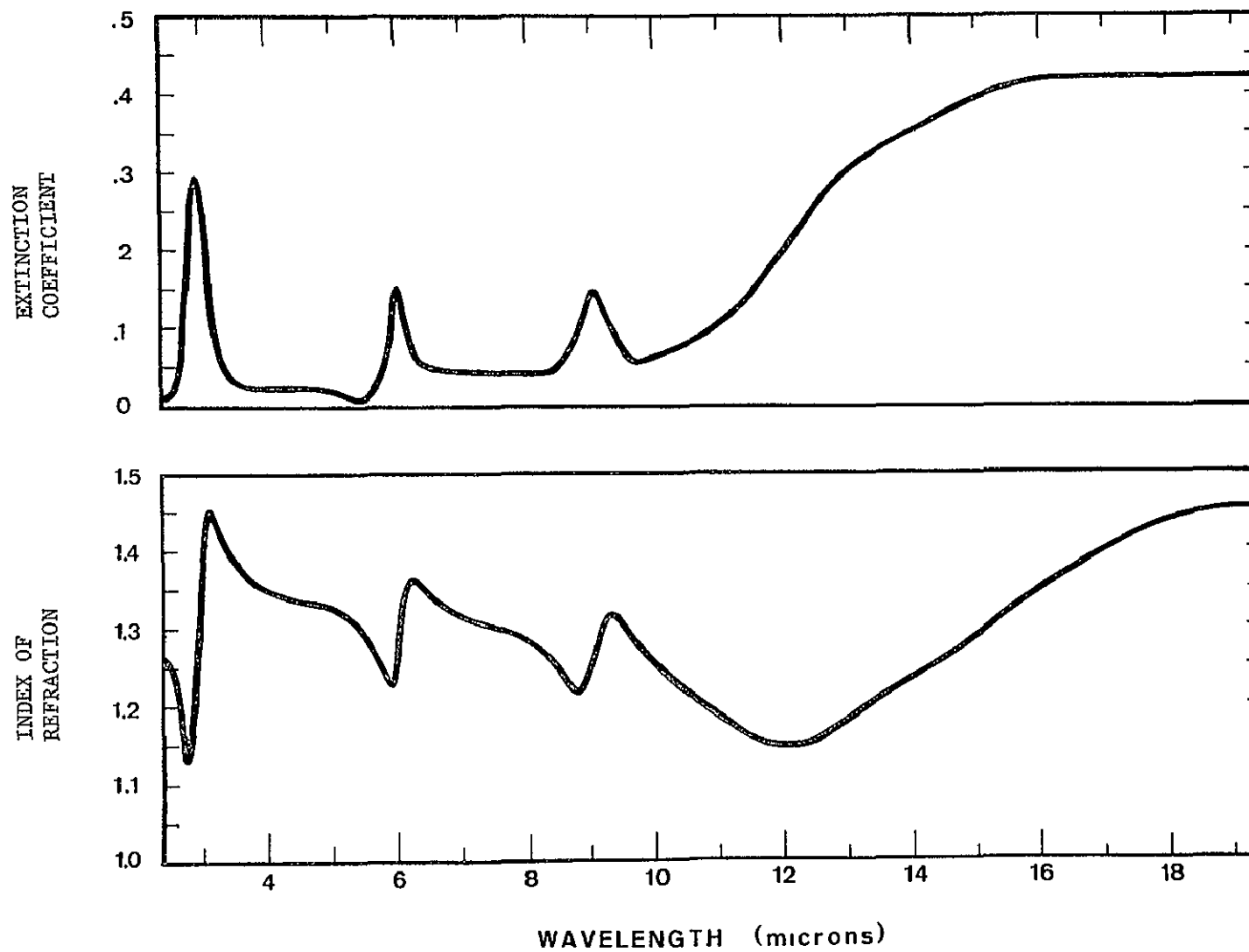


Figure 6.- The optical constants in the infrared for an aqueous solution of 0.5M K_2SO_4 .

U.M.K.C. Optical Physics Laboratory

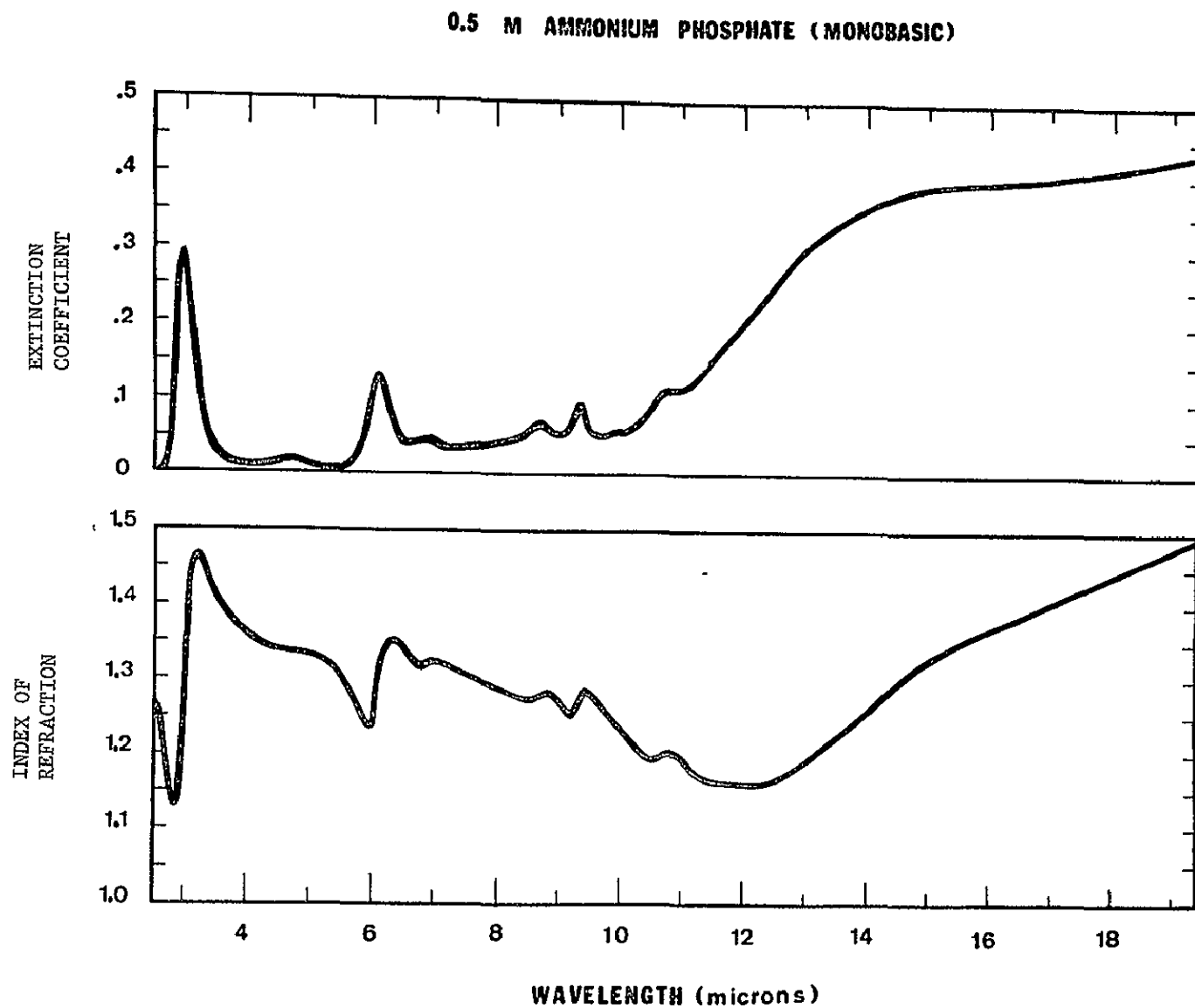


Figure 7.- The optical constants in the infrared for an aqueous solution of 0.5M $\text{NH}_4\text{H}_2\text{PO}_4$

U.M.K.C. Optical Physics Laboratory

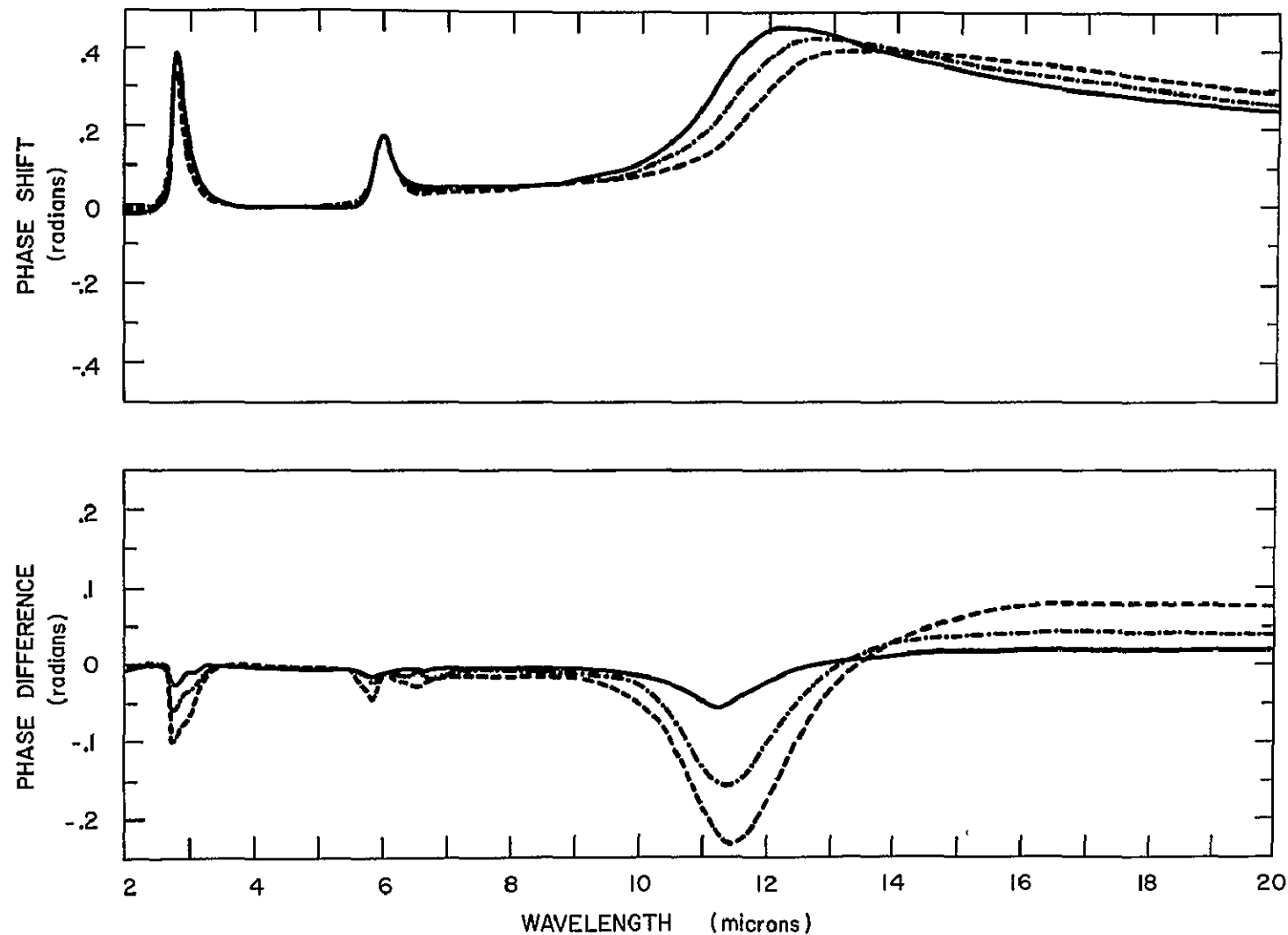


Figure 8.- Phase-difference (lower) and phase-shift (upper) spectra for aqueous solutions of 1M —, 3M — . —, and 5M — — — NaCl. These spectra result from applying the Kramers-Kronig analysis to the relative- and absolute-reflectance spectra respectively. The phase-shift is that for an electromagnetic wave reflected at the surface of the NaCl solutions. The phase-difference is the difference in phase-shifts for electromagnetic waves reflected at the surfaces of aqueous solutions and water. The angle of incidence was, 70.03°.

QUANTITATIVE RELATIONSHIP BETWEEN
REFLECTANCE AND TRANSPIRATION OF
PHREATOPHYTES--GILA RIVER TEST SITE^{1/}

By

R. C. Culler ^{2/}, J. E. Jones ^{3/}, and R. M. Turner ^{4/}

INTRODUCTION

The feasibility of using aerial photographs to estimate evapotranspiration (ET) from large parcels of the landscape has been studied by the U.S. Geological Survey at the Gila River Phreatophyte Project for several years. Repetitive color-IR (infrared) aerial photography has been used since 1967 as a means of estimating the volume of transpiring vegetation covering the project site. As plants are one of the main avenues through which water vapor is lost from a hydrologic system, a measure of plant volume should provide a means for estimating the transpiration component of ET.

Hydrologic variables such as rainfall, streamflow, ground-water levels, and soil-moisture storage have been measured at the project site since 1963. These measurements have been combined to calculate evapotranspiration as a residual in a water budget. Data from an energy-budget station was also used to compute ET from a small area of especially dense saltcedar. By subtracting an estimate of evaporative losses at the soil surface from total ET, a value for transpiration has been derived for comparison with the photogrammetric record.

The experimental design of the Gila River Phreatophyte Project prescribes removal of vegetation from the area after an initial calibration period. Mechanical vegetation removal, begun in 1968, was completed in 1971. The bare areas produced by the clearing have been reoccupied to varying degrees by perennial and ephemeral herbaceous plants. Color-IR aerial photographs have been employed to record both the vegetation changes resulting from the clearing program and the normal seasonal changes which occurred before clearing.

^{1/} Publication authorized by the Director, U.S. Geological Survey.

^{2/} Research Hydrologist, U.S. Geological Survey, Tucson, Ariz.

^{3/} Phys. Sci. Tech., U.S. Geological Survey, Tucson, Ariz.

^{4/} Research Botanist, U.S. Geological Survey, Tucson, Ariz.

The reports at previous Status Review Meetings have described the application of aerial photography to the measurement of vegetation coverage and volume (Culler and Turner, 1970; Turner, 1971). The present report will stress comparisons between adjusted densitometric measurements and estimates of ET and of transpiration,

METHOD

Color-IR photographs, using various film types, cameras, and filters, were obtained on 33 dates from 1967 through 1970. The photography and film processing was done by NASA and by the U.S. Geological Survey. All photographs were color transparencies. Most were taken from an elevation of 8,500 feet, and all were in 9-inch format.

The film images were analyzed by using a transmittance densitometer (Culler and Turner, 1970). Readings from the road surface of a concrete highway bridge located near the study site were used as a standard for scaling the densitometric data. From these standardized data, "adjusted red transmittance values" (Turner, 1971) were derived by dividing the red transmittance by the sum of the transmittance in the red, green, and blue spectral bands. All the transmittance values were derived from analytic densities as defined by Evans (1953, p. 437).

Large portions of the Gila River Site, which encompasses 2,400 hectares (6,000 acres), have been flooded at times, forcing abandonment of hydrologic data stations. For this reason, and because the probable error in some of the water-budget terms periodically exceeded acceptable limits, evapotranspiration data are available for only part of the period of study and for only certain portions of the study site.

The project area is subdivided into short segments or subreaches and separate ET estimates are made for each subreach. Vegetation clearing was performed at different times in the subreaches so that comparisons can be made between subreaches that differ mainly in the amount of vegetation they support. Data will be presented for subreach 4 (3.6 miles long) which was cleared during the winter of 1968-69 (clearing completed by April 1969) and subreach 7 (2.3 miles long) which was not cleared until recently and serves as an untreated control.

RESULTS

Uncorrected transmittance values.--In figure 1 the broken line gives relative red transmittance values. These data, taken from reach 7, do not correlate well with vegetation conditions on the ground. For example, the large differences in transmittances between the summer of 1968 and the summer of 1969 do not appear to be related to vegetation conditions since the phreatophytes were equally dense during both periods. This difference is apparently the result of two known variables: (1) different film emulsions and (2) vastly different processing employed during the two periods.

Corrected transmittance values.--These same transmittance values standardized through use of density readings from the highway bridge, and corrected for several unwanted variables such as camera elevation, film and filter changes, and processing differences, are shown by the solid line in figure 1. Here the summer values for the two years are more nearly equal, as would be expected if a correlation exists with ground conditions. Even with standardization the winter values remain too low, probably because of the low sun angles. We have not yet applied a sun angle correction and are highly skeptical of the winter values (November, December, January, and February).

Comparison of evapotranspiration and red transmittance on cleared and uncleared reaches.--ET has been calculated for several one-month periods during 1969 and 1970 (fig. 2). Separate values are given for reach 4 and reach 7. As noted earlier, ET values are not calculated for some months because of missing data or because the probable error in some of the water-budget terms exceeds acceptable limits.

Adjusted red transmittance values are given in figure 2 for those months for which acceptable ET estimates and photography are available. Note the smaller summertime ET values in the cleared reach (reach 4) than in the uncleared reach (reach 7). Also the adjusted red transmittances are greatest where ET values are correspondingly large.

Comparison of red transmittance and transpiration.--The foregoing comparison stresses the relationship between red transmittance and total water vapor losses (evapotranspiration). The image of wet bare-soil sites on infrared color film is dark green, thus the dominant adjusted transmittance is in the green and blue. The interpretation of this condition will require multiband analysis which is not warranted with present photography. Most logically the comparison should be between red transmittance and that component of ET directly related to plant volume, i.e. transpiration. Since ET includes both transpiration from plants and evaporation from the soil, transpiration can be calculated by subtracting evaporation from total ET. A comparison has been made although direct soil-evaporation data are not presently available for the Gila River Site. Such data for our area can be estimated by using published values from evapotranspirometers operated near Yuma, Arizona (McDonald and Hughes, 1968).

In order to define the relationship between transpiration and adjusted red transmittance on IR-color photography it is necessary to consider the thermal characteristics of evapotranspiration, which are not observed by remote sensing in the visual and near infrared range of the spectrum. Ground observations of climatic conditions must be incorporated into the relationship.

The widely used formula developed by Blaney and Criddle (1962) is a simple empirical equation which can be applied in developing the relation between evapotranspiration and the type of remote sensing presently available.

The equation is

$$U = K \Sigma \frac{(T) (p)}{100} \quad (1)$$

where

U = evapotranspiration during the growing period,
K = an empirical consumptive use coefficient that
is primarily dependent on the quality and species
of vegetation, which is the factor defined by
remote sensing,

p = the monthly percentage of daytime hours in the year,
and T = the mean monthly temperature, in degrees Fahrenheit.

Figure 3 shows the relationship between the computed K and the adjusted red transmittance. The value of K was computed by the Blaney-Criddle formula as

$$K = \frac{100 U}{(T) (p)} \quad (2)$$

where U is the measured monthly evapotranspiration, shown on figure 3, minus soil evaporation, and T and p were determined from local observations.

The data, shown in figure 2 for reaches 4 and 7 and one point from an energy-budget station are plotted on figure 3. In developing the regression between K and red transmittance, we have let K = 0 (no transpiration) where adjusted red transmittance = 33. This is because densitometric analysis of color-IR images of dry, bare soil on the project area gives an adjusted red transmittance of 33. Regression equation 3 is based on the data from reach 7 plus the energy-budget station; equation 4, based on data from reaches 4 and 7 plus the energy-budget station, was also developed to test the affect on the regression of the sparsely vegetated reach 4. The equations, standard errors, and correlation coefficients are shown on figure 3. The standard errors are less for equation 4 than for equation 3 because of the greater number of data points. However, the correlation coefficient is higher for equation 3 indicating that the relation between K and red transmittance is closer for dense vegetation than for sparse cover.

Comparison of costs: ground survey versus aerial photography.--

The cost of assessing the vegetation status on the Gila River Site was calculated for the two techniques that have been employed. The ground survey required 4-1/2 months, including field and office procedures, to fully assess the volume of vegetation on the 2,400 hectares (6,000 acres) of the site. All costs, including aerial photography, film, and processing to produce black-and-white photographic base maps, came to roughly \$6,620.

Cost for the color-IR aerial photography technique came to \$650 for a one-time assessment of vegetation. This cost includes aerial photography, film, processing, densitometric analysis, and computer analysis of density data.

CONCLUSIONS

The dynamic characteristics of evapotranspiration require frequent and spatially complete observations of surface conditions to provide the data for quantitative estimates. The analysis described in this paper indicates that remote sensing can be used for this purpose. The accuracy of the estimates could be improved by greater radiometric fidelity. High geometric resolution is not mandatory because most hydrologic applications are made for large heterogeneous areas and gross measures will be adequate. Consistent IR-color or multiband photography with sensitivity curves and step wedges to provide checks and controls would be desirable. Thermal sensing of surface temperatures would provide data for independent evaluations of ET as suggested by Wiegand and Bartholic (1970) or for refining the relationship between radiance in the visual and near infrared portion of the spectrum and ET. The remote sensing from ERTS-A covers the same range of the spectrum used in this analysis and will have the added advantage of greater radiometric fidelity.

REFERENCES CITED

- Blaney, H. F., and Criddle, W. D., 1962, Determining consumptive use and irrigation water requirements: U.S. Agr. Research Service Tech. Bull. 1275, 57 p.
- Culler, R. C. and Turner, R. M., 1970, Relation of remote sensing to transpiration of flood plain vegetation: Second Annual Earth Resources Aircraft Program Status Review, National Aeronautics and Space Administration, v. 3, p. 37-1 - 37-8.
- Evans, R. M., Hanson, W. R., Jr., and Brewer, W. L., 1953, Principles of color photography: New York, John Wiley & Sons, Inc., 709 p.
- McDonald, C. C., and Hughes, G. H., 1968, Studies of consumptive use of water by phreatophytes and hydrophytes near Yuma, Arizona: U.S. Geol. Survey Prof. Paper 486-F, 24 p.

- Turner, R. M., 1971, Measurement of plant community cover from aerial photographs using Ektachrome infrared aero film: Third Annual Earth Resources Aircraft Program Status Review, National Aeronautics and Space Administration, v. 3, p. 50-1 - 50-8.
- Wiegand, C. L., and Bartholic, J. F., 1970, Remote Sensing in evapotranspiration research on the Great Plains, *in* Spectral survey of irrigated region crops and soils: Annual Report, U.S. Dept. of Agric., Weslaco, Texas, work performed under NASA Contract No. R-09-038-002, p. I.1 - I.11.

VARIABLES

CAMERA K - 17
FILM 8443 - 9"
FILTERS W - 12
ALTITUDE 3600'

K - 17
8443 - 9"
W12, CC20B, CC30M
8500'

K - 17
8443 - 9" EMULSION CHANGE
W12, CC20B, CC30M
8500'

K - 17
2443 - 9"
W12, CC20B, CC30M
8500'

ADJUSTMENTS

BRIDGE CORRECTED
ALTITUDE CORRECTED
FILM NONE
FILTERS CORRECTED

CORRECTED
NONE
NONE
NONE

CORRECTED
NONE
CORRECTION FOR EMULSION
NONE

CORRECTED
NONE
CORRECTED
NONE

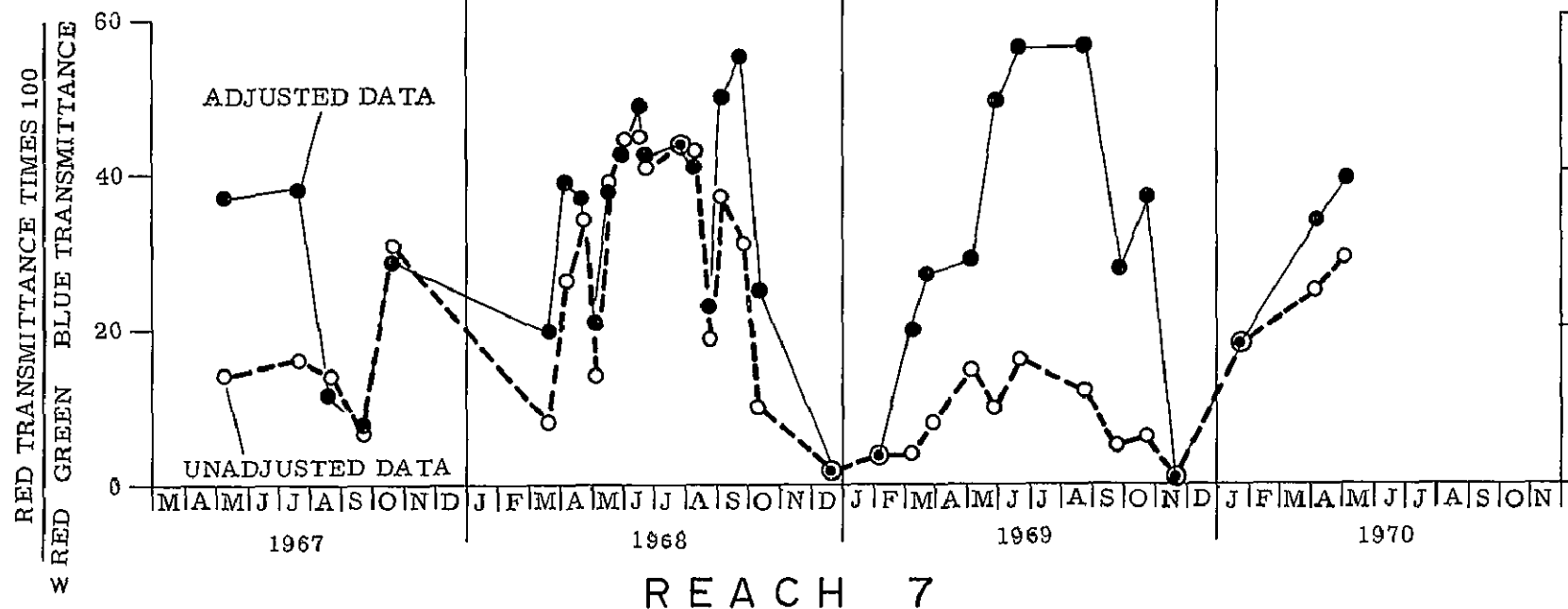


FIGURE 1.--ADJUSTED AND UNADJUSTED RED TRANSMITTANCES FOR 1967 THROUGH 1970, GILA RIVER SITE, ARIZONA. CERTAIN PHOTOGRAPHIC CONDITIONS AND ADJUSTMENTS LISTED ABOVE.

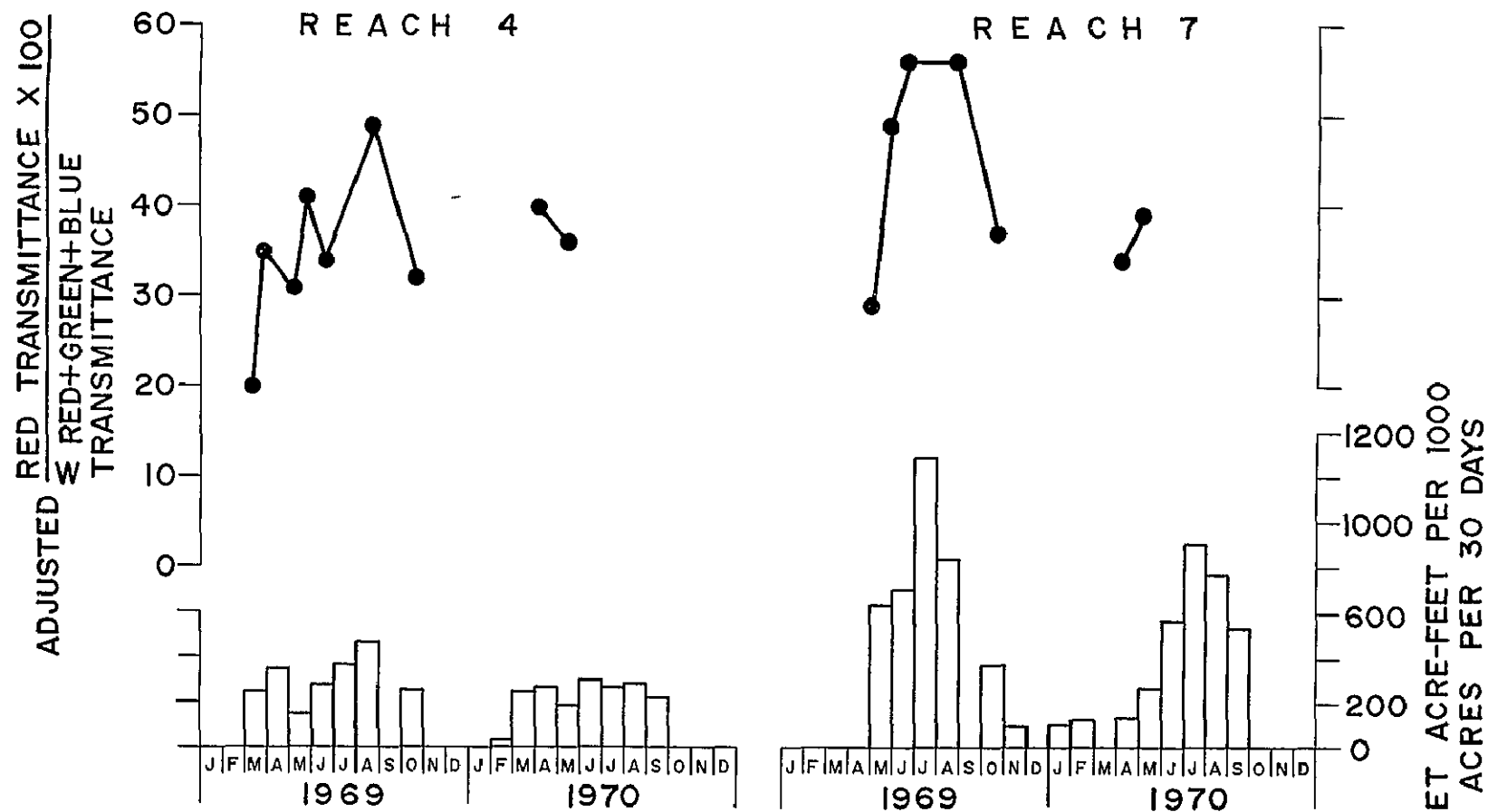


FIGURE 2.--COMPARISON OF ADJUSTED RED TRANSMITTANCES AND EVAPOTRANSPIRATION FOR TWO YEARS ON TWO REACHES OF THE GILA RIVER VALLEY, ARIZONA.

EXPLANATION

○
REACH 4

△
REACH 7

●
ENERGY BUDGET STATION

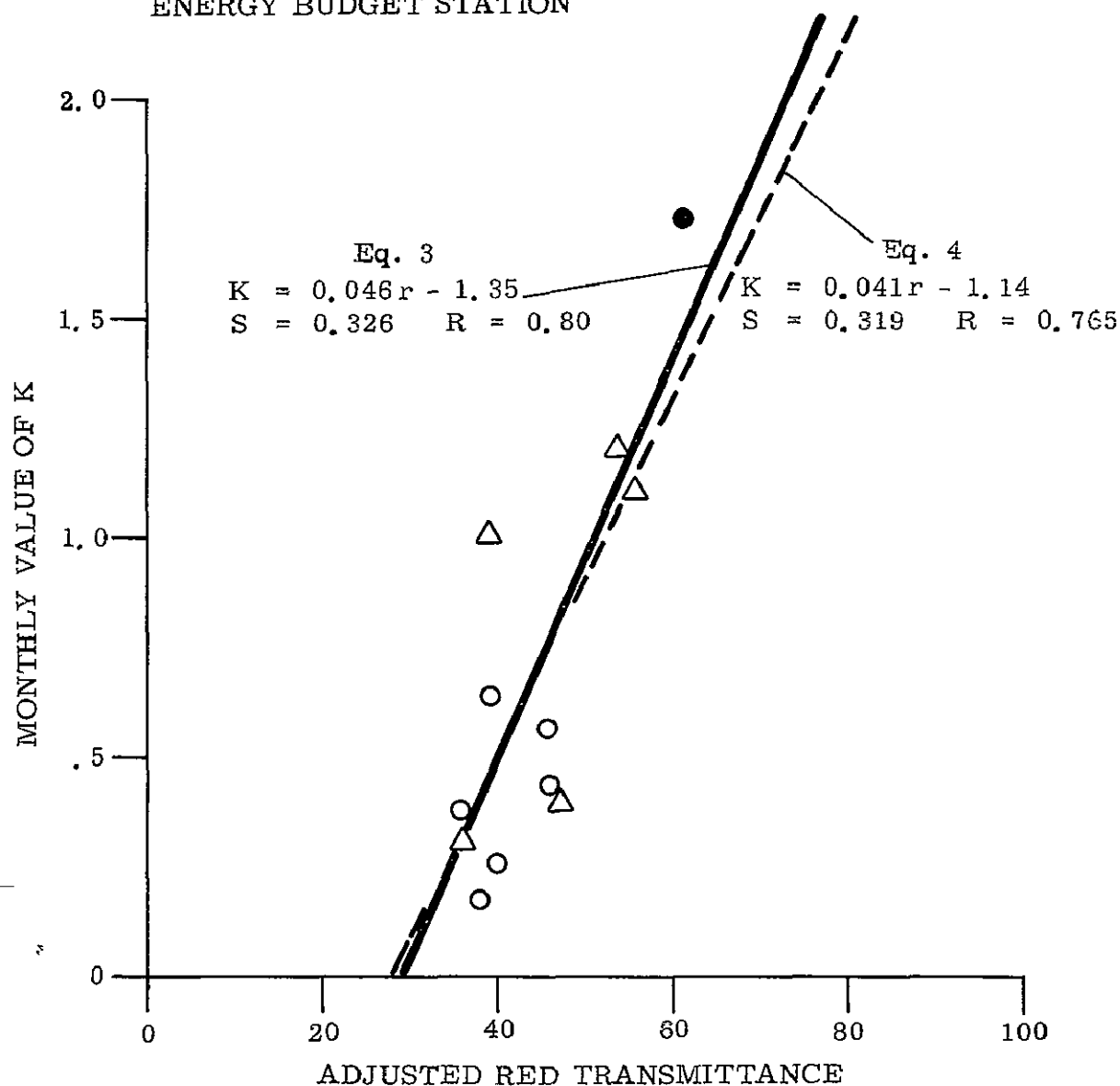


FIGURE 3. --ADJUSTED RED TRANSMITTANCE VERSUS CONSUMPTIVE USE COEFFICIENT (K). SOLID LINE DESCRIBES RELATIONSHIP BETWEEN K AND TRANSMITTANCE FOR UNCLEARED REACH, BROKEN LINE DESCRIBES RELATIONSHIP BETWEEN K AND POOLED DATA FOR CLEARED AND UNCLEARED REACHES. DATA FROM ENERGY BUDGET STATION, REPRESENTING ESPECIALLY DENSE VEGETATION, IS INCLUDED IN BOTH REGRESSION ANALYSES. (r = ADJUSTED RED TRANSMITTANCE, R = CORRELATION COEFFICIENT, S = STANDARD ERROR.)